Benzo[e]pryridoindolones, nouveaux inhibiteurs de kinases hydrosolubles à fort potentiel anti-prolifératif

Ly Thuy Tram Le

UNIVERSITÉ DE GRENOBLE

THÈSE

Pour obtenir le grade de

DOCTEUR DE L'UNIVERSITÉ DE GRENOBLE

Spécialité **: Biologie cellulaire**

Benzo[e]pyridoindolones, new hydrosoluble kinase inhibitors with high anti-proliferative activity

Présentée et soutenue publiquement par

LE Ly-Thuy-Tram

Le 18 Septembre 2013, devant le jury composé de :

Professeur Rémy SADOUL	Président
Docteur Corine BERTOLOTTO	Rapportrice
Docteur Véronique BALDIN	Rapportrice
Docteur Annie MOLLA	Directrice de thèse

Thèse préparée au sein du **Centre de Recherche INSERM –UJF U823**

Équipe 04 – Chromatine et Épigénétique

Dans **l'École Doctorale de Chimie et Science du Vivant**

ACKNOWLEDGEMENTS

This work was carried out at Instutut Albert Bonniot-INSERM U823, University of Joseph Fourier, France during the years 2010-2013. The Ministry of Education and Training of Vietnam (Project 322) is gratefully acknowledged for the fellowships during this time.

I would like to express my sincere gratitude to Dr. Annie MOLLA, my supervisor, for all supports and encouragement, not only in science but also in daily life. You were very patient and enthusiastic to help me to complete this thesis. I learned a lot from your scientific knowledge and experiences, which are surely useful for my future work.

I am grateful to Dr. Chi-Hung NGUYEN for helping me in compound synthesis in this thesis.

My special thanks to Dr.Stefan DIMITROV, director of Team 4 - IAB, for giving me the opportunity to use equipment and work in your team.

I gratefully thank Dr. Corine BERTOLOTTO and Dr. Véronique BALDIN for spending your valuable time to review my thesis. I would like also to thank Prof. Rémy SADOUL for accepting to examine my thesis with the act of the committee's presidence.

Dr. Dimitrios SKOUFIAS and Dr. Karin SADOUL are greatly acknowledged for your useful advices and constructive criticism in "Committee following my thesis" in the 2nd year.

I would also thank Bertrand for your supports in Mice xenograft experiments. Many thanks are given to Mylène, Jacques, Alexei for technical supports in microscopy and FACS experiments.

To all the current and past members in the lab, Defne, Emeline, Yohan, Carole, Aysegul, Dilek, Jessica, Sana, Damien, Thiery…, I thank you all for creating such a friendly working atmosphere; especially Lien, Sophie and Véro, who helped me a lot in experiments. Thank Kiran for your enthusiasm in editorial assistances, even during your holidays. Finally, thank Natacha and Aude for the help dealing with administration during last years.

The warmest thanks to my colleagues in Department of Biotechnology, Faculty of Chemical Engineering, Da Nang University of Technology, Vietnam for shouldering my duties at department during the time I've pursued my Ph.D.

Thanks my dear Vietnamese friends for sharing and lots of fun in daily life. You make me not feel lonely during years living far away from home.

Last but not least, all dearest thanks are given to my family, especially my husband, created the best conditions for me to pursue my dreams in study. I'm lucky to have your love beside me during last years.

Grenoble, May 29th 2013

LE Ly Thuy Tram

ABSTRACT

Benzo[e]pyridoindoles are novel potent inhibitors of aurora kinases. We performed a SAR study to improve their activity and water solubility. Amino-benzo[e]pyridoindolones were found to be potent hydrosoluble anti-proliferative molecules. They induced a massive arrest in mitosis, prevented histone H3 phosphorylation as well as disorganizing the mitotic spindles. Upon a delay, cells underwent binucleated and finally died. Taking into account their interesting preclinal characteristics, their efficiency towards xenografts in nude mice and their apparent safety in animals, these molecules are promising new anti-cancer drugs. They probably target a metabolic signaling pathway, besides aurora B inhibition.

In addition to their possible applications, these inhibitors are tools for cell biology studies. C4, a low ATP affinity inhibitor of aurora B kinase, revealed that the basal activity of the kinase is required for histone H3 phosphorylation in prophase and for chromosome compaction in anaphase. These waves of activation/deactivation of the kinase, during mitosis, corresponded to different conformations of the passenger chromosomal complex.

Key words: *Cancer, mitotic kinases, kinase inhibitor, histone H3 phosphorylation, chromosome compaction.*

RÉSUMÉ

Les benzo[e]pyridoindoles sont de puissants inhibiteurs des kinases aurora. Nous avons réalisé une étude structure/activité pour améliorer leur activité et leur solubilité. Les amino-benzopyridoindolones se révèlent être des puissantes molécules antiprolifératives. Elles induisent un fort arrêt mitotique qui s'accompagne de l'absence de phosphorylation de l'histone H3 ainsi que de la désorganisation du fuseau mitotique. Après un délai, les cellules deviennent binuclées puis, elles meurent. Compte tenu de leurs caractéristiques précliniques, de leur efficacité sur des xénogreffes implantées chez la souris nude et de leur absence apparente de toxicité chez l'animal, ces molécules sont prometteuses pour les traitements anticancéreux. Elles ciblent probablement une voie métabolique tout en inhibant la kinase Aurora B.

Au de là de leurs possibles applications, ces inhibiteurs sont des outils pour la biologie cellulaire. La molécule C4, un inhibiteur d'Aurora de faible affinité pour l'ATP, révèle l'existence d'une activité basale de la kinase requise pour la phosphorylation de l'histone H3 en prophase et pour la compaction des chromosomes en anaphase. Ces vagues d'activation/désactivation de la kinase Aurora B correspondent à différentes conformations du complexe passager.

Mots clés : *Cancer, kinases mitotiques, inhibiteur de kinase, phosphorylation de l'histone H3, compaction des chromosomes*

TABLE OF CONTENT

ABBREVIATIONS

ABL: v-abl ABelson murine Leukemia viral oncogene homolog 1

ALL: Acute Lymphoblastic Leukemia

AML: Acute Myeloid Leukemia

AMPK: AMP-activated Protein Kinase

AMPK-r: AMPK related protein Kinase

APC/C: Anaphase Promoting Complex/ Cyclosome

APS: Amonium PerSulphate

Arf6: ADP-ribosylation factor 6

Arpc1b: Actin-related protein 2/3 complex subunit 1b

ATM: Ataxia Telangiectasia Mutated

ATP: Adenosine 5'-TriPhosphate

ATR: Ataxia Telangiectasia and Rad3 Related

AXL: AXL receptor tyrosine kinase

B-NHL : B-cell Non-Hodgkin Lymphoma

BRSK2: Brain-Specific Serine/Threonine Kinase 2

BSA: Bovine Serum Albumin

BUB1: Budding Uninhibited by Benzimidazoles 1

BUBR1: Budding Uninhibited by Benzimidazoles Related 1

CAMKKβ: Calcium/Calmodulin-dependent protein Kinase Kinase 2 Beta

CCAN: Constituting Centromere-Associated Network

Cdc: Cell division cycle

Cdk: Cyclin dependent kinase

CENP: CENtromere Protein A

Cep: Centrosomal protein

Chk1/2: Checkpoint kinase 1/2

CK2: Casein Kinase 2

c-Kit: v-Kit hardy-zuckerman 4 feline sarcoma viral oncogene homolog

CM: Cutaneous Melanoma

CML: Chronic Myelogenous Leukemia

CPC: Chomosomal Passenger Complex

CSF1R: Colony Stimulating Factor 1 Receptor

Cul3: Cullin 3

DAPI: 4',6-DiAmidino-2-PhenylIndole

DDR2: Discoidin Domain-Containing Receptor 2

DMEM: Dulbecco's Modified Eagle Medium

DMSO: DiMethyl SulfOxide

DNA: Deoxyribo Nucleic Acid

DSBs: Double-Strands Breaks

Ect2: Epithelial cell transforming sequence 2 oncogene

EDTA: EthyleneDiamineTetraaceticAcid

ELISA: Enzyme-Linked Immunosorbent Assay

ESCRT: Endosomal Sorting Complex Required For Transport

FACS: Fluorescence Activated Cell Sorting

FDA: Food and Drug Administration (US)

FGFR1: Fibroblast Growth Factor Receptor 1

FRAP: Fluorescent Recovery After Photobleaching

FRET: Fluorescence Resonance Energy Transfer

HDAC: Histone DeACetylase

HEF1: Human Enhancer Of Filamentation 1

HIPK: Homeodomain Interacting Protein Kinase

HPLC: High-Performance Liquid Chromatography

INCENP: INner CENtromere Protein

IP: IntraPeritoneal injection

Jak2/3: Janus kinase 3

Kif4: Kinesin family member 4A

KLH21: Keyhole Limpet Hemocyanin 21

KLHL9/13: Kelch-Like Protein 9/13

KSP: Kinesin Spindle Protein

Lats1 /2: Large tumor suppressor kinase 1

LCK: LymphoCyte-specific protein tyrosine Kinase

LKB1: Liver Kinase B1

Mad1/2: Mitotic arrest deficient-like 1

MAP4K3/5: Mitogen-Activated Protein Kinase Kinase Kinase Kinase 3/5

MARK: Microtubule Affinity-Regulating Kinase

MCAK: Mitotic Centromere-associated Kinesin

MELK: Maternal Embryonic Leucine Zipper Kinase

Mklp1: Mitotic Kinesin-Like Protein 1

MM: Multiple Myeloma

Mps1: Monopolar Spindle 1

MRLC: Myosin Regulatory Light Chain 2

NEDD9: Neural precursor pell Expressed, Developmentally Down-Regulated 9

NHL: Non-Hodgkin Lymphoma

NPM: Nucleophosmin/B23

NSCLC: Non Small Cell Lung Cancer

NUAK1: NUAK family snf1-like kinase 1 (known as AMPK-related protein kinase 5)

OD: Optical Density

PBS: Phosphate Buffered Saline

PCM: PeriCentriolar Material

PDGFRβ: Platelet-derived growth factor receptor β

Ph+ALL: Philadelphia-positive (Ph-positive) subtype of Acute Lymphoblastic Leukemia

Phk: Phosphorylase kinase

PKB: protein Kinase B

Plk1: Polo-like kinase1

PP1: Protein Phosphatase 1

Prc1: Protein regulator of cytokinesis 1

PTK2: Protein Tyrosine Kinase 2

RacGAP: Rac GTPase Activating Protein

Ran-GTP: RAs-related Nuclear protein-GFP

Rb: Retinoblastoma protein

RhoGAP: Rho GTPase Activating Protein

RPMI medium: Medium from Roswell Park Memorial Institute

SAC: Spindle Assembly Checkpoint

SDS: Sodium Dodecyl Sulphate

SDS-PAGE: SDS polyacrylamide gel electrophoresis

SIK2: Salt-Inducible Kinase 2

Src: v-Src Sarcoma (Schmidt-Ruppin A-2) Viral Oncogene Homolog

TACC: Transforming Acid Coiled-Coil

Tak1: Epithelial transforming growth factor β-activated kinase 1

TBK1: TANK-Binding Kinase 1

TD-60: Telophase Disc 60 protein

TEMED: N,N,N',N'-TEtraMethylEthyleneDiamine

Tlk1: Tousled-like kinase 1

TORC2: Transducer Of Regulated CREB Protein 2

TPX2: Targeting Protein for Xenopus kinesine like protein 2

TRKA/B: Tropomyosin Receptor Kinase A/B

VEGFR2/3: Vascular Endothelial Growth Factor Receptor 2/3

γ-TuRC: γ-tubulin ring complexes

LIST OF FIGURES AND TABLES

Page

INTRODUCTION

CHAPTER 1: CELL CYCLE AND ITS REGULATION

CHAPTER 2: AURORA KINASES

CHAPTER 3: AURORA KINASE INHIBITORS AND ANTI-CANCER THERAPIES

CHAPTER 1: CELL CYCLE AND ITS REGULATION

Cell is the most basic functional and structural unit of life. To ensure development of an organism, new cells are constantly formed through a growth and division process called cell cycle. In prokaryotic cells, the cell cycle occurs through a process called binary fission. Whereas, in eukaryotic cells, the cell cycle can be divided into two fundamental stages: the interphase, during which the cell grows and duplicates its DNA; and the M (mitosis) phase, during which the cell is split into two distinct cells (Figure 1).

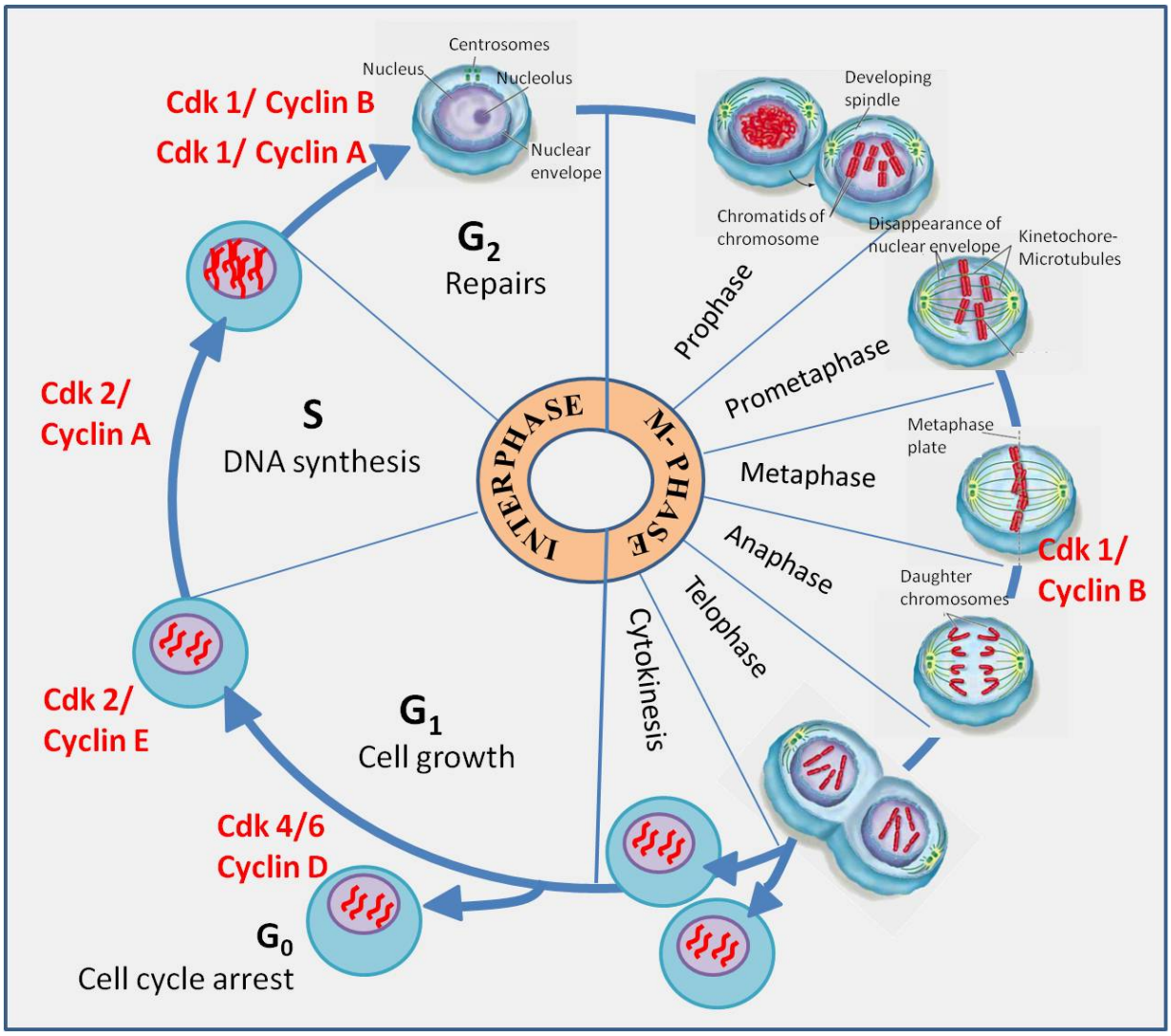

Figure 1: Stages of eukaryotic cell cycle. Interphase includes 4 phases: G_0, G_1, S and G_2, preparing materials for mitosis. In M-phase, the cell goes though 5 phases: prophase, prometaphase, metaphase, anaphase and telophase for seperation of chromosomes and finally, the cytoplasm is divided through cytokinesis to form two daughter cells. The regulatory factors (cyclin and cyclin-dependent kinases - Cdks) which control the cell cycle are also indicated (modified from O'Connor, 2008).

1.1. DESCRIPTION OF THE CELL CYCLE

1.1.1. Interphase

This is the first stage of cell cycle where the cell is engaged in metabolic activity and prepares itself for mitosis. Interphase encompasses four phases (G_0 G_1, S and G_2) and is mainly controlled by the interaction of cyclins and cyclin-dependent kinases (Cdks) (Fig. 1). In fact, G_0 phase (G = gap) is a quiescent period when the cell is unable to get through the restriction point to G_1. When stimulated by mitogenic growth factors or the availability of nutrients, Cdk4 and Cdk6 will interact with three D-type cyclins (cyclin D_1, cyclin D_2 and cyclin D_3) to form the Cdk-cyclin D active complexes. These complexes initiate partially phosphorylation of the retinoblastoma protein (Rb) that binds to the E2F transcription factors and inactivates its function as transcriptional repressor allowing the cell to enter the G_1 phase. The G_1 phase is the major period of cell growth in which the cell synthesizes RNAs, proteins and increases in size. In late G_1 phase, active Cdk2-cyclin E complexes reinforce Rb phosphorylation leading to the release of E2F which participates in the expression of genes required for G_1 to S phase transition and DNA synthesis. This transition is called the restriction point (G_1 checkpoint), which allows the cell either to pause or to continue cell division. Subsequent to G_1, the cell enters S phase for DNA synthesis. In this phase, Cdk1/2-cyclin A complexes hyperphosphorylate Rb activating checkpoint kinases to reduce DNA replication damage. Finally, G_2 phase is the period for final DNA repairs, rapid growth of organelles as well as protein synthesis before initiation of Mitotic phase (M-phase). G_2 checkpoint at the end of this gap determines whether the cells can enter mitosis or must extend G_2 for further cell growth or DNA repair. Cdk1-cyclin B complex is a key regulator of the G_2/M transition driving cells into mitosis through phosphorylation of many substrates that contribute to chromosome condensation, nuclear envelope breakdown and spindle assembly (Enserink et al., 2010; Lapenna et al., 2009).

1.1.2. Mitotic (M) phase

After successful interphase completion, somatic cells go through mitotic phase for cell division. Generally, M-phase is composed of two processes: mitosis and cytokinesis for separation of chromosomes into two identical daughter cells. Mistakes in this stage may lead to uncontrolled cell division, aneuploidy and genetic instability culminating in cancer development.

Mitosis is divided into five phases: prophase, prometaphase, metaphase, anaphase and telophase (Fig.1). At prophase, chromosome condensation begins, the duplicated centrosomes

separate, and some mitotic checkpoint proteins, including Bub1 and BubR1, are recruited to kinetochores on the chromosomes. At the entry of prometaphase, nuclear envelope breaks down. Microtubules emerging from the centrosomes at the spindle poles reach the chromosomes and attach to the kinetochores. During metaphase, the kinetochore-microtubules pull the sister chromatids back and forth until they align along the equatorial plate – an imaginary plane locating midway between two centrosome poles. The mitotic spindle checkpoint is activated by the signals from unattached kinetochores that delays progression to anaphase until all sister chromatid pairs are attached to the spindle microtubules and properly aligned. When this checkpoint is turned off, anaphase starts. Within anaphase, kinetochores provide the pulling forces which allow two sister chromatids of each chromosome to pull apart toward opposite poles. Simultaneously, the midzone is organized by a redistribution of different molecules like actin and myosin to form the cleavage furrow. Finally, at telophase, chromatids complete their movement, a new nuclear membrane is formed around each set of sister chromatids and chromosomes start to decondense into chromatin. At the end of telophase, a contractile ring called midbody is formed to initiate the process of cytokinesis.

Cytokinesis is the final stage of cell division, which distributes the cytoplasm of a parental cell into two daughter cells. The actomyosin ring constricts the plasma membrane in the equatorial region of a dividing cell to form a cleavage furrow between the cytoplasmic content of two daughter cells. The ingressing cleavage furrow compresses antiparallel microtubules of the midzone into a single large microtubule bundle that comprises the core of the midbody. A budge-like structure called the stem body is formed in the center of midbody. Midbody localizes the site of abscission where the two daughter cells will separate at the end of cytokinesis. In a recent study, Hu et al (2012) described the relocalization of midzone microtubule-interacting proteins during midbody formation. These proteins localize to three different parts of midbody: centralspindlin (Mklp1 and RacGAP1) and its partners (Cep55, Arf6 and Ect2) accumulate in the budge of midbody; Prc1 and Kif4 colocalize in the dark zone – a narrow region on the stem body unstained with tubulin; while CENP-E, Mklp1 and aurora B were observed in the flanking zone, outside of the dark zone. Mklp1 interacting with RacGAP1 forms the centralspindlin complex that might be required to recognize the antiparallel microtubule structure of the stem body (Hutterer et al., 2009). Kif4 localizes to plus-ends microtubules to inhibit their dynamics (Hu et al., 2011). Prc1 stabilizes the microtubule overlap. Together with Mklp1, Prc1 helps to transport Polo-like kinase 1 (Plk1), a key regulator of cytokinesis, on microtubules. Aurora B kinase and Plk1 act as master

regulators to ensure proper progression of abscission (Steigemann et al., 2009). Abscision, the final separation of daughter cells, requires coordination of many molecular machines, including endocytic and secretory vesicle trafficking proteins as well as ESCRT (endosomal sorting complex required for transport) proteins (Hu et al., 2012).

1.2. IMPORTANT STRUCTURES IN MITOSIS: MITOTIC SPINDLE AND CENTROMERES/KINETOCHORES – UPDATED VIEWS:

New emerging super-resolution microscopy techniques and proteomic analyses have provided new insight into these known structures.

1.2.1. Mitotic spindle

The mitotic spindle is a bipolar, self-organizing microtubule-based machine that accurately segregates sister chromatids into the daughter cells during cell division. The major structural elements of the spindle are microtubule polymers, which are nucleated from the two centrosomes, major components of the spindle poles.

As the main microtubule-organizing center of animal cells, the centrosome participates in the regulation of cell mobility, organelle positioning, intracellular transport and mitotic spindle assembly (Lawo et al., 2012). It comprises a centriole pair surrounded by a matrix of proteins called PeriCentriolar Material (PCM) (Figure 2).

Centrioles are cylindrical structures composed of nine triplets of microtubules, similar to the basal bodies of cilia and flagella that are required for the formation of centrosomes, cilia and flagella (Nigg et al., 2009). In each centriole pair, there are two unequal centrioles in which the older carries appendages that are close to its distal end. During S-phase, each parental centriole (mother centriole) is duplicated by the formation of procentriole (daughter centriole) at the proximal end. Procentrioles then elongate until maximum length at the end of G_2 and reach full maturation during late G_2 and early M phase by the acquisition of appendages. At the end of mitosis, centrioles in each pair begin separation in a process called centriole disorientation.

During centrosome maturation, the PCM increases in size and γ-tubulin ring complexes (γ-TuRC) are recruited from the cytosol, thereby promoting microtuble nucleation, the key role of centrosome. Previous studies only reported about a uniform amorphous electron-dense structure of PCM around the centrioles. Recently, by using 3D structured illumination microscopy (3D-SIM), the structure of PCM was elucidated (Figure 2). It is composed of nine centrosome components (CPAP, centrin, CEP120, CEP192, CEP152, CDK5RAP2, NEDD1,

TUBG1, PCNT) organized in a toroidal manner around the proximal end of mother centriole in interphasic cells (Lawo et al., 2012).

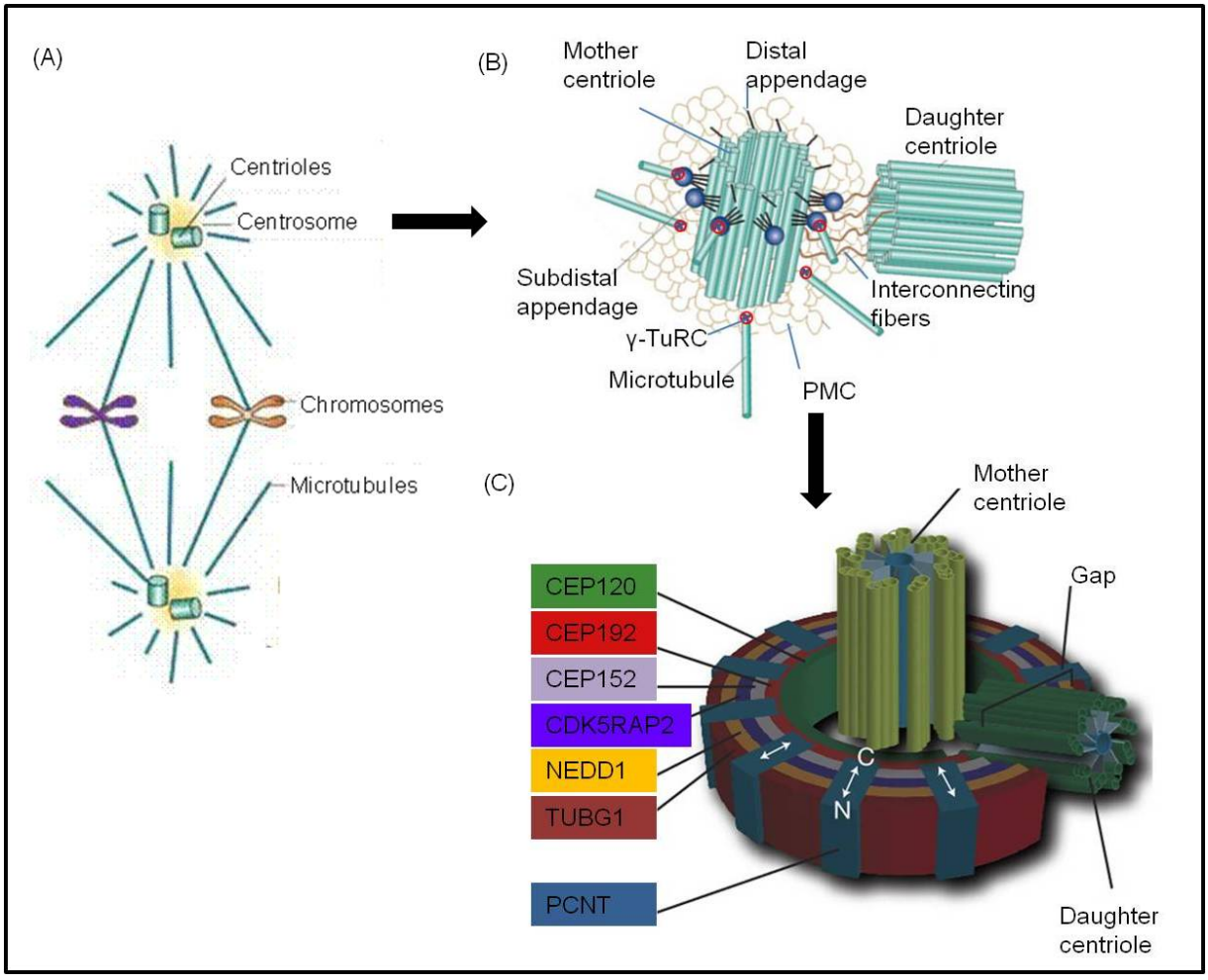

Figure 2: Structure of mitotic spindle. (A) Microtubules are nucleated from two centrosomes forming a mitotic spindle for chromosome separation in mitosis (B) Each centrosome is composed of two orthogonally arranged centrioles surrounded by an amorphous mass of pericentriolar material (PCM). Each centriole comprises nine triplets of microtubles; the older of the two centrioles (mother centriole) has two sets of appendages (additional proteins) along the exterior surface. Microtubules are nucleated from the γ-tubulin ring complexes (γ-TuRC) contained in PCM. (C) Organized-structure of PCM in interphase cells with 9 centrosome components: PCNT (Pericentrin), TUBG1 (γ-tubulin), NEDD1 (Neural precursor cell Expressed, Developmentally Down-regulated 1), CDK5RAP2 (CDK5 Regulatory subunit-Associated Protein 2), CEP120/152/192 (CEntrosomal Protein of 120/152/192 kDa) (modified from Lawo et al., 2012).

The key protein in the centrosome that nucleates assembly of microtubules is γ-tubulin (TUBG1). Complexes of γ-tubulin form ring structures that contain 13 γ-tubulin molecules and have diameters similar to those of microtubules. These γ-tubulin rings serve as nucleation sites for the assembly of microtubules and may remain bound to their minus ends. From these

points, α/β-tubulin-heterodimers are attached and polymerized at their plus end, their parallel arrangement around a hollow core form microtubules.

1.2.2. Centromere - Kinetochore

Centromere is the center region of chromosome. Centromeric chromatin is epigenetically characterized by the presence of specialized nucleosomes in which the canonical histone H3 is replaced by the variant CENP-A (centromeric protein –A) (Gues et al, 2011). HJURP (Holliday JUnction- Recognizing Protein) has been identified as a CENP-A chaperone, which directly interacts with newly synthesized CENP-A and guides CENP-A for its deposition into the centromeric nucleosomes (Dunleavy et al., 2009). The deposition of CENP-A at centromeres is an important marker for the recruitment of a group of 16 proteins constituting centromere-associated network (CCAN) (Westermann and Schleiffer, 2013) (Table 1). Recent studies have elucidated functions of CCAN proteins as an assembly platform for the microtubule-binding interface of the kinetochore, called KMN network, consisting of KNL1, Mis12 complex and Ndc80 complex. The connection between centromeric nucleosomes and microtubules through kinetochore enables for the equal chromosome segregation at anaphase.

CCAN module	Human subunit	Centromere localization dependences	Common functions
Centromeric nucleosome	CENP-A	HJURP chaperone	Centromere specification and propagation
CENP-C	CENP-C	CENP-A	Recognizes CENP-A nucleosome, Associates with Mis-12 complex of KMN
CCAN-HF	CENP-T CENP-W CENP-S CENP-X	CENP-A CENP-T CENP-T CENP-T	Associates with Ndc80-C of KMN Heterodimerizes with CENP-T Forms [CENP-S-CENP-X]$_2$ tetramer, CENP-S-X-T-W heterotramer Associates with FancM (DNA remodeling enzyme)
Module MNL	CENP-N CENP-L CENP-M	CENP-A	Associates with CENP-A nucleosome
Module HIK	CENP-H CENP-I CENP-K	CENP-C. CENP-T	Requires for Ndc80 localization
Module OPQUR	CENP-O CENP-P CENP-Q CENP-U CENP-R	CENP-C, CENP-T	No data available

Table 1: Overview of human centromere-associated network (CCAN) subunits (reviewed by Westermann and Schleiffer, 2013).

Conventional electron microscopy studies indicated that the kinetochore has a layered structure with an electron dense inner plate that contacts centromeric chromatin, an outer plate that contacts microtubles and a “fibrous corona” middle zone that extends away from the outer plate (Figure 3). In recent years, advances in biochemical and proteomic approaches have greatly identified the components of kinetochore as well as their functions. Thereby, CENP-A and CCAN subunits form a core, conserved part in the inner plate of kinetochore. CCAN proteins recruit outer kinetochore components (KMN network) that attach to the spindle microtubules. In detail, the N-terminal region of CENP-C interacts with Nnf-1 and more weakly with Nsl1, both subunits of the outer plate Mis12 complex (Screpanti et al., 2011; Przewloka et al., 2011). Through the connection with KNL1 and Ndc80 complexes, Mis12 complex enhances the binding of microtubules to kinetochores. How the microtubules are attached to kinetochore? The Ndc80 complex contains four proteins forming two dimers Ndc80/Nuf2 and Spc24/Spc25 linked by long α-helical coiled-coil rod domains. First, the Hec1/Nuf2 component of the Ndc80 complex attaches with the plus-end of microtubule; then the Spc24/Spc25 heterodimer of the Ndc80 complex interacts with the histone-fold protein Cnn1/CENP-T and Nsl1 of Mis12 complex to establish the linkage with the inner kinetochore (DeLuca and Musachio, 2012; Malvezzi et al., 2013). Meanwhile, the KNL1 complex is composed of Knl1 and Zwint1 (Zwi) proteins. The C-terminal of Knl1 protein directly interacts with Nsl 1 (Mis12 complex) and its N-terminal binds microtubules (Figure 3).

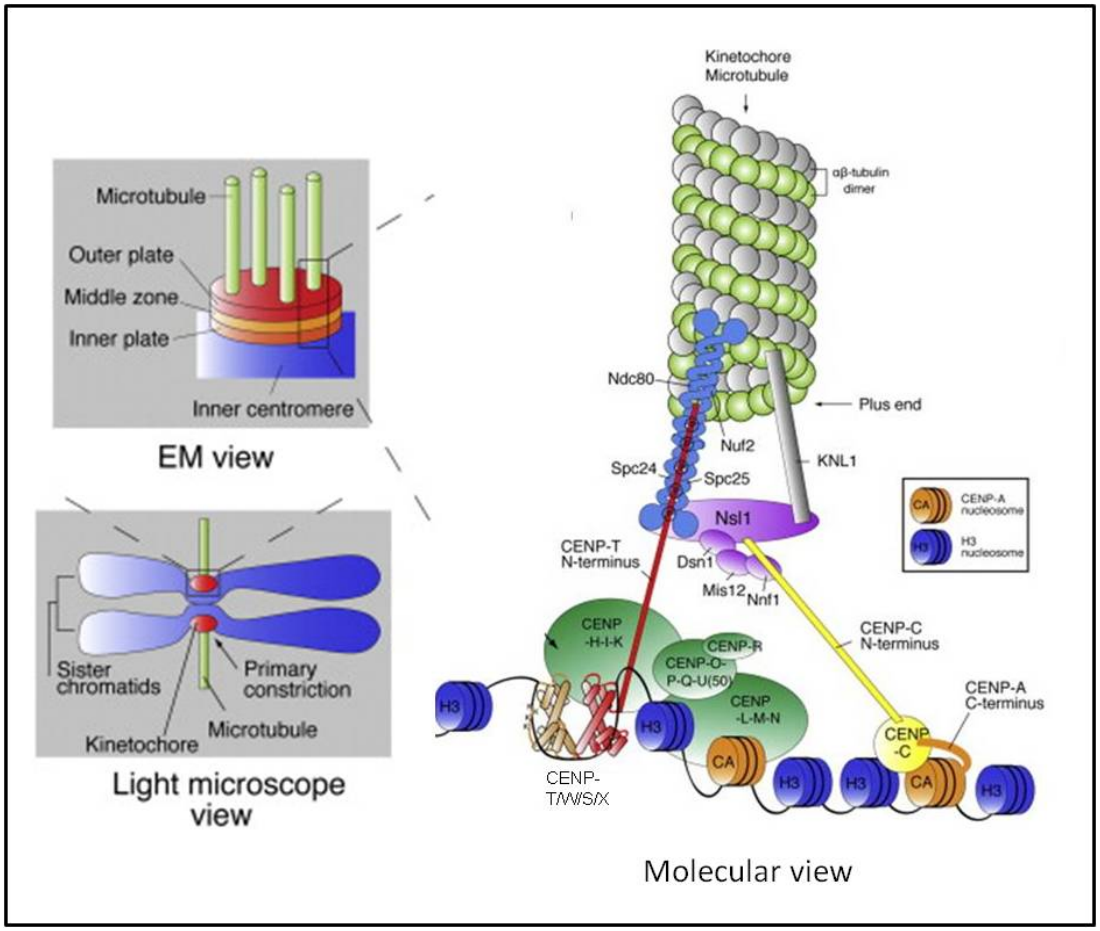

Figure 3: Eukaryotic kinetochore structure from three different views: 1) light microscopy; 2) electron microscopy (EM) and 3) biochemical and proteomic analyses to map the molecular structure. Complexes participating in kinetochore-microtubule attachment are presented. The centromere-associated network (CCAN) subunits are divided into sub-modules and assembled on the centromeric chromatin. The CENP-H/I/K- and CENP-O/P/Q/U/R-containing complexes link to CENP-T/W/S/X complex. The N-terminus of CENP-T directly interacts with the Ndc80 complex in the outer kinetochore through Spc24/25, while Ndc80/Nuf2 of Ndc80 complex binds to microtubules. In parallel, the CENP-L/M/N complex is associated with CEN-A nucleosomes. CENP-C, recruited by CENP-A, connects to Mis12 complex through Nsl1 and Nnf1. Nsl1 also binds to KNL1 complex through Knl1 proteins. All make thus a link between kinetochores and microtubules (modified from Takeuchi et al., 2012).

1.3. QUALITY CONTROL OF CELL CYCLE: CHECKPOINTS

In order to minimize mistakes in DNA synthesis as well as to ensure the proper segregation of chromosomes during cell cycle, cells have checkpoint controls at the specific phase-to-phase transitions. Normally, checkpoints consist of at least three components: a sensor for detecting the mistakes, a signal generated by the sensor via a signal transduction pathway and finally, a responsive element in the cell cycle machinery to prevent cell cycle progression until the errors are repaired (Rieder et al., 2011). There are four known checkpoint

controls during the cell cycle: the DNA damage and replication checkpoints, the spindle assembly checkpoint (SAC) and the NoCut checkpoint (Morgan, 2007; Manuel et al., 2009).

1.3.1. DNA damage/replication checkpoints

During the development of living organisms, DNA damage might happen by the impact of various chemical and environmental agents or by errors in DNA replication. These mistakes, if not repaired properly, may lead to mutation, cancer or cell death. However, from G1 to G2/M, the cells can induce DNA repair mechanisms. The DNA damage/replication checkpoints include damage sensor proteins such as the Rad9-Rad1-Hus1 (9-1-1) complex and the Rad17–RFC complex to detect DNA damages. They transduce signals to ATM, ATR, Chk1 and Chk2 kinases and finally phosphorylate p53 and Cdc25 for various responsive pathways throughout the cell cycle (Figure 4) (Jeremy and Randy, 2010).

The dominant checkpoint response to DNA damage through G1 depends on p53-p21 pathway and is responsible for a G1 arrest. Through both ATM and ATR, p53 is phosphorylated at serine 15 and subsequently stimulates the transcription of p21 CIP1/WAF1, the inhibitor of cyclin-dependent kinases. As a result, p21 inhibits Cdk2-cyclin E and thus stops G1/S progression. In addition, p21 also binds to the Cdk4-cyclin D complex and prevents Rb phosphorylation, thereby suppressing the Rb/E2F pathway and causing a sustained G1 blocking. Simultaneously, in late G1, in response to genotoxic stress the ATR-activated Chk1 increases Cdc25A phosphorylation accelerating its ubiquitilation and proteolysis, thereby inhibiting Cdk2-cyclin E. This pathway is rapidly implemented independently of p53 and only delays the G1/S transition for a few hours, unless the sustained p53-dependent signal prolongs the G1 arrest (Kastan and Bartek, 2004).

During S phase, the DNA damage/replication checkpoint is related to Cdc25A-dependent pathway. Zhou et al (2004) distinguished 3 types of S-phase checkpoints: the replication checkpoint, the S-M checkpoint and the intra-S phase checkpoint. The replication checkpoint is initiated to delay DNA replication in response to dNTP depletion or DNA polymerase inhibition. This checkpoint firstly inactivates Cdk2-cyclin E to wait for DNA repair and then, allows cell cycle ongoing (Jares et al., 2000). The S-M checkpoint is activated when cells end S phase with incomplete replicated DNA. In this case, the checkpoint inhibits Cdk1-cyclin B and stops the cell cycle. The intra-S phase checkpoint works in response to DNA Double-Strands Breaks (DSBs) occurring at any random locus in the genome. DSBs activate ATM autophosphorylation that next phosphorylates Chk2. The combination of activated Chk2 by ATM and Chk1 by ATR increases Cdc25A phosphorylation leading to

down-regulation of CDC25A, thereby inhibiting Cdk2-cyclin A and delaying S-phase (Zhou et al., 2004).

Finally, the G2/M checkpoint prevents cells from initiating mitosis if DNA damage occurs during G2 or if cells enter in G2 with unrepaired DNA lesions. The G2/M checkpoint inhibits Cdk1-cyclin B, the mitosis-promoting complex, by p53 pathway or through the degradation of CDC25C as above mentioned.

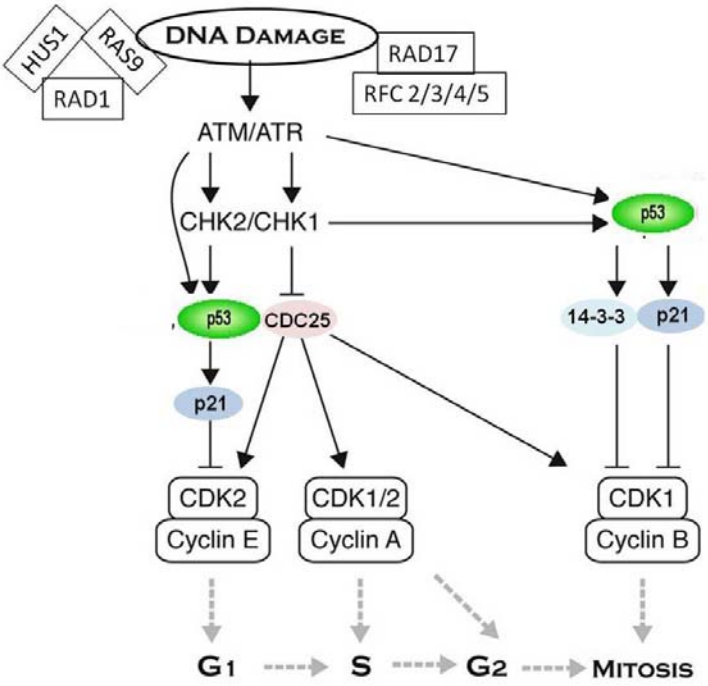

Figure 4: Schematic organization of the DNA damage checkpoints throughout cell cycle. DNA damages are specifically recognized by Rad9-Hus1-Ras1 complex or Rad17-RFC complex to activate ATM/ATR/Chk1/Chk2 kinases. While Chk1 inhibits Cdc25 pathway; Chk2 phosphorylates and activates p53 leading to the inhibition of Cdk-cyclin complexes. As a result, a delay in mitotic phases happens for DNA repair or induction of apoptosis (modified from Jeremy and Randy, 2010).

1.3.2. Spindle Assembly Checkpoint

In order to minimize the mis-segregation of chromosomes and aneuploidy during cell cycle, there is a checkpoint control at the metaphase-anaphase transition called spindle assembly checkpoint (SAC) (Muchaccio and Salmon, 2007). The mechanism of SAC is displayed in Figure 5. The SAC function delays the anaphase onset throughout inhibitory activity on Cdc20, a key cofactor of APC/C until each chromosome is bipolarly attached to spindle microtubules (Nilsson et al., 2008). Briefly, chromosome segregation is mediated by the anaphase-promoting complex/cyclosome (APC/C), an E3 ubiquitin ligase that normally

targets cyclin B for degradation by the 26S proteasome. By inhibiting the APC/C, the SAC keeps cyclin B levels high and arrests the cell in metaphase until all kinetochores are attached to spindle microtubules. Once chromosomes are properly aligned on the metaphasic plate, SAC is turned off, the inhibitory complex dissociates and APC/C gets activated initiating the onset of anaphase. At that time, separase will cleave cohesin to resolve sister-chromatids cohesion for chromosome segregation. Separase is inactivated by securin and cyclin B. Thus, when Cdc20 binds and activates APC/C, securin and cyclin B are ubiquitylated and degraded, in turn, it leads to the activation of separase for the dissociation of sister chromosomes.

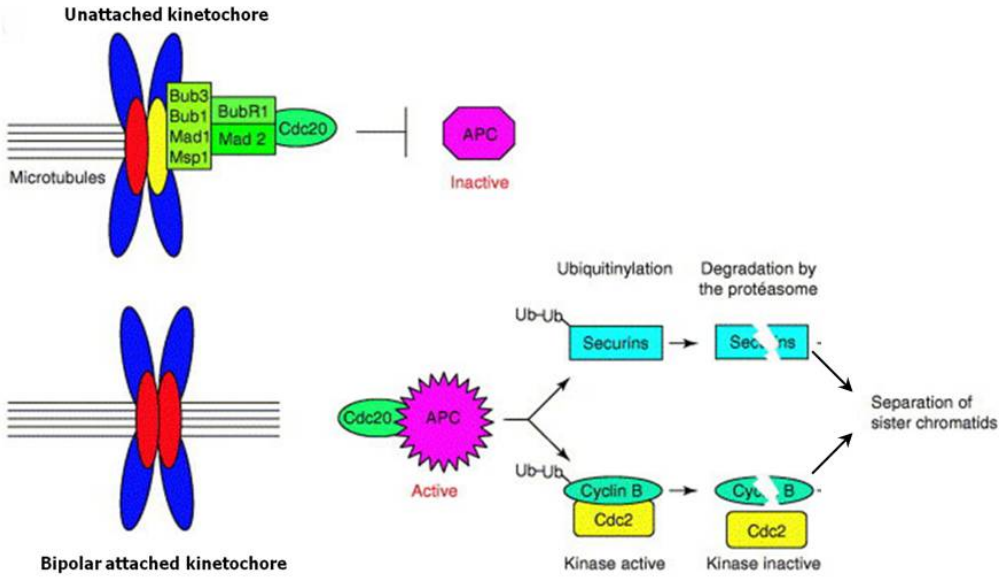

Figure 5: **The mechanism of SAC (modified from Karess, 2005)**
Chromosome segregation is triggered by the APC/C throughout the SAC turn-off. At microtubule-unattached kinetochores, SAC promotes the formation of a Cdc20 inhibitory complex, which inhibits APC/C activity. When each chromosome is bipolarly attached to spindle microtubules, SAC signaling is turned off, the inhibitory complex dissociates; Cdc20 binds to and activates APC/C promoting ubiquitylation of Securins and Cyclin B and thus, their degradations.

The core spindle checkpoint proteins are Mad1, Mad2, BubR1/Mad3, Bub1, Bub3 and Mps1 which specifically localize at the unattached kinetochores and become depleted after the proper microtubule attachment (May and Harwick, 2006). BubR1, Bub3 and Mad2, as key factors, directly bind to Cdc20 and form a mitotic checkpoint complex (MCC) which can function as an inhibitory complex preventing APC/C activity (Karess, 2005; Herzog et al., 2009). Recent studies have elucidated how the SAC proteins are recruited to unattached kinetochore and KNL1 is determined as an important factor in the kinetochore-based SAC activation (reviewed by Foley and Kapoor, 2013). KNL1 is a crucial substrate of Mps1 and its phosphorylation by Mps1 creates a docking site for the SAC kinase Bub1. Kinetochore-

localized Bub1 is necessary and sufficient for recruiting the SAC protein Bub3. BubR1 localizes at outer kinetochore in a Bub3-dependent manner. Additionally, BubR1 also functions as a mechanosensor monitoring CENP-E activity (Chan et al., 1999). CENP-E is a kinetochore motor protein, involved in the attachment of microtubule to kinetochore (Mao et al., 2010). Interaction of CENP-E and BubR1, at the unattached kinetochore is thought to stimulate BubR1 activation in the absence of microtubule attachments (Mao et al., 2005; Weaver et al., 2003) and conversely, inactivate BubR1 activity in the proper attachment of kinetochore-microtubules (Muchassio et al., 2007). BubR1 is considered to play an important role in the inhibition of the APC/C, together with Mad2 (Muchassio et al., 2007). The Mad2 attachment to kinetochore requires docking protein like Mad1. Mad1, a stably kinetochore-bound protein, is essential for Mad2 kinetochore localization. Interaction between Mad1 and Mad2 results in the conformational modification of Mad2 enabling to bind to Cdc20. Mps1 contributes to the SAC activity by recruiting Mad and Bub proteins to unattached kinetochores (Lan & Cleveland, 2010) and by promoting Mad2 activation (Hewitt et al., 2010; Maciejowski et al., 2010). Furthermore, Mps1 prevents the dissociation of the inhibitory complex (Maciejowski et al., 2010). All these numerous actors playing together integrate kinetochore functions, SAC activation, microtubule attachments and SAC silencing to ensure accurate timely chromosome segregation (Foley and Kapoor, 2013). The balance of kinase and phosphatase activities has a crucial role in kinetochore functions and is not fully described.

In the presence of spindle poison like Taxol, kinetochores are unable to form proper attachments to spindle microtubules. This leads to the permanent activation of the SAC, the prolongation of mitotic arrest for hours. However the SAC cannot prevent a slow but continuous degradation of cyclin B that ultimately drives the cell out of mitosis (Brito and Rieder, 2006). Mitotic checkpoint slippage leads to 4N-multinucleated cells exhibiting a micronuclei phenotype.

1.3.3. NoCut Checkpoint (Abscission checkpoint control)

Cell abscission is the last step of mitosis and it does not occur until all chromatids are pulled out of the cleavage plane. In budding yeast and human cells, this event is monitored by the NoCut checkpoint, which involves the activities of the chromosome passenger aurora B kinase and Plk1 (Carmena, 2012; Chen et al., 2012). When the NoCut checkpoint detects the presence of chromatins in the cleavage furrow, it is turned on. Active Plk1 phosphorylates a centrosomal protein of 55 kDa (Cep55) and prevents its association with the midbody (Bastos

and Barr, 2010). Cep55, that efficiently bundles microtubules, binds to Mklp1 *in vitro* and associates with the Mklp1-MgcRacGAP centralspindlin complex *in vivo*.

Meanwhile, aurora B still phosphorylates mitotic kinesin-like protein 1 (Mklp1) and prevents furrow ingression (Steigmann et al., 2009). Normally, aurora B activity gradually decreases at cytokinesis, to be null upon abscission. If aurora B is prematurely inactivated, the NoCut checkpoint is turned off, leading to the formation of binucleated cells (Chen et al., 2012).

At the end of mitosis, once chromosomes are segregated away from the cleavage furrow, the NoCut checkpoint is turned off, Plk1 is degraded allowing the interaction of Cep55 with kinesin Mklp1 at the midbody enabling the recruitment of subsequent midbody components for the abscission initiation. In a recent study, Carmena clarified the molecular mechanism by which the CPC controls the timing of abscission through regulation of ESCRT-III (Carmena, 2012).

The ESCRT (endosomal sorting complex required fortransport) complexes are proteins involved in membrane fission events, including six complexes (ESCRT-0, -I, -II, -III, ALIX and VSP4) in human. Different ESCRT complexes are recruited sequentially to the site of scission, ending with the recruitment of the ESCRT-III complex that brings about membrane scission (Figure 6). In cytokinesis, after Cep-55 is associated with kinesin Mklp1, it interacts with Tsg101 (ESCRT-I) and ALIX, which in turn recruit ESCRT-III, the complex responsible for the abscission activity. ESCRT-III can assemble in filaments around the abscission site and makes the membrane curve, eventually driving the final break between daughter cells (Carmena, 2012). This study defines a cellular mechanism that links centralspindlin to Cep55, which, in turn, controls the midbody structure and membrane fusion at the terminal stage of cytokinesis.

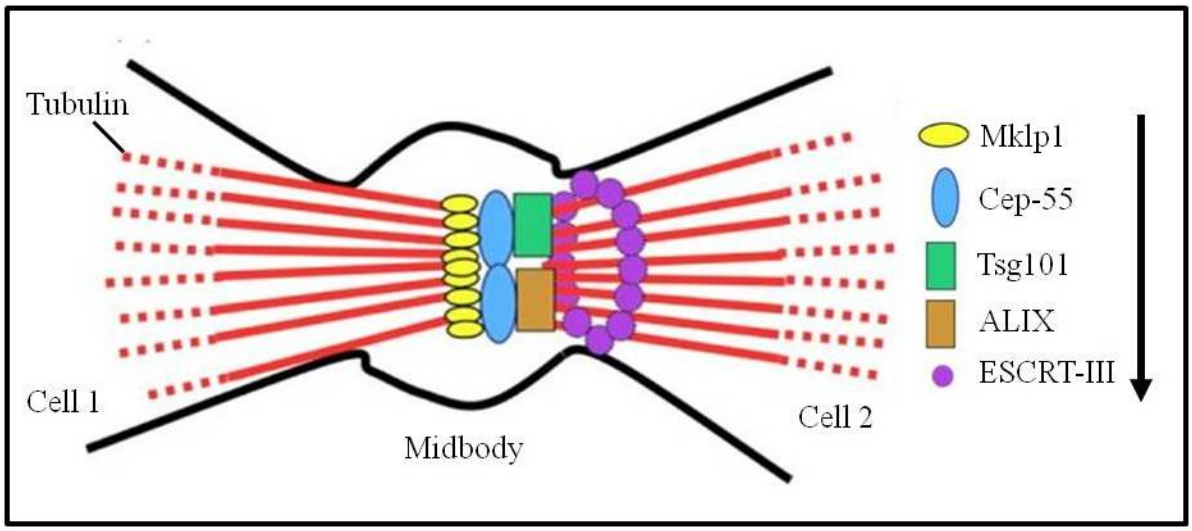

Figure 6: The sequential recruitment of ESCRT complexes to the midbody. After Plk1 degradation, dephosphorylated Cep-55 binds to Mklp1. Cep-55 then recruits Tsg101 (ESCRT-I) and ALIX, which in turn attract the ESCRT-III complex. ESCRT-III forms filaments around the abscission site and drive the final cut (Carmena, 2012).

CHAPTER 2: AURORA KINASES

Aurora kinases are a family of serine/threonine protein kinases that have been recognized as regulators of mitosis with key roles from mitotic entry to cytokinesis (Carmena et al., 2009). The first aurora kinase was discovered in *Saccharomyces cerivisae*, based on a pioneering genetic screen for mutations that lead to the increase of chromosome mis-segregation, was named IPL1 for increase-in-ploidy (Chan et al., 1993). *Schizosaccharomyces pombe* also expresses an aurora kinase, formerly called aurora-related kinase (ARK1) (Petersen et al., 2001). While yeast has only a single aurora kinase, there are two aurora kinases (aurora-A and aurora-B) in *Drosophila melanogaster*, *Caenorhabditis elegans* and *Xenopus laevis* (Schumacher et al., 1998). In mammals, this family has 3 members known as aurora kinase A, B and C (Bischoff et al., 1999). Aurora A and B are expressed in many cell types, whereas aurora C is mostly found in testicular tissue and is involved in spermatogenesis (Kimmins et al., 2007).

2.1. LOCALIZATION OF AURORA KINASES

Aurora kinases show different cellular localization during mitosis (Figure 7). At late S phase, as soon as centrioles are duplicated, aurora A localizes on the centrosomes and is still there, in prophase. Then, from metaphase to anaphase, it associates along the microtubules close to the spindle poles. Aurora A concentrates in the midbody during cytokinesis and finally, it is degraded in early G1 of the following cycle (Katayama et al., 2003). Whereas, aurora B, a member of the chromosome passenger complex (CPC), is mostly absent in interphase. In prophase, aurora B is localized first in pericentromeric chromatins, then along the length of the condensing chromosomes and it gradually concentrates in the inner centromere at prometaphase. Thereafter, it transfers from chromosomes to microtubules, localizes to the spindle midzone in anaphase. Finally, like aurora A, it is associated with the midbody during cytokinesis. Aurora C is also a chromosomal passenger protein with a similar sub-cellular location to aurora B; it is localized to centromeres during the prophase to metaphase and is redistributed to midzone microtubules during anaphase (Sasai et al., 2004; Tang et al., 2006; Chen et al., 2005).

The different localizations of aurora kinases correspond to their distinct functions during mitosis. Interestingly, recent studies reported that the mutated G198A aurora A mimicked the asparagine 142 of aurora B and rescues aurora B mitotic functions (Hans et al., 2009; Fu et al., 2009). These data demonstrated that both aurora kinases share structural

similarities but a few different key amino acids in their structure decide their distinct targets, functions and localizations.

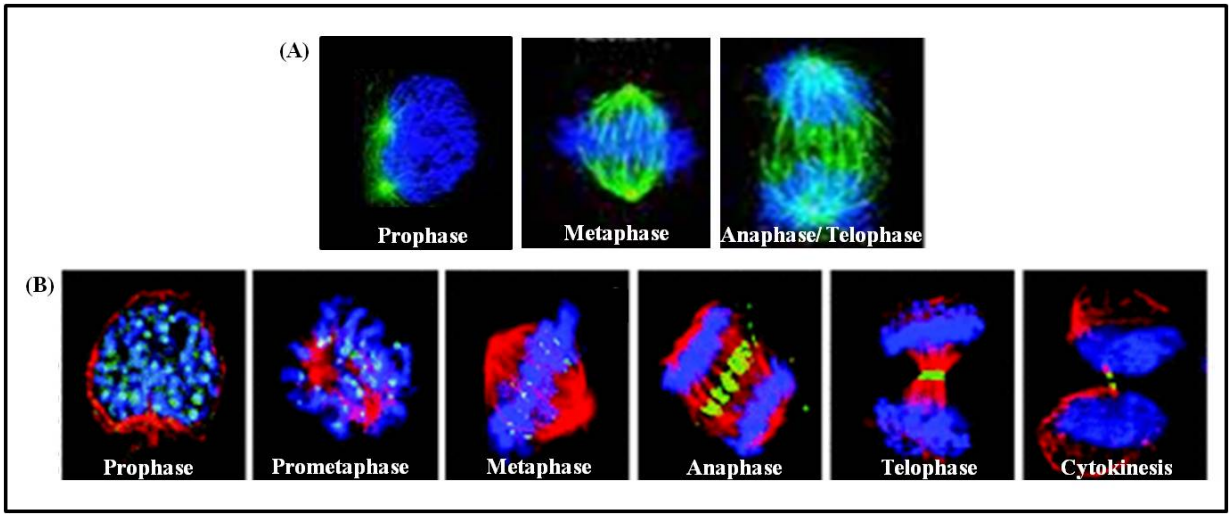

Figure 7: Comparative localizations of aurora kinases A and B during mitosis. DNA is stained in blue and microtubules are in red. (A) Aurora A (in green) localizes around centrosomes in prophase, on the microtubules near the spindle poles in metaphase and on polar microtubules during anaphase and telophase. (B) Aurora B (in green) localizes first in pericentromeric chromatins in prophase, concentrates in the inner centromere during prometaphase and metaphase, transfers to spindle mid-zone microtubules in anaphase and finally is associated with the midbody during cytokinesis (photo was modified from Kollareddy et al., 2008). Aurora C, when overexpressed in cells, shares the localization and functions of aurora kinase B.

2.2. STRUCTURE OF AURORA KINASES

Aurora kinases are composed of a highly conserved C-terminal catalytic domain and a short N-terminal domain that varies in size (Chemtham et al., 2002, Giet et al, 1999). The three mammalian aurora kinases range from 275 to 402 amino acids. Like other protein kinases, the highly conserved catalytic domain of aurora kinase consists of an activation loop, a hinge region binding ATP, a hydrophobic pocket and an allosteric site.

In efforts to develop kinase inhibitors, the structural features of ATP-binding sites of aurora kinases have been elucidated by X-ray crystallography. Until now, most of the available data on the ATP-binding site are from aurora A studies because aurora B itself has not been crystallized in the absence of its inhibitors (Girdler et al., 2008; Sessa et al., 2005). Results showed that aurora A has a peculiar DFG (Asp-Phe-Gly) motif in the ATP-binding sites that adopts different conformations: the active DFG-in and the inactive DFG- out states (Dodson et al., 2010; Martin et al., 2012; Liu and Gray, 2006). In the active DFG-in conformation, the activation loop is oriented away from the ATP site and accessible for phosphorylation.

Conversely, in the inactive-DFG state, in the presence of aurora inhibitors, the phenylalanine side chain points outwards and interacts with inhibitors, preventing the phosphorylation of the activation loop (Figure 8).

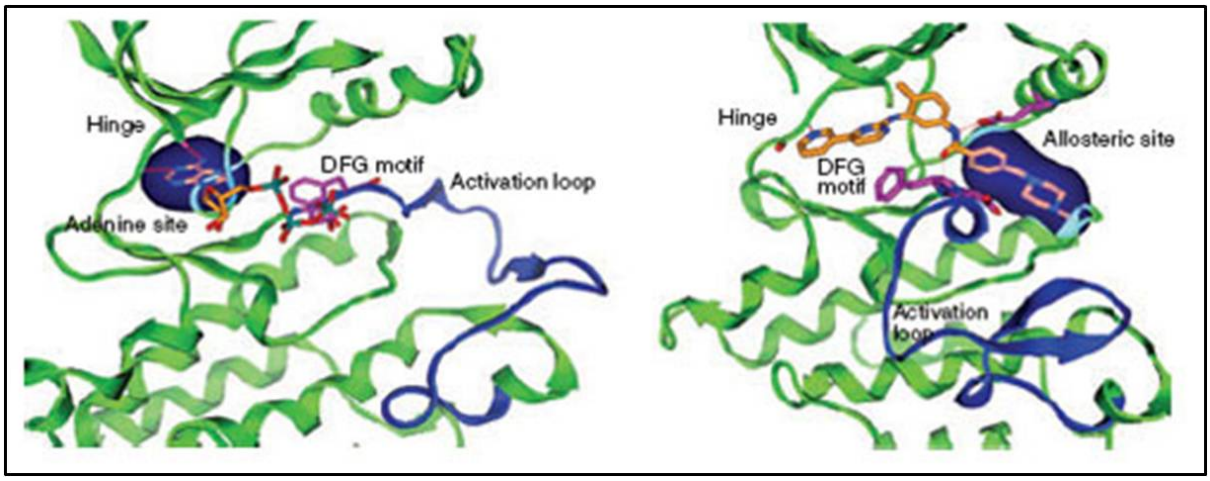

Figure 8: Conformational changes of aurora A activation loop: the active DFG-in (left) and the inactive DFG- out states (Liu and Gray, 2006)

In complex with INCENP and an aurora kinase inhibitor (VX-680), the structure of aurora B has recently been determined (Elkins et al., 2012). The overall structure of human aurora B resembles that of human aurora A with the exception of the conformation of the activation loop (Figure 9A and 9B). The catalytic domains of human aurora A and aurora B are 76% identical at the primary sequence level, and their ATP-binding pockets differ by just three amino acids in which Leu215, Thr217 and Arg220 in aurora A are replaced by Arg159, Glu161 and Lys164 respectively in aurora B (reviewed in Dodson et al., 2010). Remarkably, in complexes with the same inhibitor, both aurora kinases showed a significant spatial difference of the DFG motif (Figure 9C). In aurora A, the DFG motif is arranged with the Phe underneath the αC helix; while in aurora B, the αC helix is moved further out from the ATP- binding site and the Phe residue is to side to the helix whereas Asp is not well-ordered in the structure (Elkins et al., 2012).

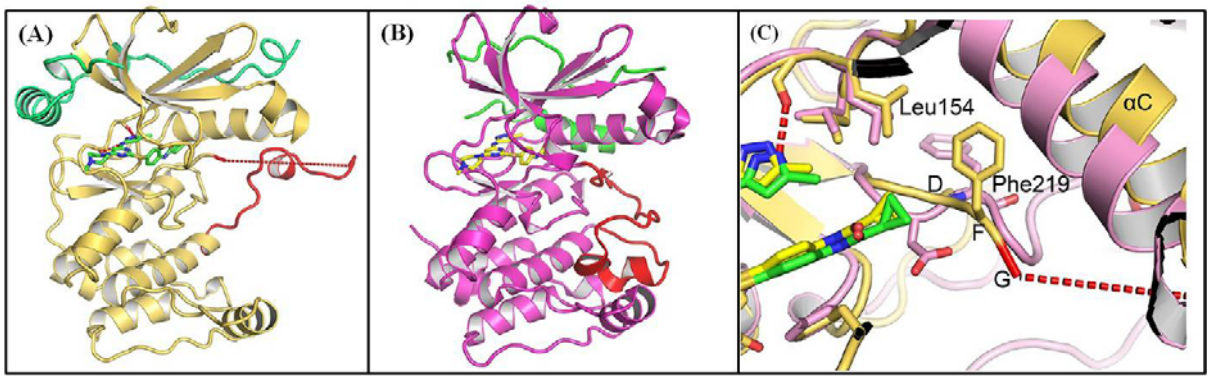

Figure 9: Comparison of human aurora A and aurora B structures. (A) Structure of human aurora B with INCENP stained green and activation loop stained red. (B) Structure of human aurora A with TPX2 colored in green and activation loop colored in red. (C) Differences in DFG motif between aurora B (in yellow) and aurora A (in pink). (modified from Elkins et al., 2012).

2.3. SUBSTRATES, FUNCTIONS AND REGULATION OF AURORA KINASES

2.3.1. Aurora A

During mitosis, aurora A interacts with different substrates for its activation and regulation, corresponding to its distinct roles (Table 2). Aurora A is involved in centrosome maturation, mitotic entry, separation of centriolar pairs, accurate bipolar spindle assembly and alignment of metaphase chromosomes. Major substrates, inter-actors and co-factors are listed in Table 2.

Aurora A is activated by its phosphorylation and by the binding of activator proteins (Dodson and Bayliss, 2012). Recent studies have described several activators of aurora A such as TPX2 (Dodson and Bayliss, 2012; Giubettini et al., 2011), HEF1 (Pugacheva et al., 2007), Bora (Hutterer et al., 2006), Arpc1b (Molli et al., 2010) and Nucleophosmin/B23 (NPM) (Reboutier et al., 2012). The role of Ajuba as aurora A activator is still controversial (Hirota et al., 2003; Sabino et al., 2011).

Autophosphorylation of aurora A on Thr-288 within its activation segments requires the binding to TPX2, a microtubule-associated protein (Dodson and Bayliss, 2012). Upon TPX2 binding, the autophosphorylation activity of aurora A is increased and its desphosphorylation by PP1 phosphatase is prevented (Eyers et al., 2003; Kufer et al., 2002; Tsai et al., 2003). The binding to TPX2 is required for the localization of aurora A to the mitotic spindle but not to the centrosome (Carmena and Earnshaw, 2009).

Besides TPX2, at G_2-M transition, aurora A binds to Bora inducing Plk1 phosphorylation and mitotic entry (Hutterer et al., 2006). Additionally, the interaction of aurora A and HEF1 is

necessary to phosphorylate and activate HDAC6, promoting ciliary disassembly at the basal body (Pugacheva et al., 2007). Alternatively, Arpc1b, a centrosomal protein, is required for the activation of aurora A and in turn, aurora A phosphorylates it on Thr21, a signal for mitotic entry (Molli et al., 2010). More recently, aurora A was found to be activated by Nucleophosmin/B23 for centrosome maturation. Nucleophosmin/B23 (NPM) binds to aurora A and strongly induces its autophosphorylation on serine 89 (Reboutier et al., 2012).

Table 2: Partners of aurora A and their roles

Substrate	Interactor	Co-factors	Function
Aurora A(T288)	TPX2		Maximal activity of aurora A
	AurKAIP1	GSK-3β	Degradation of aurora A
	HEF1		Aurora A activation (centrosome amplification)
	Arpc1b		Aurora A activation (mitotic entry)
Aurora A (S89)	NPM		Aurora A activation (centrosome maturation)
TPX2	TPX2 (Ser 204)	Plk1	Localization of aurora A to centrosome ; aurora A activation; spindle length /MT nucleation from chromosome
Plk1 (T210)	BORA	BORA	G2/M entry activation of Cdk1; liberation of aurora A and recruitment of TPX2
Xl-p53(S129/190) H-p53 (S315)	TPX2		Stabilisation of p53 (Met II meiosis) Ubiquitination by Mdm2 and proteolysis
	Cyclin B1		Stabilisation of cyclin B (prevents APC interaction)
Cdc25B (S553)			Cdk1-cyclin B_1 activation for G_2-M transition
Lats 2 (S83)			Centrosomal localisation Lats 2 kinase
Hs-TACC3 /maskin (S558) D-TACC1(S863)		MAP215	Interaction with microtubule-associated-proteins (dynamic of spindle pole MT) Stabilisation of centrosome-associated microtubules
HDAC6	HEF 1/Cas-L (NEDD9)		Primary cilium disassembly (microtubule deacetylation)
D-Par 6		Numb	Neuronal polarity/ asymetric division Spindle orientation
	Ajuba		Aurora A activation

(TPX2 : microtubule-associated protein; AurKAIP1 : aurora-A kinase interacting protein 1; HEF1 : focal adhesion scaffolding protein; Plk1: polo-like kinase 1; Lats2, a novel serine/threonine kinase, member of the Lats kinase family that includes the Drosophila tumour suppressor lats/warts; TACC : transforming acidic coiled-coil; MAP : microtubule associated protein; HDAC : histone deacetylase; NEDD9 neural precursor cell expressed, developmentally down-regulated 9; Par-6, partitioning defective 6 homolog alpha, is a regulatory subunit of atypical protein kinase C (aPKC); Xl: Xenopus laevis, D: drosophila and Hs Human sapiens) (reviewed by Molla, 2010).

In order to become fully functional after duplication and separation, in G2 phase, centrosomes must recruit several proteins in a process known as maturation. This process requires the function of aurora A. Aurora A activity depends on other kinases such as Pak1, Plk1, Cdk11 for centrosomal localization (Zhao et al., 2005; Petretti et al., 2006; Macůrek et al., 2008). Of these, Pak1 directly binds and phosphorylates aurora-A. Next, aurora A phosphorylates transforming acid coiled-coil (TACC) protein and the activated TACC-aurora A complex is recruited to the centrosome, together with microtubule-associated proteins like Msps/XMAP215, centrosomin and γ-tubulin, promoting the centrosome maturation (Ikezoe, 2008).

After maturation, the centriolar pairs separate and migrate to two opposite positions around the nuclear envelop for bipolar mitotic spindle formation. This event also requires aurora-A function; thus inhibition or depletion of aurora-A can lead to monopolar spindles and prevent chromosome segregation in mitosis (Vader and Lens, 2008). Aurora A phosphorylates Eg5, a conserved BimC-like kinesin involved in centrosome separation (Giet et al., 1999). After centrosome separation, spindle assembly initiates in early prophase. Nachury et al (2001) has shown an interaction between Ran-GTP and aurora A in spindle assembly. Ran-GTP binds to Importin-β causing the release of important microtubule-assembly factors such as TPX2 near chromosomes. The liberated TPX2 then binds to aurora A at the centrosome and this interaction is required for microtubule nucleation from chromosomes and in turn, for building a spindle of correct length (Nachury et al., 2001; Kufer et al., 2002, Bird and Hyman, 2008).

Aurora A also regulates mitotic entry through activation of Cdk1-cyclinB. During G2, aurora A together with Bora phosphorylates Plk1 at Thr-210 and Cdc25B at Ser-353 (Dutertre et al., 2004; Seki et al., 2008). Activated Plk1 regulates Cdk1-cyclinB activity through phosphorylation of Cdc25B phosphatase and degradation of the Cdk1 inhibitory activity Wee1 that allows cell to enter mitosis (Macůrek et al., 2009).

Aurora-A is degraded early in next G_1 by the proteasome and the ubiquitin- dependent pathway. Its degradation depends on both intact A and D boxes. The level of aurora A decreases in interphase due to its ubiquination by the E3-ligase Cdh1-activated APC/C (Honda et al., 2000; Walter et al., 2000).

2.3.2. Aurora B

Like aurora A, aurora B interacts with different substrates corresponding to distinct roles during mitosis as reviewed in Table 3.

Table 3: Substrates of aurora B: roles and time of action during mitosis.

Substrate	Phase in mitosis	Function
Aurora B (Thr232)	Mitose	Maximal activity of aurora B
INCENP (TSS893-895)	Mitose	Localization and activation of aurora B; checkpoint function
Histone H3 (Ser10 and 28)	G2-metaphase	Chromosome alignment
Dam1 (Ser20, Ser257, Ser265 and Ser292)	S-metaphase	Correction of improper kinetochore-microtubule connections.
Complex Ndc80 (Ser55 and 62)	Metaphase	Correction of improper kinetochore-microtubule connections.
Hs-Mis13 (Ser100 and 109)	Metaphase	Kinetochore function/recruitment of Ndc80/Hec1
CenP-A (Ser7)	Metaphase	Mitosis ongoing; cytokinesis completion
MCAK (Xl-S196, Xl-T95)	Metaphase	Kinetochore microtubule dynamic/ recruitment of MCAK on chromatin
Survivin (Thr117)	Anaphase	Anaphase onset and cytokinesis
Stathmin/Op18 (Ser16)	Anaphase	Spindle assembly
MgcRacGap (Ser387)	Cytokinesis	Cytokinesis completion
Kinesin 6 : Zen4/MKLP1(Ser708)	Cytokinesis	Cytokinesis completion
Desmin (Thr16)	Cytokinesis	Cytokinesis completion

(CenP-A :Centromeric Protein A ; CPC : Chromosomal Passenger Complex ; INCENP : INer CENtromeric Protein ; MCAK: Mitotic Centromere-associated Kinesin ; Ndc 80 complex composed of Ndc80/H-Hec, Nuf2, Spc24, and Spc25is an essential core element of kinetochores; MgcRacGap: Rac GTPase activating protein (modified from Molla, 2010).

Aurora B is a passenger protein, together with INCENP, Survivin and Borealin. They form the Chomosomal Passenger Complex (CPC). The expression of CPC members peak in mitosis and these proteins are interconnected. Invalidation of the expression of a CPC protein leads to the degradation of the partners (Klein et al., 2006). In fact this complex has a peculiar localization since it concentrates in the centromere from where it controls kinetochore tension then, when the SAC is turned off at anaphase onset, it transfers to the midzone. Finally, it concentrates in the midbody and participates to the NoCut checkpoint. The association with its partners ensures the correct localization of the kinase on the inner centromere as described in Figure 10. Aurora B is the unique enzymatic member of the CPC, and its maximal activation depends on a functional complex (Petsalaki et al., 2011). Activation of aurora B occurs through a two-step mechanism: first, aurora B binds to the C-terminal IN-box sequence of INCENP and is then autophosphorylated at threonine 232 (Thr232) within its activation loop (Honda et al., 2003; Yasui et al., 2004). In the second step, aurora B phosphorylates INCENP

at the TSS sequence and is subsequently fully activated.

Together with INCENP, Survivin and Borealin also participate in the right localization of the entire passenger protein complex to centromeres through the recognition of two specific epigenetic marks present on chromatin: 1) Haspin-dependent phosphorylation of histone H3 on Thr3 (H3-Thr3ph) and 2) Bub1-dependent phosphorylation of histone H2A on Thr120 (H2A-Thr120ph) (Xu et al., 2009). In details, the Bir domain of Survivin recognizes phospho-histone H3 (Thr3), allowing its recruitment on chromatin. Meanwhile, in centromeric nucleosomes, histone H2A is phosphorylated by Bub1, on Thr 120, in turn, recruiting Shugoshin that interacts with Borealin, a CPC member. The concomitance of the two phosphorylations on centromeres triggers the specific recruitment of the CPC (Figure 10) (Campbell and Desai, 2013; Kelly et al., 2010). Simultaneously, Mps1 activity enhances H2A-T120ph and is also critical for Shugoshin recruitment to centromeres, thereby promoting aurora B centromeric localization (van de Walls et al., 2012). As shown in Figure 10, when fully activated, aurora B exercised a retro control on Haspin. (Wang et al., 2011)

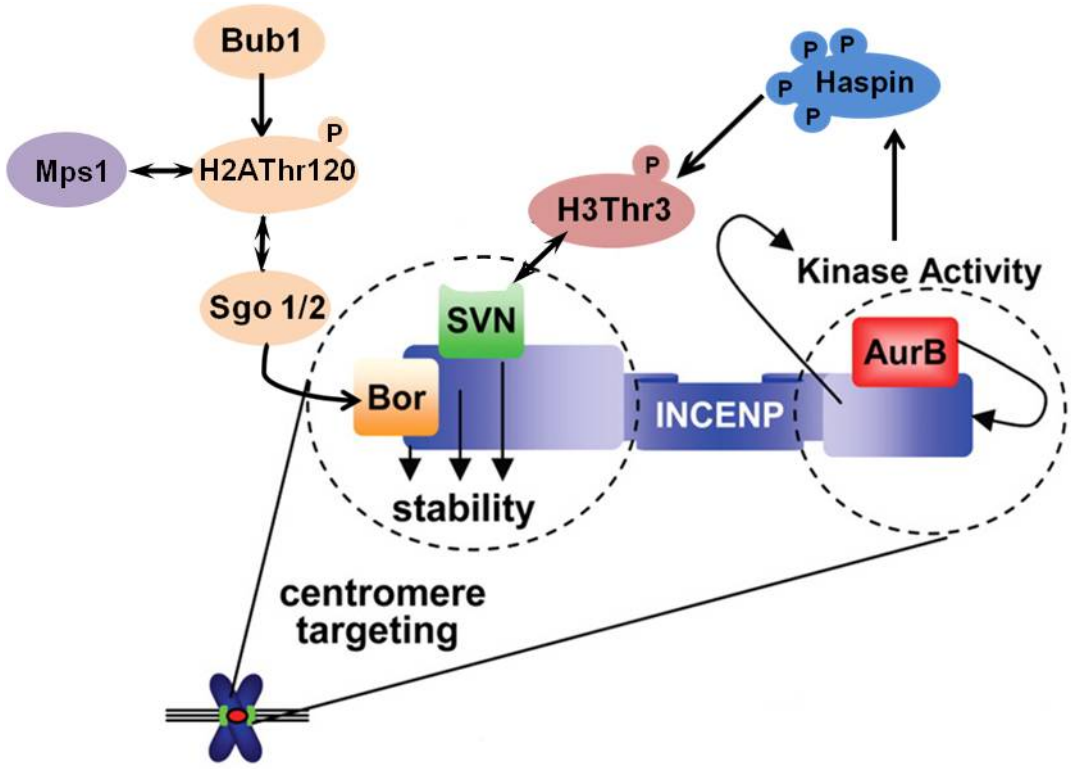

Figure 10: Recruitment of the CPC on centromere. Concomitance of the phosphorylations of histone H3 on Thr3 (H3Thr3P) and histone H2A on Thr120 (H2AThr120P) allows the recruitment of the CPC at the centromere. Survivin (SVN) interacts directly with chromatin whereas the stabilisation is provided by the interaction of Borealin (Bor) with Shugoshin (Sgo1/2). Within the CPC, aurora B is fully activated and exercises a retro control on Haspin (modified from Xu et al., 2009).

Interestingly, aurora kinase B activity is also enhanced through priming of its substrates. A recent report shows that the phosphorylation of Survivin on Ser20 by Plk1 also activates aurora B in centromeres (Chu et al., 2011). Moreover, the full CPC activation requires two cofactors: the telophase disc 60 protein (TD-60) and microtubules (Rosasco-Nitcher et al., 2008; Wang et al., 2011).

Besides, there are two other kinases directly involved in the activation of aurora B: the Checkpoint kinase 1 (Chk1) and Tousled-like kinase 1 (Tlk1). Chk1 kinase is a major component of DNA damage and DNA replication checkpoints. It was recently found to phosphorylate aurora B on Ser331 during unperturbed pro-metaphase and during spindle disruption by Taxol. This phosphorylation is required for optimal phosphorylation of INCENP on its TSS sequence, a motif involved in aurora B full activation (Petsalaki et al., 2011). Related to Tlk1, in *C. elegans*, it is a substrate and activator of AIR-2 (the *C. elegans* homolog of aurora B) and this activation requires the presence of the *C. elegans* homolog of INCENP (ICP-1) (Han et al., 2005). However, evidence for a role of Tlk1 in aurora B activation in mammal is unknown at the moment.

Aurora B is involved in chromosome condensation and cohesion, microtubule-kinetochore attachment, mitotic spindle checkpoint regulation, chromosome segregation and cytokinesis.

- Chromosome condensation: Condensation of chromosome into compact structures is a prerequisite for the accurate segregation of chromosomes and is driven by Condensin complexes (Condensin I and II in human) (Takemotor et al., 2007; Hirano, 2006). Depletion of aurora B impairs the localization of Condensin I on chromosomes and consequently, chromosome condensation (Lipp et al., 2007) showing the role of aurora B in this process. Moreover, aurora B is a well-known primary mitotic kinase responsible for the phosphorylation of histone H3 on Ser10 and Ser28 during mitosis (Baek, 2011). This phosphorylation has long been thought to regulate chromosome condensation during mitosis (Wei et al., 1999; Cerutti and Mollano, 2009). Other reports demonstrated that histone H3 phosphorylation is only required for the initiation rather than the maintenance of condensed state of chromatin (Van Hoosser et al., 1998); and is also dispensable for meiotic chromatin condensation (Schmitt et al., 2002). Therefore, the role of aurora B and histone H3 phosphorylation in chromosome condensation is still controversial and needs further studies.

- **Chromosome cohesion**: During S phase DNA is replicated then, it condenses into chromosomes in G2. Therefore the two sister chromatids require a cohesion system to keep

together. This is accomplished by a ring-like Cohesin complex that consists of Smc1, Smc3, Scc/Rad21 and Scc3/SA (Nasmyth and Haering, 2009). The cohesin complex is released from chromatin in two steps: along chromatid arms in prophase and finally, at centromere in anaphase (Remeseido and Losada, 2013). Aurora B is reported to promote the chromosome recruitment of separase for the complete removal of cohesin, in anaphase (Yuan et al., 2009).

- **Bi-oriented microtuble-kinetochore attachment**: In order to ensure the proper chromosome segregation, microtubules must attach sister kinetochores to opposite sides of the mitotic spindle (bi-orientation). Errors such as syntelic attachments (both kinetochores bind microtubules from the same pole); merotelic attachments (one kinetochore attaches to both mitotic spindle poles) or monotellic attachments (single attachment of one kinetochore in two sister chromatids) exert the less tension on kinetochore-to-pole connection (Figure 11). Aurora B triggers the phosphorylation of kinetochore substrates in a tension dependent manner and thereby, facilitates the bi-orientation of kinetochore-spindle pole connection. Studies in yeast showed that aurora B/Ipl1 corrects syntelic attachment by the phosphorylation of an important kinetochore-microtubule-capture factor (Dam1-ring complex), which facilitates the turnover of kinetochore-microtubule attachments (Keating et al., 2009). Similarly, the phosphorylation of Ndc/Hec1 in KMN by aurora B is observed to increase in the merotelic attachment correction (DeLuca et al., 2006). Another study shows the enrichment of MCAK, at points of merotelic attachment, in an aurora B-dependent manner. The kinesin-13 microtubule depolymerase MCAK is phosphorylated and could then depolymerize the improperly attached microtubules (Knowlton et al., 2006). However, how aurora B senses tensions for correction is still controversial to date. Using FRET (fluorescence resonance energy transfer)-based biosensors (with labeled centromere- and kinetochore-specific substrates), Liu and Lampson (2009) proposed a mechanism by which tensions can be converted into biochemical changes in the cell, through modulation of the spatial separation of aurora B from its substrates. In weak tension, at the inner centromere, aurora B is close to its kinetochore substrates and induces their phosphorylation for correcting wrong attachments. Conversely, when spindle microtubules pull bi-oriented sister kinetochores in opposite directions, away from the inner centromere, kinetochore substrates are dephosphorylated favoring the microtubule attachment stability.

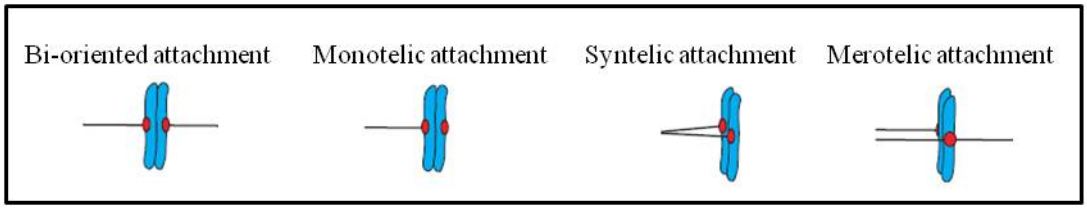

Figure 11: The model of kinetochore-microtubule attachments. Aurora B corrects abnormal mis-attachments such as monotelic, syntelic or merotelic attachments and induces bi-oriented attachments (Cimini and Degrasssi, 2005).

- Mitotic spindle checkpoint regulation: Aurora B also plays a role for spindle assembly checkpoint (SAC). It activates the spindle checkpoint in response to a lack of kinetochore tension and prevents the activation of APC/C until proper bipolar spindle attachments are formed (Hauf and Watanabe, 2004). Aurora B targets two proteins for this regulation. Actually, the failure of microtubule stabilization caused by depletion of the chromosomal passenger complex was rescued by co-depletion of the microtubule-depolymerizing kinesin MCAK, whose activity is negatively regulated by aurora B (Sampath et al., 2004) and the microtubule-destabilizing protein Stathmin/Op18 activity (Gadea and Ruderman, 2006).

- **Cytokinesis**: At anaphase onset, aurora B relocalizes to both the central spindle and the cell cortex to regulate cleavage furrow formation (Bringmann, 2005; Yabe et al., 2009). Aurora B inactivation induces the delocalization of ZEN4/MKLP1, which is necessary for formation of the central spindle during anaphase (Guse et al., 2005). Further, aurora B phosphorylates Desmin, a protein of the cleavage furrow, leading to the destabilization of intermediate filaments, which are essential for the last stage of cytokinesis (Kawajiri et al., 2003).

Moreover, aurora B also phosphorylates MgcRacGAP in the midbody, at Ser387. This modification induces the conversion of MgcRacGAP to a RhoGAP, which is required for the contractile ring formation and the proper cytokinesis (Minoshima et al., 2003). Finally, aurora B is demonstrated to participate in the NoCut checkpoint as referred to in 1.3.3 above.

In summary, aurora B plays key roles during mitosis and its activity is also regulated through degradation. Related to the degradation of aurora B from metaphase chromosome arms, it is indicated to require a Cullin 3 (Cul3)-based E3 ubiquitin ligase. KLHL9 and KLHL13 form a complex with Cul3, which is necessary for ubiquitination of aurora B (Sumara et al., 2007). Similarly, the degradation of aurora B at the central spindle is also through Cul3-dependent ubiquination when bound to KLH21 (Maerki et al., 2009). Moreover, in cytokynesis, aurora B interacts with APC/C through the Cdc27 subunit, it is ubiquitinated and then degraded by a proteosome pathway (Nguyen et al., 2005).

2.3.3. Aurora C

Aurora C is the least studied member of the aurora kinase family. Unlike aurora A and B, it is only present in germ cells and is involved in male meiotic cytokinesis (Dieterich et al., 2009). As reported, aurora C localizes on chromosomes from prophase to metaphase and at the midbody from anaphase to telophase, like aurora B. Exceptionally, in tumor cells, it may be present at centrosome, in G2, like aurora A does (Dutertre et al., 2005). Aurora kinase C expression appears to be testis specific and this kinase is required for spermatogenesis and male fertility in mice (Kimmins et al., 2007). Tsou et al. (2011) found that the overexpression of aurora C, localized in centromeric region, decreases aurora B level resulting in tumourigenicity of epithelial cells. Additionally, aurora C is also reported to interact and phosphorylate Ser288 of TACC1, at midbody, for cytokinesis (Gabillard et al., 2011).

2.4. COORDINATING ACTION OF AURORA WITH OTHER KINASES IN MITOSIS

During mitosis, aurora kinases have interaction with other kinases for enhancing their activity. The understanding of this functional crosstalk might help us to well-approach the development of new anti cancer drugs.

First, we could mention Polo-like kinases (Plk), a serine/threonine kinase family. Mammalian polo-like kinases include Plk1 (*Xenopus* Plx1), Plk2/Snk (*Xenopus* Plx2), Plk3/Prk/FnK (*Xenopus* Plx3), Plk4/Sak and Plk5. Other species have only one form of Plk: Polo (*Drosophila*), Plo1 (*Schizosaccharomyces pombe*) and Cdc5 (*Saccharomyces cerevisiae*). Among them, Plk1 has been the most studied. Besides Cdks and aurora kinases, Plk1 is also responsible for cell-cycle-dependent protein phosphorylations, which has been implicated in the regulation of centrosome maturation, bipolar spindle assembly, sister chromatid cohesion, activation of APC/C, and initiation of cytokinesis (Lowery et al., 2005; Lénárt et al., 2007; Petronozki et al., 2008). Aurora A, together with its cofactor hBora, was found to initiate the phosphorylation of Plk1, on Thr210, at G_2/M transition which relates to its localization and activity during mitosis. In turn, Plk1 and Cdk1 induce the phosphorylation of hBora and target it for the proteosomal degradation (Chan et al., 2008; Seki et al., 2008). Interestingly, the coordination of aurora A and Plk1 activates Cdk1-cyclin B that is necessary for recovering from cell cycle arrest induced by DNA damage, and achieving a synergic effect (Zou et al., 2011). Thus, the combined use of aurora A and Plk1 inhibitors after chemotherapy or radiography is potent in anti-cancer therapy.

Meanwhile, the Plks activity at kinetochore requires aurora B for its activation. Their collaboration regulates the kinetochore-microtubule attachments. Aurora B phosphorylates Polo/Plk1 at centromeres, relocalizing it from centromeres to kinetochores and promoting the detachment of kinetochore without tension. When tension stretches kinetochores, Polo/Plk on the outer kinetochore, moves away from aurora B presenting on the inner centromere, leading to the Polo/Plk dephosphorylation and thus the stabilization of attachment (Archambault and Carmena, 2012). Besides, Plk1 also indirectly enhance aurora B activity by phosphorylating its substrates. Briefly, the phosphorylation of Survivin on Ser20 by Plk1 also activates aurora B activity in the centromere (Chu et al., 2011).

Secondly, Lats kinases are mostly known for their participation in the Hippo signalling cascade, which controls cell proliferation and apoptosis but they are also pivotal effectors of mitotic progression, including mitotic exit and cytokinesis (Bothos et al., 2005; Yabuta et al., 2007; Pan, 2010). Yabuta et al (2007) have proposed that aurora kinases A and B are linked by the large tumor suppresors 1 and 2 (Lats1 and Lats2). Actually, aurora A was demonstrated to phosphorylate Lats2 on Ser83 and Ser380 during mitosis. The Ser380-phosphorylated Lats2 protein colocalized at the central spindle with aurora B and in turn, aurora B is phosphorylated by Lats1. The Lats1/2 kinases "connect" the two aurora kinases to form an aurora A-Lats1/2-aurora B axis that ensures accurate chromosome segregation. Moreover, the expression of mitotic regulators such as aurora B and Plk1 is suspected to be controlled by Lats2, thus indicating multiple interconnections between Last and mitotic kinases.

2.5. AURORA KINASE ROLE IN TUMOR DEVELOPMENT

Because aurora kinases play essential roles during mitosis, changes in their signalling could result in mitotic errors and have been closely associated with chromosomal aneuploidy and genomic instability in cancer (Dar et al., 2010). Several studies reported the involvement of aurora kinases in cancer progression and even development.

Human aurora A gene is located on chromosome 20q13.2, which is a region frequently altered in human cancers. In fact, overexpression of aurora kinase A was reported in many human cancers such as breast, glioblastoma, ovarian, cervical, colon, lung and pancreatic cancer (Katayama et al., 2003). Recently, the role of aurora A in tumorigenesis has been well-studied.

In non-transformed cells, aurora A is high expressed in G2/M transition for centrosome and mitotic spindle functions and then, it is degraded at cytokinesis. Meanwhile, in tumor cells,

it may be diffusely detected in all the cytoplasm, which allows the over-phosphorylation of substrates during G1/S or the wrong targeting of cytoplasmic proteins, resulting in neoplastic transformation. Moreover, overexpression of aurora A also affects the G_2 checkpoint; thereby, cells with DNA damage still enter in mitosis and perform cell division. Additionally, the SAC can be perturbed allowing cell cycle to continue despite of improper mitotic spindle (Warren et al., 2009).

The defects in centrosome maturation related to aurora A function have been described in breast, cervical and prostate carcinomas (Pihan et al., 2003). Centrosome amplification inducing multipolar mitotic spindle has been reported in head and neck cancers (Tasuka et al., 2009). Additionally, the abnormal mitotic spindles cause cytokinesis failure and as a consequence, polyploid cells are present which likely result in aneuploidy (Meraldi et al., 2002). In turn, aneuploid cells still undergo cell division due to G1 checkpoint inactivation. The abolishment of G_1 checkpoint can be caused through a p53 pathway. Aurora A, in fact, phosphorylates p53, a tumour suppressor protein, at the serine 215 residue, inducing an inactivation of its transactivation activity (Liu et al., 2004) and at the serine 315 residue, facilitating MDM2-mediated p53 degradation (Katayama et al., 2004).

Besides, in human ovarian and breast cancers, aurora A is found to bind c-Myc sites on the telomerase promoter, inducing its transcription and thus increasing its expression as well as its activity (Yang et al., 2004). Furthermore, the overexpression of aurora A potentiates oncogenic Ras-induced transformation suggesting that it may be responsible for oncogenic growth of cancer cells (Tasuka et al., 2009). Therefore, aurora A may play a role in malignant transformation and in tumor growth.

Based on these strong lines of evidence, the enthusiasm of exploring anticancer therapeutic targets has initially been focused on aurora A, but recent studies have demonstrated that aurora B is also eligible. Aurora B is located on chromosome 17p13.1, in the close vicinity with p53 gene. Aurora B can directly phosphorylate p53, resulting in the loss of p53 activity, thereby accelerating tumorigenesis in transgenic mice (Lacroix et al., 2006). Although aurora B has not been mentioned as an oncogene, its overexpression is also found in several cancers such as hepatocellular carcinoma (Aihara et al., 2010, Lin et al., 2010), gastric (Honma et al., 2013), multiforme glioblastoma (Zeng et al., 2007), epithelial ovarian cancer (Chen et al., 2009), malignant mesothelioma (Lopez-Rio et al., 2006), hematological malignancies (Ikezoe et al., 2007)… More interestingly, the overexpression of aurora B, but not of aurora A,

might contribute to DNA aneuploidy in gastric cancers by promoting chromosomal instability (Honma et al., 2013).

The inhibition of aurora B decreases the tumorigenic potency in many cases suggesting that it is an attractive target in anti-cancer therapy. For instance, using aurora B-null liver cells, a delayed DNA replication and a premature mitotic exit were observed, that could be explained by $p21^{Cip1}$ pathway (Trakala et al., 2013). In the absence of aurora B, the $p21^{Cip1}$, a Cdk inhibitor, is induced strongly and Cdk1 is diminished. Since Cdk1 activity is reduced, cells may eventually exit from the metaphase with high level of cyclin B as an adaptation to the SAC. As a result, the formation of tumors in the liver is hampered. In the other view, a recent study proposed a new pathway in using aurora B to prevent tumor growth (Sharma et al., 2013). Aurora B is confirmed as a target downstream of ^{V600E}B-Raf in the MAP kinase signaling cascade relating to cell growth. ^{V600E}B-Raf is a popular target in melanoma cancer treatment but limited by drug resistance. Therefore, the inhibition of aurora B that is described to reduce the oncogenic growth of melanoma cells is a good alternative (Bonet et al., 2012; Sharma et al., 2013).

The involvement of aurora C in carcinogenesis has been the least explored among aurora kinases. A few studies showed that aurora C was overexpressed in colorectal, breast and prostate cancer (Sasai et al., 2004). Furthermore, the phenotype obtained upon Aurora C overexpression (polyploid cells containing abnormal centrosome numbers) is aggravated in the absence of a functional p53 like in HeLa cells (Dutertre et al., 2005). These data suggested that aurora C might also be a target for cancer treatment, especially in the presence of mutated p53.

In summary, the involvement of aurora kinases in tumor development makes them considered as potential targets in anticancer chemotherapy. Recently, a number of aurora kinase inhibitors have been developed and have attracted much attention from pharmaceutical companies. Further informations will be discussed in the next chapter.

CHAPTER 3: AURORA KINASE INHIBITORS AND CANCER THERAPY

Even though much effort has been made in decreasing cancer mortality, cancer is still one of the major causes of death over the world. Up to date, anti-cancer therapy mainly relies on surgery, radiation therapy and chemotherapy, which can be used alone or in combination. Both surgery and radiotherapy are only local treatments and cannot control the metastatic tumors; whereas, chemotherapy is a systemic therapy in cancer treatment. Most chemotherapeutic anti-cancer drugs used in the clinic today target the cell cycle in order to inhibit the over-proliferation state of tumor cells and then inducing apoptosis (Lee and Schmitt, 2003).

Classical anti-cancer drugs interfere with DNA synthesis, DNA damage, or inhibit the function of the mitotic spindle. Among them, microtubule-binding drugs are the most exceptionally successful chemotherapeutic compounds currently used in the clinic.

3.1. MICROTUBULE BINDING ANTI-CANCER DRUGS

Traditional antimitotic chemotherapeutics, including taxanes and various Vinca alkaloids, are currently used to treat patients with breast, ovarian and non-small cell lung cancers (Lister-Sharp et al., 2000; O'Shaughnessy et al., 2013; Socinski et al., 2013; Ueda et al., 2013). Both types of drugs create unattached kinetochores in mitosis by altering microtubule dynamics and cause long-term mitotic arrest.

Vinca alkaloids are a group of mitotic and spindle inhibitors that were originally extracted from the periwinkle plant *Vinca rosea*. Among them, only four drugs (vinblastine, vincristine, vinorelbine and vindesine) are approved for clinical uses in US and Europe. They bind to β-tubulin and disrupt the microtubules formation leading to the metaphase arrest (William et al., 2000). Their actions are highly dependent on the drug concentration. At relatively high concentrations, they cause microtubule depolymerization, dissolve spindle microtubules and arrest cells at mitosis. At even higher concentrations (milliMolar), they induce the aggregation of tubulin into paracrystalline arrays. In contrast, at low concentrations, the vinca alkaloids suppress microtubule dynamics without depolymerizing spindle microtubules, but remain able to arrest mitosis and induce apoptosis (Zhou and Giannakakou, 2005). Vinca alkaloids are used to treat both hematological malignancies like leukemias and lymphomas and solid tumors of various organs like breast, ovary, testis, lung, colon, central nervous system, melanomas as well as Kaposi sarcomas.

Like Vinca alkaloids, taxanes are successful chemotherapeutic agents. The taxane paclitaxel/taxol is derived from the Pacific yew tree, *Taxus brevifolia*, and docetaxel/taxotere is a semisynthetic derivative of a compound from the European yew tree, *Taxus baccata*. The former was approved for anticancer treatment in 1992, and the latter, in 1996. Both agents stabilize microtubules by binding to β-tubulin, practically lining the inside of microtubules (Jordan and Wilson 2004). Interestingly, the effects of taxol or taxotere on additional cellular targets enhance their anticancer activity by promoting apoptosis and inflammation and inhibiting angiogenesis. Resistance mechanisms to taxol include mutation of the paclitaxel binding site of β-tubulin, lowering stability of microtubules especially as the wild type allele is lost (Wang *et al.* 2005, Hari *et al.* 2006). Taxanes are employed against a broad range of cancers: the breast, ovary, prostate, non small-cell lung, head and neck, esophagus, stomach, bladder and Kaposi's sarcoma and they are also used when other chemotherapy regimens have failed.

However, the drawback of these drugs is that they also inhibit the function of microtubules in normal cells. Lowering the blood counts and inducing peripheral neuropathies are the most common unwanted side effects. Therefore, current attempts not only try to improve novel anti-microtubule drugs, but also to develop drugs towards novel mitotic targets such as mitotic kinesins and mitotic kinases.

3.2. MITOTIC KINESIN TARGETING DRUGS

Kinesins are a large superfamily of microtubule motor proteins that bind and move towards the plus end of microtubules in an ATP-dependent manner. To date, approximately 45 unique kinesin superfamily genes have been identified in mammals, them self divided into 14 families. They participate in intracellular transport of vesicles and organelles as well as various mitotic functions such as centrosome separation, spindle assembly and cytokinesis (Wordemann, 2010).

Among kinesins, the mitotic kinesin motor protein Eg5/KSP (kinesin spindle protein) is responsible for the establishment of spindle bipolarity by moving the duplicated centrosomes to opposite sides of the cell (Blangy *et al.* 1995). Inhibition of Eg5/KSP prevents centrosome separation leading to the formation of a monoastral spindle, which activates the spindle checkpoint and results in mitotic arrest. Upon prolonged treatment, cells escape from mitotic arrest and initiate apoptosis. Inhibition of Eg5/KSP is expected to be specific for mitosis and, thus, effective solely in proliferating cells. Therefore, Eg5/KSP inhibitors should not have the side effects associated with microtubule binding drugs. Especially, Eg5/KSP inhibitors are

effective even in taxol resistant cancer cells (Tao et al., 2007, Woessner et al., 2009). These data showed that kinesin proteins are new promising alternatives for replacing traditional anti-microtubules drugs.

Monastrol was the first Eg5/KSP inhibitor to be identified (Mayer *et al.* 1999). Subsequently, more potent inhibitors like KSP-IA (Tao et al. 2005), Ispinesib (SB-715992 and its derivative SB-743921, GlaxoSmithKline; Davis et al. 2006), MK-0731 (Merck; Stein et al. 2006) and ARRY-520 (Array Biopharma; Woessner et al. 2007) were developed and exhibited potent anti-proliferative efficacy in hematological tumors, breast and ovarian cancers, in clinical trials.

3.3. KINASE TARGETING DRUGS

Because of the drawbacks of microtubule targeting agents, many kinases, overexpressed in several types of cancer, have been identified as new potential targets in the development of anti-cancer drugs. The first validation of small molecules targeting the ATP-binding site of a kinase, in cancer therapy, was obtained with Bcr-Abl inhibitors.

3.3.1. Bcr-Abl inhibitors - the first kinase inhibitor in human cancer treatment

Development of chronic myeloid leukemia (CML), a lethal hematopoietic stem cell malignancy, is characterized by t(9;22)(9q34.1)(22q11.2) chromosomal translocation leading to the production of the fusion oncogene Bcr-Abl. This oncoprotein is a constitutively active tyrosine kinase that perturbs numerous signal transduction pathways, causing uncontrolled cell proliferation and inducing apoptosis (Jabbour et al., 2007). Discorvered in 1992, Imatinib (Gleevec), the first generation of Bcr-Abl tyrosine kinase inhibitors, was first approved in the treatment of human cancer, in 2001. Imatinib is an ATP competitive inhibitor that prevents cell proliferation. More importantly, Imatinib targets specifically Bcr-Abl; hence it only inhibits the development of peculiar cancer cells, but do not kill all dividing cells. With the encouraging results in clinical trials, great hopes were opened in the use of this new target in anti-cancer therapy (Manly et al., 2002) and highlighted kinases as cancer targets.

Despite the obvious benefits of Imatinib over prior treatments, some patients may be intrinsically resistant to it, whereas others may acquire resistance during treatment. Resistance to Imatinib occurs at an annual rate of approximately 4% in patients with newly diagnosed CML and more often, in advanced-phase disease (Jabbour et al., 2007). In order to overcome drug resistance, many second generation of Bcr-Abl targeting drugs have been developed such as Dasatinib (BMS-345825) and Nilotinib (AMN107). Dasatinib is a multi-target kinase

inhibitor of five critical oncogenic enzymes: Bcr-Abl, Src, c-Kit, platelet-drived growth factor receptor (PDGFR) and ephrin A receptor kinases. Meanwhile, Nilotinib is a multi-target inhibitor of Bcr-Abl, PDGF and c-Kit receptors. Both compounds demonstrated the comparative effective clinical activity in chronic myeloid leukemia patients (Signorovitch et al., 2011) and have been FDA approved for patients with resistance to Imatinib. They are being currently studied further in response to other tumors.

3.3.2. Mitotic kinase inhibitors

a. Cyclin dependent kinase (Cdk) inhibitors

Cdks are deregulated in several human cancers because of various genetic and epigenetic events that affect their regulatory pathways (Lapenna et al., 2009). Their overall effect is the loss of checkpoint control integrity, causing uncontrolled proliferation. Therefore, targeting Cdks probably limits tumor cell division. Moreover, the improved understanding of how Cdks regulate DNA damage and the repair pathway opens a potential approach by combining Cdks inhibition and DNA-damaging agents for the treatment of cancer (Johnson and Shapiro, 2010)

Many Cdk inhibitors have been developed and are undergoing clinical trials (reviewed by Lapenna et al., 2009 and listed in table 4). However, until now, no Cdks inhibitor has reached the marketplace (Galons et al., 2013) suggesting that they need further investigations.

b. Polo-like kinase (Plk) inhibitors

The members of the Plk family of serine/threonine kinases function in centrosome maturation, Cdk1 activation at the G_2/M transition, spindle assembly, regulation of the APC/C, chromosome segregation, and cytokinesis (Strebhardt and Ullrich, 2006, van Vugt and Medema, 2005). The development of Plk inhibitors for chemotherapy focused attention on Plk1 because it is often overexpressed in a variety of human cancers (Takai et al. 2005) and its function-targeting agents induce mitotic arrest and then, cell death (Guan et al., 2005; Liu and Erikson, 2003; Sumara et al., 2004; Schmidt et al., 2007; van Vugt et al., 2004).

Two Plk1 inhibitors are in clinical trials and many others are currently in preclinical phase. One of the most common Plk1 inhibitors is BI2536 (Boehring Ingelheim). Results showed that BI2536 had anticancer activity in murine xenograft models especially solid tumors (Mross et al., 2005). It is currently in phase II of clinical trial for various tumor indications. Another Plk1 inhibitor is GSK461364A (GlaxoSmithKline), an ATP-competitive inhibitor. GSK461364A is currently in phase I for advanced solid malignancies (Olmos et al., 2013).

Inhititors (Company)	IC50 Invitro	Clinical trial
SNS-032 (Sunesis)	CDK9 (IC50 = 4 nM) CDK7 (IC50 = 38 nM) CDK2 (IC50 = 62 nM)	•Phase I: B-lymphoid malignancies and advanced solid tumours
ZK-304709 (Bayer Schering Pharma AG)	CDK2 (IC50 = 4 nM) CDK9 (IC50 = 5 nM) CDK1 (IC50 = 50 nM) CDK4 (IC50 = 61 nM) CDK7 (IC50 = 85 nM)	• Phase I: advanced solid tumours
PD-0332991 (Pfizer)	CDK4 (IC50 = 11 nM) CDK6 (IC50 = 16 nM)	• Phase I: advanced cancer and mantle cell lymphoma. •Phase I–II: multiple myeloma (in combination with bortezomib and dexamethasone), hormone receptor-positive advanced breast cancer (in combination with letrozole)
AT-7519 (Astex)	CDK9 (IC50 < 10 nM) CDK5 (IC50 = 13 nM) CDK2 (IC50 = 47 nM) CDK4 (IC50 = 100 nM)	• Phase I: advanced or metastatic solid tumours, or refractory non-Hodgin leukemia (NHL)
P276-00 (Nicholas Priomal)	CDK9 (IC50 = 20 nM) CDK4 (IC50 = 63 nM) CDK1 (IC50 = 79 nM) CDK2 (IC50 = 4 nM) CDK7 (IC50 = 85 nM)	• Phase I–II: multiple myeloma, mantle cell lymphoma, head and neck cancers, and cyclin D1-positive melanoma
R-547 (Hoffmann LaRoche)	CDK 1,2,4: Ki=1-3 nM	• Phase I: advanced solid tumours and trial completed (2008)
Flavopiridol, (Sanofi–Aventis)	CDK9 (IC50 = 3 nM) CDK4 (IC50 = 20-40 nM) CDK6 (IC50 = 60 nM) CDK1 (IC50 = 30-400 nM) CDK2 (IC50 = 100 nM) CDK7 (IC50 = 110-300 nM)	•Phase I–II: various cancers, including leukaemia, multiple myeloma, lymphoma, sarcoma and solid tumours (as a single agent and in combination with DNA-damaging or other cytotoxic drugs)
Roscovitine, also known as CYC202 and seliciclib (Cyclacel)	CDK2 (IC50 = 220 nM) CDK9 (IC50 = 230 nM) CDK5 (IC50 = 270 nM) CDK1 (IC50 = 330 nM) CDK7 (IC50 = 800 nM)	• Phase I–II: NSCLC •Trials completed (2009); when administered at 800 mg twice daily for 7 days, it elicited limited tumor responses and dose-limiting toxicities (fatigue, skin rash and hypokalaemia)

Table 4: Second-generation CDK inhibitors in confirmed clinical trials. Cdks inhibitors exhibit high activity towards *in vitro* Cdks and anti-proliferative potency in a variety of solid tumors and leukemia. (reviewed in Lapenna et al., 2009)

3.4. AURORA KINASE INHIBITORS

As mentioned in chapter 2, aurora kinases are key regulators of mitosis that are responsible for centrosome function, mitotic entry, spindle assembly, chromosome segregation, microtubule dynamics, spindle checkpoint and cytokinesis. Furthermore, they are frequently overexpressed in various human tumors, and such an overexpression correlates with a poor prognosis for patients, exemplifying their significance for tumor formation and progression. Therefore, aurora kinases have focused attention as potential targets in the development of anticancer drugs.

Because the domain kinase of aurora kinases are highly homologous, it is difficult to obtain aurora kinase inhibitors that are specific for one kinase. Consequently, most aurora kinase inhibitors in the market target multiple aurora kinase members. A series of pan-aurora kinase inhibitors are developed and undergoing in clinical trials as indicated in Table 5.

Among pan aurora kinase inhibitors, Tozasertib (VX-680, MK-0457) was the first aurora kinase inhibitor to be tested in clinical trials. It targets three aurora kinases *in vitro* with IC50 of 0.7; 18 and 4.6 nM for A, B and C, respectively (Harrington et al., 2004). Preclinical tests reveal that it inhibits the tumor growth in prostate (Lee et al., 2006), thyroid (Arlot-Bonnemains et al., 2008), ovarian (Lin et al., 2008), and oral squamous (Pan et al., 2008) cancer cell lines with IC50 values ranging from 15 to 130 nM. It induces the accumulation of cells arrested in a pseudo-G_1 state with a 4N DNA content or the accumulation of cells with >4N DNA content, the latter population representing cells that exit mitosis and subsequently proceed through S phase in the absence of cell division. Continuous proliferation in the presence of aberrant mitosis and failed cytokinesis presumably result in cell death (Gizatullin et al., 2006). Tozasertib was reported to induce apoptotic cell death in aurora A-high primary leukemic blasts, but not in aurora-A-low acute myeloid leukemia (AML) or in normal bone marrow mononuclear cells (BMMCs); this suggests its potentially therapeutic use for some leukemia patients (Huang et al., 2008). More interestingly, Tozasertib showed *in vitro* activity against Bcr-Abl bearing the Imatinib-resistant T315I or the Dasatinib-resistant V299L mutations (Giles et al., 2007; Young et al., 2006), opening the great hopes for these patients resistant to the former inhibitors.

The same positive effect towards the Imatinib-resistant cell lines harboring the T315I Brc-Abl mutation was reported upon PHA-739358 and AT-9283 treatment, two other pan aurora kinase inhibitors (Gontarewicz et al., 2008; Tanaka et al., 2008). The safety, tolerability

and preliminary efficacy of these compounds are currently evaluated in Phase I/II clinical studies.

Cells invalidated by siRNA for either aurora A or aurora B or both in combination, exhibited biological consequences and potential clinical outcomes, in accordance with the different functions of each kinase (Warner et al., 2006). In all cases, aurora kinase inhibitors lead to apoptosis and cell death. However, a rapid induction of apoptosis is observed in the cells without aurora A, whereas cells without aurora B show a gradual induction of apoptosis (Warner et al., 2006). The question is which aurora kinase is the best drugs target? Preclinical results demonstrated that targeting aurora A rather than aurora B is effective for pancreatic cancer cells (Warner et al., 2006). In contrast, aurora B is proposed for colon cancer treatment (Girdler et al., 2006). This demonstrated that the alternative role of auroras kinases depends on the type of tumor cells. Therefore, many specific aurora kinase inhibitors were developed and are undergoing clinical tests, as listed in Table 5. More interestingly, some pan aurora inhibitors such as upon ZM447439, with equal potency to aurora A and B in *in-vitro* kinase assay, exhibited an obvious aurora B inhibition phenotype in colon cancer cells (Girdler et al., 2006). Similar observations were maid upon AT9283 treatment in aggressive B non-Hodgkin lymphomas (Qi et al., 2012). This suggests that aurora B currently seems an attractive anti-cancer drug target.

From this hypothesis, our group started to search for aurora kinase inhibitors. A high throughput screen was performed on the French patrimonial library (around 10000 molecules). The test was based on an *in vitro* assay with recombinant aurora A catalytic domain and Histone H3 as substrate. The kinase and the substrate were expressed in *E. coli* and purified to homogeneity. The assay was run in the presence of a limited amount of ATP. The test started by the addition of the enzyme. The molecules were present at the concentration of 15 µM and Staurosporin was used as positive control. Remaining ATP was monitored by luminescence. The hits were confirmed at the concentration of 1.5 µM. The patrimonial library was formerly screened for CK2 inhibitors, we therefore withdrawn the common hits inhibiting both kinases and focused on the new hits. We realized that among them, benzo[e]pyridoindoles were over-represented (Hoang et al., 2009). These molecules belong to the Institut Curie library and were synthesized by the Dr Chi-Hung Nguyen at CNRS (Orsay). Other hits were identified in the NIH library but we decided to focus our attention on the benzo[e]pyridoindole family.

Among this family, the most potent hit was recalled C1 (Figure 12A) and was evaluated *in vitro* as well as in cells. This work was formerly ~~as~~ described in HOANG-Nhung's thesis and in the publication (Hoang et al., 2009).

C1 was found to be an ATP-competitive inhibitor with a sharp selectivity in the kinome (Hoang et al., 2009). Within the aurora kinase family, it exhibited a broad specificity with a slight prevalence for aurora B (Figure 12 B). The potency of C1 towards aurora kinases was found to be similar to that of VX-680, the reference aurora kinase inhibitor (Cohen et al., 2007).

Moreover, the *ex vivo* assays conducted in HeLa cells showed that C1 inhibited the activity of Aurora B mimicking the phenotype obtained after siRNA suppression of aurora B expression, and prevented cell division as well as delaying the development of tumor xenografts. These data confirmed that aurora B is a potential target for preventing cell proliferation and that benzo[e]pyrydoindoles are a new family of aurora kinase inhibitors.

(A)

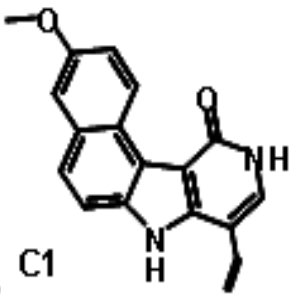

C1

(B)

Kinase	IC50 of C1 nM	IC50 of VX-680 nM
Aurora A	**61**	13
Aurora B	**29**	37
Aurora C	**124**	117

Figure 12: The structure of the hit aurora B inhibitor C1 (A) and the *in-vitro* IC50 towards aurora kinases of C1 and VX-680 (B).

3.5. PERSPECTIVE OF ANTI-CANCER THERAPY WITH AURORA KINASE INHIBITORS

The preclinical and clinical findings on the efficiency of aurora kinase inhibitors towards the growth of tumor cells, as listed in Table 5, demonstrated that aurora kinase inhibitors could be potential anticancer drugs in the future.

In anti-cancer chemotherapy, we are presently facing drug resistance in patients after prolonged treatment. Mutations of the oncogenic tyrosine kinase Bcr-Abl, in leukemia, is such an example of resistance upon inhibitor treatment. Luckily, as mentioned above, aurora kinase inhibitors have shown cross-reactivity with the mutated kinase and potency against drug resistant Bcr-Abl, opening great prospects in the treatment of leukemia patients.

In order to improve the anti-proliferative activity of the aurora kinase inhibitors in the clinic, the combined therapy with cytotoxic anticancer agents, radiotherapy, or other targeted agents might be a solution in the future. Many recent preclinical studies have proven for this strategy. For instance, the aurora A inhibitor (MLN8237) enhanced vincristine or docetaxel chemosensitivity in aggressive B-cell non-Hodgkin lymphoma (B-NHL) (Mahadevan et al., 2012). Similarly, pan-aurora inhibitor SNS-314 also enhanced antitumor activity of microtubule-targeting agents in a colon carcinoma model (Vander-Porten et al., 2009). Treatment with AZD1152, an aurora B inhibitor, was found to be synergistic with a variety of chemotherapeutic agents, including irinotecan, docetaxel, vinorelbine, gemcitabine, oxaliplatin, and 5-fluorouracil (Nail et al., 2004), and with vincristine and topoisomerase inhibitors, in leukemia cell lines (Yang et al., 2007). Moreover, this compound also potentiates the radiation response in p53-deficient cancer cells, suggesting synergy with radiotherapy (Tao et al., 2007).

Besides, analysis for various off-targets is also required in the development of aurora kinase inhibitors. Cross-talk activity of aurora kinases with other mitotic kinases promises new pathways in increasing anti-tumor activity as well as overcoming the drug resistance of kinases inhibitors.

Compound (company)	Aurora kinase inhibition	Pre-clinical trial	Clinical trial
Pan aurora inhibitors			
VX-680 (Vextec)	Aurora A (IC_{50}: 0.7 nM) Aurora B (IC_{50} : 18 nM) Aurora C (IC_{50} :4.6 nM)	-Blocking cell cycle progression -Inducing apoptosis in human leukemia xenografts	- Phase II: colorectal cancer, NSCLC, ALL, CM - Potency against drug resistant mutants of Brc-Abl.
PHA-739358 (Pfizer/ Nerviano)	Aurora A (IC_{50}: 13 nM) Aurora B (IC_{50} : 79 nM) Aurora C (IC_{50} : 61 nM)	-Inhibiting FGFR1, BCR–ABL, RET and TRKA -Increasing p53 leading mitotic arrest with 4N DNA cells in wild types - Without mitotic arrest (4N) but > 8N DNA stage and then apoptosis in p53-deficient cells -Antitumor activity in different human tumour xenografts in nude mice	- Phase II: CML and Ph+ALL - Potency against drug resistant mutants of Brc-Abl
AT-9283 (Astex)	Aurora A (IC_{50}: 3 nM) Aurora B (IC_{50} : 3 nM)	-Inhibiting JAK3 (1.1 nM), JAK2 (1.2 nM) and ABL (4 nM) - Inhibiting the tumor growth of HCT116 cells (IC50: 30 nM) -Synergic effect in the combination with Docetaxel - Antitumor activity in lymphoma human tumour xenografts in nude mice	-Phase I–II: advanced or metastatic solid tumours, NHL, AML, ALL, CML and myelofibrosis
CYC-116 (Cyclacel)	Aurora A (IC_{50}: 44 nM) Aurora B (IC_{50} : 19 nM) Aurora C (IC_{50} : 65 nM)	-inhibiting VEGFR2 (IC50= 69 nM) -inhibiting the spindle checkpoint and cytokinesis, resulting in polyploidy and induction of apoptosis - Inhibiting the tumor growth of AML cell line, MV4-11 (IC50: 30 nM) -Antitumor activity in various human solid tumour and leukemia xenograft models	-Phase I: advanced solid tumors
SNS-314 (Sunesis)	Aurora A (IC_{50}: 9 nM) Aurora B (IC_{50} : 31 nM) Aurora C (IC_{50} : 3.4 nM)	-inhibiting TRKA, TRKB, VEGFR3, CSF1R, DDR2 and AXL (IC50 < 100 nM) - inducing defects in spindle checkpoint and cytokinesis, leading to multiple rounds of endoreduplication and cell death - preventing tumor growth in mice bearing a human colon carcinoma xenograft	-Phase I: advanced solid tumors
SUS-6668 (Sugen)	Aurora A(IC_{50}: 850 nM) Aurora B (IC_{50} : 47 nM)	- inhibiting VEGFR2, PDGFRβ, FGFR1 and TBK1 - Inhibited angiogenesis and tumor growth in a diverse panel of human tumor xenografts • Preventing colon cancer liver metastasis in mice	-Phase I: advanced solid tumors

Aurora A inhibitors			
MLN8054 (Millennium)	Aurora A (IC_{50}:4 nM) Aurora B (IC_{50} :172 nM)	-Inhibiting LCK (3.2 μM), PHA(19 μM), Chk2 (28 μM) and CK2 (20.5 μM) -Killing Hct116 through the development of deleterious aneuploidy -Binding to DNA-double-strand breaks leading to the radiosensity of androgen-resistant prostate cancer	- Phase I: advanced solid tumours and other malignancies; trials discontinued
MLN8237 (Millennium)	Aurora A (IC_{50}:1.2 nM) AuroraB (IC_{50}: 396 nM) (The second generation of MLN8054)	-Inducing cytotoxicity and cell cycle arrest in G2–M phase in multiple myeloma cellular (MM) models (at 0.25 mM) - Up-regulating p53 and tumor suppressor genes p21 and p27 -Synergic effect in MM cells in the combination with dexamethasone, doxorubicin, or bortezomib - Daily oral administration (20 mg per kg twice daily) to mice bearing lymphoma or leukaemia xenografts was well tolerated and significantly reduced tumour growth	- Phase I–II: paediatric solid tumours or ALL -Phase II: adult NHL, leukaemia and MDS, and ovarian, fallopian tube and peritoneal carcinoma -Phase I: advanced solid tumours and haematological malignancies
ENMD2076	Aurora A (IC_{50}:14 nM) Aurora B (IC_{50} :350 nM)	-inhibiting VEGFR2(80nM), KIT(40nM) PTK2(5 nM) SRC (100 nM) -preventing the tumor growth in various xenograft models such as breast, colon cancer and leukemia. -Synergic cytotoxic activity in the combination with lenalodomide in myeloma cell lines.	-Phase II: platinum-resistant ovarian cancer
Aurora B inhibitors			
AZD1152 (AstraZeneca)	Aurora A(IC_{50}:1368 nM) Aurora B (IC_{50} :0.37 nM) Aurora C (IC_{50} :4.6 nM)	- Inducing growth arrest, polyploidy and promoted apoptosis in various human tumour xenografts (colon, lung and hematologic) and AML cell lines - Synergic effect in the combination with viscristine and a topoisomerase II inhibitor, against the growth of MOLM13 and PALL-2 cells. - inducing apoptotic in myeloma cells at 500 nM - enhance radiotherapy-sensity of tumor cells	-Phase II: Metastatic Solid Tumors and AML.
GSK1070916 (GlaxoSmith Kline)	Aurora A (K_i: 490 nM) Aurora B (K_i :0,38 nM) Aurora C (K_i: 1,5 nM)	- inhibition of phosphorylation on serine 10 of Histone H3 -Antitumor activity in different human tumour xenografts in nude mice (breast, colon, lung, and two leukemia models)	-Phase I: advanced solid tumors

Table 5: Selected inhibitors of aurora kinases in clinical trials (Reviewed from How and Jee, 2012)

OBJECTIVES OF THE THESIS

Since aurora kinases have been evaluated as potentially druggable targets in anti-cancer therapy, our group started to search for aurora kinase inhibitors. By *in-vitro* high-throughput screening in the molecule library of Institut Curie (France), we identified aurora kinase inhibitory activity of the benzo[e]pyridoindole family (Hoang et al., 2009). In this family, molecule 1 (C1) was confirmed as the most potent anti-proliferative compound based on its *in-vitro* and *in-cellulo* activities (Hoang et al., 2009). However, C1 exhibits a low water-solubility that impairs its applications. A structure-activity relationship (SAR) study was undertaken to design more active and hydrosoluble molecules (partly described in the thesis of HongLien VU, 2011). As a result, a series of new compounds were synthesized and their aurora kinase inhibitory activities were initially confirmed in *in-vitro* assays. The first results from SAR study indicate the requirements for aurora kinase inhibition and give some directions for modifying the molecule and improving its potency.

Moreover, among benzo[e]pyridoindoles, the molecule 4 (C4) was reported to only inhibit the phosphorylation of histone H3 in prophase, but not in metaphase. This is an unusual profile of histone H3 phosphorylation in mitosis, which is probably interesting in cell biology research.

On the basis of these findings, the objectives of the thesis were:

- To study the aurora B activity in mitosis through the unusual inhibition of histone H3 phosphorylation by compound C4.

- To improve the activity and water-solubility of benzopyridoindoles through SAR study and to identify the highest anti-proliferative compound.

- To characterize the selected molecule, named C710 and to evaluate its anti-proliferative potency in human tumor cells as well as in mice xenograft models.

In order to address these objectives, all experiments were designed as described in the scheme presented on the following page.

OUTLINE OF EXPERIMENTS IN THE THESIS

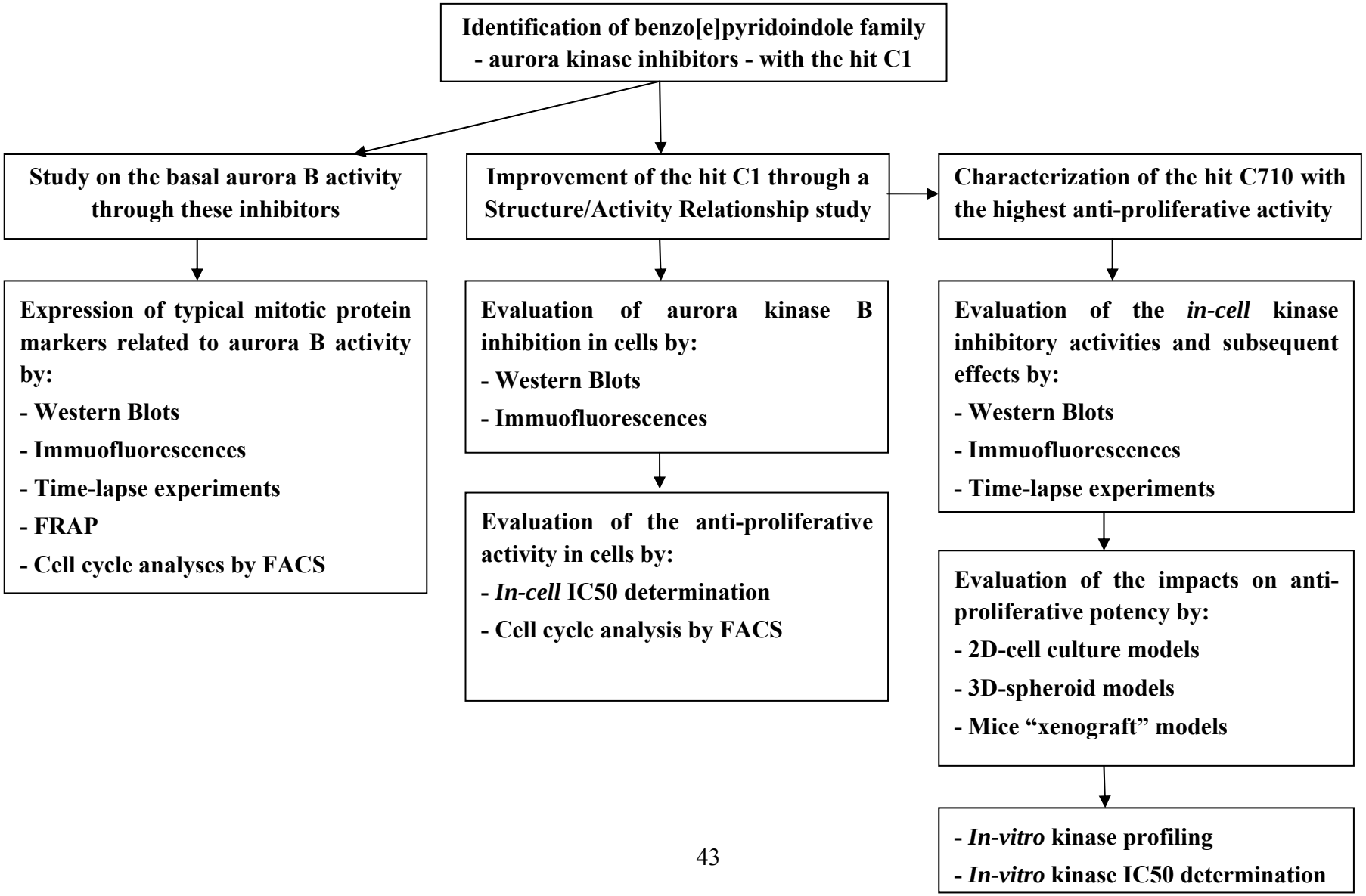

MATERIALS AND METHODS

1. MATERIALS

1.1. CELL LINES

Different human cancer cell lines were used in this thesis, to evaluate in-cell activity of compounds (Table 6). These cells were stored in liquid nitrogen or at minus 80^0C and were obtained from ATCC.

1.2. COMPOUND SYNTHESIS

Benzo[e]pyridoindoles used in all experiments of this thesis were synthesized by Dr. Chi-Hung Nguyen (CNRS- Institut Curie, Orsay, France). The syntheses of compounds were described in Nguyen et al., 1990; Nguyen et al., 1992; Escude et al., 1995; Nguyen et al., 1998; and that of new compounds are present in this thesis.

The purity of compounds was estimated to be more than 95% by thin layer chromatography (TLC). The solubility of compounds was checked by the "shake-flask" method on a TechMed platform (Strasbourg, France). Briefly, 1 mg of compound was dissolved in 100 µL of water, the mixture was stirred for 1h at room temperature and then centrifuged. The supernatant was diluted 1:100 in water/acetonitril (1/1). The concentration of the supernatant was analysed by HPLC by comparison with the stock solution in DMSO.

1.3. REAGENTS

Antibodies were purchased from different companies listed in method below. Cell culture materials (culture medium, foetal bovine serum, penicillin/streptomycine, trypsin-EDTA) were supplied from PAA-GE Healthcare (USA). Nocodazole and Taxol are from Sigma. Reference inhibitors of aurora kinase such as VX-680 and AZD-1152 were supplied from Kavatechnology and Sigma, respectively. Salts and buffer reagents were of analytical grade and purchased from Sigma-Aldrich (USA), EuroBio (France), Euromedex (France).

2. METHODS

2.1. CELL CULTURE AND MAINTENANCE

2.1.1. Culture of human cells

The frozen cells were rapidly thawed by placing the cryovial in a 37°C water bath until only a few ice crystals were remaining. Thawed cells were resuspended in 9 mL their prewarmed complete growth medium, and then centrifuged at 1200 rpm for 5 minutes. Supernatant was discarded, the cell pellet was gently resuspended in 10 mL prewarmed complete growth medium,

and then distributed with the ratio 1:1 and 1:10 into two petri dishes Ø10 cm (for adherent cells) or filtered cap flasks 15 mL (for non-adherent cells).

Cell lines	Origin	Complete growth medium
MCF-7	Breast	DMEM (4.5 g/l Glucose) + 1 mM sodium pyruvate + 0.1 mM NEAA
BT20	Breast	DMEM (1 g/l Glucose) + 1 mM Sodium pyruvate + 0.1 mM NEAA + 7.5% sodium bicarbonate
HeLa	Cervix	DMEM (1 g/l Glucose) + 1 mM sodium pyruvate
Hct116	Colon	McCoy's 5A
U251	Glioblastoma (brain)	DMEM (4.5 g/l Glucose) + 1 mM Sodium pyruvate
U87	Glioblastoma (brain)	DMEM (4.5 g/l Glucose) + 1 mM Sodium pyruvate
Hek293	Kidney	DMEM (1 g/l Glucose) + 1 mM Sodium pyruvate
Malhavu	Liver	DMEM (4.5 g/l Glucose) + 1 mM sodium pyruvate + 0.1 mM NEAA
Hep3B	Liver	DMEM (4.5 g/l Glucose) + 1 mM sodium pyruvate
Focus	Liver	RPMI
H358	Lung	RPMI
JurKat	T lymphocyte	RPMI
BL41	Lymphoma	DMEM (4.5 g/l Glucose) + 1 mM Sodium pyruvate
U2OS	Sarcoma	McCoy's 5A
HaCaT	Skin	DMEM (4.5 g/l Glucose) + 1 mM Sodium pyruvate
SKMel28	Skin	DMEM (4.5 g/l Glucose) + 1 mM Sodium pyruvate
WM793	Skin	DMEM (4.5 g/l Glucose) + 1 mM Sodium pyruvate
A431	Skin	DMEM (4.5 g/l Glucose) + 1 mM Sodium pyruvate

Table 6: List of human cancer cell lines and growth medium *(All medium were completed with 10% (v/v) FBS + 2 mM L-gtutamine and 100 IU/mL peniciline/streptomycine*).

Cells were cultured at 37°C in a humidified incubator with 5% CO_2 in various medium as described in Table 6. The sub-culturing was performed after 2-3 days. Trypsin-EDTA solution (0.05% (w/v) trypsin, 0.02% (w/v) EDTA in PBS) was used to detach cells from the culture dish in the case of adherent cells. Briefly, 2 mL trypsin solution was added and cells were incubated for 5 minutes at 37^0C. After detachment from petri dishes, cells were harvested in 10 mL complete growth medium. The cells were then collected by centrifugation at 1200 rpm for 5 minutes for sub-culturing.

2.1.2. Conservation of cells

For long term preservation of cell lines, healthy cells were recovered by centrifugation as described above and suspended in freezing solution (complete growth medium with 10% (v/v) DMSO); then transferred into a 1,5mL cryovial at the density of 10^6cells/mL. The vials were put into a passive freezer tank filled with isopropanol at minus 80^0C overnight and then stored at minus 80^0C or in liquid nitrogen.

2.2. PROTEIN ANALYSIS BY WESTERN BLOT

Cells were treated in different conditions, then harvested and lysed in 9M urea supplemented with LaemmLi sample buffer. LaemmLi sample buffer 6X contains 10.28% (v/v) sodium dodecyl sulphate (SDS), 36% (v/v) glycerol, 5% (w/v) β-mercaptoethanol, 0.012% (w/v) bromophenol blue and 0.35M Tris-HCl, pH 6.8. Lysates were mixed carefully and boiled for 10 minutes, at 100^0C. They were used for protein analysis by Western blot and stored at 4^0C for use later.

Proteins were resolved by electrophoresis in 8-15% SDS polyacrylamide gels, depending on the size range of the proteins of interest. Polyacrylamide gels were prepared by free-radical induced polymerisation of acrylamide with N,N'-methylenebisacrylamide as cross-linker. Amonium persulphate (APS) and N,N,N',N'-tetramethylethylenediamine (TEMED) were added as provider and stabiliser of free radicals respectively. The separating gel solution was prepared with ingredients as follows:

Gel concentration	**8%**	**10%**	**12%**	**15%**
Acrylamide 30%	1.4 mL	1.7 mL	2 mL	2.5 mL
Tris-HCl pH 8.8	1.3 mL	1.3 mL	1.3 mL	1.3 mL
SDS 10%	0.05 mL	0.05 mL	0.05 mL	0.05 mL
APS 10%	0.05 mL	0.05 mL	0.05 mL	0.05 mL
H_2O	2.2 mL	1.9 mL	1.6 mL	1.1 mL
TEMED	0.002 mL	0.002 mL	0.002 mL	0.002 mL

Polymerization started with the addition of TEMED. The solution were mixed well and poured into the gap between two glass plates of the slab gel system (Biorad) and carefully overlaid by water subsequently. When polymerization was completed after 30 min, the overlay is poured off and the excess was completely removed with the edge of a Whatman 3MM paper. Next, the stacking gel solution was prepared (1.4 mL H_2O, 0.33 mL acrylamide 30%, 0.02 mL SDS 10%, 0.02 mL APS 10%, 0.25 mL Tris-HCl pH 6.8 and 0.002 mL TEMED added finally)

and poured onto the separating gel, together with inserting immediately comb to form wells for loading sample. After completing polymerization, the comb was removed and the slab gel system was inserted in the electrophoresis chamber (Biorad), filled with the electrophoresis buffer 1X (3 g Tris base, 18.8 g glycine, 5 mL SDS 20%, filled by H_2O to 1000 mL).

Protein samples were loaded on the stacking gel wells, together with protein ladder 10 ÷ 250 kDa (Biorad). The gel was run in electrophoresis buffer at the current of 40 mA for 5 min to concentrate all samples on the same starting position before separation; subsequently at 20 mA per gel and the voltage was set up maximum. After SDS polyacrylamide gel electrophoresis (SDS-PAGE), separated proteins were transferred to nitrocellulose membrane (GE Healthcare) immediately after electrophoresis. The transfer sandwich was assembled in transfer buffer: on the black side of the transfer cassette, near the cathode site, the order was: a porous pad, a sheet of three Whatman 3MM papers, the gel, the nitrocellulose membrane, another sheet of three Whatman 3MM papers; rolling a plastic sheet over sandwich to remove air bubbles and finally a porous pad. The cassette was inserted in the blotting chamber with the membrane towards the anode. The chamber was filled with transfer buffer (20% (v/v) absolute ethanol, electrophoresis buffer 0.5X and H_2O) to completely cover the electrode panels. The transfer was performed at the voltage of 110 V and the current was set up maximum, for 1 hour, at room temperature.

After transfer, membrane was incubated in the blocking buffer (either 5% (w/v) non-fat milk or BSA in PBS) to cover free binding sites. Next, it was incubated with a primary antibody diluted in buffer I (PBS containing 0.05% (v/v) tween 20 and either 5% (v/v) lamb serum or 5% (w/v) BSA). The precise concentrations and incubation times are indicated in Table 7. Subsequently, membrane was incubated with secondary antibodies conjugated with horseradish peroxidase (Sigma, 1:5000) in buffer II (PBS containing 1% (w/v) non-fat milk, 0.2% (v/v) Tween20). After each antibody incubation step, membrane was washed 3 times by water; washed extensively with PBS-0.05% Tween 20 for 5 minutes and finally washed 3 times by water. Blots were developed using Luminata™ Forte Western HRP Subtrate Kit (Milipore) and imaged by ChemiDoc™ MP System (Biorad).

Antibody	Company	Source	WB dilution	Incubation
α-tubulin	Sigma	Mouse IgG_1	1:5000/serum	1 hour, t^0room
β-actin	Sigma	Mouse IgG_1	1:5000/serum	1 hour, t^0room
Histone H3-P-Ser10	Upstate	Rabbit	1:2000/serum	1 hour, t^0room
Histone H3-P-Ser28	Upstate	Rabbit	1:2500/serum	1 hour, t^0room
Histone H3-P-Thr3	Abcam	Rabbit	1:2000/BSA	Overnight, 4^0C
Aurora B	Epitomics	Rabbit	1:5000/serum	3 hour, t^0room
Aurora A-P-Thr288	Cell signaling	Rabbit	1:1000/BSA	Overnight, 4^0C
Aurora B-P-Thr232	Stressgen	Rabbit	1:1000/serum	1 hour, t^0room
MPM2	Millipore	Mouse	1:1000/serum	3 hour, t^0room
CENPA-P-Ser7	Cell signaling	Rabbit	1:1000/serum	Overnight, 4^0C
Anti-mouse IgG Peroxidase	Roche	Sheep	1:5000	1 hour, t^0room
Anti-rabbit IgG Peroxidase	Roche	Donkey	1:5000	1 hour, t^0room

Table 7: Antibodies used in Western Blot (WB) experiments

2.3. MICROSCOPY TECHNIQUE

2.3.1. Immunofluorescence

Cells (10 000 cells/coverslips) were seeded on 12-mm-diameter glass coverslips (Knittel Glasser) in the 24-well-plates with 500µL of medium until they adhered to the coverslips. Depending on the experiment, they are treated with different compounds for 20 hours. After washed once by PBS, cells were fixed by warm paraformaldehyde 4% (Sigma) (200 µL/well) for 15 min, at 37^0C and then, washed twice with PBS, 5 min per each time. The protocol was carried out at room temperature. Cells were permeabilized by Triton X-100 in PBS (0.2% v/v) (100 µL/ well) for 5 min and then washed once by PBS. To reduce background, free binding sites were blocked by BSA (0.5 mg/mL) (200 µL /well), for 15 min. The cells were incubated first with specific antibodies diluted in buffer I at the concentrations indicated in table 2.3, for 30 min (200 µL/well) and then, with fluorescence conjugated antibodies (1:500 in buffer I; 30 min, table 8). DNA was stained with Hoechst 33342 (Sigma) (1µg/mL in PBS). Each antibody incubation step was followed by washing 3 times with PBS + 0.2% Tween 20, 5 min per wash to remove non-specific binding antibodies. Finally, coverslips were mounted on slides with fluorescent mounting medium (Dakocytomation). Images were collected by ZEISS LSM510 or LSM710 laser scanning confocal microscope with a 63x oil-immersion objective and were analysed by

LSM510 or ZEN2010 software. Lasers were Argon2, Helium-Neon and biphoton Titanium (Tsunami) for excitation at 488 nm, 543 nm and 720 nm, respectively.

Antibody	Company	Source	IF dilution
α-tubulin	Sigma	Mouse IgG_1	1:2000
Histone H3-P-Ser10	Upstate	Rabbit	1:2000
Histone H3-P-Thr3	Abcam	Rabbit	1:250
Aurora B	Epitomics	Rabbit	1:2000
MPM2	Millipore	Mouse	1:1000
Histone H3-P-Ser28	Upstate	Rabbit	1:2000
Aurora A	Abcam	Mouse	1:1000
Human centromere	Immunovision	Human	1:2000
Survivin	Norvus	Rabbit	1:300
INCENP	Abcam	Rabbit	1:1000
β-tubulin III	Epitomics	Rabbit	1:250
Shugoshin	Abcam	Mouse	1:200
Anti-mouse Hylite fluor^{TM}647-labeled	Anaspec	Goat	1:500
Anti-rabbit Hylite fluor^{TM}488-labeled	Anaspec	Goat	1:500
Anti-mouse Cy3	Eurogentec	Goat	1:500
Anti-rabbit Cy3	Eurogentec	Goat	1:500
Anti-mouse Cy2	Eurogentec	Goat	1:500
Anti-human Dylight fluor^{TM}488-labeled	Invitrogen	Goat	1:500

Table 8: Antibodies used in Immunofluorescence (IF) experiments

2.3.2. Time-lapse experiments

Hek cells stably expressing histone H2A-GFP and Tubulin-GFP as well as Hela cells stably expressing Survivin-GFP, INCENP-GFP and Aurora B-GFP were available (Delacour-Larose et al., 2007; Delacour-Larose et al., 2004; Hoang et al., 2009). Cells were grown on Lab-Tex chambered coverglass (Nalge Nunc International) for at least 24 hours. During imaging, live cells were still maintained under standard culture conditions (37^0C, 5% CO_2). Images were acquired on a ZEISS LSM510 or LSM710 microscope using a Planapochromat 40x water-immersion objective. GFP was excited with a 488 nm Argon2 laser (power varying from 0.1 to

2%). In each experiment, approximately 15 mitotic cells were followed and three independent experiments were performed.

2.3.3. FRAP (Fluorescent Recovery After Photobleaching)

One application of FRAP technique is to measure the dynamic of a molecule. FRAP experiments were performed on HeLa cells stably expressing GFP-INCENP or survivin-GFP or aurora kinase B-GFP. Cells were grown on Lab-Tek chambered coverglass (Nalge Nunc International) and maintained at 37°C, under controlled cell culture conditions. Photobleaching was performed on a ZEISS LSM510 system using a PlanApochromat 40x-water immersion objective. GFP was excited with a 488-nm Argon2 laser (power varying from 0.1 to 1%). For FRAP (Fluorescence Recovery After Photobleaching) experiments, outlined regions were bleached by 10 iterations of a full power laser and recovery was monitored every 20 seconds for 4–5 minutes. Fluorescence intensities were quantified with homemade software and bleaching due to the acquisition was corrected. It was less than 10% in all experiments. Arbitrarily, the intensity of the region prior to bleaching was set at 1 while that of the background was set at 0. Relative intensities are represented as a function of time. Data were recovered in two independent experiments and 8 to 10 cells were followed in each mitotic stage. In mitotic cells, movement of fluorescent objects could be wrongly interpreted as a recovery of fluorescence. Therefore, we performed 3D-reconstitution all along the experiment.

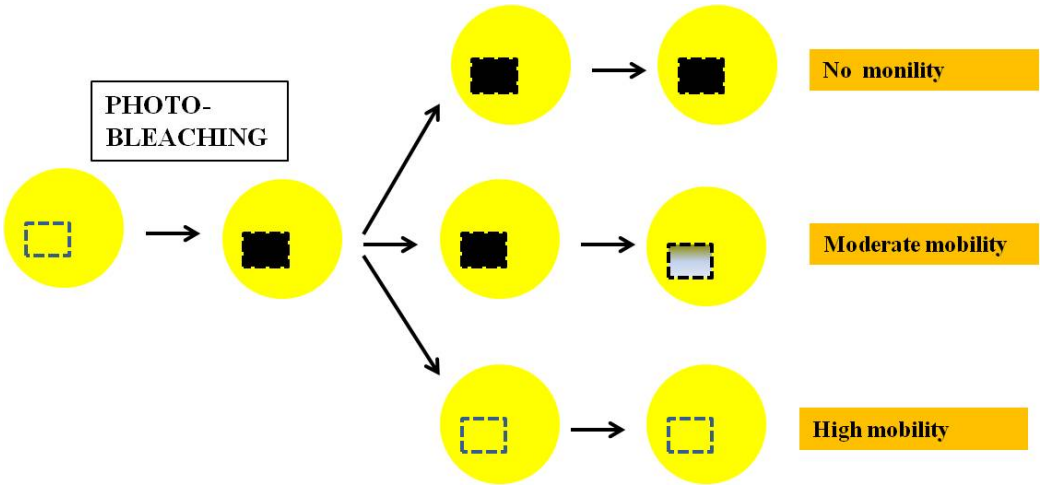

Figure 13: Scheme of the possible situations in a FRAP experiment. The square is the bleached fluorescent region and it appears black after photobleaching. Then the experiment consists in analyzing the fluorescent recovery area. Three situations can occur: 1) either the protein is fully mobile and it is immediately recruited in the bleach area or 2) it is fully immobile and the bleached area will not be fluorescent anymore or 3) in case of moderate mobility, the area will progressively recover fluorescent proteins.

2.4. Cell cycle analysis by FACS (Fluorescence Activated Cell Sorting)

2.4.1. Principle of the method

The DNA content varied during the cell cycle and its analysis requires its staining with a nucleic acid-specific fluorochrome such as propidium iodide (PI), which binds stoichiometrically to DNA and is excited with blue light (488 nm) in a flow cytometer. To allow the penetration of the dye, cells must be fixed by cold ethanol before staining. Moreover, PI can also bind RNA so that it is necessary to digest RNA from the cells by incubation with RNAase.

Besides, to ensure the homogeneity of cell population, it is important to synchronize the cells in the same phase of the cell cycle before compound treatments.

2.4.2. Protocol

a/ Synchronization of the cell

- *Synchronization of cells at G_o/G_1 by serum starvation*

For Hela cells, the absence of serum in the culture medium induces a stop of the cell population in G_0. In this experiment, cells were seeded into the petri dishes (Ø60 mm) at around 40% of confluence (10^5 cells/ plate) and then incubated overnight. The next day, cells were washed once by PBS and the medium replaced by DMEM without serum; the culture was kept, for 48 hours, under such conditions. Upon this treatment, cells were arrested at G_0/G_1 phase.

- *Synchronization of mitotic cells by Nocodazole arrest*

This method was used for all cell lines because nocodazole prevents microbule polymerization. Cells were seeded into the petri dishes (Ø60 mm) with 10^5 cells/ plate and incubated overnight for cell adherence. Next, nocodazole (100 ng/mL) (Sigma) was added in complete medium and the culture kept for 15 hours. Then, nocodazole was removed by gentle washing with PBS. Upon this treatment, cells were arrested at prometaphase of mitosis.

- *Synchronization of cells at S phase by serum starvation and thymidine block*

In the case of synchronizing cells at S phase, immediately following serum starvation as described above, cells were released into complete medium in the presence of 3 mM thymidine (Euromedex) for 20 hours. Upon this treatment, cells were mostly arrested at S phase.

b/ Preparing cells for cell cycle analysis by FACS

After synchronizeation and incubation with compounds, at different concentrations, for various periods of time, cells were collected by centrifugation at 1200 rpm, for 5 minutes. The

pellet was washed once in PBS and cells carefully dispersed before being fixed in 5 mL of ice-cold ethanol (70%) for 1 hour, at -20^{0}C. Next, the pellets were collected by centrifugation, washed once with PBS and then, incubated with a propidium iodide solution (50 mg/mL) in the presence of 0.2 mg/mL RNAase for 15 minutes, at 37°C. DNA content was measured using the BD Accuri C6 flow cytometer (BD Biosciences, US) and cell cycle profiles were analyzed by CFlow Plus software.

2.5. MEASUREMENT OF CELL PROLIFERATION

In this project, two methods were used for evaluating cell proliferation:

2.5.1. Viable cell counting via Trypan blue exclusion method

Trypan blue is a vital stain, the cells excluding it are viable.

Viable cell numbers were accessed by counting cells using a Malassez haemocytometer (0,2 mm, 0,0025 mm^2; Marienfeld, Germany) under a phase contrast microscope (Olympus, Japan), at 10x magnification. 50 µL of cell suspension from the cell culture were diluted 1:1 with Trypan blue (Sigma, Poole, UK 0.4% (w/v) in water). The mixture was transferred into the chamber of the hemocytometer. The unstained cells were counted in 5 grids and the number of viable cells was calculated as follows:

$$\text{Cell viability} = \frac{\text{Number of cells counted}}{5} \times 2 \times 10^4 \text{ cells/mL}$$

2.5.2. Viable cell counting by using Colorimetric Cell Viability Kit 1

This method is based on the mitochondrial reductase activity of viable cells (Figure 14). Briefly, a yellow tetrazolium salt WST-8 (2-(2-methoxy-4-nitrophenyl)-3-(4-nitrophenyl)-5-(2,4-disulfophenyl)-2H-tetrazolium, monosodium salt) was bioreducted by alive cells to an orange formazan product, soluble in culture medium. This reaction only took place in living cells and involved the mitochondrial enzyme succinate-dehydrogenase. The amount of orange formazan produced was directly proportional to the number of alive cells and can be measured by an ELISA photometer, at 450 nm wavelength.

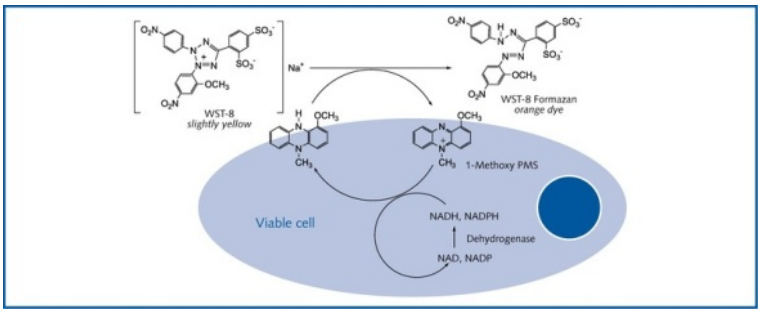

Figure 14: The mechanism of Colorimetric Cell Viability Kit 1

In order to evaluate anti-proliferative activity of compounds, we determined in-cell IC50 (50% inhibititory concentration) value; IC50 means the concentration of compound reducing cell proliferation by half over a period of treatment (96 hours) Cells were seeded in a 96-well plate with different cell numbers depending on cell lines (500 ÷ 2000 cells/ well). In the next day, they were treated under various conditions (compounds and concentrations of compound). Controls without cell and without treatment were simultaneously run. After 4 days of treatment, 10 µL of WST-8 solution were added, into each well, to the 100 µL of cell culture and incubation was pursued for 4 hours in the dark. The absorptions (OD) at 450 nm were measured. The ΔOD was calculated by deducting OD value of control without cell. OD values of untreated controls were set up at 100% of cell growth and the percentage of cell growth of treated samples was calculated based on this control. Mean IC50 was the average of at least three independent reproducible statistically significant measurements.

2.6. KINASE PROFILING AND *IN VITRO* IC50 DETERMINATION

Assays were performed using a radioactive (^{33}P-ATP) filter-binding assay (MRC, Dundee). The kinase profilings were determined with a range of recombinant kinases. Compound C710 was tested at the final concentration of 250 nM. All assays were run in duplicate and the ATP concentration adjusted at the Km value for of each kinase.

For *in vitro* IC50 determination, C710 was also tested against 6 kinases (NUAK1, PHK, Aurora B, SIK2, MELK, CHK2) in the assay by MRC (Dundee). ATP concentration adjusted at the Km value for each kinase. The compound was tested, in duplicate, at 10 concentrations varying from 0.03 nM to 1 µM, with serial 3-fold dilutions. Compound *in vitro* IC50 towards each kinase was defined as the concentration of compound inhibiting by 50% the kinase activity.

Besides, 13a, 13b and C710 were also tested against selected kinases in another assay performed by Reaction Biology Corp (USA). ATP concentration was 1 µM. Compounds were

tested, in duplicate, at 10 various concentrations from 2 pM to 10 µM with serial 3-fold dilutions. Staurosporine was used as internal control and tested at 10 concentrations.

2.7. EVALUATION OF COMPOUNDS' EFFECTS INTO THE TUMOR GROWTH.

2.7.1. The multicellular tumor spheroid (MTS) model

We have adapted the hanging-drop method to produce spheroids of similar diameters. A mixture of agarose 2% – culture medium (1:1) was coated on 24-well plates (500 µL /well) and then 500 µL culture medium was added. A drop of Hct116 cell suspension (20 µL with 750 cells) was put on the lid of an agar coated 24-petri dish containing culture media. Cells were kept under standard culture conditions for spheroid formation. After 48 hours, the spheroids (approximately 0.01 mm) were transferred to the culture medium and after 1 day, they were treated with different concentrations of C710M (350 nM and 1µM) for 2 weeks. Control Hct116 spheroids were grown under the same conditions, but without drug treatment. Spheroid volumes were measured before drug treatment (V_0) and each two days during the drug treatment (V_n). The size of each spheroid was determined by measuring 2 orthogonal diameters (d_1 and d_2) using an inverted microscope. The volume was calculated according to the formula:

$$\mathbf{V = 4/3\pi r^3 \text{ in which } r = 1/2\ \sqrt{d_1} \times d_2.}$$

Spheroid growth was calculated by measuring the variations in volume during the drug treatment using the formula: $\mathbf{(V_n - V_0)/V_0}$. The mean values were determined by following at least 6 spheroids.

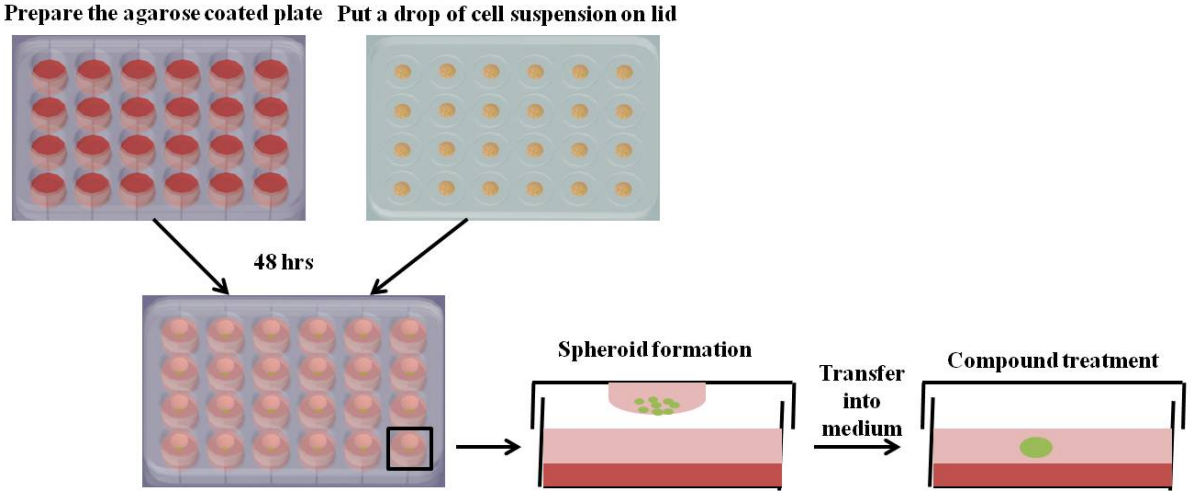

Figure 15: MTS formation by the hanging-drop method.

2.7.2. *In vivo* test: Xenograft models

The protocole was evaluated by the local ethic committee and was conducted by a habilitated researcher. *In-vivo* experiments were performed on four-week old female Swiss nude mice (Janvier, France). After one week of adaptation of the mice with their environment conditions in the animal keeping-house of Institut Albert Bonniot, cells were injected subcutaneously. Cells resuspended in PBS were mixed 1:1 with cold growth factor free matrigel (Beckton Dikinson) and $3.5x10^6$ cells per mouse used for the establishment of Mahlavu tumours. Glioblastoma tumors were got by injection of $6x10^6$ cells per mouse (U251).

Tumors were established after 13 days (Mahlavu) or 9 days (U251-GFP), ready for compound injection. At this time, the mice were randomly divided into 3 groups, with the equivalent mean tumor size among groups. Each group (6 mice) received the treatment of either C710M or C21 in NaCl 0.45% (200 µg compound per each 20 gr of mouse weight) by an intraperitoneal injection (IP injection); whereas, the control group was only injected with NaCl 0.45%. The injections were carried out 4 times per week, stopped 1 day between 2 continuous times. Mice received 11 injections in the experiment with Mahlavu, and 13 injections in the case of U251. The size of the tumor and the weight of each mouse were determined twice per week. Tumor volume was determined by measuring two perpendicular diameters using a clipper and then calculated as follows: $V = \mathbf{d_1 \times d_1 \times d_2}$ in which d_1 and d_2 are the smallest and the largest diameter, respectively. The mean values for each group (6 mice) were determined and compared using Student's t test. At the end of the protocole, 38^{th} day (Mahlavu tumor) or 48^{th} day (U251 tumor), mice were autopsied by a veterinary, tumors were collected and weighted.

RESULTS

CHAPTER 1: STUDY ON AURORA B ACTIVITY IN MITOSIS THROUGH BENZO[e]PYRIDOINDOLONE C4

CHAPTER 2: STRUCTURE-ACTIVITY RELATIONSHIP (SAR) STUDY OF BENZO[e]PYRIDOINDOLES

CHAPTER 3: CHARACTERIZATION OF BENZO[e]PYRIDOINDOLONE C710M EXHIBITING HIGH ANTI- PROLIFERATIVE ACTIVITY

CHAPTER 1:

STUDY ON AURORA B ACTIVITY IN MITOSIS THROUGH BENZO[e]PYRIDOINDOLONE C4

Aurora kinase B plays key roles during mitosis through its activity towards various substrates. However, how it interacts selectively with substrates in different phases of mitosis is still an interesting question to be elucidated.

When studying the benzo[e]pyridoindole aurora kinase inhibitors, we paid attention on compound C4 with an unusual profile of histone H3 phosphorylation. We realized that this compound only inhibits histone H3 phosphorylation in prophase but not in metaphase. Since histone H3 phosphorylation is the hallmark of mitosis and is required for mitotic events, we decided to follow what happens during mitosis upon C4 treatment.

The results showed that without histone H3 phosphorylation in prophase, cells enter into mitosis normally, assemble chromosomes and progress to metaphase. This reinforced the hypothesis of no relationship between histone H3 phosphorylation and chromosome condensation, which was suggested in previous studies (De la Barre et al., 2001; Hans and Dimitrov, 2001; Prigent and Dimitrov, 2003). More interestingly, except inhibition of histone H3 phosphorylation in prophase, the expression and other activities of aurora kinase B were unchanged in these phases. In addition, we observed chromosome compaction defects in anaphase and afterwards, lagging chromosome leading to a delay in mitotic exit upon C4 treatment. We demonstrated that anaphase defects were not related to the absence of histone H3 phosphorylation, in prophase. Simultaneously, aurora kinase B was partly mis-localized in anaphase.

We reproduced the same mitotic defects by treated cells with a selective well-known aurora kinase inhibitor, at a very low concentration. This result leads us to postulate that C4 inhibited the low ATP-affinity of aurora B kinase, in other words its basal activity. Taking account of the independence of the noted defects: the absence of histone H3 phosphorylation in prometaphase and the compaction defects in anaphase, we could hypothesize the existence of waves of aurora kinase activation in mitosis.

Moreover, in previous studies, we showed by FRAP experiments that the mobility of survivin varied from metaphase to anaphase suggesting the existence of different conformations for the chromosomal passenger complex (CPC) (Delacour-Larose et al., 2004). To complete this study, we analyzed the mobility of INCENP, in prophase, by FRAP. The overall FRAP data indicate the existence of different conformations for the CPC that correlates with the aurora kinase activation waves.

In conclusion, the histone H3 phosphorylation in prophase and the anaphase chromosome compaction required the basal activity of aurora B.

All the above results were accepted for publication in Biology Open. Additional data and further discussion will be presented in the article hereafter.

Basal aurora kinase B activity is sufficient for histone H3 phosphorylation in prophase

Ly-Thuy-Tram Le[1,*], Hong-Lien Vu[1,‡], Chi-Hung Nguyen[2] and Annie Molla[1,§]

[1]CRI INSERM UJF U823, Institut Albert Bonniot, 38 706 La Tronche Cedex, France
[2]UMR 176 CNRS, Institut Curie, Bâtiment 110 Centre Universitaire, 91405 Orsay Cedex, France

*Permanent address: Da Nang University of Technology, Da Nang City, Vietnam
‡Permanent address: Ho Chi Minh University of Natural Sciences, Ho Chi Minh City, Vietnam
§Author for correspondence (annie.molla@ujf-grenoble.fr)

Biology Open 000, 1–8
doi: 10.1242/bio.20133079
Received 13th September 2012
Accepted 7th January 2013

Summary

Histone H3 phosphorylation is the hallmark of mitosis deposited by aurora kinase B. Benzo[e]pyridoindoles are a family of potent, broad, ATP-competitive aurora kinase inhibitors. However, benzo[e]pyridoindole C4 only inhibits histone H3 phosphorylation in prophase but not in metaphase. Under the C4 treatment, the cells enter into mitosis with dephosphorylated histone H3, assemble chromosomes normally and progress to metaphase, and then to anaphase. C4 also induces lagging chromosome in anaphase but we demonstrated that these chromosome compaction defects are not related to the absence of H3 phosphorylation in prophase. As a result of C4 action, mitosis lasts longer and the cell cycle is slowed down.

We reproduced the mitotic defects with reduced concentrations of potent pan aurora kinase as well as with a specific aurora B ATP-competitive inhibitor; we therefore propose that histone H3 phosphorylation and anaphase chromosome compaction involve the basal activity of aurora kinase B. Our data suggest that aurora kinase B is progressively activated at mitosis entry and at anaphase onset. The full activation of aurora kinase B by its partners, in prometaphase, induces a shift in the catalytic domain of aurora B that modifies its affinity for ATP. These waves of activation/deactivation of aurora B correspond to different conformations of the chromosomal complex revealed by FRAP.

The presence of lagging chromosomes may have deleterious consequences on the daughter cells and, unfortunately, the situation may be encountered in patients receiving treatment with aurora kinase inhibitors.

Key words: Cancer, Chromosome compaction, Aurora kinase, Kinase inhibitors, Survivin, Chromosomal passenger complex, Histone H3 phosphorylation

Introduction

Histone phosphorylation plays a direct role in major cell events like mitosis, cell death, repair, replication and recombination (Baek, 2011). The same residue phosphorylation may have dual role. For example, histone H3 phosphorylations on Ser10 and Ser 28 were reported both in interphase where chromatin needs to be decondensed for transcriptional activation of genes, and in mitosis where chromatin condensation is necessary (Hans and Dimitrov, 2001). Their definitive roles in these processes have not yet been elucidated.

In late G2 phase, the phosphorylation of histone H3 only occurs on pericentromeric chromatin. Then it spreads along the chromosomes and is complete in prophase. At the end of mitosis, histone H3 is dephosphorylated. Aurora kinase B is a well-known primary mitotic kinase responsible for histone H3 phosphorylation on Serine 10 and 28 (Baek, 2011).

Aurora kinases are a family of serine/threonine protein kinases that play a key role in mitosis progression (Carmena et al., 2009; Vader and Lens, 2008). In human, three aurora kinases have been identified: A, B and C. Aurora A is first associated with centrosomes and then with spindle microtubules whereas aurora B is a chromosomal passenger protein travelling from centromeres to microtubules. Aurora A is required for centrosome duplication, entry into mitosis, formation of bipolar spindle and mitotic checkpoint (Hannak et al., 2001; Sardon et al., 2008; Seki et al., 2008). Aurora B is essential for chromosome condensation, kinetochore functions, spindle checkpoint activation and cytokinesis completion (Carmena et al., 2009; Lens and Medema, 2003; Mendoza et al., 2009; Saurin et al., 2011). Aurora C is mostly involved in spermatogenesis (Vader and Lens, 2008).

Both aurora A and B kinases are activated through interactions with their substrates or partners and priming by other kinases. Activation of aurora B occurs through a two-step mechanism: first, aurora B binds to the C-terminal IN-box sequence of INCENP and is then autophosphorylated at threonine 232 (Thr232) within its activation loop (Honda et al., 2003; Yasui et al., 2004). In the second step, the kinase phosphorylates INCENP and is subsequently fully activated. Aurora kinase B activity is enhanced through its phosphorylation by Chk1 and

priming of its substrates by Plk1 and Mps1 (Jelluma et al., 2008; Petsalaki et al., 2011; Rosasco-Nitcher et al., 2008). Despite this description of the aurora kinase B activation, the physicochemical properties of the enzyme are poorly documented since aurora B itself has not been crystallized in the absence of inhibitors (Girdler et al., 2008; Sessa et al., 2005). Most of the available data derive from the study of the ATP-binding pocket of aurora A (Dodson et al., 2010; Martin et al., 2012). The catalytic domains of human aurora-A and aurora-B are 76% identical at the primary sequence level, and just differ by three amino acids in their ATP-binding sites. With the aim to derive specific kinase inhibitors, efforts are devoted to the description of the different conformations adopted by the ATP-binding sites.

Aurora kinases A and B, exclusively expressed in mitosis, are over-represented in many cancers, including primary colon and breast cancers (Sen et al., 1997; Vader and Lens, 2008). In the light of these observations, aurora kinases have emerged as potential promising targets in the development of anti-cancer therapy and small molecule inhibitors of aurora kinase have been identified (Garuti et al., 2009; Girdler et al., 2006; Harrington et al., 2004; Hoang et al., 2009; Soncini et al., 2006). Several of these ATP-competitive inhibitors are currently in clinical development. Preliminary data from clinical trials generally indicate disease stabilization, the best response being achieved in solid tumours or in refractory chronic myeloid leukemia (Cheetham et al., 2007; Kollareddy et al., 2012; Vu et al., 2010).

Besides their possible efficiency in therapy, aurora kinase inhibitors are tools for describing these enzymes. In a previous study, we found that benzo[e]pyridoindoles are potent ATP-competitive inhibitors of aurora kinases (Hoang et al., 2009). *In vitro*, they inhibited aurora kinases at nanomolar range; in cells, they prevented mitosis progression. In this study, playing with these aurora kinase inhibitors, we showed that the phosphorylation of histone H3 (Ser10 and 28) is not a prerequisite for chromosome assembly and is accounted for by basal aurora kinase B activity. Moreover, at anaphase onset, the compaction of DNA was also perturbed by low concentrations of ATP competitive inhibitors. These data revealed modifications of the ATP-binding site of aurora kinase B during mitosis and their consequences are discussed.

Results

By high throughput screening, we found that benzo[e]pyridoindoles are potent aurora kinase inhibitors (Hoang et al., 2009). *In vitro*, they prevented histone H3 phosphorylation on Ser10. C1 was the first hit and C4 was the fourth inhibitor of this series. The efficiency of molecules C1 and C4, at two different concentrations, is recalled in Fig. 1A. C1, the more potent of the two molecules, was already shown to be an ATP competitive inhibitor of aurora kinase B that prevents mitosis progression (Hoang et al., 2009). By immunofluorescence, we showed that histone H3 phosphorylation was fully inhibited in all mitotic cells by C1 (1 µM) but only in prophase by C4 (3 µM) (Fig. 1A).

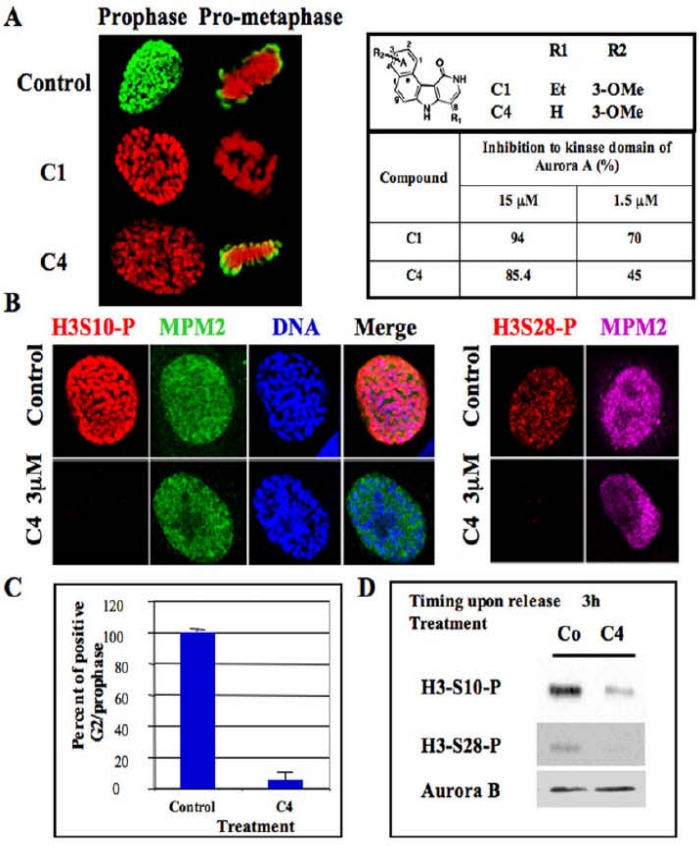

Fig. 1. Delay of histone H3 phosphorylation at mitotic entry upon C4 treatment. (**A**) C1 and C4 are two benzo[e]pyridole inhibitors of the catalytic domain of aurora kinase A (Hoang et al., 2009). Molecules and their efficiency *in vitro* towards aurora A catalytic domain are recalled (Hoang et al., 2009). These data derived from the high throughput screening performed under non-saturating conditions. *In vitro*, IC_{50} of C1 towards aurora A, B are 61 nM and 31 nM respectively (Hoang et al., 2009). Immunofluorescences of histone H3 (Ser10) phosphorylation on HeLa cells treated by either C1 (1 µM) or C4 (3 µM) are represented; Histone H3 (Ser10) phosphorylation is shown in green whereas DNA is in red. Both prophase and pro-metaphase are imaged and compared to control cells. (**B**) Immunofluorescence of Histone H3 (Ser10 and Ser 28) phosphorylations on MPM2 positive HeLa cells. (**C**) Analysis of the percentage of positive histone H3-phospho Ser 10 at mitotic entry. Two independent experiments were conducted and 100 cells in G2/prophase scored in each. (**D**) Western blots were realized on cells synchronized by a MG-132 block and then released for 3 hours. Histone H3 (Ser10 and Ser 28) phosphorylations were analyzed. The same membrane was also revealed using an antibody against aurora kinase B for estimation of the amount of mitotic cells.

MPM2 recognizing phospho-mitotic epitopes allowed the detection of early mitotic cells. The normal MPM2 signal in the presence of C4 demonstrated that C4 did not induce an overall inhibition of phosphorylation in prophase, but only inhibited histone H3 phosphorylation on both Ser 10 and 28 (Fig. 1B). At the concentration of 3 µM, C4 completely abolished histone H3 phosphorylation since 94±4% of the cells in G2/prophase were scored negative with this marker (Fig. 1C). This inhibition was further confirmed by immunoblotting with the reduction of Ser 10 and Ser 28 phospho-histone H3 signals in C4 treated cells (Fig. 1D).

By immunoblotting, we followed the appearance of histone H3 phosphorylation on Ser 10 and Ser 28 in synchronized cells (Fig. 2A). These signals were reduced in C4 treated cells, at mitotic entry, but they were quite similar to control cells, 8 hours later (supplementary material Table S1), showing that C4 only inhibited the histone H3 phosphorylation at G2/prophase. Meanwhile, we did not observe any differences in activity of aurora kinases A and B. They were respectively evaluated through the autophosphorylation of aurora A and the phosphorylation of CenP-A on Ser 7, these two phosphorylations occurring upon priming by the partners (Fig. 2A; supplementary material Fig. S1). By immunofluorescence, we noticed that, in prometaphase, under C4 treatment, although chromosomes were well-condensed, histone H3 was only partly phosphorylated (Fig. 2B). The centromeres, detected through the survivin signal, were found positive for phospho-H3 whereas the chromosome arms were still mostly negative. This pattern is consistent with the enrichment of aurora kinase B on centromeres (Fig. 2C). In the C4 treated cells, aurora kinase B was also found on the whole chromosomes in prometaphase (Fig. 2C), co-localizing with survivin. In the presence of C4, the level of aurora kinase B was found similar to the control (supplementary material Table S1).

Time-lapse experiments on cells expressing fluorescent histone H2A suggested a delay in mitosis progression. The anaphase chromosome compaction was perturbed and lagging chromosomes were observed (Fig. 3). Around 60% of cells in anaphase were scored abnormal under the treatment and only few in the control (Fig. 6A). The screening was stringent; abnormal meant at least two chromosomes from one pole connected to one opposite chromosome. This segregation defects are thus a major consequence of the C4 treatment. Knowing that both aurora kinases A and B are key enzymes in anaphase (Mora-Bermúdez et al., 2007; Hégarat et al., 2011), we looked to their localization. In late anaphase, we did not observe any modification of aurora kinase A localization whereas aurora kinase B was partly found in the midzone and on the chromatin (Fig. 4A). At anaphase onset, passenger proteins like aurora kinase B and survivin are instantly transferred on microtubules when chromosomes start to segregate. Therefore we followed survivin and aurora kinase B localizations by time lapse (Fig. 4B,C) during mitosis.

In control cells, survivin-GFP was transferred to microtubules and fully concentrated in the midbody (Fig. 4B). Conversely in the C4 treated cells, survivin-GFP was present mostly on microtubules but fluorescence was detected outside the midzone (Fig. 4B, indicated by arrows). Finally the survivin signal was also detected outside the midbody in cytokinesis. The localization of aurora B-GFP was found very similar to survivin-GFP and again the kinase was partly mis-localized in late anaphase and telophase (Fig. 4C). The partial mislocalization of

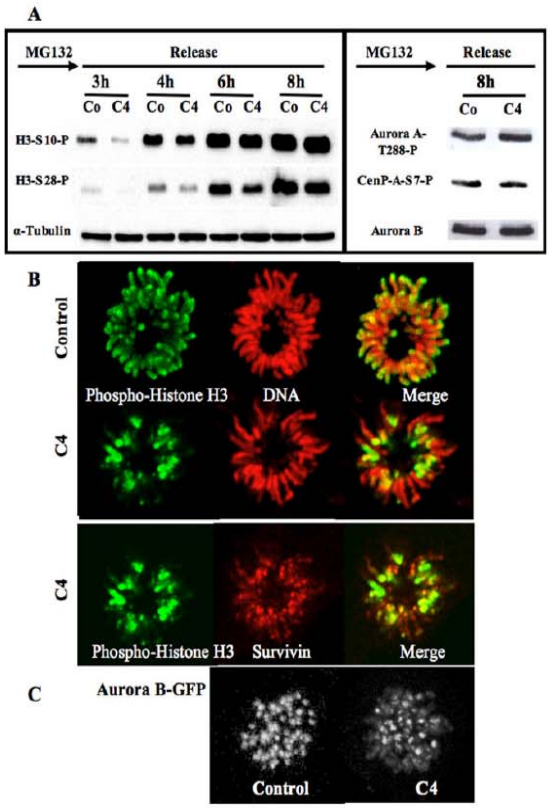

Fig. 2. Histone H3 phosphorylation appears at prometaphase upon C4 treatment. (**A**) Western blots were realized on cells synchronized at mitotic entry in the presence of MG-132 and then released for varying times. Histone H3 (Ser10 and Ser 28) phosphorylations were analyzed in control (Co) and C4 treated cells (C4). The same membrane was also revealed using an antibody against α-tubulin for estimation of the amount of cells. The signals were quantified and the results are in supplementary material Table S1. The phosphorylations of Cenp-A (Ser 7) and aurora kinase A (Thr 288) are also shown in control (Co) and C4 treated cells (C4). Aurora kinase B detection is used for estimation of the amount of mitotic cells. Its level was quantified using α-tubulin as internal standard (supplementary material Table S1; Fig. S2). (**B**) Detection of histone H3 (Ser10) phosphorylation on control and C4 treated cells. Phospho-histone H3 is in green and DNA in red. On the same C4-treated cells, the histone H3 (Ser10) phosphorylation signal (in green) colocalized with survivin (represented in red). (**C**) Detection of aurora kinase B on prometaphasic cells. Z stacks were imaged and 3D-projections are shown. The settings were kept identical for both conditions.

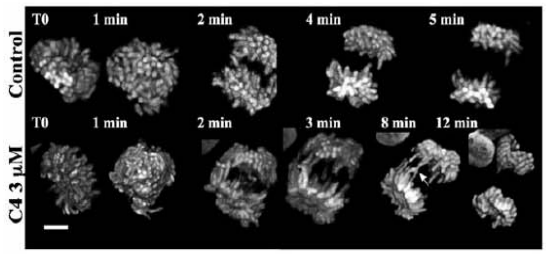

Fig. 3. Time lapse on mitotic cells. Mitotic Hek stably expressing histone H2A-GFP were continuously imaged. Z stacks were acquired and 3D-projections are shown. The settings were kept identical for all conditions. Representative control and C4 treated cells are shown and elapse times indicated on each image. Scale bar: 5 µm.

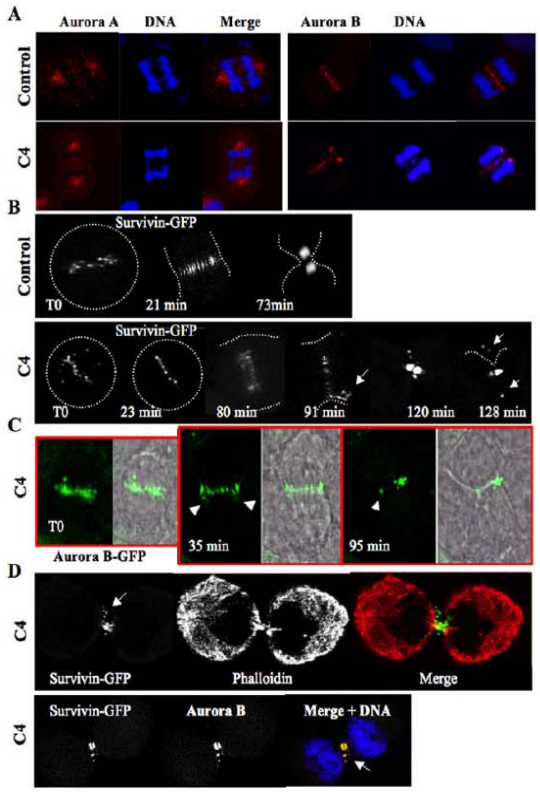

Fig. 4. Consequences of chromosome compaction defects. (**A**) Localization of aurora kinases A and B by immunofluorescence in control and C4 treated cells. A late anaphase is imaged. (**B**) Time lapse on mitotic HeLa cells stably expressing survivin-GFP. Time-lapse microscopy of mitotic HeLa cells expressing the survivin-GFP fusion was performed in the absence (Control) or in the presence of C4 (at 3 µM). The compound was added to the cell culture and then mitotic cells were continuously imaged. Representative photos, made at the times indicated, are presented. For a better understatement, the shape of the cells is recalled by a white dotted line on each fluorescent image. Two independent experiments were conducted and at least 15 cells were followed in each. (**C**) Time lapse on mitotic HeLa cells stably expressing aurora B-GFP. The experiment described in B was reproduced with HeLa cells stably expressing aurora B-GFP. A representative cell is shown and the fluorescent signal is merged with the wide field image. Elapsed times are indicated. (**D**) Immunofluorescence was realized on HeLa cells expressing survivin-GFP. Cells in cytokinesis were imaged. The cell was labelled with phalloidin-TRITC in order to visualize its shape meanwhile aurora kinase B was revealed with antibodies.

passenger proteins was confirmed by immunofluorescence (Fig. 4D). Survivin and aurora kinase were mostly concentrated in the midbody but the passenger complex was also detected on the plasma membrane. The shape of the cell was highlighted by phaloidin labelling (Fig. 4D). Other major actors of cytokinesis like MKPL1 were also partly delocalized in the vicinity of the passengers (data not shown). We found that tubulin was disorganized in the midzone (supplementary material Fig. S2), it may be a consequence of the presence of lagging chromosomes in this area.

The next question was whether cells could complete mitosis and progress in the cell cycle upon C4 treatment. We determined by FACS the repartition of the cells, at different times of treatment (Fig. 5; supplementary material Table S2). The C4

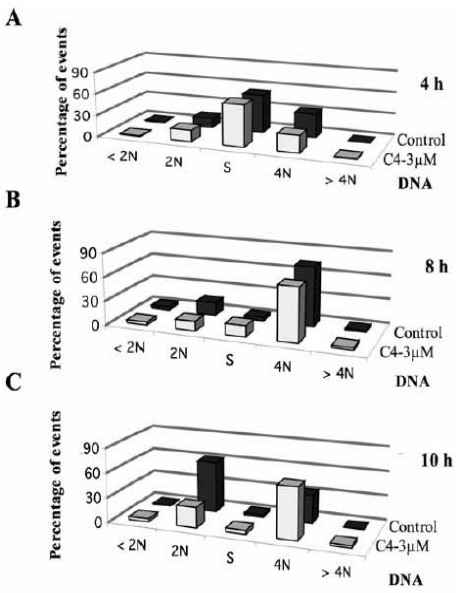

Fig. 5. Cell cycle progression upon C4 treatment. FACS analyses show the repartition of synchronized HeLa cells treated by either C4, at the concentration of 3 µM, for 4 (**A**), 8 (**B**) and 10 (**C**) hours in comparison to non-treated cells. DNA was stained with propidium iodine and the samples were analyzed with the BD Accuri C6 flow cytometer (BD Biosciences, US). The percentage of cells in the different phases is indicated in supplementary material Table S1.

treatment did not significantly modify the timing of mitotic entry (Fig. 5; 4 hours) but delayed mitosis exit (Fig. 5; 8 and 10 hours). In the presence of C4, we did not observe any increase of cell ploidy and the cell viability was also not affected (Fig. 5; supplementary material Table S1). Thus, benzo[e]pyridoindole C4 targeted mostly mitotic events.

We wonder whether chromosome compaction defects could be a consequence of the absence of histone H3 phosphorylation, at mitosis entry. To address this question, we synchronized cells in prometaphase and we treated them by C4 at two separated stages: before and (or) after prometaphase (Fig. 6). Cells treated by C4 upon prometaphase release had a normal phospho-histone H3 level but exhibited a high percentage of anaphase chromosome compaction defects (around 40%). Conversely, cells that entered into mitosis in the presence of C4, and were released from prometaphase in its absence, recovered and showed only 11.5% of lagging chromosomes in anaphase (Fig. 6A). Consequently the absence of histone H3 phosphorylation in prophase and the chromosome compaction defects in anaphase were two independent actions of the molecule C4. As aurora kinase B is the main kinase phosphorylating histone H3 on Ser 10 and 28 and is also involved in chromosome compaction (Mora-Bermúdez et al., 2007), we hypothesised that C4 targeted a low ATP dependent activity of aurora kinase B. If so, the observed defects could be reproduced with other aurora kinase inhibitors at low concentrations.

In cells treated by C4 (3 µM), only 4% of the cells in prophase were positive for histone H3 phosphorylation, 67% had few positive dots, and 29% were negative whereas all the cells in metaphase were scored positive (Fig. 6B). When cells were treated by a low concentration of benzo[e]pyridoindole C1

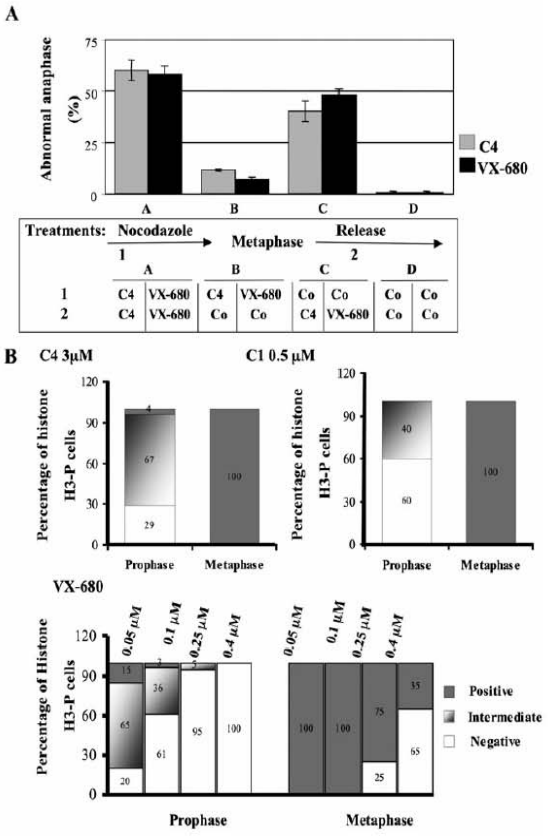

Fig. 6. Quantification of the mitotic defect induced by C4. (**A**) Abnormal anaphases presenting connecting chromosomes were scored by immunofluorescence. DNA was labelled by Hoechst. Cells were synchronized in prometaphase by nocodazole (0.33 µM) for 16 hours and anaphase was induced upon release (post-anaphase onset, 3 hours). Compounds C4 (3 µM) and VX-680 (0.1 µM) were present in different steps: either in (pro)metaphase (1) and (or) post-metaphase (2). In assays A, compounds were added in both steps (1) and (2). In assays B, compounds were only present in prometaphase and were then withdrawn in (2); conversely in assays C, compounds were added after metaphase (step 2). Co means control experiments without compound. Control assays in the absence of compounds are in D. A view of the course of the experiment is shown. Around 200 mitotic cells were analysed in each condition and two independent experiments were conducted. (**B**) The percentage of phospho-histone H3 (Ser 10) was defined by immunofluorescence, in both prophasic and metaphasic HeLa cells treated either by C4 (3 µM), C1 (0.5 µM) or VX-680 (the concentration of VX-680 varied from 0.05 µM to 0.4 µM). Cells were scored as positive, negative or intermediate. Intermediate signal means a significant reduction of the phosphorylation compared to the control. Around 100 cells were scored in each assay and two independent experiments were conducted.

(0.5 µM), a known aurora kinase inhibitor (Hoang et al., 2009), we observed a decrease of histone H3 phosphorylation in prophase (60% were negative and 40% scored intermediate) whereas histone H3 was fully phosphorylated in metaphase (Fig. 6B). Taking into account that C1 and C4 belong to the same family of molecules and in order to avoid the possible involvement of a common off-target, we reproduced the experiment with varying concentrations of VX-680, a reference ATP-competitive aurora kinase inhibitor (Harrington et al., 2004). At 50 nM and 100 nM, VX-680 prevented histone H3 phosphorylation in prophase but not in metaphase (Fig. 6B). We searched for chromosome compaction defects, at anaphase onset, upon VX-680 (0.1 µM) treatment (Fig. 6A) and found that 58% of the anaphasic cells exhibited lagging chromosomes. Again these defects were independent of the inhibition of H3 phosphorylation at mitotic entry and appeared when prometaphasic cells were released in the presence of VX-680 (around 48% of abnormal anaphases, Fig. 6A).

As benzo[e]pyridoindoles C1 and C4 as well as VX-680 are pan-aurora kinase inhibitors, we checked whether AZD-1152, a selective inhibitor for aurora kinase B, could fully reproduce the observed effects. At the concentration of 25 nM, AZD-1152 induced a delay in mitosis exit (Fig. 7A) but cells could then start a new cycle. When cells entered into mitosis, histone H3 (S10) was not phosphorylated (Fig. 7B), the phosphorylation signal was then detected near centromeres (Fig. 7C) and it was found maximal in metaphase (Fig. 7B). We have noted the presence of lagging chromosomes and the partial mis-localization of aurora kinase in late anaphase (Fig. 7D). When AZD-1152 was added upon metaphasic release, around 30% of the anaphase exhibited lagging chromosomes. Therefore the mitotic defects induced by C4 were mostly accounted for by aurora kinase B. However, the possible participation of aurora kinase A in the anaphase compaction defects upon C4 treatment cannot be dismissed.

Our data suggest that aurora kinase B is submitted to activation waves. Previously we showed, by FRAP experiments, that the chromosomal passenger complex could adopt different conformations (Delacour-Larose et al., 2007; Delacour-Larose et al., 2004). Whereas aurora kinase B is immobile all along mitosis, survivin is only mobile in (pro)metaphase. As shown in Fig. 8, INCENP was found mobile in G2/prophase when the partners were immobile. Then, in prometaphase and metaphase, survivin was mobile conversely to others, and finally the complex was stuck on microtubules. Therefore the binary data analysis, which defined mobile and immobile proteins, reveals that the basal activity of aurora kinase B correlates to conformational changes within the chromosome passenger complex. The low-ATP activity is first observed when the CPC moves from pericentromeric chromatin to centromeres and similarly, shortly after its transfer to microtubules (Fig. 8).

Discussion

Successful cell division requires the temporal and spatial integration of chromosomal and cytoskeletal events. One key integrator is the chromosomal passenger complex (CPC) composed of INCENP, aurora kinase B, borealin, and survivin (reviewed by van der Waal et al., 2012). Spatially regulated activity of the CPC is essential for the correction of kinetochore microtubule attachment errors, bipolar spindle stability, and completion of cytokinesis (van der Waal et al., 2012). Aurora kinase B is the unique enzymatic member within the complex; it phosphorylates numerous substrates, during mitosis, such as histones H3 and CenP-A, as well as its partners (INCENP and survivin). Aurora B is known to reach different levels of activations through interactions with CPC members and by phosphorylations (Honda et al., 2003; Jelluma et al., 2008; Petsalaki et al., 2011; Rosasco-Nitcher et al., 2008; Yasui et al., 2004). How these different activation steps are related to the mitotic activities is poorly documented. Recently, by incorporating mutant INCENP, Xu et al. revealed that the full activation is at least required for transferring the CPC to the midzone at anaphase onset (Xu et al., 2009).

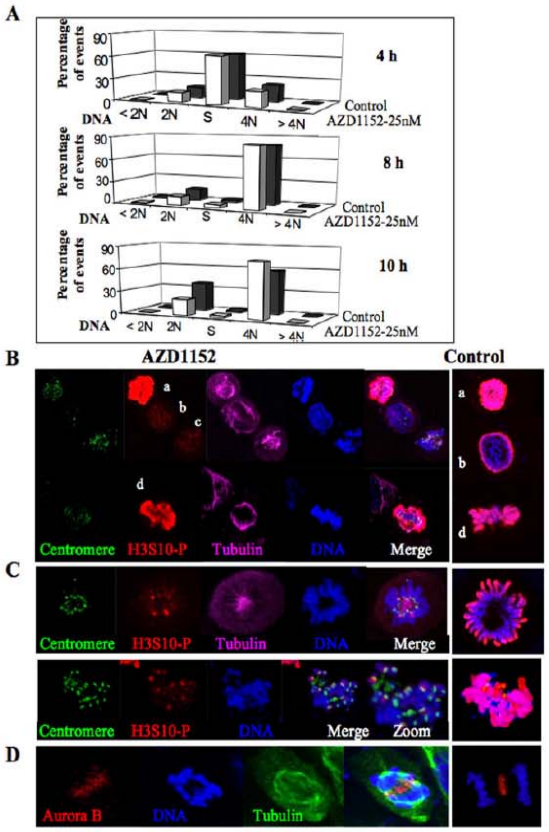

Fig. 7. Effect of low concentrations of AZD1152. (**A**) Cell cycle progression upon AZD1152 treatment FACS analyses show the repartition of synchronized HeLa cells treated by either AZD1152, at the concentration of 25 nM, for 4, 8 and 10 hours in comparison to non-treated cells. DNA was stained with propidium iodide and the samples were analyzed with the BD Accuri C6 flow cytometer (BD Biosciences, US). (**B**) Immunofluorescence of HeLa cells treated by AZD1152, for 15 hours, at the concentration of 25 nM. Centromeres are revealed in green, histone H3(S10) phosphorylation (H3S10-P) is in red, α-tubulin in far red and DNA in blue. Control cells are shown on the right, H3(S10) phosphorylation (H3S10-P) is in red and DNA in blue. Cells **a** and **d** are in metaphase, **b** in prophase and **c** in prometaphase. (**C**) Same experiments as in B. Centromeres are detected by a specific antibody and represented in green. Two different prometaphasic cells are imaged. For an easy visualisation of the colocalization, an enlarged merge is shown in one case. Control cells are shown on the right, H3(S10) phosphorylation (H3S10-P) is in red and DNA in blue. (**D**) Cells were synchronized by nocodazole and imaged 3 hours after release. Most of the cells in anaphase (around 30%) present compaction defects. Aurora kinase B is revealed in red, DNA in blue, α-tubulin in green. A control cell is shown on the right, aurora kinase B is in red, DNA in blue.

When studying the benzo[e]pyridoindole aurora kinase inhibitors, we noticed that some compounds like C4 only inhibited histone H3 phosphorylation in prophase. Then phospho-histone H3 reached its normal level in prometaphase. We reproduced this transitory inhibition by decreasing the concentration of potent aurora kinase inhibitors. These inhibitors being ATP competitive inhibitors, it means that, in prometaphase, a shift occurring in the catalytic domain of aurora B modifies its affinity for ATP. We noticed that the compound C4 (8-H) differed from the counterpart C1 (8-Et) by the absence of an alkyl group on the summit 8. The largest molecule was found to better fit with the ATP binding site. The activation loop of aurora kinase B contains a DFG (Asp-Phe-Gly) motif like most AGC kinases. But it seems that in aurora kinases, this ATP-binding motif could adopt more complex conformations; a DFG-up conformation was described for aurora kinase A in addition to the active DFG-in and the inactive DFG-out states (Dodson et al., 2010; Martin et al., 2012). The existence of this unusual conformation in aurora B and its possible involvement in the observed shift of affinity for ATP remain to be investigated.

Conversely to what was observed when BubR1 or Melk are inhibited, inhibition of aurora kinase did not accelerate the timing of mitotic entry (Park et al., 2009). We observed that cells still assembled chromosomes in the absence of phospho-histone H3. The role of this epigenetic mark is still in debate. *In vitro* assays demonstrated that the phosphorylation is not required for chromosome condensation in *Xenopus* egg extracts (de la Barre et al., 2001). *In vivo* experiments, in *Drosophila*, revealed a very weak correlation between the level of histone H3 phosphorylation and the degree of chromosome compaction (Adams et al., 2001). Our group has postulated that the mark was a ready-to-go label that implied no relationship between chromosome condensation and histone H3 phosphorylation (Hans and Dimitrov, 2001; Prigent and Dimitrov, 2003). Once the cell has arrived in metaphase its chromosomes should be phosphorylated, and this is independent of their state of condensation (Hans and Dimitrov, 2001). In this study we observed the spreading of the phosphorylation on well-organized chromosomes. The absence of mitotic consequences of this delayed phosphorylation favours the label hypothesis for the role of H3 phosphorylation.

Benzo[e]pyridoindole C4 as well as low concentrations of C1 or VX-680 or AZD-1152 revealed the basal activity of aurora kinase B. The two independent consequences of the inhibition of basal activity are the absence of phosphorylation in prophase and chromosome compaction defects in anaphase. Aurora kinase B full activation was not required for H3 phosphorylation, this fits with the observations of Xu and collaborators (Xu et al., 2009). By preventing INCENP expression, they mildly decreased histone H3 phosphorylation. Xu et al. reported a gradient of kinase activity when mitosis progressed whereas Tan and Kapoor described the existence of gradients of phosphorylation of CPC substrates (Tan and Kapoor, 2011; Xu et al., 2009; Xu et al., 2010). The use of competitive inhibitors suggests at least two activation waves of aurora kinase B, the basal activity seems sufficient in prophase and post anaphase onset. Similarly, low level of cyclin B1–cdk1 activity was found to be required during prophase compared to later mitotic steps (Gavet and Pines, 2010). As a consequence aurora kinase B exhibited a full activity in prometaphase and metaphase as required for transferring the CPC from centromere to microtubule (Meldi and Brickner, 2011; Xu et al., 2009). The observed chromosome compaction defects, in anaphase, in the presence of low-ATP competitors, revealed a shift to basal activity when the kinase lies on microtubules. These different steps correspond to different CPC conformations as revealed by FRAP experiments.

The induction of lagging chromosomes at anaphase onset by low concentration of kinase inhibitors is somewhat worrying. The consequences might be the loss of midbody proteins, a non-identical repartition of proteins, the induction of aneuploidy or DNA mislocalization in the daughter cells. These drawbacks are important since the inaccurate localization of DNA in the nucleus impairs gene expressions (Meldi and Brickner, 2011). This situation may be encountered, at distance from the treatment, in

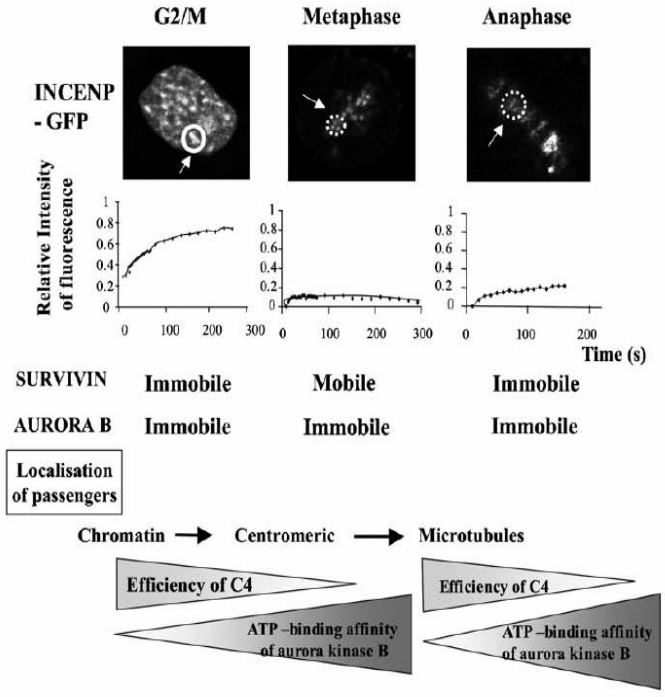

Fig. 8. Compared mobilities of passenger proteins in G2/M-prophase, metaphase and anaphase. FRAP experiments were performed on HeLa cells stably expressing GFP-INCENP or survivin-GFP or aurora kinase B-GFP. The bleached zone is indicated by the dotted line. The recovery of fluorescence was registered at the times indicated and expressed as relative intensities. The kinetics of recovery are shown on the right side of the cell images. Time is in seconds. Survivin and aurora recovering are already published (Delacour-Larose et al., 2004; Delacour-Larose et al., 2007) and recalled in the figure for comparison. The localization of passenger proteins during mitosis progression is indicated as well as the timing of efficiency of C4 (from G2/M to prometaphase and at anaphase onset). The proposed variations of aurora kinase B affinity for ATP are visualized with arrows.

patients treated by aurora kinase inhibitors if long lived compounds are used.

In conclusion, the perturbation of protein kinases with small inhibitors is a powerful approach to dissect kinase function in complex biological systems. In the presence of low-ATP competitors of aurora kinase, cells entered into mitosis without the main mitotic epigenetic mark, the phosphorylation of histone H3, confirming its non-essential role in chromosome assembly. Aurora kinase B activity was found at basal level in prophase, fully activated on centromere and reduced again on microtubules. These waves of activation/deactivation correspond to different conformations of the CPC as described by FRAP.

Materials and Methods

Materials

VX-680 was purchased from Kava Technology, Inc. MG132, thymidine, nocodazole, phalloidin-TRITC, propidium iodide and AZD-1152 were from Sigma–Aldrich. RNase A was supplied by Euromedex. Benzo[e]pyridoindole synthesis and characterization were already described (Hoang et al., 2009; Nguyen et al., 1992).

Cell lines

HeLa cells and Hek-293 were cultured in growth medium (DMEM 1 g/l of glucose with 10% heat-inactivated foetal bovine serum (Gibco–Invitrogen), 2 mM L-glutamine, 100 UI/ml penicillin–streptomycin) at 37℃ in a humidified atmosphere with 5% CO_2.

HeLa cells stably expressing survivin-GFP or aurora kinase B-GFP or INCENP-GFP and Hek-293 expressing histone H2A-GFP were already described (Delacour-Larose et al., 2007; Delacour-Larose et al., 2004; Hoang et al., 2009).

HeLa cells were synchronized at S phase by serum deprivation for 2 days followed by a thymidine block (3 mM) for 20 hours. After PBS washing, cells were then either allowed to grow in normal conditions or arrested at mitosis entry by MG132 treatment (3 hours, 10 µM). HeLa cells were synchronized in prometaphase by nocodazole (0.33 µM).

Immunofluorescence

Hela cells grown on glass coverslips were treated by C4 (3 µM), AZD1152 (25 nM) or DMSO (control) in different trials and then fixed by formaldehyde 4% for 10 minutes at 37℃. Immunofluorescence was performed as described previously (Delacour-Larose et al., 2004). Coverslips were incubated with the antibodies directed against the following antigens: phospho-histone H3-Serine10 (Upstate, 1:2000); phospho-histone H3-Serine 28 (Upstate, 1:2000); aurora kinase B (Epitomics, 1:2000); phospho-MPM2 (Milipore, 1:1000); human anti-centromere HCT-0100 (Immunovision, 1:2000); aurora kinase A (Abcam, 1:1000); α-tubulin (Sigma, 1:1500). Actin was stained by phalloidin-rhodamin (1 µg/ml). DNA was visualized with Hoechst 33342 (Sigma, 0.5 µg/ml). Images were collected with a ZEISS 710 Laser Scanning Confocal microscope with a 63× immersion oil objective. Slices of 0.5 µm are shown.

Western Blot

Synchronized cells were treated by C4 (3 µM) or DMSO (control) for 3, 4, 6 and 8 hours, then harvested and lyzed in 9M urea, finally supplemented with Laemmli sample buffer as described previously. Western blots were performed using the following antibodies: rabbit anti-phospho-histone H3 (Ser10) (Upstate, 1:2000); rabbit anti-phospho-histone H3 (Ser28) (Upstate, 1:1000); rabbit anti-aurora B (Epitomics, 1:5000); rabbit anti-phospho-aurora A (Thr288) (Cell Signaling, 1:1000); rabbit anti-phospho-CENP-A (Ser 7) (Cell Signaling, 1:1000). Bands were visualized by horseradish peroxidase labelled antibodies and ECL technique (Amersham Bioscience). Images were observed by ChemiDoc MP system (Biorad).

Cell cycle analysis

HeLa cells were synchronized at S phase. After release, they were treated by C4 (3 µM), AZD1152 (25 nM) or DMSO (control) for 4, 8, 10, 12, 25 and 30 hours. For determination of cell cycle profiles, cells were fixed by ice-cold 70% ethanol, for 1 hour, and then, incubated with propidium iodide solution (50 µg/ml) in the presence of 0.2 mg/ml RNase A for 15 minutes, at 37℃. DNA content was measured using the BD Accuri C6 flow cytometer (BD Biosciences, US) and CFlow Plus software.

Time lapse

Ex vivo experiments were conducted on cells grown on Lab-Tek chambered coverglass (Nalge Nunc International) and maintained under standard culture conditions (37℃, 5% CO_2). Images were acquired on a Zeiss dynascope confocal microscope using a PlanApochromat 40× water immersion objective. Images were analyzed with the Zen software provided by Zeiss.

FRAP

Cells were grown on Lab-Tek chambered coverglass (Nalge Nunc International). For imaging, cells were maintained at 37℃ on a temperature and CO_2 controlled stage. Photobleaching was performed, as described (Delacour-Larose et al., 2004;

Delacour-Larose et al., 2007), on a ZEISS LSM510 system using a PlanApochromat 40× water immersion objective. GFP was excited with a 488-nm Argon2 laser (power varying from 0.1 to 1%). For FRAP (Fluorescence Recovery After Photobleaching) experiments, outlined regions were bleached by 10 iterations of a full power laser and recovery was monitored every 20 seconds for ~4–5 minutes. Fluorescence intensities were quantified with homemade software and bleaching due to the acquisition was corrected. It was less than 10% in all experiments. Arbitrarily, the intensity of the region prior to bleaching was set at 1 while that of the background was set at 0. Relative intensities are represented as a function of time. Data were recovered in two independent experiments and 8 to 10 cells were followed in each mitotic stage. In mitotic cells, movement of fluorescent objects could be wrongly interpreted as a recovery of fluorescence. Therefore, as already described (Delacour-Larose et al., 2004), we performed 3D-reconstitution all along the experiment.

Acknowledgements

L.-T.-T.L. and H.-L.V. were funded by a Vietnam/French program. This work was supported by INSERM, UJF, CNRS, Institut Curie. The authors greatly thank Dr Stéfan Dimitrov for his encouragement during this work. Microscopy experiments were conducted on the IBISA platform of the CRI INSERM/UJF U823.

Competing Interests

The authors have no competing interests to declare.

References

Adams, R. R., Maiato, H., Earnshaw, W. C. and Carmena, M. (2001). Essential roles of *Drosophila* inner centromere protein (INCENP) and Aurora B in histone H3 phosphorylation, metaphase chromosome alignment, kinetochore disjunction, and chromosome segregation. *J. Cell Biol.* **153**, 865-880.

Baek, S. H. (2011). When signaling kinases meet histones and histone modifiers in the nucleus. *Mol. Cell* **42**, 274-284.

Carmena, M., Ruchaud, S. and Earnshaw, W. C. (2009). Making the Auroras glow: regulation of Aurora A and B kinase function by interacting proteins. *Curr. Opin. Cell Biol.* **21**, 796-805.

Cheetham, G. M. T., Charlton, P. A., Golec, J. M. C. and Pollard, J. R. (2007). Structural basis for potent inhibition of the Aurora kinases and a T315I multi-drug resistant mutant form of Abl kinase by VX-680. *Cancer Lett.* **251**, 323-329.

de la Barre, A.-E., Angelov, D., Molla, A. and Dimitrov, S. (2001). The N-terminus of histone H2B, but not that of histone H3 or its phosphorylation, is essential for chromosome condensation. *EMBO J.* **20**, 6383-6393.

Delacour-Larose, M., Molla, A., Skoufias, D. A., Margolis, R. L. and Dimitrov, S. (2004). Distinct dynamics of Aurora B and Survivin during mitosis. *Cell Cycle* **3**, 1418-1426.

Delacour-Larose, M., Thi, M. N., Dimitrov, S. and Molla, A. (2007). Role of survivin phosphorylation by Aurora B in mitosis. *Cell Cycle* **6**, 1878-1885.

Dodson, C. A., Kosmopoulou, M., Richards, M. W., Atrash, B., Bavetsias, V., Blagg, J. and Bayliss, R. (2010). Crystal structure of an Aurora-A mutant that mimics Aurora-B bound to MLN8054: insights into selectivity and drug design. *Biochem. J.* **427**, 19-28.

Garuti, L., Roberti, M. and Bottegoni, G. (2009). Small molecule Aurora kinases inhibitors. *Curr. Med. Chem.* **16**, 1949-1963.

Gavet, O. and Pines, J. (2010). Progressive activation of CyclinB1-Cdk1 coordinates entry to mitosis. *Dev. Cell* **18**, 533-543.

Girdler, F., Gascoigne, K. E., Eyers, P. A., Hartmuth, S., Crafter, C., Foote, K. M., Keen, N. J. and Taylor, S. S. (2006). Validating Aurora B as an anti-cancer drug target. *J. Cell Sci.* **119**, 3664-3675.

Girdler, F., Sessa, F., Patercoli, S., Villa, F., Musacchio, A. and Taylor, S. (2008). Molecular basis of drug resistance in Aurora kinases. *Chem. Biol.* **15**, 552-562.

Hannak, E., Kirkham, M., Hyman, A. A. and Oegema, K. (2001). Aurora-A kinase is required for centrosome maturation in *Caenorhabditis elegans*. *J. Cell Biol.* **155**, 1109-1116.

Hans, F. and Dimitrov, S. (2001). Histone H3 phosphorylation and cell division. *Oncogene* **20**, 3021-3027.

Harrington, E. A., Bebbington, D., Moore, J., Rasmussen, R. K., Ajose-Adeogun, A. O., Nakayama, T., Graham, J. A., Demur, C., Hercend, T., Diu-Hercend, A. et al. (2004). VX-680, a potent and selective small-molecule inhibitor of the Aurora kinases, suppresses tumor growth *in vivo*. *Nat. Med.* **10**, 262-267.

Hégarat, N., Smith, E., Nayak, G., Takeda, S., Eyers, P. A. and Hochegger, H. (2011). Aurora A and Aurora B jointly coordinate chromosome segregation and anaphase microtubule dynamics. *J. Cell Biol.* **195**, 1103-1113.

Hoang, T. M.-N., Favier, B., Valette, A., Barette, C., Nguyen, C. H., Lafanechère, L., Grierson, D. S., Dimitrov, S. and Molla, A. (2009). Benzo[e]pyridoindoles, novel inhibitors of the Aurora kinases. *Cell Cycle* **8**, 765-772.

Honda, R., Körner, R. and Nigg, E. A. (2003). Exploring the functional interactions between Aurora B, INCENP, and survivin in mitosis. *Mol. Biol. Cell* **14**, 3325-3341.

Jelluma, N., Brenkman, A. B., van den Broek, N. J. F., Cruijsen, C. W. A., van Osch, M. H. J., Lens, S. M. A., Medema, R. H. and Kops, G. J. P. L. (2008). Mps1 phosphorylates Borealin to control Aurora B activity and chromosome alignment. *Cell* **132**, 233-246.

Kollareddy, M., Zheleva, D., Dzubak, P., Brahmkshatriya, P. S., Lepsik, M. and Hajduch, M. (2012). Aurora kinase inhibitors: progress towards the clinic. *Invest. New Drugs* **30**, 2411-2432.

Lens, S. M. A. and Medema, R. H. (2003). The survivin/Aurora B complex: its role in coordinating tension and attachment. *Cell Cycle* **2**, 507-510.

Martin, M. P., Zhu, J.-Y., Lawrence, H. R., Pireddu, R., Luo, Y., Alam, R., Ozcan, S., Sebti, S. M., Lawrence, N. J. and Schönbrunn, E. (2012). A novel mechanism by which small molecule inhibitors induce the DFG flip in Aurora A. *ACS Chem. Biol.* **7**, 698-706.

Meldi, L. and Brickner, J. H. (2011). Compartmentalization of the nucleus. *Trends Cell Biol.* **21**, 701-708.

Mendoza, M., Norden, C., Durrer, K., Rauter, H., Uhlmann, F. and Barral, Y. (2009). A mechanism for chromosome segregation sensing by the NoCut checkpoint. *Nat. Cell Biol.* **11**, 477-483.

Mora-Bermúdez, F., Gerlich, D. and Ellenberg, J. (2007). Maximal chromosome compaction occurs by axial shortening in anaphase and depends on Aurora kinase. *Nat. Cell Biol.* **9**, 822-831.

Nguyen, C. H., Bisagni, E., Lavelle, F., Bissery, M. C. and Huel, C. (1992). Synthesis and antitumor properties of new 4-methyl-substituted- pyrido[4,3-b]indoles (gamma-carbolines). *Anticancer Drug Des.* **7**, 219-233.

Park, S.-Y., Kim, S., Cho, H., Kwon, S.-H., Chae, S., Kang, D., Seong, Y.-S. and Cho, H. (2009). Depletion of BubR1 promotes premature centrosomal localization of cyclin B1 and accelerates mitotic entry. *Cell Cycle* **8**, 1754-1764.

Petsalaki, E., Akoumianaki, T., Black, E. J., Gillespie, D. A. F. and Zachos, G. (2011). Phosphorylation at serine 331 is required for Aurora B activation. *J. Cell Biol.* **195**, 449-466.

Prigent, C. and Dimitrov, S. (2003). Phosphorylation of serine 10 in histone H3, what for? *J. Cell Sci.* **116**, 3677-3685.

Rosasco-Nitcher, S. E., Lan, W., Khorasanizadeh, S. and Stukenberg, P. T. (2008). Centromeric Aurora-B activation requires TD-60, microtubules, and substrate priming phosphorylation. *Science* **319**, 469-472.

Sardon, T., Peset, I., Petrova, B. and Vernos, I. (2008). Dissecting the role of Aurora A during spindle assembly. *EMBO J.* **27**, 2567-2579.

Saurin, A. T., van der Waal, M. S., Medema, R. H., Lens, S. M. A. and Kops, G. J. P. L. (2011). Aurora B potentiates Mps1 activation to ensure rapid checkpoint establishment at the onset of mitosis. *Nat. Commun.* **2**, 316.

Seki, A., Coppinger, J. A., Jang, C.-Y., Yates, J. R. and Fang, G. (2008). Bora and the kinase Aurora A cooperatively activate the kinase Plk1 and control mitotic entry. *Science* **320**, 1655-1658.

Sen, S., Zhou, H. and White, R. A. (1997). A putative serine/threonine kinase encoding gene BTAK on chromosome 20q13 is amplified and overexpressed in human breast cancer cell lines. *Oncogene* **14**, 2195-2200.

Sessa, F., Mapelli, M., Ciferri, C., Tarricone, C., Areces, L. B., Schneider, T. R., Stukenberg, P. T. and Musacchio, A. (2005). Mechanism of Aurora B activation by INCENP and inhibition by hesperadin. *Mol. Cell* **18**, 379-391.

Soncini, C., Carpinelli, P., Gianellini, L., Fancelli, D., Vianello, P., Rusconi, L., Storici, P., Zugnoni, P., Pesenti, E., Croci, V. et al. (2006). PHA-680632, a novel Aurora kinase inhibitor with potent antitumoral activity. *Clin. Cancer Res.* **12**, 4080-4089.

Tan, L. and Kapoor, T. M. (2011). Examining the dynamics of chromosomal passenger complex (CPC)-dependent phosphorylation during cell division. *Proc. Natl. Acad. Sci. USA* **108**, 16675-16680.

Vader, G. and Lens, S. M. A. (2008). The Aurora kinase family in cell division and cancer. *Biochim. Biophys. Acta* **1786**, 60-72.

van der Waal, M. S., Hengeveld, R. C., van der Horst, A. and Lens, S. M. A. (2012). Cell division control by the Chromosomal Passenger Complex. *Exp. Cell Res.* **318**, 1407-1420.

Vu, H. L., Hoang, T. M. N., Favier, B. and Molla, A. (2010). Aurora kinases and passenger proteins as targets for cancer therapy: an update. *Current Enzyme Inhibition* **6**, 19-25.

Xu, Z., Ogawa, H., Vagnarelli, P., Bergmann, J. H., Hudson, D. F., Ruchaud, S., Fukagawa, T., Earnshaw, W. C. and Samejima, K. (2009). INCENP-Aurora B interactions modulate kinase activity and chromosome passenger complex localization. *J. Cell Biol.* **187**, 637-653.

Xu, Z., Vagnarelli, P., Ogawa, H., Samejima, K. and Earnshaw, W. C. (2010). Gradient of increasing Aurora B kinase activity is required for cells to execute mitosis. *J. Biol. Chem.* **285**, 40163-40170.

Yasui, Y., Urano, T., Kawajiri, A., Nagata, K.-i., Tatsuka, M., Saya, H., Furukawa, K., Takahashi, T., Izawa, I. and Inagaki, M. (2004). Autophosphorylation of a newly identified site of Aurora-B is indispensable for cytokinesis. *J. Biol. Chem.* **279**, 12997-13003.

Biology Open

Supplementary Material

Ly-Thuy-Tram Le et al. doi: 10.1242/bio.20133079

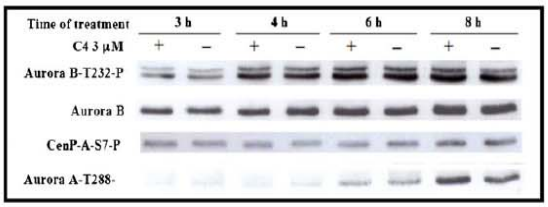

Fig. S1. Kinetics of phosphorylation. Western blots were realised on cells synchronized at S-phase and then released for varying times. The phosphorylations of aurora kinase B (T232), CenP-A (Ser 7), and aurora kinase A (Thr 288) are also shown in control (−) and C4 treated cells (+). Aurora kinase B detection is used for estimation of the amount of mitotic cells.

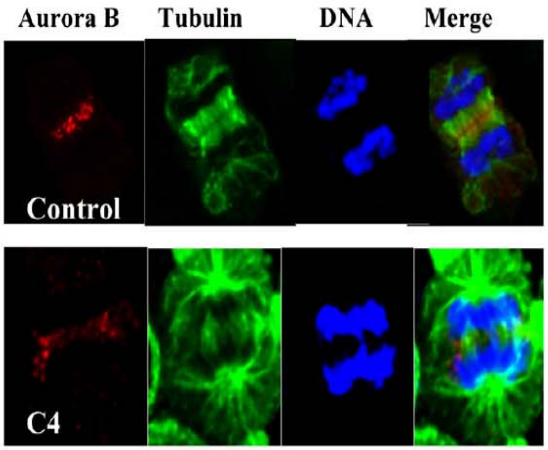

Fig. S2. Localisation of aurora B kinase and α-tubulin in late anaphase in control and C4 treated HeLa cells.

Table S1. Analysis of WB signals. The signals of Western blots were quantified by the Image J software. Two determinations were done for each band. First we analyzed the kinetic of histone H3 phosphorylations (on Ser 10 and 28) presented in Fig. 2A, then we quantified the signal of aurora kinase B in metaphase (blot shown in supplementary material Fig. S1). Briefly the integrate density (area×intensity) was measured twice for each signal and the average is reported in the table. Then the tubulin signals were used to calculate the relative intensity.

Kinetic	Tubulin integrated density	Relative intensity tubulin	H3-Ser10 integrated density	Relative intensity H3-Ser 10	H3-Ser28 integrated density	Relative intensity H3-Ser 28
Co-3h	3386	100	1661	49±1	349	10±0.5
C4-3h	3387	100	327	10±0.2	23	1±0.1
Co-4h	3644	100	3607	99±2	2251	61±1
C4-4h	3939	100	3012	76±2	1303	33±2
Co-6h	3504	100	5734	164±3	5134	147±2
C4-6h	4208	100	5356	127±5	4029	96±4
Co-8h	3853	100	7334	190±3	8366	217±4
C4-8h	4221	100	7776	184±4	6494	154±3

Kinetic	Tubulin integrated density	Relative intensity tubulin	Aurora B integrated density	Relative intensity aurora B
Co-8h	1630	100	3370	207±8
C4-8h	1359	100	3198	235±8

Table S2. Cell cycle analysis. The percentage of Hela cells in each cell cycle phase after 4, 8, 10, 12, 25 and 30 hours under C4 (3 µM) treatment or DMSO (Control) : <2N represents apoptotic cells; 2N for cells in G0/G1; S for cells in S phase; 4N for cells in G2/M and >4N for polyploid cells.

DNA	<2N	2N	S	4N	>4N
4-hour control	1	13	53	33	0
4-hour C4 3 µM	1	16	58	24	1
8-hour control	4	16	4	74	2
8-hour C4 3 µM	4	12	14	67	3
10-hour control	1	62	3	34	0
10-hour C4 3 µM	4	25	5	63	3
12-hour control	3	76	4	15	2
12-hour C4 3 µM	2	50	4	41	3
25-hour control	2	42	13	39	4
25-hour C4 3 µM	5	48	20	25	2
30-hour control	2	65	7	22	4
30-hour C4 3 µM	7	54	13	23	3

CHAPTER 2:

STRUCTURE-ACTIVITY RELATIONSHIP (SAR) STUDY OF BENZO[e]PYRIDOINDOLES

2.1. Improvement of anti-proliferative activity and water-solubility of benzo[e]pyridoindoles through SAR study

2.2. Development of new hydrosoluble benzo[e]pyridoindolones with high anti-proliferative activity

2.1. IMPROVEMENT OF ANTI-PROLIFERATIVE ACTIVITY AND WATER-SOLUBILITY OF BENZO[E]PYRIDOINDOLES THROUGH STRUCTURE-ACTIVITY RELATIONSHIP (SAR) STUDY

Benzo[e]pyridoindoles are a family of tetra-heterocyclic compounds which were identified as novel potent inhibitors of aurora kinases. Taking into account that the hit C1 bears 3 possible lateral chains that may be modified by the chemist, the initial data described in the Ph.D thesis of HongLien VU (2011) suggested some strategies to enhance the aurora B inhibition activity of benzo[e]pyrydoindoles. Hereby, a SAR study was performed with modifications in the 3 lateral chains of the hit C1. *In-cellulo* aurora B inhibition potency of alternatives were evaluated through the histone H3 phosphorylation by immunoblotting and immunofluorescence. By the enlargement of SAR study in molecules of benzo[e]pyridoindole family, we determined the requirements for aurora kinase B inhibition as follows: an oxo group at position 11, a large alkyl substituent at position 8 and an ether group at position 3 of the tetra-heterocyclic structure.

In order to improve the water-solubility of benzo[e]pyridoindoles, we introduced an amine group on position 3, such a substituent could allow the synthesis of the corresponding hydrosuble maleate salt. The methoxy group at position 3 in C1 was replaced by a dialkylaminoalkoxy substituent. Dialkylaminoalkoxy-benzo[e]pyridoindolones 13a and 13b were synthesized. The question was whether these modifications influenced aurora B inhibitory activity in cells. Very interestingly, the results showed the improved activity of these molecules in comparison to C1.

In addition, their effects toward the cell cycle of HeLa cells were also examined. FACS experiment showed that cells were arrested longer in G2/M phases (4N populations) upon 13a or 13b treatment than controls. By immunofluorescence, we observed the bi-nucleation of the cell population. These results were confirmed by time-lapse experiments. Hereby, these compounds delayed mitotic exit and prevented the separation of the two daughter cells, giving rise to large mitotic cells with two connected nuclei. Upon compounds treatment for 48 h, we have noted a significant increase of the sub-G_0 population, a signature of apoptosis induction. Consequently, compound 13a and 13b prevented cell proliferation. Their anti-proliferative potency was also confirmed through the viability of tumor HeLa cells. Upon compounds 13a and 13b treatment for 96h, respective IC50 values of 174 nM and 53 nM were measured for HeLa cell viability.

More interestingly, the hydrosolute maleate salts, 13aM and 13bM, exhibited similar activities than the corresponding free-base counterparts (13a and 13b). The hydrosoluble 13aM

and 13bM strongly inhibited aurora B kinase and exhibited a high anti-proliferative potency towards HeLa cells, with respective IC50 values of 114 and 63 nM.

In conclusion, through SAR study, we developed two new benzo[e]pyridoindolones with improved activity and solubility compared to the hit C1. Their anti-proliferative potency is comparable with the top 10 best aurora kinase inhibitors currently tested in clinical trials. These results is thus opening potential approaches in the development of benzo[e]pyridoindole family as anti-cancer drugs in the future. The full SAR study is presented in the article recently published in ChemMedChem.

DOI: 10.1002/cmdc.201200479

Hydrosoluble Benzo[*e*]pyridoindolones as Potent Inhibitors of Aurora Kinases

Ly-Thuy-Tram Le,[a] Hong-Lien Vu,[a] Delphine Naud-Martin,[b] Marianne Bombled,[b] Chi-Hung Nguyen,*[b] and Annie Molla*[a]

Aurora kinases play an essential role in mitotic progression and are potentially druggable targets in cancer therapy. We identified benzo[*e*]pyridoindoles (BePI) as powerful aurora kinase inhibitors. Their efficiency was demonstrated both in enzymatic inhibition studies and in cell culture assays. New BePI molecules were synthesized, and a structure–activity relationship study was conducted with the aim of improving the activity and solubility of the lead compound. Tetracyclic BePI derivatives are characterized by a particular curved shape, and the presence of an oxo group on the pyridine ring was found to be required for aurora kinase B inhibition. New hydrosoluble benzo[*e*]pyridoindolones were subsequently designed, and their efficacy was tested by a combination of cell-cycle analysis and time-lapse experiments in live cells. The most active BePI derivative, **13b**, inhibited the cell cycle, drove cells to polyploidy, and eventually induced apoptosis. It exhibited high antiproliferative activity in HeLa cells with an IC_{50} value of 63 nM. Relative to compounds tested in clinical trials, this antiproliferative potency places **13b** among the top 10 aurora kinase inhibitors. Our results justify further in vivo evaluation in preclinical animal models of cancer.

Introduction

Aurora kinases are a family of serine/threonine protein kinases that play key roles in mitotic progression.[1,2] In humans, three aurora kinases have been identified: A, B, and C. Aurora A is initially associated with centrosomes and then with spindle microtubules, whereas aurora B is a chromosomal passenger protein travelling from centromeres to microtubules. Aurora A is required for centrosome duplication, entry into mitosis, formation of bipolar spindles, and mitotic checkpoints.[3–5] Aurora B is essential for chromosome condensation, kinetochore functions, spindle checkpoint activation, and cytokinesis completion.[2,6–8] Aurora C is poorly described and is likely to be involved in spermatogenesis.[1]

Aurora kinases A and B are overexpressed in many cancers, including primary colon and breast cancers.[1,9] In light of these observations, aurora kinases have emerged as potential druggable targets for anticancer therapy, and many small molecule inhibitors of aurora kinases have been developed.[10–14] Several of these ATP-competitive inhibitors are currently in clinical development. Preliminary data from clinical trials generally indicate disease stabilization, with the best responses achieved in patients with solid tumors or in those suffering from refractory chronic myeloid leukemia.[15–17]

In a previous study, we identified benzo[*e*]pyridoindoles (BePI), represented in Scheme 1 A, as novel potent inhibitors of the aurora kinases.[14] The best hit, compound **1**, is an ATP-competitive inhibitor with nanomolar in vitro aurora kinase inhibitory activity. In cells, it prevented the phosphorylation of histone H3 and induced mitotic exit without chromosome segregation, a known phenomenon associated with aurora B inactivation.[6] In addition, it prevented the growth of cell lines derived from different carcinomas. However, these BePI compounds were poorly soluble in water and therefore have been limited in use.

The BePI structure contains a privileged scaffold to which multiple biological activities have been ascribed. BePI was originally identified as a synthetic triple helix-specific ligand[18,19] and as an agent inhibiting both topoisomerases I and II with the selection of an intoplicine compound for clinical trials.[20,21]

More recently, protein kinase casein kinase 2 inhibition by BePI derivatives has been implicated in antitumor activity.[22] The specificity of the biological action in the latter case was a result of hydroxy and chloro substituents at the 3- and 11-positions, respectively. As the scaffold is highly modifiable, we designed new BePI compounds with the added key advantage of water solubility and tested their capacity to inhibit the function of aurora kinase B. Our results are described below.

Our previous set of BePI derivatives **1**–**7** was expanded with the new analogues **8**–**13** described in this study. The aim of this study was to improve the activity and solubility of hit compound **1**.[14] Upon evaluating the ability of these benzo[*e*]-

[a] *L.-T.-T. Le,[+] Dr. H.-L. Vu,[++] Dr. A. Molla*
Biology Laboratory, CRI-INSERM/UJF U823, Institut Albert Bonniot
Université Joseph Fourier, 38706 La Tronche (France)
E-mail: annie.molla@ujf-grenoble.fr

[b] *D. Naud-Martin, M. Bombled, Dr. C.-H. Nguyen*
Chemistry Laboratory, UMR 176 CNRS, Institut Curie
Bat 110 Centre Universitaire, 91405 Orsay (France)
E-mail: chi.hung@curie.u-psud.fr

[+] *Permanent address: DaNang University of Technology (Vietnam)*

[++] *Permanent address: Ho Chi Minh University of Natural Sciences (Vietnam)*

Supporting information for this article is available on the WWW under http://dx.doi.org/10.1002/cmdc.201200479.

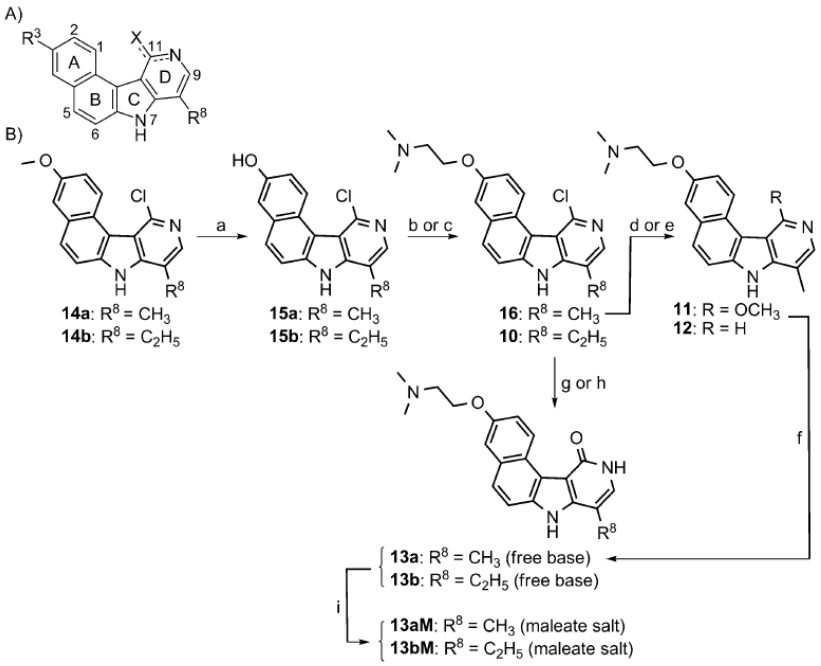

Scheme 1. A) Structure of benzo[*e*]pyridoindoles and their atom numbering. B) Synthesis of 8-alkyl-3-dimethylaminoethoxy-7*H*-10*H*-benzo[*e*]pyrido[4,3-*b*]indol-11-ones **13a** and **13b**. *Reagents and conditions:* a) $BnNEt_3Cl$, concd HCl; b) 2-chloro-*N*,*N*-dimethylethanamine, NaOH, *n*BuOH/H_2O, RT then reflux for 1 h; c) 2-(dimethylamino)ethanol, diisopropyl azodicarboxylate, PPh_3, THF, RT, 18 h; d) NaOMe/MeOH (30:70), 130 °C, 48 h; e) H_2 (1 atm), Pd/C; f) 1 N HCl in AcOH, RT, 18 h; g) Ac_2O; h) 0.13 M NaOAc in AcOH, reflux, 18 h; i) maleic acid.80 °C, 5 min.

pyridoindoles to inhibit aurora kinase B, we found that the oxo group on ring D is required for aurora kinase B inhibition. The inhibitory activity increased with the bulkiness of the R^8 alkyl group (Me, Et) on ring D. A dialkylaminoalkoxy substituent at the 3-position of ring A enabled the possibility of synthesizing a hydrosoluble counterpart. Both the free base and the maleate salt of each hydrosoluble BePI were evaluated and were shown to exhibit high antiproliferative activity in HeLa cells. Based on these studies, we conclude that these hydrosoluble BePI are potent aurora kinase inhibitors that are worthy of in vivo evaluation in preclinical animal models of cancer.

Results and Discussion

New benzo[*e*]pyridoindoles

We previously identified benzo[*e*]pyridoindoles **1** and **2** as potent inhibitors of aurora kinases by high throughput screening, and their activities were confirmed both in vitro and in cells.[14] Major features of **1** and **2** are described in table S1 (Supporting Information). In the order to improve hit **1**, we decided to define the important requirements for aurora kinase B inhibition. We therefore increased the number of available benzo[*e*]pyridoindoles by varying positions 3, 8, and 11 (Scheme 1 A); syntheses illustrated in Scheme 1 B.

Requirements for aurora kinase B inhibition in cells

As aurora kinase B is responsible for the phosphorylation of histone H3 on the Ser10 residue, an important epigenetic mark in mitosis,[23] its activity was determined through this mitotic signal. The inhibitory activities of benzo[*e*]pyridoindole molecules in mitosis were evaluated by western blot and immunofluorescence (Figure 1 and figure S1, Supporting Information). Immunoblotting and immunofluorescence were carried out on U2OS cells that were treated overnight with compounds at a concentration of 1 μM; cells were collected by mitotic shake-off. The percentage of phospho-histone H3-positive mitotic cells was estimated for immunofluorescence assays (Figure 1).

The comparison of histone H3–Ser10 signals upon treatment with **1**, **2**, or **4** showed that **1** was the most efficient inhibitor (Figure 1). Focusing on their structures, we realized that these molecules differ at position R^8: **1** has an ethyl group, **2** has a methyl, and **4** has a hydrogen atom. Our results demonstrate that the bulkiness of the R^8 alkyl group plays an important role for aurora B inhibition. However, the replacement of this alkyl group by a benzo-fused ring at the 8,9-position (compound **7**) led to a complete loss of inhibitory potency (Figure 1).

Deletion of the ether functional group at position R^3 (in **3**), or replacement of this group by a hydroxy moiety (in **8**) or an ester functionality (in **9**), did not maintain the inhibitory activity (Figure 1). Moreover, the position of this ether functional group at R^3 is crucial, and moving this group to position 4 resulted in an inactive corresponding compound **5** (Figure 1). This indicates that the ether at position R^3 of the benzopyridoindole is necessary for aurora B inhibition. Moreover, in spite of the simultaneous preservation of R^3 and R^8, the 5,6-dihydroxy derivative **6**, with a mild planarity modification on ring B, exhibited no activity.

Based on these initial data, two questions arose: was the oxo group at position 11 important for aurora kinase B inhibition, and would it be possible to replace the methoxy substituent at position 3 by an O-alkylamino-substituted chain without altering the biological activity? To answer these queries, the oxo group at position 11 was replaced by either a methoxy group, a chlorine, or a hydrogen. The corresponding respective compounds **11**, **10**, and **12** were designed and are presented

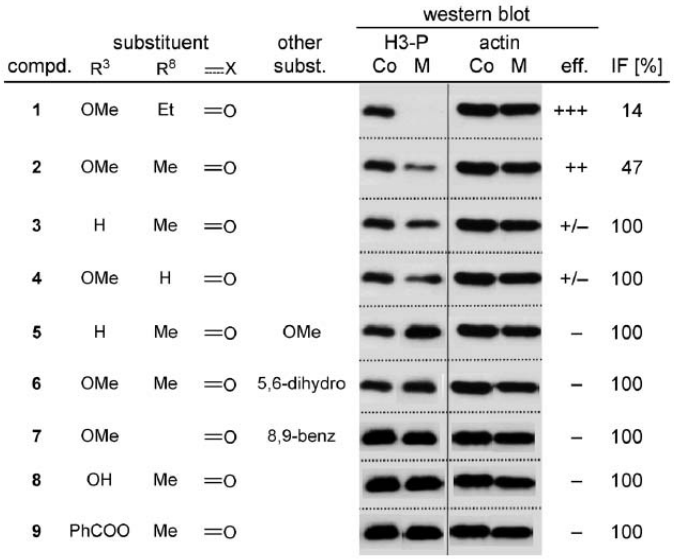

Figure 1. Inhibition of aurora kinase B by benzo[*e*]pyridoindole molecules **1**–**9** with an oxo group at position 11: U2OS cells were treated overnight with the test compounds at 1 μM in the presence of nocodazole (50 nM). Aurora kinase B activity was evaluated both by western blots and by immunofluorescence (IF) with a specific antibody against phosphoserine 10 histone H3 (H3-P). For western blots, the efficiency of the test molecule (M) is compared with control (Co, DMSO), and actin is used as an internal loading control. Data are reported as follows: (+ + +): strong inhibition, (+ +): significant inhibition, and (+/–): a slight decrease in signal, whereas (–) reveals no difference from control. The full western blots are given in figure S1 (Supporting Information). For immunofluorescence, the percentage of positive phospho-Ser 10 histone H3 is indicated. Two different experiments were conducted, and 100 mitotic cells were scored.

in Figure 2A. These compounds **10**–**12** and their oxo counterparts **13a** and **13b**, fitted with a lateral chain [-O-CH_2CH_2N-$(CH_3)_2$] at position 3, allowed us to study the SAR within this family of aurora inhibitors. However, substitution of the pyrrole amine with a methyl group resulted in an inactive compound (data not shown).

The ability of these benzo[*e*]pyridoindole molecules to inhibit histone H3 phosphorylation in mitosis was evaluated by immunofluorescence (Figure 2A) and western blotting (Figure 2B). Two compounds, **13a** and **13b**, were found to be more potent than lead compound **1** (Figure 2B and C). A comparison of the activities of these five new molecules (**10**–**13a** and **13b**) clearly revealed that the oxo group at position 3 is required for aurora kinase B inhibition. Indeed, compounds **11** and **12**, which differ from **13a** by replacement of the oxo group with an ether group (OMe) and a hydrogen atom, respectively, had no inhibitory activity (Figure 2). Similarly, chloro derivative **10** was inactive when we compared its activity with **13b**, the most potent aurora B inhibitor in this series. Evaluation of these molecules confirmed the correlation between inhibitory potency and the bulkiness of the R^8 alkyl substituent observed in the former series (**13b** was slightly superior to **13a**, while **1** was better than **2** and **4**).[14] The evaluation of H3 phosphorylation signals at different compound concentrations revealed that in cells, **13b** inhibited aurora kinase B at a level similar to VX-680, the reference aurora kinase inhibitor.[24]

Inhibitory activities toward recombinant aurora kinases confirmed that **13b** is a more powerful aurora B inhibitor than **13a** (IC_{50} values of 13 nM versus 22 nM, see Figure 2D). Neither compound exhibited selectivity toward the aurora kinases, with aurora A also inhibited at nanomolar levels in vitro (Figure 2D). Compound **13b** was found to be approximately threefold more potent than lead compound **1** toward aurora B. Benzo[*e*]pyridoindoles bearing a methyl at position 8 (**2** and **13a**) inhibited aurora kinases A and B to the same extent, whereas **1** and **13b**, with an ethyl substituent at this position, were more efficient toward aurora kinase B than aurora A (Figure 2D). Conversely, VX-680 inhibited aurora A threefold more efficiently than aurora B (Figure 2D). Moreover, casein kinase 2, targeted by BePIs with hydroxy and chloro substituents at the 3- and 11-positions, respectively[14,22] was not affected by **1** or **13a** (Figure 2D). In summary, within the BePI family, the requirements for an aurora kinase B inhibitor are as follows: an oxo group at position 11, a large alkyl substituent at R^8, and an ether group at R^3. The R^3 site enables addition of a long chain without affecting aurora kinase activity, a possibility that was later exploited for deriving hydrosoluble salts corresponding to **13a** and **13b**.

Outcome of cells treated by dialkylaminoalkoxybenzo[*e*]pyridoindolones 13a and 13b

Next, we tested the behavior of cells treated with compounds **13a** and **13b**. HeLa cells were synchronized at the S phase, and the compounds were added upon release. The results of experiments following 12 and 48 h of compound treatment are presented in Figure 3A. After 12 h, cells in the control entered a new cycle (71% in G_1) whereas **13a**- and **13b**-treated cells were primarily arrested in G_2/M populations (84 and 86%, respectively). These 4N populations were identified by immunofluorescence as binucleate cells (Figure 3B). The connection between the two nuclei was clearly visible in late telophase (Figure 3B, **13a-1**). Conversely, compound **1** and VX-680 gave rise to micronuclei as a result of mitotic exit following delayed metaphase (Figure 3B).[14] At micromolar concentrations, **13a** and **13b** prevented ongoing mitosis, thus confirming the inhibition of mitotic target(s).

To understand how these binucleate cells arose, we performed time-lapse microscopy on HeLa cells stably expressing aurora B–GFP. Cells were treated with either DMSO (control) or with compound (500 nM) and were imaged immediately. In the control experiments, aurora B–GFP localized on aligned centromeres (Figure 4, 10 min), followed by relocation to the midzone (~45 min) and final concentration at the mid-body (1 h). In the presence of **13a**, the centromeres aligned quite normally (T0 and 18 min), and aurora B appeared to localize in the midzone at anaphase onset (40 min, 2 h). However, the two daughter cells did not separate, and each mitotic cell gave rise to a large spread cell (4 h). The duration of mitosis was

A)

compd.	R^3	R^8	=X	IF (H3-P)
10	$(CH_3)_2N(CH_2)_2O$	Et	—Cl	–
11	$(CH_3)_2N(CH_2)_2O$	Me	—OMe	–
12	$(CH_3)_2N(CH_2)_2O$	Me	—H	–
13a	$(CH_3)_2N(CH_2)_2O$	Me	=O	+++
13b	$(CH_3)_2N(CH_2)_2O$	Et	=O	+++

B)

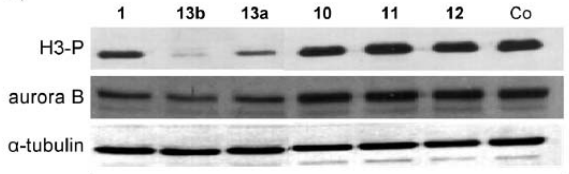

C)

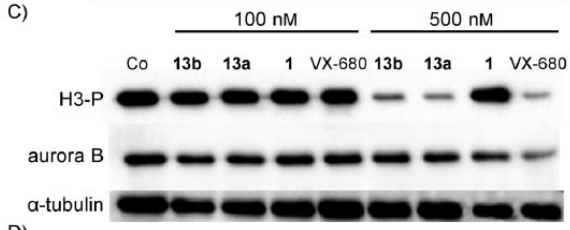

D)

compd.	IC_{50} [nM] aurora A	IC_{50} [nM] aurora B	CK2 inhib. at 1 μM [%]
1	61	33	0
2	40	47	0
13a	29	22	7
13b	50	13	ND
VX-680	13	37	ND

Figure 2. Efficiency of the new 3-dialkylaminoalkoxy-BePI derivatives **10**–**13** in inhibiting aurora B kinase: A) Immunofluorescence (IF) with phospho-Ser10 histone H3 antibodies. Percentage phospho-Ser10 histone (H3-P) is qualitatively represented as follows: (+ + +) indicates strong inhibition with no positive mitosis detected, whereas (–) reveals no difference from control. Two different experiments were conducted, and 100 mitotic cells were scored. B) Immunoblot analysis of histone H3 phosphorylation. HeLa cells were incubated overnight with nocodazole (50 nM) in the presence of either DMSO (Co) or test compounds (1 μM) as indicated. Cells were then collected and lysed; identical amounts of the lysed cell samples were separated by SDS-PAGE (15% acrylamide). After transfer, the blot was revealed with an antibody against phosphorylated histone H3. The same membrane was also revealed by using antibodies against α-tubulin and aurora B for estimation of the amount of loaded proteins and mitotic cells, respectively. C) Comparison of the inhibition potency: the experiment described in panel B was reproduced with two concentrations of compounds (100 and 500 nM). Inhibitory activity observed with **13a** and **13b** were compared with the signals obtained with lead compound **1** and VX-680 under the same conditions. D) Compound concentrations required to inhibit kinase activity by 50% (IC_{50} values) were determined by in vitro assays and are listed for aurora kinases A and B. Percent inhibition of casein kinase 2 (CK2) at 1 μM is indicated where available (ND: not determined).

longer than for the control (compare Co and **13a**). The effects were observed in all of the cells that were followed, and they appeared with no delay, suggesting good cell permeability of this compound. It is possible that the chromatin detected in the mid-region (Figure 3B) might activate the NoCut checkpoint, delay mitosis exit, and prevent cytokinesis.[9] Interestingly, binucleation was not observed with compound **1**; instead, **1** led primarily to micronuclei formation.[14] These differences may be due to: 1) increased efficiency toward aurora kinases, 2) better permeability, or 3) differential selectivity among mitotic kinases.

After compound treatment for 48 h, while control cells were still cycling, the bulk of the **13a**- and **13b**-treated populations were detected in the sub-G_0 gated population (Figure 3A). Therefore, we investigated the viability of tumor HeLa cells upon treatment with **13a** or **13b** and compared these to the effects observed for **1** and **2**.[14] HeLa were grown as adherent cells, and concentrations that inhibit growth (IC_{50}) were determined (Figure 5D). Compounds **13a** and **13b** exhibited high antiproliferative activity in HeLa cells (IC_{50} values of 174 ± 46 nM and 53 ± 3 nM were determined, respectively). Extension of the lateral R^3 chain significantly increased the antiproliferative activity of benzo[*e*]pyridoindole derivatives (7- and 18-fold, respectively, for **13a** and **13b** relative to **1** and **2**). The antiproliferative capacity varied in the same way as the inhibition of aurora kinase B and increased with the length of the chain at position R^8 (**13b** was found threefold more active than **13a**). Moreover, the best compound (**13b**) was found to be 27-fold more efficient for preventing HeLa proliferation than VX-680, the reference inhibitor for aurora kinases (Figure 5D).[14,23] The improvement in antiproliferative activities observed with **13a** and **13b** cannot be solely explained by increased inhibition of aurora kinases. Instead, the reason may be better biodistribution of the molecule or simultaneous activity toward another target. Profiling of **13a** revealed a rather narrow selectivity, as only 15 of the 121 kinases were inhibited by more than 70% at 1 μM of **13a** (table S2, Supporting Information). Targeted mitotic kinases included Nuak1, Chk2, Chk1, and the aurora kinases.

Development of new hydrosoluble benzopyridoindolones

To enable the use of a drug in clinical practice, it is valuable to synthesize hydrosoluble compounds. We focused our attention toward the introduction of an aminoalkoxy side chain at position 3 of BePI, which was likely to give a hydrosoluble salt. The question remained to determine whether activity would be retained by the hydrosoluble maleate salts corresponding to **13a** and **13b**, which we designated **13aM** and **13bM**, respectively. The results in Figure 5A–C show that both compounds inhibited aurora kinase B, and their efficiencies were found to be similar to those for their free base counterparts (Figure 5A–C). Compounds **13aM** and **13bM** exhibited high antiproliferative activity toward HeLa cells, with respective IC_{50} values of 114 and 63 nM (Figure 5C).

Conclusions

This structure–activity study led to the improvement of a lead identified by high throughput screening.[14] Although the BePI structure is built upon a privileged scaffold which has multiple biological capacities, the specificity of the biological activity is introduced by the lateral substitutions. A chloro group at position 11 led to a casein kinase 2 inhibitor, whereas exchange to an oxo group at this position induced the specific inhibition of

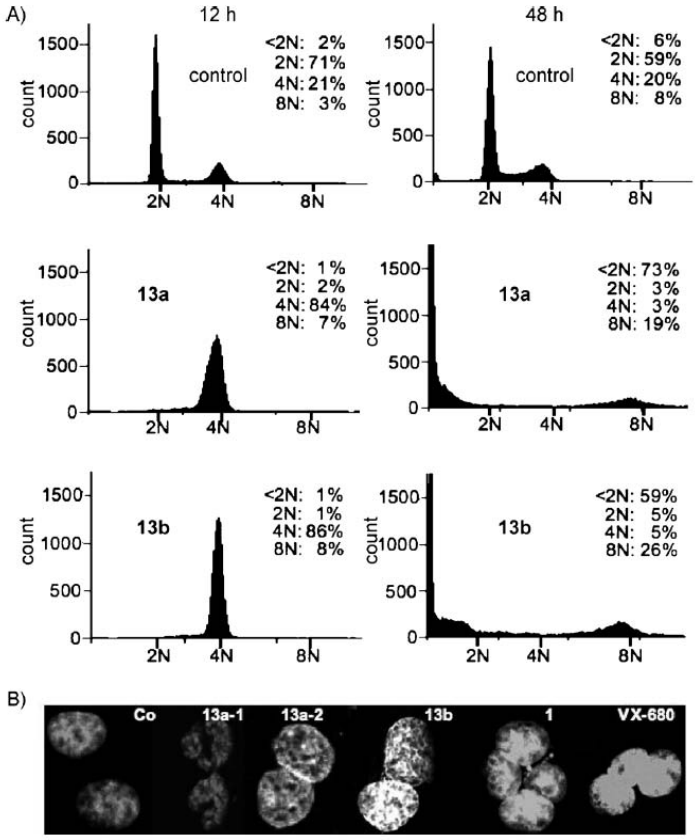

Figure 3. Cell-cycle repartition upon treatment with aurora kinase B inhibitors: A) FACS analyses show the repartition of synchronized HeLa cells treated by either **13a** or **13b** at 0.5 μM for 12 (left) and 48 h (right) in comparison with untreated cells (control). DNA was stained with propidium iodide, and the samples were analyzed with a FACS analyzer (Becton–Dickinson). The percentages of cells in various phases are indicated. B) Representative binucleated cells following 18 h treatment with **13a** and **13b** (500 nM). DNA was stained by Hoechst 33342 (Sigma–Aldrich). A bridge between the two nuclei is clearly visible at late telophase (**13a-1**). For comparison, micronuclei induced by compound **1** (1 μM) and VX-680 (300 nM) are shown.

aurora kinases without activity toward casein kinase 2. The best molecule, 8-ethyl-3-dimethylaminoethoxy-7*H*-10*H*-benzo[*e*]pyrido[4,3-*b*]indol-11-one maleate (**13bM**), is a hydrosoluble inhibitor of aurora kinases which exhibits antiproliferative activity in the nanomolar range. Furthermore, the optimized synthetic scheme developed and presented in this study is permissive for large-scale synthesis of this cell-permeable hydrosoluble molecule.

The antiproliferative potency of **13b** is similar to data reported for the best aurora kinase inhibitors currently in clinical trials (table S3, Supporting Information).[25] Based on cell proliferation capacity, compound **13b** was among the top 10 best aurora kinase inhibitors. The next step will include evaluation of this compound in preclinical cancer animal models. Although there are currently several aurora kinase inhibitors in clinical trials, additional molecules are expected to be tested in protocols when resistance to used drugs appears. Each inhibitor has a peculiar spectrum of off-target molecules; thus, different applications are expected for each aurora kinase inhibitor.

Experimental Section

Chemistry

General: All solvents were reagent grade, purchased from Sigma–Aldrich, and used without purification. All reactions were monitored by thin layer chromatography (TLC) using Merck 60 F_{254} pre-coated silica gel or neutral aluminum oxide plates. Flash column chromatography was performed with the indicated solvents using either silica gel 60 (particle size 0.035–0.070) or neutral alumina. Proton NMR spectra were recorded on a Bruker AC-300 (300 MHz) spectrometer at ambient temperature using an internal deuterium lock. Chemical shifts (δ) are reported in ppm (s, d, t, q, m, and br for singlet, doublet, triplet, quadruplet, multiplet, and broad, respectively). Elemental analyses and solubility measurements were performed by the Service Central de Microanalyse du CNRS, Gif-sur-Yvette (France) and the Plateforme de chimie biologique intégrative de Strasbourg, Illkirch (France), respectively.

Synthesis: The BePI structure with its numbering is shown in Scheme 1A. The syntheses of compounds **1**,[26] **2**–**3**,[27] **4**,[26] **5**,[28] **6**,[27] and **7**[29] have been described previously. The 3-hydroxy derivative **8** was obtained by demethylation of the corresponding methoxy precursor[27] and was esterified under standard conditions, resulting in benzoate derivative **9**. The syntheses of compounds **10**–**13** are shown in Scheme 1B. In alkali conditions, the condensation of 8-alkyl-11-chloro-3-hydroxy BePI derivatives **15a**[30] and **b** with 2-chloro-*N*,*N*-dimethylethanamine gave the corresponding 3-dimethylaminoethoxy intermediates **16** and **10**. Alternatively, starting from **15a**, under Mitsunobu conditions, intermediate **16** was also obtained using diisopropyl azodicarboxylate (DIAD), triphenylphosphine (PPh_3), and 2-(dimethylamino)etha-

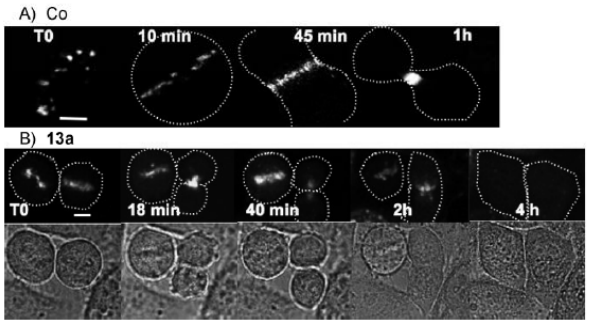

Figure 4. Time-lapse microscopy of mitotic HeLa cells expressing the aurora B–GFP fusion protein were performed in the A) absence (Co: control) or B) presence of **13a** (500 nM). The compound was added to the cell culture, and the mitotic cells were continuously imaged; representative photos are shown, taken at the times indicated. For clarification, cell shapes are outlined by white dotted lines. For cells treated with **13a**, both the fluorescent aurora B–GFP signal (top) and the corresponding transmission field (bottom) are shown at each indicated time. In the presence of **13a**, the two mitotic cells shown (T0) gave rise to two large spread cells (4 h). Three independent experiments were conducted, and at least 15 cells were followed in each case (bar: 5 μm).

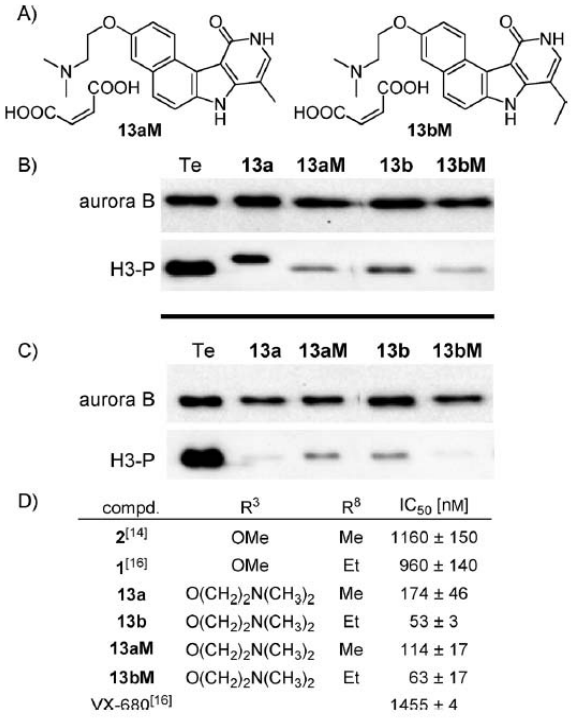

D)

compd.	R^3	R^8	IC_{50} [nM]
2[14]	OMe	Me	1160 ± 150
1[16]	OMe	Et	960 ± 140
13a	$O(CH_2)_2N(CH_3)_2$	Me	174 ± 46
13b	$O(CH_2)_2N(CH_3)_2$	Et	53 ± 3
13aM	$O(CH_2)_2N(CH_3)_2$	Me	114 ± 17
13bM	$O(CH_2)_2N(CH_3)_2$	Et	63 ± 17
VX-680[16]			1455 + 4

Figure 5. Effect of hydrosoluble benzo[*e*]pyridoindolones (**13a** and **13b**) in cells: A) The maleate salts corresponding to benzo[*e*]pyridoindolones **13a** and **13b** are shown as **13aM** and **13bM**, respectively. Their potency to inhibit aurora kinase B at 1 μM was evaluated in B) U2OS and C) HeLa cells (Te: Control). Blots were revealed by using an antibody against phospho-Ser10 histone H3 (H3-P); the same membrane was also revealed by using an antibody against aurora kinase B for estimation of the number of mitotic cells. D) Cell growth and viability were tested under standard conditions in 96-well culture plates with the MTT cell viability assay (Promega). Average IC_{50} values ±SD of three independent experiments are listed; data for **1**, **2**, and VX-680 were reported previously by Hoang et al.,[14,16] and are indicated for comparison. The lateral chain of each molecule is noted, with the six molecules bearing an oxo group at position 11.

nol. These methods provide flexibility for the introduction of various side chains. The conversion of 11-chloro intermediate **16** to the final pyridone **13a** was initially carried out in a two-step transformation via demethylation by HCl/AcOH of methoxy derivative **11**. Alternatively, experiments using either acetic anhydride or acetic acid in the presence of NaOAc were found to be convenient, as the final products, **13a** and **13b**, were obtained in a single step from chloro intermediates **16** or **10** (Scheme 1B). However, the latter method is preferred, as it resulted in higher yields, and the purification of the final compounds was easier. Finally, 11-unsubstituted compound **12** was synthesized from chloro derivative **16** by palladium-catalyzed hydrogenation. All compounds were fully characterized by MS and NMR. Microanalyses ensured the purity of compounds.

3-Hydroxy-8-methyl-7*H*,10*H*-benzo[*e*]pyrido[4,3-*b*]indol-11-one (8): A mixture of 3-methoxy-8-methyl-7*H*,10*H*-benzo[*e*]pyrido[4,3-*b*]indol-11-one[27] (83 mg, 0.3 mmol), benzyltriethylammonium chloride (480 mg, 2.1 mmol) and 37% HCl (4 mL) was heated in a 5 mL sealed tube in an oil bath at 140 °C for 24 h. The reaction mixture was evaporated in vacuo, then H_2O (10 mL) was added. The medium was rendered basic by addition of 28% NH_4OH (1 mL), and the resulting solid was collected by filtration, washed with H_2O, and then dried using a vacuum desiccator. The intermediate (3-hydroxy-8-methyl-7*H*,10*H*-benzo[*e*]pyrido[4,3-*b*]indol-11-one) was obtained as a brown powder (yield: 50 mg, 63% yield): ^{1}H NMR ([D$_6$]DMSO) δ = 11.95 (br s, 1H), 10.88 and 10.86 (2 br s, 1H), 10.18 (d, 1H), 9.38 (br s, 1H), 7.68–7.50 (m, 2H), 7.21–7.16 (m, 1H), 7.12–7.03 (m, 2H), 2.29 ppm (s, 3H); MS: 265.2 [*M*+H]; Anal. calcd for $C_{16}H_{12}N_2O_2 \cdot 0.5\,H_2O$: C 70.33, H 4.76, N 10.25, found: C 70.81, H 4.89, N 9.96.

3-Benzoyloxy-8-methyl-7*H*,10*H*-benzo[*e*]pyrido[4,3-*b*]indol-11-one (9): A mixture of 3-hydroxy-8-methyl-7*H*,10*H*-benzo[*e*]pyrido[4,3-*b*]indol-11-one (35 mg, 0.13 mmol), benzoic anhydride (140 mg, 0.6 mmol), and pyridine (1 mL) was heated in an oil bath at 135 °C for 1 h. The volatile material was co-evaporated with toluene in vacuo. H_2O (5 mL) was added, and the medium alkalinized with solid $NaHCO_3$. The liquid was discarded, and the residue was washed with H_2O (2×2 mL), then boiling EtOH was added (4 mL). The resulting precipitate was filtered, washed with a minimal amount of EtOH, and then dried in vacuo to give the expected compound (yield: 20 mg, 41%): ^{1}H NMR ([D$_6$]DMSO) δ = 12.22 (s, 1H), 11.03 & 11.01 (2 s, 1H), 10.48 (d, 1H), 9.26–8.19 (m, 2H), 7.87 (d, 1H), 7.85–7.75 (m, 3H), 7.68–7.61 (m, 2H), 7.78 (dd, 1H), 7.14 (d, 1H), 2.32 ppm (s, 3H); MS: 367.1 [*M*−H]; Anal. calcd for $C_{23}H_{16}N_2O_3 \cdot 0.25\,H_2O$: C 74.09, H 4.43, N 7.52, found: C 73.76, H 4.46, N 7.29.

11-Chloro-3-(2-*N*,*N*-dimethylaminoethoxy)-8-ethyl-7*H*-benzo[*e*]pyrido[4,3-*b*]indole (10): *Step 1:* In a sealed 50 mL tube, a mixture of 11-chloro-8-ethyl-3-methoxy-7*H*-benzo[*e*]pyrido[4,3-*b*]indole **14b**[26] (600 mg, 1.9 mmol), benzyltriethylammonium chloride (2.80 g, 12 mmol), and 37% HCl (45 mL) was heated in an oil bath at 140 °C for 24 h. The reaction mixture was evaporated in vacuo, then H_2O (10 mL) was added. The medium was basified by addition of 28% NH_4OH (2 mL), and the resulting solid was collected by filtration, then washed with H_2O and dried using a vacuum desiccator to yield intermediate 11-chloro-8-ethyl-3-hydroxy-7*H*-benzo[*e*]pyrido[4,3-*b*]indole (**15b**) as a brown powder (yield: 450 mg, 78%); MS: 296.1/298.1 [*M*+H]; Anal. calcd for $C_{17}H_{13}ClN_2O \cdot 0.25\,H_2O$: C 67.78, H 4.52, N 9.30, found: C 67.90, H 4.62, N 9.56.

Step 2: The protocol described for the synthesis of compound 11-chloro-3-(2-*N*,*N*-dimethylaminoethyloxy)-8-methyl-7*H*-benzo[*e*]pyrido[4,3-*b*]indole **16** by method 1 was applied, starting from 11-chloro-3-hydroxy-8-ethyl-7*H*-benzo[*e*]pyrido[4,3-*b*]indole and using 2-chloro-*N*,*N*-dimethylethanamine hydrochloride to give the title compound (yield: 37% yield): ^{1}H NMR ($CDCl_3$) δ = 9.76 (d, 1H), 8.73 (br s, 1H), 8.13 (s, 1H), 7.86 (d, 1H), 7.62 (d, 1H), 7.43–7.34 (m, 2H), 4.25 (t, 2H), 2.97 (q, 2H), 2.84 (t, 2H), 2.40 (s, 6H), 1.46 ppm (t, 3H); MS: 368.2 and 370.2 [*M*+H].

11-Methoxy-3-(2-*N*,*N*-dimethylaminoethoxy)-8-methyl-7*H*-benzo[*e*]pyrido[4,3-*b*]indole (11): A mixture of 11-chloro-3-(2-*N*,*N*-dimethylaminoethoxy)-8-methyl-7*H*-benzo[*e*]pyrido[4,3-*b*]indole **16** (80 mg, 0.22 mmol) and 30% NaOMe in MeOH (12 mL) was heated in a 25 mL sealed tube in an oil bath at 130 °C for 48 h. The reaction mixture was cooled, poured into H_2O (30 mL), and extracted with CH_2Cl_2. The organic layer was washed with brine, dried over $MgSO_4$, and evaporated in vacuo. The residue was purified by flash chromatography (neutral alumina, EtOAc gradient from 0 to 20% in CH_2Cl_2) to give the methoxy compound **11** (yield: 75 mg, 94%): ^{1}H NMR ($CDCl_3$) δ = 9.64 (d, 1H), 8.82 (br s, 1H), 7.85 (s, 1H), 7.73 (d,

1H), 7.58 (d, 1H), 7.35 (dd, 1H), 7.30 (d, 1H), 4.27–4.22 (m, 5H), 2.83 (t, 2H), 2.46 (s, 3H), 2.39 ppm (s, 6H).

3-(2-*N*,*N*-Dimethylaminoethyloxy)-8-methyl-7*H*-benzo[*e*]pyrido-[4,3-*b*]indole (12): Pd/C (10%, 150 mg) was added to a solution of 11-chloro-3-(2-*N*,*N*-dimethylaminoethyloxy)-8-methyl-7*H*-benzo[*e*]-pyrido[4,3-*b*]indole **16** (300 mg, 0.84 mmol) in absolute EtOH (30 mL). At atmospheric pressure, hydrogen was introduced, and the mixture was stirred for 18 h at room temperature. The catalyst was then removed by filtration, washed with hot EtOH, and the solvent was removed under reduced pressure. The residue was purified by flash chromatography (neutral alumina, EtOH gradient from 0 to 2% in CH_2Cl_2) to give the expected compound **12** as a beige solid (190 mg, 71%): ^{1}H NMR ([D$_6$]DMSO) δ = 12.39 (s, 1H), 9.73 (s, 1H), 8.77 (d, 1H), 8.37 (s, 1H), 7.99 (d, 1H), 7.86 (d, 1H), 7.68 (d, 1H), 7.47 (dd, 1H), 4.48 (t, 2H), 2.79 (s, 6H), 2.65 (s, 3H), 2.53 ppm (m, 2H); Anal. calcd for $C_{20}H_{21}N_3O{\cdot}0.25H_2O$: C 74.18, H 6.64, N 12.98, found: C 74.21, H 6.67, N 12.71.

11-Chloro-3-(2-*N*,*N*-dimethylaminoethoxy)-8-methyl-7*H*-benzo[*e*]-pyrido[4,3-*b*]indole (16): A mixture of 11-chloro-3-hydroxy-8-methyl-7*H*-benzo[*e*]pyrido[4,3-*b*]indole **15a**[30] (400 mg, 1.4 mmol), *n*BuOH (40 mL), and H_2O (24 mL) was stirred for 30 min at room temperature, then a solution of NaOH (300 mg) in H_2O (5 mL) was added. Stirring was continued for an additional 15 min, then 2-chloro-*N*,*N*-dimethylethanamine hydrochloride (240 mg, 1.7 mmol) was added, and the mixture was heated at reflux for 1 h. The reaction mixture was cooled and the organic layer was separated. The aqueous layer was extracted with EtOAc, and the organic layers were combined, washed with brine, dried over $MgSO_4$, and evaporated in vacuo. The residue was purified by flash chromatography (neutral alumina, EtOH gradient from 0 to 2% in CH_2Cl_2) to give the expected compound as a beige solid (yield: 220 mg, 44%): ^{1}H NMR ($CDCl_3$) δ = 9.76 (d, 1H), 8.79 (brs, 1H), 8.10 (s, 1H), 7.85 (d, 1H), 7.62 (d, 1H), 7.39 (dd, 1H), 7.35 (d, 1H), 4.24 (t, 2H), 2.83 (t, 2H), 2.56 (s, 3H), 2.40 ppm (s, 6H); Anal. calcd for $C_{20}H_{20}ClN_3O{\cdot}0.7H_2O$: C 65.64, H 5.85, N 11.48, found: C 65.29, H 5.49, N 11.31.

3-(2-*N*,*N*-Dimethylaminoethoxy)-8-methyl-7*H*,10*H*-benzo[*e*]pyrido[4,3-*b*]indol-11-one (13a): A mixture of 11-chloro-3-(2-*N*,*N*-dimethylaminoethoxy)-8-methyl-7*H*-benzo[*e*]pyrido[4,3-*b*]indole **16** (290 mg, 0.82 mmol), NaOAc (172 mg, 2.1 mmol), and AcOH (16 mL) was heated at reflux for 18 h. The volatile material was first evaporated in vacuo, then co-evaporated with toluene. H_2O (100 mL) was added, and the medium was basified by addition of NaOH (2 N). The aqueous layer was extracted with EtOAc and EtOH, dried over $MgSO_4$,and evaporated in vacuo to give the free base **13a** (yield: 274 mg, 100%): ^{1}H NMR ($CDCl_3$) δ = 10.28 (d, 1H), 8.89 (brs, 1H), 8.60 (brs, 1H), 7.70 (d, 1H), 7.56 (d, 1H), 7.37 (dd, 1H), 7.29 (d, 1H), 7.02 (s, 1H), 4.24 (t, 2H), 2.84 (t, 2H), 2.40 (s, 6H), 2.35 ppm (s, 3H); ^{13}C NMR ([D$_6$]DMSO) δ = 159.97, 154.67, 144.21, 133.64, 130.85, 129.97, 128.01, 124.44, 123.64, 119.48, 116.67, 113.24, 108.83, 108.14, 103.01, 65.61, 57.81, 45.57, 13.18; MS: 336.3 ppm [*M*+H]; Anal. calcd for $C_{20}H_{21}N_3O_2{\cdot}1.8H_2O$: C 65.32, H 6.69, N 11.43, found: C 65.36, H 6.28, N 11.17.

3-(2-*N*,*N*-Dimethylaminoethoxy)-8-methyl-7*H*,10*H*-benzo[*e*]pyrido[4,3-*b*]indol-11-one maleate (13aM): A solution of the free base **13a** (120 mg) in boiling absolute EtOH (10 mL) was poured into a solution of maleic acid (50 mg) in hot absolute EtOH (2 mL). The resulting homogenous solution was evaporated in vacuo, and the residue was triturated with acetone. The resulting solid was collected by filtration, washed with acetone, and dried in a desiccator to afford maleate salt **13aM** (yield: 160 mg, 99%): Anal. calcd for $C_{20}H_{21}N_3O_2{\cdot}C_4H_4O_4{\cdot}0.5H_2O$: C 62.61, H 5.65, N 9.31, found: C 62.51, H 5.80, N 9.42.

3-(2-*N*,*N*-Dimethylaminoethoxy)-8-ethyl-7*H*,11*H*-benzo[*e*]pyrido-[4,3-*b*]indol-11-one (13b): The method described above for the synthesis of **13a** was applied, starting from compound **10**, to give the free base **13b** (yield: 100%): ^{1}H NMR ([D$_6$]DMSO) δ = 12.02 (s, 1H), 10.98 and 10.96 (2s, 1H), 10.27 (d, 1H), 7.74–7.67 (m, 2H), 7.40 (d, 1H), 7.18 (dd, 1H), 7.05 (d, 1H), 4.17 (t, 2H), 2.77–2.67 (m, 4H), 2.26 (s, 6H), 1.27 ppm (t, 2H); ^{13}C NMR ([D$_6$]DMSO) δ = 159.91, 154.64, 143.43, 133.65, 130.82, 129.95, 126.96, 124.43, 123.60, 119.41, 116.65, 113.25, 109.25, 108.97, 108.15, 65.59, 57.82, 45.58, 20.48, 13.85 ppm; MS: 350.1 [*M*+H]; Anal. calcd for $C_{21}H_{23}N_3O_2{\cdot}H_2O$: C 68.66, H 6.81, N 11.44, found: C 68.96, H 6.78, N 11.36.

3-(2-*N*,*N*-Dimethylaminoethoxy)-8-ethyl-7*H*,11*H*-benzo[*e*]pyrido-[4,3-*b*]indol-11-one maleate (13bM): A solution of free base **13b** (120 mg) in boiling absolute EtOH (12 mL) was poured into a solution of maleic acid (62 mg) in hot absolute EtOH (2 mL). The resulting homogenous solution was evaporated in vacuo, and the residue was triturated with acetone. The resulting solid was collected by filtration, washed with acetone, and dried in a desecrator to afford maleate salt **13bM** (yield: 147 mg, 92%): Anal. calcd for $C_{21}H_{23}N_3O_2{\cdot}C_4H_4O_4{\cdot}0.25H_2O$: C 63.89, H 5.85, N 8.94, found: C 63.41, H 6.28, N 8.76.

Solubility: The solubility of **13aM** and **13bM** was estimated by the "shake-flask" method[31] on a TechMed platform (Strasbourg, France). Briefly, 1 mg of compound was dissolved in 100 µL of H_2O, and the mixture was stirred for 1 h at room temperature and then centrifuged. The supernatant was diluted 1:100 in H_2O/MeCN (1:1). The concentration of the supernatant was analyzed by HPLC and compared with the stock solution in DMSO. Under these conditions, the solubility was estimated to be >22.8 and 24.8 mM for **13aM** and **13bM**, respectively, knowing that saturation was not obtained under such conditions.

Biology

In vitro kinase assay: Kinase assays were performed by Reaction Biology (USA). The assay included recombinant human aurora kinases A or B, the peptide substrate [H-LRRASLG], and [^{33}P]ATP (1 µM, specific activity: 0.01 µCi µL^{-1}). The reaction buffer used for these experiments contained 10 mM $MgCl_2$, 1 mM EGTA, 0.02% Brij 35, 0.02 mg mL^{-1} BSA, 0.1 mM Na_3VO_4, 2 mM DTT, 1% DMSO, and 20 mM HEPES at pH 7.5. IC_{50} values were determined through a ten-dose assay, starting at a compound concentration of 2 µM, with a dilution factor of 3. The pan-kinase inhibitor staurosporine was used as an internal control. Kinase profiling was performed with **13a** under similar conditions at the MRC (Dundee) with a panel of 121 kinases; the concentration of **13a** was 1 µM.

Cell culture: HeLa cells were grown in DMEM (1 g L^{-1} glucose) supplemented with 10% heat-inactivated fetal bovine serum (Gibco–Invitrogen), L-glutamine (2 mM), penicillin (100 UI mL^{-1}), and streptomycin (100 µg mL^{-1}). HeLa (aurora–GFP) stable cell lines have already been described elsewhere.[32] Cell proliferation assays were conducted in 96-well culture plates. Assays were run in triplicate. Serial dilutions of compounds were prepared from 10 nM to 2 and the viable cell number was determined at day 4 by the addition of MTT cell counting (Promega).

Western blot: Cells were treated with compounds, then harvested and lysed in 9 M urea, supplemented with LaemmLi sample buffer as previously described.[32] Western blotting was performed using

the following antibodies: rabbit anti-phospho-histone H3 (Ser10) (Upstate, 1:2000), rabbit anti-aurora B (Epitomics, 1:4000), mouse anti-actin (Sigma, 1:5000) and mouse anti-tubulin (Sigma, 1:5000). Bands were visualized using horseradish peroxidase-labeled antibodies and the ECL technique (Amersham Bioscience).

Cell-cycle analysis: HeLa cells were synchronized at the S phase of the cell cycle by serum starvation for 48 h and by subsequent thymidine treatment (3 mM) for 20 h. After release, cells were treated with **13a** and **13b** (0.5 μM) for 12 h and 48 h. For determination of cell-cycle profiles, cells were fixed by ice-cold 70% EtOH for 1 h, then incubated with propidium iodide solution (50 mL^{-1}) in the presence of 0.2 $mg\,mL^{-1}$ RNase for 15 min at 37 °C. DNA content was measured using a FACS flow cytometer (Becton–Dickinson, San Diego, CA, USA) and CellQuest software.

Immunofluorescence: U2OS cells were seeded on glass coverslips and treated with compounds at a concentration of 1 μM for 20 h. Immunofluorescence was performed as described in Ref. [33]. The primary antibody used was phospho-histone H3 (Ser10; Upstate, 1:2000). Specific staining was revealed using Hylite Fluor488-conjugated secondary antibodies (Anaspec). DNA was visualized with 0.1 mM Hoechst33342 (Sigma–Aldrich). Images were collected with a ZEISS 510 laser scanning confocal microscope with a 63× oil-immersion objective. Slices of 0.5 μm are shown.

Time-lapse experiments: Ex vivo experiments were conducted on HeLa cells grown on Lab-Tek chambered cover glass (Nalge Nunc International) and maintained under standard culture conditions as described in Ref. [14,33]. Images were acquired on a Zeiss LSM510 system using a Planapochromat 40× water-immersion objective. GFP was excited with a 488 nm Argon 2 laser (power varying from 0.1 to 2%). In each experiment, approximately 15 mitotic cells were followed, and three independent experiments were performed. Representative confocal slices are shown.

Acknowledgements

L.-T.-T.L. and H.-L.V. were supported by a Vietnam/France program. This work was supported by INSERM, UJF, CNRS, and Institut Curie, and we also acknowledge La Ligue Nationale contre le Cancer (Equipe labelisée La Ligue, Stéfan Dimitrov). Microscopy experiments were conducted at the IBISA platform of the CRI INSERM/UJF U823. We thank Thierry Pagnier and Kiran Padmanabhan (CNRS and INSERM, respectively) for editorial assistance. The authors declare no competing financial interests.

Keywords: antitumor agents · aurora kinases · cancer · inhibitors · structure–activity relationships

[1] G. Vader, S. M. A. Lens, *Biochim. Biophys. Acta. Rev. Cancer* **2008**, *1786*, 60–72.
[2] M. Carmena, S. Ruchaud, W. C. Earnshaw, *Curr. Opin. Cell Biol.* **2009**, *21*, 796–805.
[3] T. Sardon, I. Peset, B. Petrova, I. Vernos, *EMBO J.* **2008**, *27*, 2567–2579.
[4] E. Hannak, M. Kirkham, A. A. Hyman, K. Oegema, *J. Cell Biol.* **2001**, *155*, 1109–1116.
[5] A. Seki, J. A. Coppinger, C.-Y. Jang, J. R. Yates, G. Fang, *Science* **2008**, *320*, 1655–1658.
[6] S. M. A. Lens, R. H. Medema, *Cell Cycle* **2003**, *2*, 507–510.
[7] A. T. Saurin, M. S. van der Waal, R. H. Medema, S. M. A. Lens, G. J. P. L. Kops, *Nat. Commun.* **2011**, *2*, 316.
[8] M. Mendoza, C. Norden, K. R. Durrer, H. F. Uhlmann, Y. Barral, *Nat. Cell Biol.* **2009**, *11*, 477–483.
[9] S. Sen, H. Zhou, R. A. White, *Oncogene* **1997**, *14*, 2195–2200.
[10] L. Garuti, M. Roberti, G. Bottegoni, *Curr. Med. Chem.* **2009**, *16*, 1949–1963.
[11] F. Girdler, K. E. Gascoigne, P. A. Eyers, S. Hartmuth, C. Crafter, K. M. Foote, N. J. Keen, S. S. Taylor, *J. Cell Sci.* **2006**, *119*, 3664–3675.
[12] J. R. Jackson, D. R. Patrick, M. M. Dar, P. S. Huang, *Nat. Rev. Cancer* **2007**, *7*, 107–117.
[13] C. Soncini, P. Carpinelli, L. Gianellini, D. Fancelli, P. Vianello, L. Rusconi, P. Storici, P. Zugnoni, E. Pesenti, V. Croci, *Clin. Cancer Res.* **2006**, *12*, 4080–4089.
[14] T. M.-N. Hoang, B. Favier, A. Valette, C. Barette, C. H. Nguyen, L. Lafanechère, D. S. Grierson, S. Dimitrov, A. Molla, *Cell Cycle* **2009**, *8*, 765–772.
[15] G. M. T. Cheetham, P. A. Charlton, J. M. C. Golec, J. R. Pollard, *Cancer Lett.* **2007**, *251*, 323–329.
[16] N. T. M. Hoang, M. Delacour-Larose, A. Molla, *Curr. Enzyme Inhib.* **2008**, *4*, 153–159.
[17] H.-L. Vu, T. M. N. Hoang, B. Favier, A. Molla, *Curr. Enzyme Inhib.* **2010**, *6*, 19–25.
[18] J. L. Mergny, G. Duval-Valentin, C. H. Nguyen, L. Perrouault, B. Faucon, M. Rougée, T. Montenay-Garestier, E. Bisagni, C. Hélène, *Science* **1992**, *256*, 1681–1684.
[19] C. Escudé, C. H. Nguyen, S. Kukreti, Y. Janin, J.-S. Sun, E. Bisagni, T. Garestier, C. Hélène, *Proc. Natl. Acad. Sci. USA* **1998**, *95*, 3591–3596.
[20] M. C. Bissery, C. H. Nguyen, E. Bisagni, P. Vrignaud, F. Lavelle, *Invest. New Drugs* **1993**, *11*, 263–277.
[21] J. F. Riou, P. Fossé, C. H. Nguyen, A. K. Larsen, M. C. Bissery, L. Grondard, J. M. Saucier, E. Bisagni, F. Lavelle, *Cancer Res.* **1993**, *53*, 5987–5993.
[22] R. Prudent, V. Moucadel, C.-H. Nguyen, C. Barette, F. Schmidt, J.-C. Florent, L. Lafanechère, C. F. Sautel, E. Duchemin-Pelletier, E. Spreux, *Cancer Res.* **2010**, *70*, 9865–9874.
[23] S. H. Baek, *Mol. Cell* **2011**, *42*, 274–284.
[24] J. Bain, L. Plater, M. Elliott, N. Shpiro, C. J. Hastie, H. McLauchlan, I. Klevernic, J. S. C. Arthur, D. R. Alessi, P. Cohen, *Biochem. J.* **2007**, *408*, 297–315.
[25] M. Kollareddy, D. Zheleva, P. Dzubak, P. S. Brahmkshatriya, M. Lepsik, M. Hajduch, *Invest. New Drugs* **2012**, *30*, 2411–2432.
[26] C. H. Nguyen, E. Bisagni, F. Lavelle, M. C. Bissery, C. Huel, *Anticancer Drug Des.* **1992**, *7*, 219–233.
[27] C. H. Nguyen, J. M. Lhoste, F. Lavelle, M. C. Bissery, E. Bisagni, *J. Med. Chem.* **1990**, *33*, 1519–1528.
[28] C. Escudé, C. H. Nguyen, J.-L. Mergny, J.-S. Sun, E. Bisagni, T. Garestier, C. Hélène, *J. Am. Chem. Soc.* **1995**, *117*, 10212–10219.
[29] C. H. Nguyen, C. Marchand, S. Delage, J.-S. Sun, T. Garestier, C. Hélène, E. Bisagni, *J. Am. Chem. Soc.* **1998**, *120*, 2501–2507.
[30] S. Vinogradov, V. Roig, Z. Sergueeva, C. H. Nguyen, P. Arimondo, N. T. Thuong, E. Bisagni, J.-S. Sun, C. Hélène, U. Asseline, *Bioconjugate Chem.* **2003**, *14*, 120–135.
[31] A. Avdeef, *Adv. Drug Delivery Rev.* **2007**, *59*, 568–590.
[32] M. Delacour-Larose, M.-N. H. Thi, S. Dimitrov, A. Molla, *Cell Cycle* **2007**, *6*, 1878–1885.
[33] M. Delacour-Larose, A. Molla, D. A. Skoufias, R. L. Margolis, S. Dimitrov, *Cell Cycle* **2004**, *3*, 1418–1426.

Received: October 19, 2012
Published online on December 28, 2012

2.2. DEVELOPMENT OF NEW HYDROSOLUBLE BENZOPYRIDOINDOLONES WITH THE HIGH ANTI-PROLIFERATIVE ACTIVITY

With the aim of developing new hydrosoluble compounds, we continued to focus on the alternatives of O-alkylamino chain at position 3 of the benzo[e]pyridoindolone scaffold. Three new compounds (named C710, C07, C711) were designed as in Figure 31 and their potencies were evaluated through firstly aurora kinase B inhibition and then, anti-proliferation assays in cell.

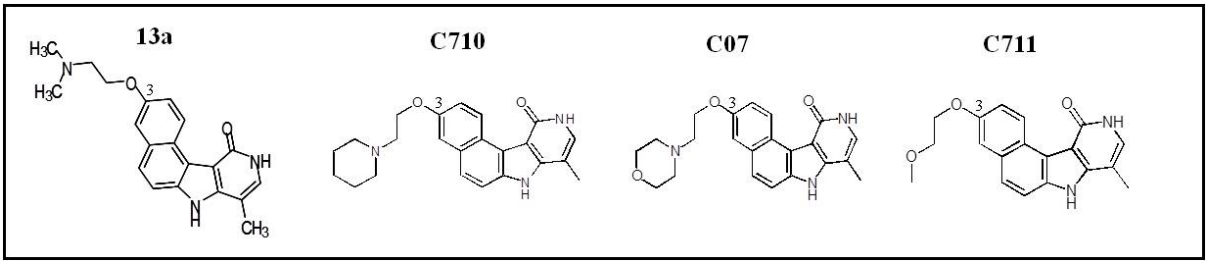

Figure 31: Structure of new benzo[e]pyridoindolones

At position 3, a piperidine-ethoxy group, morpholin-ethoxy group and methoxy-ethoxy group replaced the amino-ethoxy group present in compound **13a**. These molecules were respectively named C710, C07 and C711.

2.2.1. Evaluating aurora B inhibition potency of these new compounds in cell

Aurora kinase B activity was determined by western blot and by immunofluorescence analysis, through the histone H3 phosphorylation on Serine 10 as substrate (Figure 32).

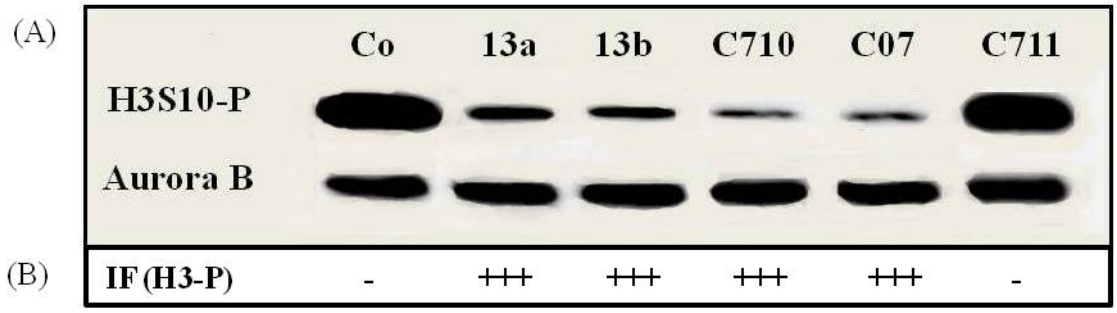

Figure 32: Comparison of the aurora B inhibition in HeLa cell

(A) HeLa cells were incubated with Nocodazole (0.1 mg/ml, 15 h) in the presence of either DMSO (Co) or compounds (0.5 µM, 24 h) as indicated. The western Blot was performed with an antibody against phosphorylated histone H3 on serine 10, a marker of aurora B kinase activity. The same membrane was also revealed with an antibody against aurora B for estimation of the amount of mitotic cells. (B) Immunofluorescence (IF) were performed under the same conditions as in (A) and both phospho-Histone H3 and DNA were detected. The percentage of phospho-Ser10-Histone H3 (H3-P) is qualitatively represented as follows: (+++) indicates strong inhibition with no positive mitosis detected, whereas (-) reveals no inhibition. Two different experiments were performed and 100 mitotic cells were scored.

From figure 32, we realized that the replacement of the [-O-CH_2CH_2N-$(CH_2)_2$] chain by the [-O-CH_2CH_2-O-CH_3] group at position 3 (compound C711) resulted in a complete loss of inhibitory potency. The amino group seems therefore to be required for aurora B kinase inhibition. The cyclisation of the amino-chain increases the inhibition potency (comparison of C13a with C710 and C07) (Fig. 32A).

Based on this result, the corresponding hydrosoluble maleate salts were synthesized and named C710M and C07M, respectively (Fig. 33A). Their effect on aurora kinase B was evaluated by western blot analysis with phospho-serine10 histone H3 marker. The results in Figure 33B showed that both compounds inhibited aurora B activity as their free base counterparts.

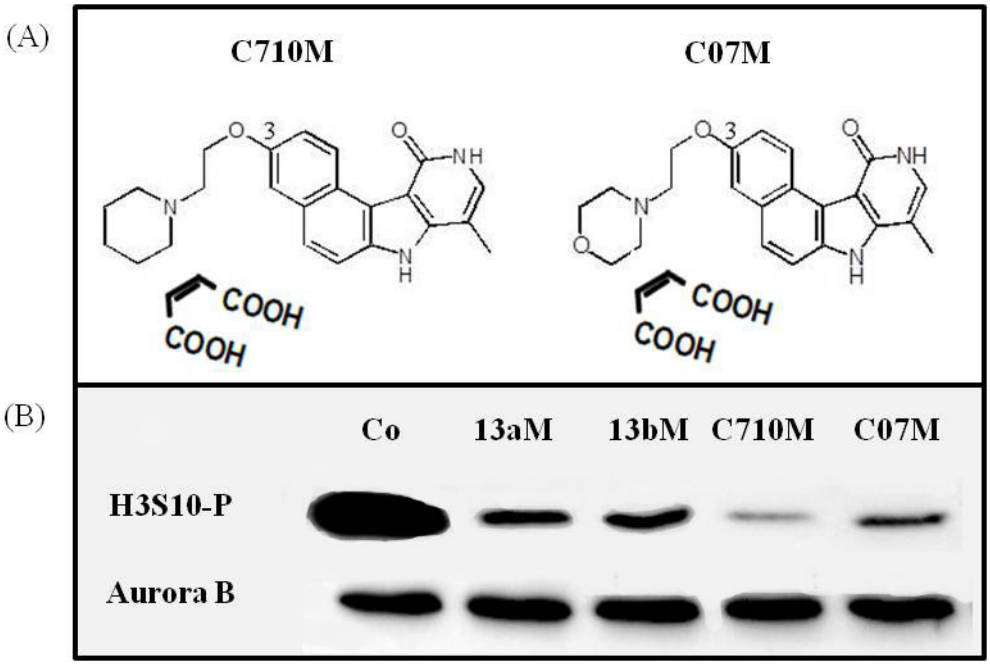

Figure 33: Aurora B inhibition efficiency of hydrosoluble compounds.

(A) The C710M and C07M hydrosoluble maleate salts are shown.

(B) Western blott revealing aurora B activity in HeLa cells without treatment (Co) or in the presence of benzo[e]pyridindolone maleate salts (13aM, 13bM, C710M and C07M; 0.5 µM for 20 h). Simultaneously, mitotic cells were enriched by Nocodazole (0.1 µg/mL for 14 h). Aurora B signal is used to quantify the proportion of mitotic cells.

2.2.2. Evaluating the anti-proliferative activity of the compounds

As aurora kinase B plays a key role in mitotic progression, its inhibition could lead to disorders in mitosis and results in non-proliferation of cells. We thus evaluated the anti-proliferative activity of these new compounds through the viability of tumor HeLa cells, upon 96h treatment.

The anti-proliferative activity of the former identified compound 13a and 13b is recalled in Table 11 for comparison. Among the two novel molecules, C710 is two fold more potent than C07 for preventing HeLa cell proliferation, IC50 value of 72 nM and 155 nM were respectively determined. The anti-proliferative potencies of C710M and 13bM are quite similar, respective cell-IC50 of 83 nM and 77 nM were determined.

IC50 (nM) in HeLa cell		
	Free-base	Hydro-soluble (*M)
13a	102 ± 20	131 ± 38
13b	119 ± 49	77 ± 19
C710	72 ± 6	83 ± 8
C07	155 ± 45	335 ± 35

Table 11: Comparision of the anti-proliferative activities of compounds in HeLa cell

IC50: the concentration of compound that reduced by half cell proliferation after 96 h of compound treatment. Both the free base as well as the hydrosoluble maleate salt (-M) of each compound were evaluated. Note that most results with the free base and the corresponding salt are similar at the exception of a slight increase for CO7M compared to CO7.

We have thus identified new hydrosoluble inhibitors of aurora kinase B that exhibited anti-proliferative activity. Taking into account that 13b was partly described in Le et al. (2013), we decided to evaluate the potency and consequences of C710 treatment in cells to compare it with 13b and to evaluate the possible applications of these new molecules.

CHAPTER 3

CHARACTERIZATION OF BENZO[e]PYRIDOINDOLONE C710M EXHIBITING HIGH ANTI-PROLIFERATIVE ACTIVITY

3.1. ANTI-PROLIFERATIVE EFFICIENCY OF C710M IN CELLS

In the previous chapter, we showed that C710M inhibited aurora kinase B and prevented efficiently the growth of HeLa cells. To better describe its anti-proliferative potency, we continued to evaluate the viability of a panel of cell-lines upon C710M treatment (Table 12).

Mahlavu cells, a liver cancer model, showed high sensitivity to C710M with an in-cell IC50 of 84 ± 6 nM, similar to data obtained with HeLa cells. Besides, C710M also inhibited efficiently the growth of many cancer cell-lines originating from different organs such as Jurkat (T lymphocyte), MCF-7 (breast), Hek293 (kidney), Hct116 (colon) and A431 (skin) with IC50 values of 133 nM, 138 nM, 210 nM, 347 nM and 350 nM, respectively. However, its impact seemed not to be identical among cell-lines from the same organs. C710M exhibited poor potency towards Focus (liver), SKMel28 (skin), WM793 (skin), BT20 (breast) or BL41 (lymphoma) cells. Interestingly, its effect was not related to p53 pathway since the cell-proliferative inhibition by C710M between Hct116 p53(+) and p53(-) cells was not different (data not shown). Moreover, C710M had no effect on lung cancer cells (H358), conversely to what was observed with C1 in the past.

Cell line	Tissue/Cancer	IC50 of C710M (nM)
HeLa	Cervix /carcinoma	83 ± 8
Malhavu	Liver/carcinoma	84 ± 6
JurKat	T lymphocyte/T cell leukemia	133
MCF-7	Breast/adenocarcinoma	138
Hek293	Embryonic Kidney	210
Hct116	Colon/carcinoma	347 ± 4
A431	Skin/ epidermoid carcinoma	350
HaCaT	Skin/ keratinocyte	480
Hep3B	Liver/ carcinoma	950
U-251	Brain/ Glioblastoma	1195± 58
Focus	Liver/ carcinoma	1750
U87	Brain/ Glioblastoma	> 1000
SKMel28	Skin/ Melanoma	>2000
WM793	Skin / Melanoma	>2000
BT20	Breast/carcinoma	>2000
BL41	B cells/ Burkitt's Lymphoma	>2000
H358	Lung/carcinoma	>2500

Table 12: C710M anti-proliferative efficiency towards different cell-lines

(IC50: the concentration of compound reducing by half cell proliferation, after 96 hours of treatment)

2.2. EFFECT OF C710M ON CELL CYCLE PROGRESSION

In order to understand how C710M affected cell cycle progression, the behavior of cells in the presence of C710M was analyzed by FACS. HeLa cells were synchronized at S phase, and C710M (100 nM) was added upon release. The results of kinetics are reported in Figure 34. After 3 h of C710M treatment, there was no difference compared to the control, most of cells were in S phase (61% upon C710M treatment and 59% in control) and they started to enter mitosis. Eight hours after release, the bulk of the population was in mitosis; whereas in the control, some cells (16%) started a new cycle. The delay in mitosis exit induced by C710M was more clearly visible after 11 hours since 92 % of the cells were still scored as 4N. Meanwhile, in the control experiment, cells were cycling normally (52% in 2N population). Following the progression in the cell cycle, C710M had induced a major polyploidisation of the population after 30 h (65 % of the cells being scored as >4N) and finally, 72h later, the cells were dying (70 % scored as < 2N). In fact, C710M induced apoptosis since this cell population was stained by annexin V (data not shown).

Furthermore, the addition of C710M to HeLa cells upon release from a G_0/G_1 block did not influence mitotic entry. There were no differences in cell cycle progression in the presence and in the absence of C710M, till the cells were in mitosis (data not shown). Therefore, C710M was not involved in G_1 and S phase progression.

In order to understand how C710M inhibited ongoing mitosis and how polyploid cells were formed, time-lapse microscopy was performed on Hek293 cells stably expressing either Histone H2A-GFP or tubulin-GFP.

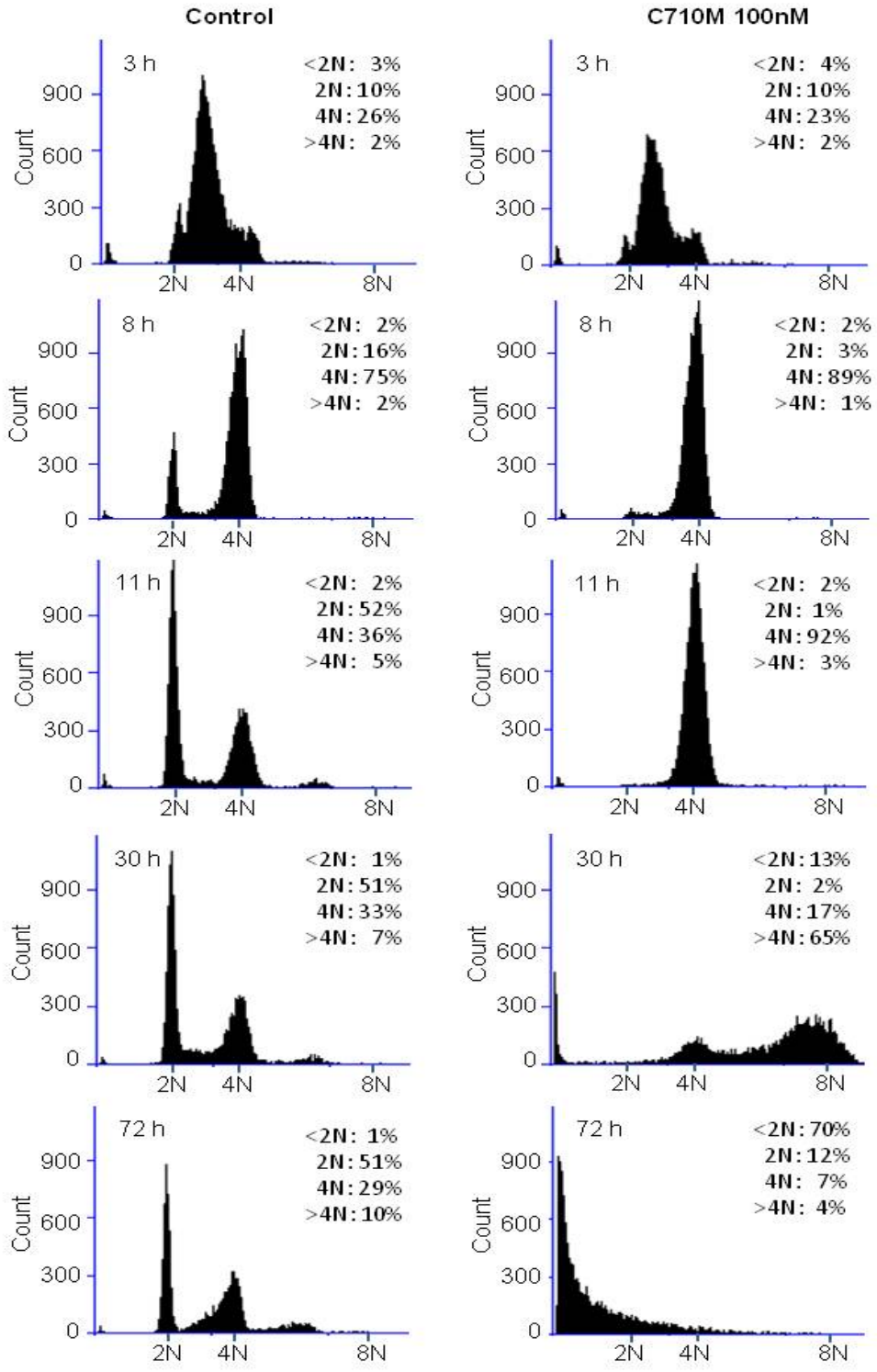

Figure 34: Effect of C710M on the cell cycle

FACS experiments were performed to show cell cycle progression upon C710M treatment in comparison to control (without C710M). HeLa cells were synchronized in S phase by serum deprivation (48 h) and then, by thymidine block (20 h). Upon release, they were incubated subsequently with C710M (100 nM; on the right) or DMSO as a control (on the left) for 3 h, 8 h, 11 h, 30 h and 72 h. DNA was stained with propidium iodide and samples were analyzed with a FACS analyzer. The percentage of cells in the different phases was indicated in each panel.

3.3. C710M REDUCES MITOTIC SPINDLES AND INDUCES THE FORMATION OF BI-NUCLEATED CELLS

Hek293 cells stably expressing tubulin-GFP and histone H2A-GFP were continuously imaged upon C710M treatment by Time-lapse microscopy as shown in Figure 35. We observed the shortening in pole-to-pole length of the spindle microtubules after 20 minutes of C710M treatment versus control (Fig.35A, T_0). Cells exhibited only a few kinetochore-microtubles and were unable to organize a ordered mitotic spindle as seen in control cells (Fig.35A, T 34 min). As a consequence, chromosomes could not be fully separated and cells escaped mitosis as large binucleated cells (Fig.35B, T 2 h).

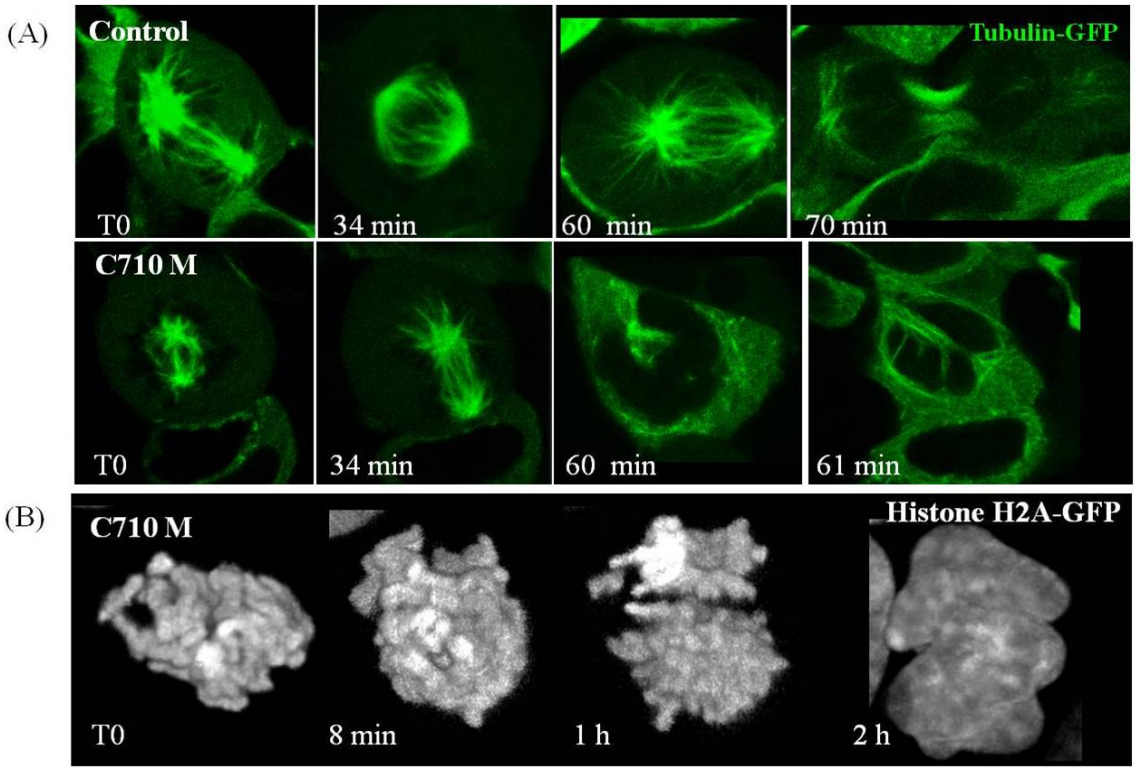

Figure 35: Time-lapse experiments on mitotic cells in the presence or the absence of C710M (200 nM) (A) on Hek293 cells stably expressing Tubulin-GFP. C710M was added 20 minutes before imaging. Mitotic cells were continuously imaged and elapsed time is indicated on each photo. Representative cells are shown. (B) Time lapse of mitotic Hek cells stably expressing Histone-H2A-GFP in the presence of C710M (200 nM). The prometaphase, imaged at T0, gave rise to a binucleated cell within 2 hours.

3.4. EFFECT OF C710M ON TUMOR GROWTH

The above results revealed the high anti-proliferative potency of compound C710M in many cancer cell-lines. However, these experiments were limited cells cultured as mono-layers where the compound is in direct contact with the cells. We wanted to know whether the compound could diffuse from cell to cell in a tumor. To mimic the 3D-organized structure of a tumor, a spheroid model was utilized and finally, cell xenografts were implanted in nude mice.

3.4.1. In MTS model

By the hanging-drop method, we succeeded in producing Hct116 spheroids. In order to evaluate the effect of the compound for a long-term period on 3D-organized cells, we treated spheroids, for 2 weeks, by C710M, at two concentrations: 350 nM (concentration corresponding to the IC50 in Hct116 cells) and 1 µM. The results in Figure 36 and Table 13 showed that in the control, spheroids grew exponentially and a 16-fold increase in size was noted at Day 14; whereas, both concentrations of C710M prevented very dramatically the growth of spheroids. An immediate effect of C710M (1 µM) was observed from the 2nd day, with a 2/10 reduction of spheroid size, demonstrating that C710M diffused easily inside. Long-term effects were noted with C710M since the size of the spheroid gradually decreased till Day 14. Meanwhile, at the concentration of 350 nM, C710M exhibited a slightly slower inhibitory effect than at 1 µM, spheroids still grew on the 2nd day, even moderately, and only started to decrease in size from the 4th day of treatment. This result was understandable because 350 nM was the minimum concentration of C710M reducing cell proliferation by a half, after 4 days. Despite this slight difference, the inhibitory potency of both concentrations of C710M was similar in the long-term treatment, with the same ratios of spheroid growth from the 6th day of treatment (Table 13). Consequently, cells died on prolonged C710M treatment with the spheroids eventually breaking into fragments. Interestingly, the efficiency of C710M seemed similar in 2D- and 3D-cultures, at least for the lowest concentration (IC50), indicating an easy diffusion of this compound in spheroids.

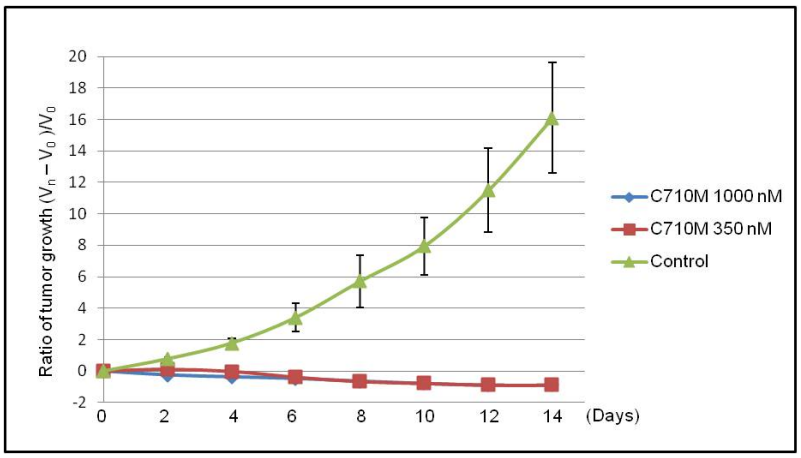

Figure 36: Effect of C710M on the growth of Hct116 spheroids

Hct116 spheroids (approximately 0.1 mm^3) were incubated with C710M (350 nM in red; 1 µM in blue) or without compounds (control, in green) from Day 0 to Day14. The spheroid sizes were measured each 2 days for 2 weeks. The growth of spheroids was calculated by the formula: $[(V-V_0)/V_0]$ with V_0 being the volume at Day 0. For treated spheroids, the error bar was included in the label.

Days of treatment	Control	C710M 350 nM	C710M 1000 nM
0	0	0	0
2	0.78 ± 0.11	0.10 ± 0.07	-0.24 ± 0.15
4	1.78 ± 0.30	-0.03 ± 0.10	-0.36 ± 0.11
6	3.41 ± 0.90	-0.39 ± 0.15	-0.46 ± 0.11
8	5.71 ± 1.67	-0.66 ± 0.11	-0.63 ± 0.06
10	7.94 ± 1.84	-0.77 ± 0.07	-0.78 ± 0.07
12	11.49 ± 2.67	-0.88 ± 0.06	-0.89 ± 0.04
14	16.11 ± 3.49	-0.89 ± 0.05	-0.89 ± 0.04

Table 13: The ratio of tumor growth $[(V_n - V_0)/V_0]$ upon C710M for 14 days.
(-) meaning the reduction in size of spheroids versus the first day of treatment.

3.4.2. In Xenograft model in "Nude" mice

The efficiency of compound C710M was also evaluated in nude mice bearing tumors either U-251 or Mahlavu tumors (Figure 37 and 38). After tumor establishment, the mice were randomly dispatched in three batches: the control batch received the vehicule, the others received a benzo[e]pyridoindole: either C710M or C21. C21, a kinase inhibitor with different specificity from C710M, was analyzed, in this experiment, as a control compound. Mice were healthy after repetitive injections of both compounds and grew normally, without difference in body weight among batches (Figure 37A, 38A). Figure 37C and 38C showed the tumor growth upon different treatments.

U-251, glioblastoma cells, grew slowly when engrafted in mice (Figure 37C). C710M was found to have a slight effect since a 30 % decrease of the tumor volume was noted upon IP treatment. The control compound C21 reduced tumor volume by 2 (Figure 37 B and D) and the effect was found significant at days 42, 44 and 48 (Student test, $p = 0.03$, 0.02 and 0.01, respectively). The treatment ended at day 30, long-term effects were thus observed. U-251 tumors were found homogeneous and poorly vascularized (Figure 37D).

Mahlavu tumors derived from liver cells developed quickly in mice and attracted many vessels as obvious on the photos (Figure 38D). C21 seems to increase the size of Mahlavu tumors, the final average weight increased by 25 %. Conversely, C710M prevented the growth of Mahlavu tumors and the final average tumor weight decreased by a half (Figure 38B). The effect was still observed at distance from the last injection and was found significant from day 31 to 38 by the Student test ($p < 0.05$) (Figure 38C). We did not observe differences of vascularization of the Mahlavu tumors according to the different treatments. More interestingly, when the mice were autopsied at the end of the experiment, we realized that C710M did not have any impacts on internal organs.

To note the results obtained with these two examples of xenografts fitted perfectly with the data recovered on 2D-cell line cultures (Table 10 and data not shown). Upon C710M treatment, in-cell IC50 of viability determined for Mahlavu and U251 were 84 nM and 1195 nM respectively (Table 10). Whereas C21 was found to efficiently prevent U251 growth (Hong-Lien Vu, PhD thesis, 2011) and we showed that it is efficient towards U251 xenografts. The proliferation test conducted on 2D-cultures seemed predictive of the efficiency towards cells xenofrafts in mice and this interesting point could indicate that these compounds diffused well in the body, when peritonealy injected, meanwhile maintaining their activity. The contrasting results obtained with the two compounds suggested that the different benzo[e]pyridoindoles had different potentialities, linked to specific targeting.

Hence, C710M exhibited potency for preventing tumor growth and its repetitive injection in mice seemed not to induce adverse effects. We decided thus to further characterize this molecule. We investigated both its pharmacological characteristics and tried to gain some information on its mechanism of action.

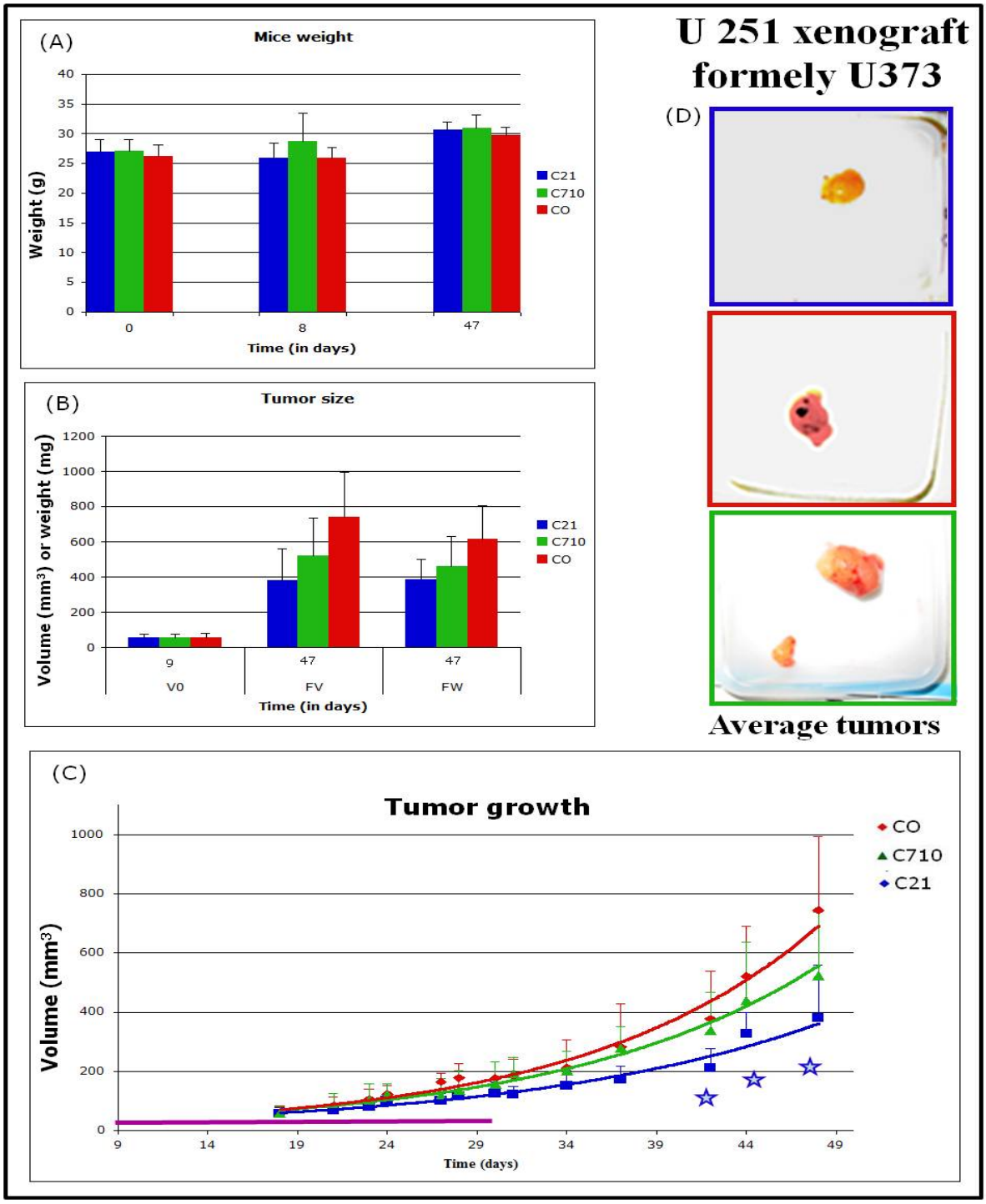

Figure 37: Effect of C710M, C21 on the growth of U251-xenograft. Mice were treated 13 times by either C710M or C21 (10 µg compound/g of mice weight) or NaCl 0.45% (Control, CO), by IP injections, 4 times per week. The period of compound injection was shown as the violet bar (A) Comparison of mice weight among groups, on the first day (tumor injection), 10th day (the first injection of compound) and 48th day (mice autopsy). The size of tumors in each group was presented in (C) in function of the elapsed time (in days). Blue stars indicated significant differences of C21 versus the control, determined by the Student test ($p < 0.03$). At the end of the experiment, the final tumor weight was compared to the tumor size in (B) and a tumor exhibiting the average weight was shown in (D)

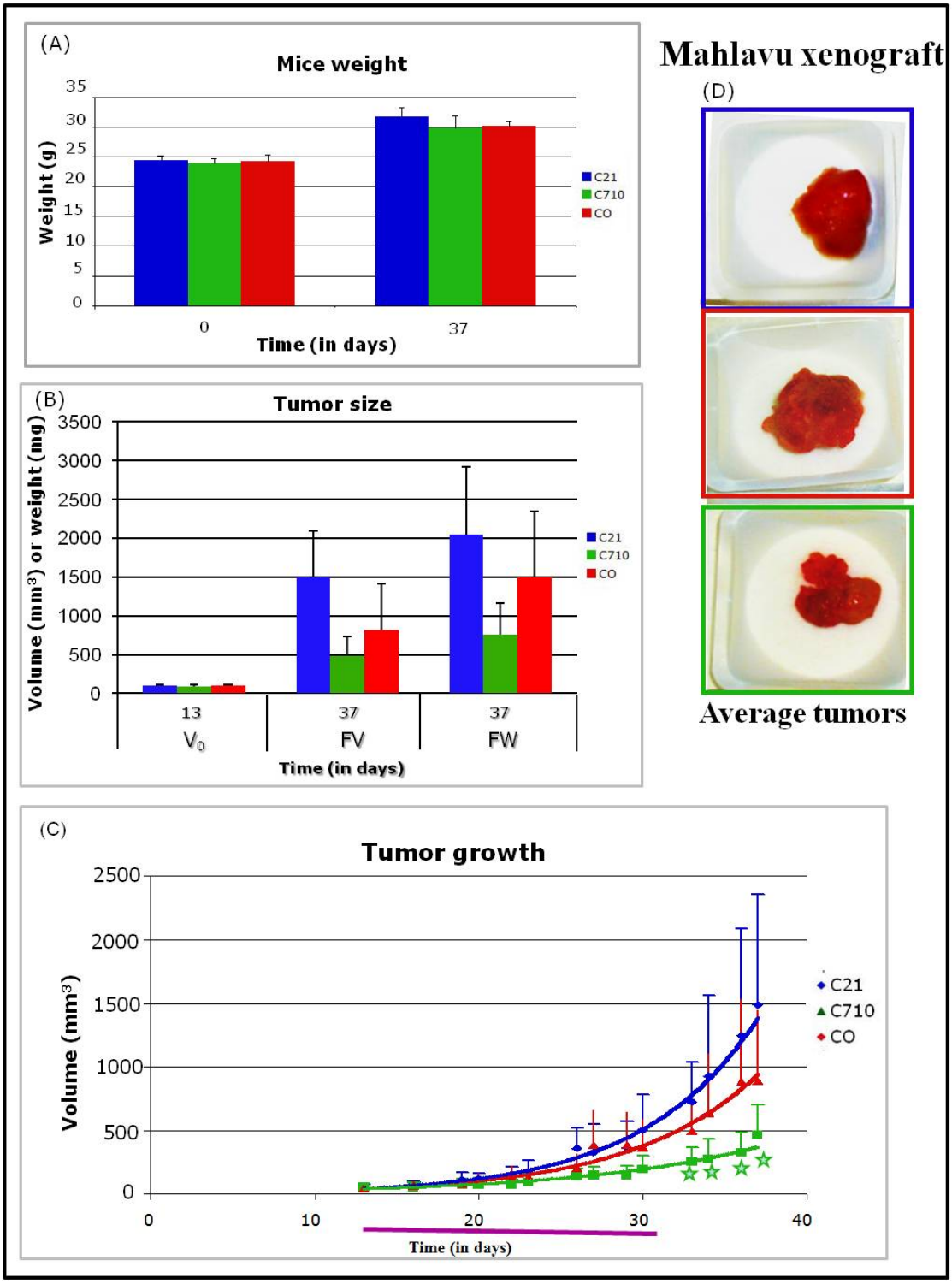

Figure 38: Effect of C710M, C21 on the growth of Mahlavu-xenograft. Mice were treated 11 times by either C710M or C21 (10 µg compound/g of mice weight) or NaCl 0.45% (Control, CO), by IP injection, 4 times per week. The period of compound injection was shown as the violet bar (A) Comparison of mice weight among groups, on the first day (tumor injection) and 38th day (mice autopsy). The size of tumors in each group was presented in (C) in function of the elapsed time (in days). Green stars indicated significant differences of C710 versus the control, determined by the Student test ($p < 0.05$). At the end of the experiment, the final tumor weight was compared to the tumor size in (B) and a tumor exhibiting the average weight was shown in (D).

3.5. PHARMACOKINETIC CHARACTERISTICS OF C710M

To evaluate the possible use in clinical trial, some pharmacokinetic characteristics of compound C710M were recorded on the CNRS TechMed platform in Strasbourg (Table 14). The reaction with maleic acid formed the hydrosoluble C710M salt; but its solubility in water was unknown. We found that the solubility of C710M in water was over 6 mg/mL; but it decreased to less than 1 mg/ml in physiological medium (0.9 % NaCl).

We checked the passive permeability of C710M compound across artificial barriers at physiological, pH 7.4. C710 crossed the lipid barrier slowly (Pe = 4.62×10^{-9} cm/sec, log Pe = -8.34 ± 0.29) in comparison to Antipyrine, a common ear-drop medicine (logPe = - 6.14). However the time-lapse experiments suggested that C710 was quickly available inside the cell upon addition, indicating its active transportation.

C710 was found to poorly attach to reconstituted membrane (around 9 % were retained). It is efficiently retained by plasmatic proteins, 80 % of it was stuck on plasma proteins, but similar data (83 %) were reported for Propanolol, a common drug used in treatment of high blood pressure. In the body, we could expect its transportation by the blood especially as this compound was found very stable in mice plasma. After 1 hour of incubation, no loss was noted either in mice plasma or in human liver microsomes.

These results are encouraging for the potential use of C710 in preclinical trials.

Test	C710M	References
Solubility in NaCl 0.45%	2 mg/ml	
PAMPA pH 7.4 Passive permeability	Pe = 4.62×10^{-9} cm/sec logPe = -8.34 ± 0.29	Antipyrine : logPe = - 6.14
Binding to plasmatic proteins	80 ± 1%	Propanolol 83%
Binding to membranes	9 ± 7%	
Stability in mice plasma, 1h	100 ± 1 %	Procaine 10 %
Metabolic stability in human liver microsomes (cytochrome P450), 1h	100 %	Half-life of Testosterone: 40 min

Table 14: Pharmacokinetic characteristics of C710M

3.6. *IN-VITRO* KINASE PROFILING OF COMPOUND C710

To obtain a general view about C710 specificity, we determined the *in-vitro* kinase inhibition profile of this compound. The activity of 138 recombinant kinases was determined in the presence of C710 (250 nM). The percentage of remaining activity for each kinase was reported in Table 15.

Kinase	Remaining activity (%)	Kinase	Remaining activity (%)	Kinase	Remaining activity (%)	Kinase	Remaining activity (%)
NUAK1	**1 ± 0**	BTK	45 ± 8	LKB1	85 ± 1	IRR	99 ± 3
TrkA	**1 ± 0**	MARK1	50 ± 3	TESK1	85 ± 3	JNK1	99 ± 10
MAP4K3	**1 ± 0**	RIPK2	52 ± 1	CAMK1	86 ± 12	PIM3	99 ± 10
TAK1	**4 ± 0**	Src	52 ± 4	PLK1	86 ± 4	GCK	100 ± 2
PHK	**5 ± 1**	ULK1	52 ± 2	CDK2-CycA	87 ± 12	TTBK2	101 ± 4
SIK2	**5 ± 0**	TTK1	53 ± 29	TAO1	87 ± 11	EIF2AK3	101± 3
HIPK1	**6 ± 0**	MARK2	56 ± 5	CK2	89 ± 6	p38dMAPK	101 ± 5
CHK2	**7 ± 2**	MKK6	57 ± 0	EPH-A2	89 ± 10	PKBb	101 ± 5
MAP4K5	**8 ± 1**	YES1	58 ± 3	HER4	89 ± 11	MPSK1	103 ± 11
VEGFR	**8 ± 1**	HIPK2	61 ± 4	MNK1	89 ± 6	OSR1	103 ± 2
MELK	**9 ± 0**	MST2	61 ± 22	TGFBR1	89 ± 1	PAK6	103 ± 2
JAK2	**10 ± 1**	RSK2	61 ± 5	NEK2a	90 ± 6	PIM1	103 ± 0
CAMKKb	12 ± 2	MARK4	64 ± 6	ROCK2	90 ± 9	Lck	104 ± 9
IR	12 ± 2	FGF-R1	65 ± 3	EPH-B4	91 ± 5	MST4	104 ± 49
BRSK2	12 ± 1	BRK	66 ± 6	TTBK1	91 ± 11	PKCa	104 ± 5
IRAK4	13 ± 0	PRK2	68 ± 3	**Aurora A**	**91 ± 1**	SRPK1	104 ± 18
Aurora B	**14 ± 1**	CLK2	69 ± 3	JNK2	92 ± 3	IKKb	105 ± 10
AMPK-human	**16 ± 6**	PAK4	69 ± 17	SIK3	93 ± 17	MAPKAP-K3	105 ± 8
IRAK1	17 ± 1	S6K1	69 ± 4	TIE2	93 ± 7	p38gMAPK	105 ± 7
MLK3	17 ± 4	SmMLCK	69 ± 2	DYRK1A	94 ± 4	p38aMAPK	106 ± 9
CHK1	19 ± 8	PDK1	70 ± 2	EPH-B2	94 ± 3	ZAP70	106 ± 6
PKD1	19 ± 4	DDR2	71 ± 1	CSK	95 ± 9	ERK1	107 ± 0

MKK1	23 ± 1	PDGFRA	74 ± 1	MNK2	95 ± 7	ERK2	108 ± 4
STK33	26 ± 9	PRAK	74 ± 1	PAK5	95 ± 15	CK1γ2	108 ± 3
MARK3	28 ± 7	DAPK1	76 ± 7	PKCz	95 ± 10	TLK1	109 ± 15
AMPK	30 ± 6	IKKe	76 ± 1	GSK3b	96 ± 8	PKBa	113 ± 0
ULK2	31 ± 5	MST3	76 ± 2	PKA	96 ± 6	MEKK1	114 ± 19
BRSK1	37 ± 10	MKK2	77 ± 8	PKCγ	96 ± 1	NEK6	114 ± 4
MLK1	38 ± 2	JNK3	78 ± 8	EPH-A4	97 ± 3	HIPK3	115 ± 10
TSSK1	38 ± 6	ABL	79 ± 4	PIM2	97 ± 4	PAK2	115 ± 1
IGF-1R	40 ± 7	ERK5	80 ± 1	CK1δ	98 ± 5	MAPKAP-K2	121 ± 4
TBK1	40 ± 16	DYRK2	82 ± 0	DYRK3	98 ± 9	WNK1	125 ± 8
MINK1	43 ± 0	p38bMAPK	82 ± 1	CDK9-CycT1	98 ± 7	EF2K	134 ± 7
RSK1	43 ± 4	SGK1	83 ± 4	EPH-B3	99 ± 3		
SYK	43 ± 7	EPH-B1	85 ±3	ERK8	99 ± 5		

Table 15: In-vitro kinase inhibition profile of C710 at the concentration of 250 nM.

This assay was performed, in duplicate, by the MRC (Dundee University) on 138 recombinant kinases. The percentage of remaining activity for each kinase was determinated. Kinases belonging to the AMPK pathway affected by C710 are in red; other AMPKr kinases are in blue.

The results showed that C710 specifically inhibits few kinases. Among the panel, ten kinases were inhibited by more than 90 % in the presence of C710, at 250 nM. We have noted the presence of several AMPK-related kinases in this top ten (Nuak, Sik2 and Melk) as well as two AMPK upstream regulator kinases (Tak1 and CaMKKß). However, the whole AMPK-related kinase family was not affected; for example, MARKs, Sik3 and Brsk1 were not inhibited. Note that C710 inhibited AMPK and aurora kinase B at the same level. This profiling indicated that C710 was a specific aurora kinase B inhibitor, aurora A was not affected (91 % activity in the presence of C710, 250 nM). Other major off-targets are MAP4K3, Tak1, Phosphorylase kinase Phk, HIPK, Chk2, MAP4K5 as well as VEGFR.

Based on kinase profiling, we determined *in-vitro* IC50 of C710 towards the main kinase targets. We compared the kinase inhibitory activity of C710 and compound 13b, the former benzo[e]pyridoindolone with similar anti-proliferative potency (Table 16).

Kinases	In-vitro IC50 (nM) of compound			Km ATP
	13b[#]	C710[#]	C710[*]	
Aurora A	50	58	Sup 250 nM	5
Aurora B	13	12	118.3 ± 27.9	20
ARK5/NUAK1	6	0.4	4.8 ± 0.4	20
CHK1	54	5	ND	20
CHK2	43	5	13.6 ± 0.5	20
TAK1	133	6	ND	5
FLT1/VEGFR1	274	37	ND	20
SIK2	ND	ND	12.4 ± 0.7	50
MELK	ND	ND	13.3 ± 2	50
PHK	ND	ND	18.5	50

Table 16: In-vitro IC50 of compounds towards main targeted kinases.

(#) This assay was performed by Reaction Biology Corp (USA) with recombinant kinases in the presence of 1 µM ATP. Compounds were tested, in duplicate, at 10 various concentrations from 2 pM to 10 µM with serial 3-fold dilutions. Staurosporine was used as internal control and tested at 10 concentrations. In-vitro IC50 was the concentration of compound inhibiting by 50% the kinase activity.

(*) This assay was performed by the MRC (Dundee University) with recombinant kinases. The ATP concentration was adjusted at the Km value for each kinase. Compounds were tested in duplicate, at 10 concentrations varying from 0.03 nM to 1 µM, with serial 3-fold dilutions.

Data in Table 16 revealed that both compounds had the same inhibitory potency towards aurora kinases. Especially, both compounds efficiently targeted aurora B than A. In addition, they also had similar off-targets but C710 was found to be far more efficient than 13b. Both compounds inhibited very efficiently Nuak1, an AMP-related protein kinase whose activation is directly regulated by Akt, and that has been reported to be a key player in tumor malignancy (Suzuki et al., 2004) and in c-myc deregulated tumors (Liu et al.,2012). An IC50 of 4.8 nM was determined for C710 towards Nuak1 whereas IC50 of 12.4 and 13.3 nM were recorded towards Sik2 and Melk, two AMPKr members. Both 13b and C710 affected chekpoint kinases 1 and 2 and nanomolar IC50 values were measured. These compounds might thus interfere with DNA reparation in cells. *In vitro*, both molecules affected the tyrosine kinase receptor VEGF-R and phosphorylase kinase.

On the whole, C710M was a very potent hydrosoluble kinase inhibitor, targeting many kinases. Beside aurora B, it also targeted other kinases, such as AMPK and AMPKr-kinases. In fact, we also found that C710 blocked cell progression in mitosis but the observed effects could

not be fully accounted for by aurora kinase B inhibition (Figure 35). Upon C710M, cells did not escape mitosis through mitotic slippage. As evidence, we observed binucleate cells arose from cells without accurate chromosome segregation. We did not observe micronuclei as the consequence of known aurora kinase inhibitors (VX-680, C1). One possibility might be the presence of a reduced spindle that could not be stabilized due to actomyosin defects. AMPK inactivation has recently been shown to create such defects (Thaiparambil et al., 2012). Moreover, AMPK and AMPKr were described to play a role in mitosis ongoing (Motoshima et al., 2006, Banko et al., 2011). Together with the *in-vitro* kinase profiling of C710M, we hypothesized the possible involvement of AMPK and AMPKr-kinases in C710 action mechanism, beside aurora B. This hypothesis has been tested and recently we have had some evidence for possible involvement of AMPK in C710M action.

For a better description of the C710M impact on mitotic spindles, confocal Z stacks were acquired and 3D-reconstitutions were built. 3D views are presented with a depth color code to appreciate the relative localisation of the two poles. In control cells, quickly after duplication, centrosomes moved to two opposite poles and a nice spindle was constituted. As shown with the depth color code, on the 3D-reconstituted views, both spindle poles were at similar z levels in the cell (Fig. 39A, T 38 min and 83 min). At 83 min, the two poles moved away and the cell entered in anaphase. The orientation of the spindle was conserved during mitosis and figured the direction of cytokinesis (T: 100 min).

Conversely, on C710M treated cells (Fig. 39B and C), mitotic cell started with an oriented bipolar spindle (Fig. 39B, T_0 and T 27 min). But afterwards, during mitosis ongoing, the spindle turned around as indicated by the arrows. The direction of the spindle did not prefigure the sense of separation. Note that the two spindle poles were not in exactly the same z as in control (Fig 39B, T 27min and 65 min, 3Dc as well as Fig. 39C, T 46 min and 48 min, 3D-color forward and back). Most of the observed spindles were reduced in size as shown previously (Fig.35). Observing Fig. 39B, we might suggest that the spindle could be organized normally, but it is progressively reduced (compare between T_0 and T 65 min). The lack of stabilisation of the spindle by C710M may impair the dynamic of microtubules on the kinetochores and leads to the mitotic exit as binucleated cells. This preliminary result showed the possible involvement of AMPK in C710M action, but further investigations are required to confirm this hypothesis.

(A)

Tubulin-GFP

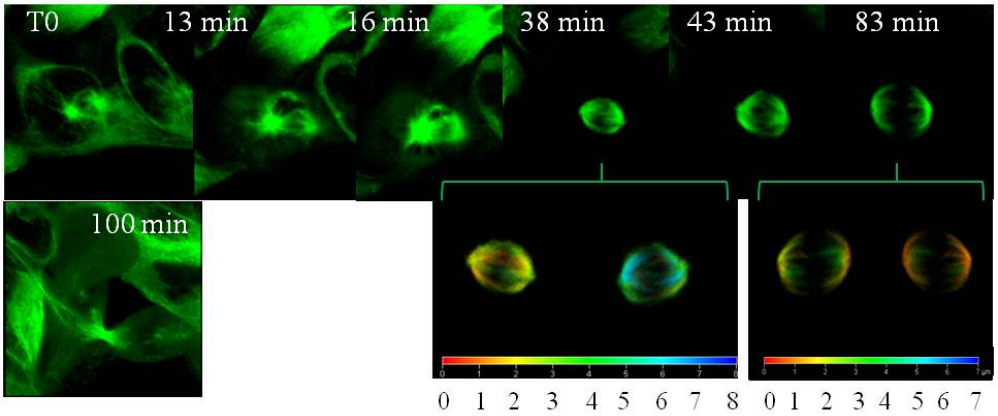

(B)

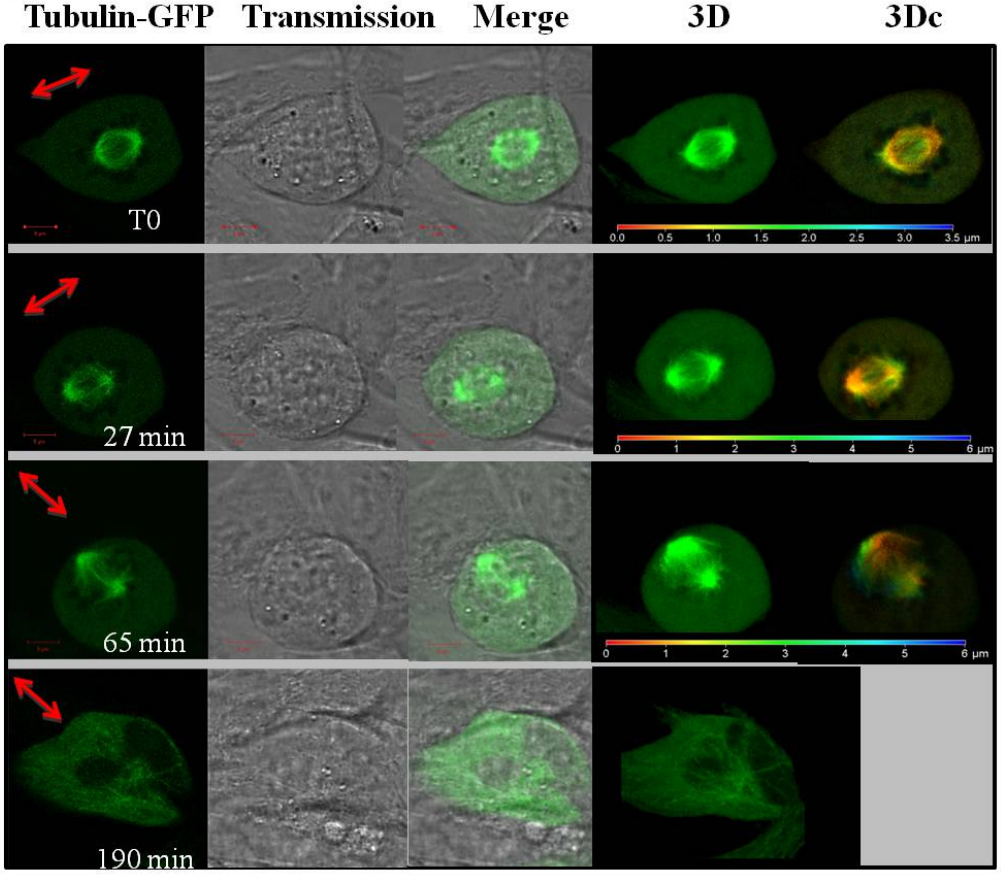

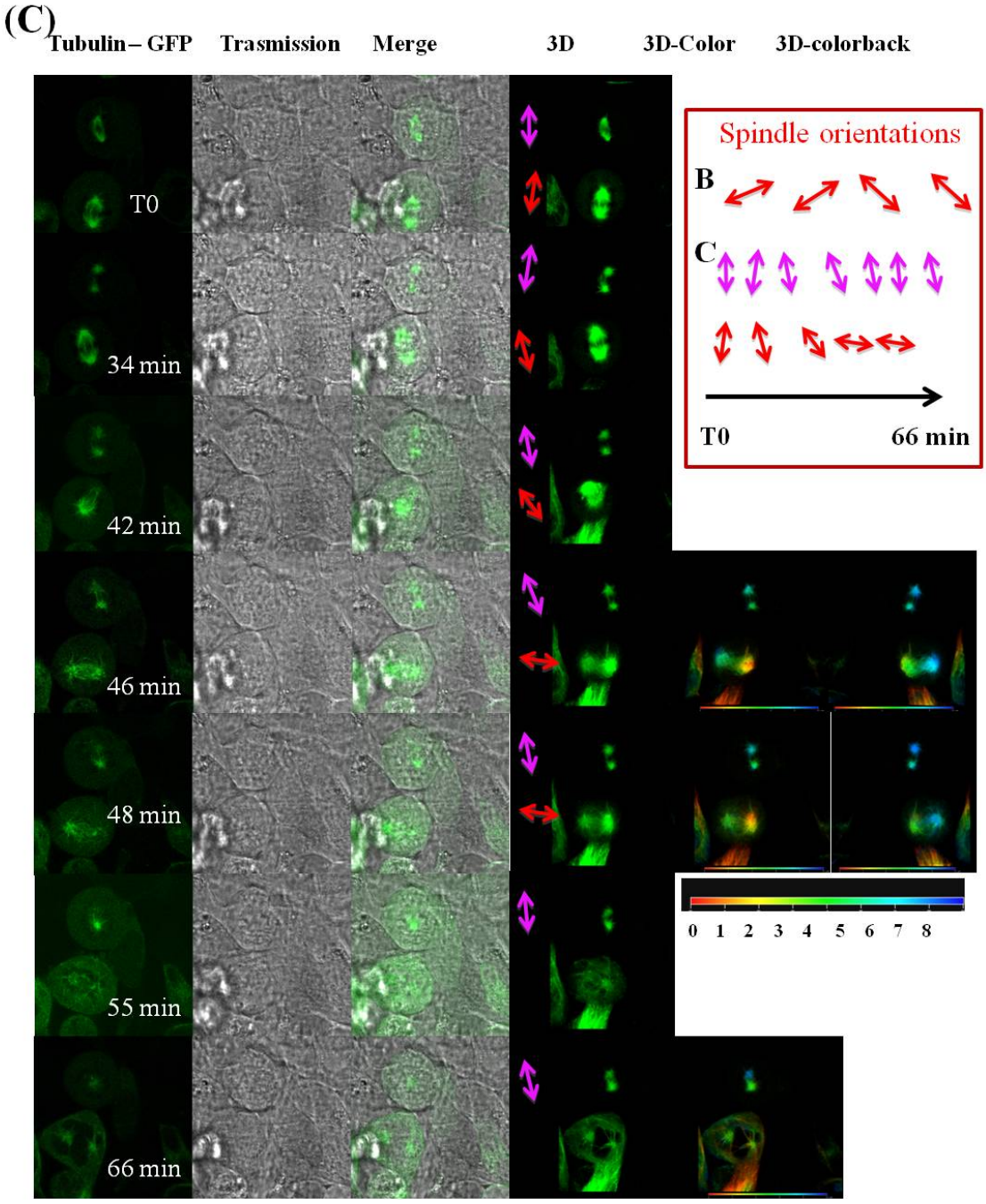

Figure 39: Time-lapse microscopy on mitotic Hek cells expressing tubulin-GFP. Control cells in the absence of treatment were represented in A and compared to C710M (200 nM) treated cells (in B and C). 3D –reconstitution views were shown in green as well as in a depth color code (forward and back views, depth values in microM on the bar scale). The elapse time was indicated on each photo.

For treated cells in B and C, in addition to the 3D reconstitution views, a representative plane was shown (Tubulin-GFP, Transmission and merge). Moreover, the orientation of the spindle was recalled by an arrow (pink and red) on each image.

A summary of the varying orientations for the three followed spindles (one in B and two in C) is shown in (C).

DISCUSSION

AND

PERSPECTIVES

DISCUSSION

Aurora kinases play key roles in mitosis and are overexpressed in many tumors. Hence, they have been considered as potential targets in anti-cancer therapy. Several aurora kinase inhibitors have been identified and are currently evaluated in clinical trials. Among them, we found that benzo[e]pyridoindoles were novel potent ATP-competitive inhibitors of aurora kinases.

Besides their therapeutic potency, these small kinase inhibitors are also interesting tools in cell biology research. Therefore, benzo[e]pyridoindole C4 attracted our interest due to its abnormal inhibition of histone H3 phosphorylation, only in prophase, and its induction of lagging chromosomes in anaphase. Herein, some questions arose: what is the role of histone H3 phosphorylation in mitotic prophase? Does C4 target aurora kinases? How does aurora kinase B activity vary during mitosis?

In fact, in mitosis, the role of histone H3 phosphorylation is still controversial and our data demonstrate that this epigenetic mark is not required for chromosome condensation. Once the cells progress in metaphase, their chromosomes should hold phospho-Ser10- histone H3 for ongoing anaphase. This result sustains the tag hypothesis proposed by Stéfan Dimitrov group (Hans and Dimitrov, 2001; Prigent and Dimitrov, 2003).

Which kinase is the target of C4, leading to the inhibition of histone H3 phosphorylation, specifically in prophase? C4 belongs to the benzo[e]pyridoindole family that we have identified as ATP-competitive aurora kinase inhibitors; but it is less potent than the hit C1. We propose that C4 has a lower affinity for the ATP-binding site than C1 and it could only target the basal activity of aurora kinases. Indeed, we reproduced its effects by low concentrations of several aurora kinase inhibitors and especially with AZD-1152, a specific aurora kinase B inhibitor. From these data we could conclude that aurora kinase B activity varies during mitosis. As suggested by Xu et al. (2009), the maximal activation of aurora B is necessary for ongoing anaphase but then its activation decreases during its transfer on microtubules. We show that defects in anaphase are independent of the absence of H3-phosphorylation in prometaphase and instead correlate with oscillations of aurora kinase B activation. These waves of activation corresponds to different conformations of the CPC complex as shown by the variations in the mobility of the proteins evaluated by FRAP.

By a combination of different kinase inhibitors and microscopy techniques we described aurora kinase B activation in mitosis. We found that aurora kinase inhibitors with low ATP affinity did not prevent mitosis ongoing but induced lagging chromosomes in anaphase. This might be deleterious for the cells since aneuploidy or DNA mislocalization may arise in the daughter cells (Meldi and Brickner, 2011). This situation should be considered in clinical trials with patients treated by aurora kinase inhibitors, especially by compounds with long half lives whose level gradually decreases over time from the start of the treatment. Therefore, the short-lived molecules should be priority in the development of these anti-cancer drugs.

In another approach, we continued to develop new molecules in the bezo[e]pyridoindole family for use in clinical applications. From the hit C1 identified through high-throughput screening, we performed a structure-activity relationship study to improve the activity and solubility of benzo[e]pyridoindoles. These molecules belong to the Institut Curie library and are synthesized by the Dr Chi-Hung Nguyen. Benzo[e] pyridoindoles are a privileged scaffold exhibiting different biological activities (Hoang et al., 2009) and we have identified benzo[e]pyridoindolones as aurora kinase inhibitors. The SAR study was then limited to two positions: R8 and R3 of the hit C1. Our data indicate that the bulkiness of the alkyl group at position R8 plays a role for aurora B inhibition. The ether group at position R3 is a requirement for preventing aurora kinase activity. Our work has highlighted the possible modifications of this R3 lateral chain. New derivatives bearing an amine functional group at this position are very efficient aurora kinase inhibitors. Especially, these molecules are suitable for producing hydrosoluble salts by the reaction to organic acids, like maleic acid in our case.

Subsequently, we characterized several of these inhibitors: 13a and 13b as well as C710. Interestingly, their corresponding salts were found as active as their base counterpart. This is a tremendous improvement for preclinal applications. These molecules were shown to be potent aurora kinase inhibitors, and were more efficient towards aurora B than aurora A. In fact, they prevented histone H3 phosphorylation in mitotic cells, exhibiting the *in-cell* aurora B inhibition. They delayed mitotic exit inducing polyploidisation of the cells and finally induced apoptosis. Consequently, these compounds exhibited high anti-proliferative potency in HeLa cells. In the comparison with data reported for the best aurora kinase inhibitors currently in clinical trials, these molecules are among the top 10 best aurora kinase inhibitors. The more potent inhibitor C710M of this series was demonstrated by efficient prevention of Hct116 spheroid growth at the concentration of 350 nM and by an decrease in the development of Mahlavu xenograft in nude mice. Mice were still healthy and grew normally upon repetitive C710M intraperitoneal

injections and the autopsy of mice revealed no adverse visible effects. In other words, these new hydrosolube benzo[e]pyridoindoles are promising kinase inhibitors. Therefore, we decided to further characterize these compounds.

Upon 13aM or C710M treatment, aurora B was inactivated and the histone H3 phosphorylation was inhibited. However, the phenotype of the cells treated by 13aM (Le et al., 2013) and by C710M did not fit with a specific aurora B kinase inhibition. Indeed, in the absence of aurora B activity, we expect cells to escape mitosis without segregating chromosomes and then, the appearance of micronuclei (Hoang et al., 2009). However, upon 13aM or C710M treatment, the organization of the microtubule spindle was perturbed, such a phenotype has been never observed by aurora kinase inhibito. Meanwhile, aurora B was mostly found to be concentrated on centromeres, even it was inactive. More interestingly, the chromosomal passenger complex was partly transferred to microtubules, probably as a result of SAC inactivation. Again the transfer on microtubule was prevented with most aurora kinase inhibitors (Hoang, 2009). However, cells could not divide due to the mis-segregation of chromosomes. Such defects might be a consequence of a lack of tension on the chromatid pairs due to spindle defects. Time-lapse experiments on Hek cells stably expressing tubulin-GFP revealed that the spindle orientation varied during mitosis upon C710M. In controls, the bipolar spindle was oriented parallel to the substratum, with spindle poles in similar z sections. The oscillation of the mitotic spindles might be due to the inhibition of AMPK or AMPK-related kinases. This possibility is highly probable since: 1) AMPK was recently shown to be involved in mitosis ongoing (Banko et al., 2011), 2) AMPK was reported to prevent the anchorage of the spindle on the acto-myosin network (Thaiparambil et al., 2012). Moreover Sik2, an AMPKr kinase seemed to be involved in centrosome maturation (Ahmed et al., 2010), 3) C710 compounds was found to efficiently target AMPK and AMPKr kinases (like Nuak1, Melk and Sik2), at least *in vitro*.

Our hypothesis is that the benzo[e]pyridoindolones studied target both aurora B and AMPK, these conjugate inhibitions turn the SAC off and trigger anaphase onset. Then, the absence of tension prevents the correct segregation of chromosomes and the presence of chromatin in the midzone maintains the No-Cut checkpoint ”on”, leading to binuclate cells. Finally, the accumulation of these defects leads to apoptosis. These benzo[e]pyridoindolones prevent cell proliferation through a new pathway which was not investigated before. Currently, only a few AMPK inhibitors are published, mostly working at micromolar concentrations and their possible intervention, as anti-proliferative molecule has not been explored yet. Conversely, AMPK activators were proposed as possible targets in anti-cancer therapy in peculiar

applications. AMPK is under the control of a complex signaling network and the situation may vary depending on the activation level of upstream kinases like Tak1, CaMKKß or the tumor suppressor LKB1. Note that both Tak1 and CaMKKß were identified as C710M targets, *in vitro.* Although best known for its effects on metabolism, AMPK has many other functions, including, regulation of transcription and mitochondrial biogenesis, autophagy, cell polarity, and cell growth and proliferation (Hardie, 2011). Their implication in these pathway is quite new and needs more investigations.

The possibility that benzo[e]pyridoindolones are dual kinase inhibitors is very interesting since pharmaceutical companies are worried about the side effect of aurora kinase inhibitors. Indeed, the clinical trial of VX-680, a known aurora inhibitor, was stopped due to its observed QTs-prolongation effect and the death of one patient during treatment. Whether it is a specific effect of the molecule or a drawback of aurora kinase inhibitors is an open question. Till now, none of aurora kinase inhibitors has been approved by FDA for anti-cancer therapy. Therefore, current efforts focus on new inhibitors with combined but selective activity on few targets to address the current problem of side effects.

In conclusion, benzo[e]pyridoindolones were found to be potent antiproliferative drugs targeting a new signaling pathway. Our first preclinical characterizations were encouraging further development of these molecules hold promise for anti-cancer therapy. Our group registered a patent for these compounds (Nguyen CH, Molla A, Le LTT, "International Patent", April 2012) and in the future, Institut Curie is in charge of their validation in preclinical and clinical trials.

PERSPECTIVES

The kinase profiling of new benzo[e]pyridoindolones reveals that these compounds may target AMPK and AMPKr, beside aurora kinase B. In future work, we will validate the involvement of these targets in the activity of benzo[e]pyridoindolones, in cells. The phosphorylation of putative substrates such as MRLC, TORC2, AMPKα1 or AMPKα2, P27 or HDAC4 will be investigated to determine the selectivity of these inhibitors. We will combine the identification of substrates with time-lapse microscopy to define the mechanism of action of these molecules. Our efforts will be dedicated to test the hypothesis of the simultaneous targeting of aurora kinase B and AMPK. We also expect to determine precisely which AMPKr kinase is involved among those identified by the kinase profiling. The possibility of the simultaneous targeting of other kinases could not be dismissed and has to be taken into account.

We have noted the correlation of the anti-proliferative potency of C710M *in cellulo* and in xenograft models. Therefore, we will enlarge the panel of cell lines to evaluate the possible efficiency of these molecules. The analysis of a larger set of data may be helpful for defining the application of these molecules as anti-cancer drugs.

Although the studied benzo(e)pyridoindolones exhibit similar anti-proliferative potency, the kinase profiling are slightly different suggesting distinct mechanisms of action. We will compare the mechanism of these different molecules in lines with possible applications in anti-cancer therapy. In collaboration with Dr Chi-Hung Nguyen, the SAR study is still in precess and in the future, crystallization of these inhibitors with their targets will be performed in collaboration with the Institute of Structural Biology, in Grenoble.

Till now the efficiency of these compounds has been mostly evaluated as single treatments but combined therapy should also be considered. Finally, we will focus on developing an accurate drug delivery system. One strategy is to integrate the compounds and nano particles within a nano-network. The effectiveness of drugs in this system will also be investigated and validated in mice.

APPENDIX

1. **Synthesis of compound C07 (3-(2-(Morpholin-4-yl)ethoxy)-8-methyl-7*H*,10*H*-benzo(e)pyrido(4,3-b)indol-11-one)** : C07 was synthesized via C05

11-Chloro-3-(2-(morpholin-4-yl)ethoxy)-8-methyl-7*H*-benzo(e)pyrido(4,3-b)indole(C05):

A mixture of 11-chloro-3-hydroxy-8-methyl-7*H*-benzo(e)pyrido(4,3-b)indole (1,0 g, 3.5 mmol) (Vinogradov et al., 2003), n-butanol (60 mL) and water (40 mL) was stirred during 30 min and a solution of NaOH (860 mg) in water (10 mL) was then added. After stirring during 15 min, 4-(2-chloroethyl) morpholine hydrochloride (770 mg, 4,1 mmol) was added and the mixture was heated under reflux for 2 h. The reaction mixture was cooled and organic layer was separated. The aqueous layer was extracted by AcOEt and the organic layers were combined, washed with brine, dried over $MgSO_4$ and evaporated under vacuum. The residue was purified by flash chromatography (neutral alumina, gradient of ethanol (0 to 3%) in dichloromethane) to give the expected compound as beige solid (660 mg, 47 %). ^{1}H NMR (300 MHz, DMSO-d_6) δ (ppm): 12.94 (br s, 1H), 9.62 (d, 1H), 8.06 (d, 1H), 7.99 (d 1H), 7.80 (d, 1H), 7.59 (d, 1H), 7.35 (dd, 1H), 4.25 (t, 2H), 3.64-3.58 (m, 4H), 2.78 (t, 2H), 2.56 (s, 3H), 2.54-2.49 (m. overlapped by DMSO signals). Microanalyses, calculated for $C_{22}H_{20}ClN_3O_2 \cdot 0.5\ H_2O$: C, 65.34; H, 5.69; N, 10.39, found: C,65.75; H,5.73; N,10.37. MS 394.1 & 396.1 [M-1].

3-(2-(Morpholin-4-yl)ethoxy)-8-methyl-7*H*,10*H*-benzo(e)pyrido(4,3-b)indol-11-one(C07):

A mixture of compound C05 (290 mg, 0.82 mmol), sodium acetate (245 mg, 3 mmol) and AcOH (20 mL) was heated under reflux for 18 h. The volatile was evaporated under vacuum followed by a co-evaporation with toluene. Water (100 mL) was added and the medium was rendered basic by addition of 2 N sodium hydroxide. The aqueous layer was extracted by AcOEt and EtOH, dried over $MgSO_4$ and evaporated under vacuum to give the exected compound (270 mg, 100%). ^{1}H NMR (300 MHz, DMSO-d_6) δ (ppm): 12.03 (br s, 1H), 10.94 & 10.92 (2 s, 1H), 10.26 (d, 1H), 7.75-7.64 (m, 2H), 7.42 (d, 1H), 7.18 (dd, 1H), 7.07 (d, 1H), 4.21 (t, 2H), 3.66-3.56 (m, 4H), 2.77 (t, 2H), 2.57-2.46 (m. overlapped by DMSO signals). Microanalyses, calculated for $C_{22}H_{23}N_3O_3 \cdot 1.2\ H_2O$: C, 66.23; H, 6.37; N, 10.54, found: C, 66.28; H, 6.55; N, 10.10. MS 400.1 [M+Na].

Formation of the maleate salt: A solution of this free base (150 mg) in boiling absolute ethanol (10 mL) was poured into a solution of maleic acid (55 mg) in hot absolute ethanol (4 mL). The homogenous solution obtained was evaporated under vacuum and the residue was triturated with

acetone giving a solid which was collected by filtration, washed with acetone and dried in a dessicator affording the maleate salt (160 mg). Microanalyses, calculated for $C_{22}H_{23}N_3O_3 \cdot C_4H_4O_4 \cdot 0.4\ H_2O$: C, 62.37; H, 5.56; N, 8.40 ; found: C, 62.66; H, 6.00; N, 7.95.

2. **Synthesis of compound C710 (3-(2-(Piperidin-1-yl)ethoxy)-8-methyl-7*H*,10*H*-benzo(e)pyrido(4,3-b)indol-11-one):** C710 was synthesized via C09

11-Chloro-3-(2-(piperidin-1-yl)ethoxy)-8-methyl-7*H*-benzo(e)pyrido(4,3-b)indole (C09):

A mixture of 11-chloro-3-hydroxy-8-methyl-7*H*-benzo(e)pyrido(4,3-b)indole (1,0 g, 3.5 mmol) (Vinogradov et al., 2003), n-butanol (60 mL) and water (40 mL) was stirred during 30 min and a solution of NaOH (885 mg) in water (10 mL) was then added. After stirring during 15 min, N-(2-chloroethyl) piprridine hydrochloride (790 mg, 4,2 mmol) was added and the mixture was heated under reflux for 2.5 h. The reaction mixture was cooled and organic layer was separated. The aqueous layer was extracted by AcOEt and the organic layers were combined, washed with brine, dried over $MgSO_4$ and evaporated under vacuum. The residue was purified by flash chromatography (neutral alumina, gradient of ethanol (0 to 4%) in dichloromethane) to give the expected compound as beige solid (1.1 g, 79 %). ^{1}H NMR (300 MHz, DMSO-d_6) δ (ppm): 12.48 (br s, 1H), 9.61 (d, 1H), 8.06 (s, 1H), 7.99 (d 1H), 7.79 (d, 1H), 7.58 (d, 1H), 7.34 (dd, 1H), 4.22 (t, 2H), 2.74 (t, 2H), 2.56 (s, 3H), 2.51-2.45 (m. overlapped by DMSO signals), 1.56-1.47 (m, 4H), 1.45-1.30 (m, 2H),,. Microanalyses, calculated for $C_{23}H_{24}ClN_3O_2$: C, 70.13; H, 6.14; N, 10.67, found: C, 69.63; H, 6.38; N, 10.44. MS 394.1 & 396.1[M+1].

3-(2-(Piperidin-1-yl)ethoxy)-8-methyl-7*H*,10*H*-benzo(e)pyrido(4,3-b)indol-11-one(C710):

A mixture of compound C09 (300 mg, 0.76 mmol), sodium acetate (278 mg, 3.4 mmol) and AcOH (20 mL) was heated under reflux for 18 h. The volatile was evaporated under vacuum followed by a co-evaporation with toluene. Water (100 mL) was added and the medium was rendered basic by addition of 2N sodium hydroxide. The aqueous layer was extracted by AcOEt and EtOH, dried over $MgSO_4$ and evaporated under vacuum to give the exected compound in quantative yield (300 mg). ^{1}H NMR (300 MHz, DMSO-d_6) δ (ppm): 12.03 (br s, 1H), 10.94 & 10.92 (2 br s, 1H), 10.26 (d, 1H), 7.73-7.63 (m, 2H), 7.41 (d, 1H), 7.17 (dd, 1H), 7.08 (d, 1H), 4.18 (t, 2H), 2.73 (t, 2H), 2.56-2.43 (m, overlapped by DMSO signals), 2.29 (s, 3H), 1.57-1.48 (m, 4H), 1.44-1.35 (m, 2H). Microanalyses, calculated for $C_{23}H_{25}N_3O_2 \cdot H_2O$: C, 70.22; H, 6.87; N, 10.68, found: C, 70.16; H, 6.92; N, 10.42. MS 376.2 [M+1].

Formation of the maleate salt: A solution of this free base (160 mg) in boiling absolute ethanol (14 mL) was poured into a solution of maleic acid (60 mg) in hot absolute ethanol (4 mL). The

homogenous solution obtained was evaporated under vacuum and the residue was triturated with acetone giving a solid which was collected by filtration, washed with acetone and dried in a dessicator affording the maleate salt (180 mg). Microanalyses, calculated for $C_{23}H_{25}N_3O_2 \cdot C_4H_4O_4 \cdot 0.5\ H_2O$: C, 64.80; H, 6.00; found: C, 64.41; H, 6.37.

3. Synthesis of compound C711 (3-(2-Methoxyethoxy)-8-methyl-7*H*,10*H*-benzo(e)pyrido(4,3-b)indol-11one): C711 was synthesized via C08

11-Chloro-3-(2-methoxyethoxy)-8-methyl-7*H*-benzo(e)pyrido(4,3-b)indole (C08):

A mixture of 11-chloro-3-hydroxy-8-methyl-7*H*-benzo(e)pyrido(4,3-b)indole (1,0 g, 3.5 mmol) (Vinogradov et al., 2003), n-butanol (60 mL) and water (40 mL) was stirred during 30 min and a solution of NaOH (914 mg) in water (10 mL) was then added. After stirring during 15 min, 1-chloro-2-methoxyethane (460 mg, 4,8 mmol) was added and the mixture was heated at 70°C for 4 h. The reaction mixture was cooled and organic layer was separated. The aqueous layer was extracted by AcOEt and the organic layers were combined, washed with brine, dried over $MgSO_4$ and evaporated under vacuum. The residue was purified by flash chromatography (neutral alumina, gradient of ethanol (0 to 2%) in dichloromethane) to give the expected compound as beige solid (50 mg, 4 %). ^{1}H NMR (300 MHz, $CDCl_3$) δ (ppm): 9.78 (d, 1H), 8.70 (br s, 1H), 8.11 (s, 1H), 7.86 (d, 1H), 7.63 (d, 1H), 7.41 (dd, 1H), 7.36 (d, 1H), 4.30 (t, 2H), 3.86(t, 2H), 3.51 (s, 3H), 2.57 (s, 3H). MS 341.0 & 343.0 [M-1].

3-(2-Methoxyethoxy)-8-methyl-7*H*,10*H*-benzo(e)pyrido(4,3-b)indol-11-one (C711):

A mixture of compound C08 (39 mg, 0.11 mmol), sodium acetate (48 mg, 0.6 mmol) and AcOH (2 mL) was heated under reflux for 18 h. The volatile was evaporated under vacuum followed by a co-evaporation with toluene. Water (100 mL) was added and the medium was rendered basic by addition of 2N sodium hydroxide. The aqueous layer was extracted by AcOEt and EtOH, dried over $MgSO_4$ and evaporated under vacuum to give the exected compound (30 mg, 81%). ^{1}H NMR (300 MHz, DMSO-d_6) δ (ppm): 12.09 (br s, 1H), 11.01 & 10.99 (2 s, 1H), 10.33 (d, 1H), 7.80-7.70 (m, 2H), 7.46 (d, 1H), 7.26 (dd, 1H), 7.15 (d, 1H), 4.28 (t, 2H), 3.80 (t, 2H), 3.41 (s, 3H), 2.35 (s, 3H). MS 345.2 [M+Na].

REFERENCES

Ahmed, A.A., Lu, Z., Jennings, N.B., Etemadmoghadam, D.L., Jacamo, R.O., et al. (2010). SIK2 is a centrosome kinase required for bipolar mitotic spindle formation that provides a potential target for therapy in ovarian cancer. *Cancer Cell*. **18**, 109-21.

Aihara, A., Tanaka, S., Yasen, M., Matsumura, S., Mitsunori, Y., et al. (2010). The selective Aurora B kinase inhibitor AZD1152 as a novel treatment for hepatocellular carcinoma. *J Hepatol.* **52**, 63-71.

Archambault, V. and Carmena, M. (2012). Polo-like kinase-activating kinases: Aurora A, Aurora B and what else?. *Cell Cycle*. **11,** 1490-5.

Arlot-Bonnemains, Y., Baldini, E., Martin, B., Delcros, J.G., Toller, M., et al. (2008). Effects of the Aurora kinase inhibitor VX-680 on anaplastic thyroid cancer-derived cell lines. *Endocr Relat Cancer.* **15**, 559-68.

Baek, S.H. (2011).When signaling kinases meet histones and histone modifiers in the nucleus. *Mol Cell.* **42**, 274-84.

Banko, M.R., Allen, J.J., Schaffer, B.E., Wilker, E.W., Tsou, P., (2011). Chemical genetic screen for AMPKα2 substrates uncovers a network of proteins involved in mitosis. *Mol Cell.* **44**, 878-92.

Bastos, R.N., Barr, F.A. (2010). Plk1 negatively regulates Cep55 recruitment to the midbody to ensure orderly abscission. *J Cell Biol.* **191,** 751-60.

Bird, A.W., Hyman, A,A. (2008). Building a spindle of the correct length in human cells requires the interaction between TPX2 and Aurora A. *J Cell Biol.***182,** 89-300.

Bischoff, J.R., Plowman G.D. (1999). The Aurora/Ipl1p kinase family: regulators of chromosome segregation and cytokinesis. *Trends Cell Biol.* **9**, 454-9.

Blangy, A., Lane, H.A., d'Hérin, P., Harper, M., Kress, M., Nigg, E.A. (1995). Phosphorylation by p34cdc2 regulates spindle association of human Eg5, a kinesin-related motor essential for bipolar spindle formation *in vivo*. *Cell.* **83**,1159-69.

Bonet, C., Giuliano, S., Ohanna, M., Bille, K., Allegra, M., Bertolotto, C. et al. (2012). Aurora B is regulated by the mitogen-activated protein kinase/extracellular signal-regulated kinase (MAPK/ERK) signaling pathway and is a valuable potential target in melanoma cells. *J Biol Chem.* **287**, 29887-98.

Bothos, J., Tuttle, R.L., Ottey, M., Luca, F.C., Halazonetis, T.D. (2005). Human LATS1 is a mitotic exit network kinase. *Cancer Res.* **65**, 6568-75.

Bringmann, H. (2005). Cytokinesis and the spindle midzone. *Cell Cycle*. **4**, 1709-12.

Brito, D.A., Rieder, CL. (2006). Mitotic checkpoint slippage in humans occurs via cyclin B destruction in the presence of an active checkpoint. *Curr Biol*. **16**, 1194-200.

Campbell, C.S., Desai, A. (2013). Tension sensing by Aurora B kinase is independent of survivin-based centromere localization. *Nature*. **497**, 118-21.

Carmena, M., Earnshaw, W.C. (2003). The cellular geography of aurora kinases. *Nat Rev Mol Cell Biol.* **4**, 842-54.

Carmena, M., Ruchaud, S., Earnshaw, W.C. (2009). Making the Auroras glow: regulation of Aurora A and B kinase function by interacting proteins. *Curr Opin Cell Biol.* **21**, 796-805.

Carmena, M. (2012). Abscission checkpoint control: stuck in the middle with Aurora B. *Open Biol.* **2**, 120095.

Cerutti, H., Casas-Mollano, J.A. (2009). Histone H3 phosphorylation: universal code or lineage specific dialects?. *Epigenetics*. **4,** 71-5.

Cimini, D., Degrassi, F. (2005). Aneuploidy: a matter of bad connections. *Trends Cell Biol.* **15**, 442-51.

Chan, E.H., Santamaria, A., Silljé, H.W., Nigg, E.A. (2008). Plk1 regulates mitotic Aurora A function through βTrCP-dependent degradation of hBora. *Chromosoma.* **117**, 457–69.

Chan, C.S., Botstein, D. (1993). Isolation and characterization of chromosome-gain and increase-in-ploidy mutants in yeast. *Genetics.* **135,** 677-91.

Chan, G.K., Jablonski, S.A., Sudakin, V., Hittle, J.C., Yen, T.J. (1999). Human BUBR1 is a mitotic checkpoint kinase that monitors CENP-E functions at kinetochores and binds the cyclosome/APC. *J Cell Biol*. **146**, 941-54.

Cheeseman, I.M,, Desai, A. (2008). Molecular architecture of the kinetochore-microtubule interface. *Nat Rev Mol Cell Biol*. **9**, 33-46.

Cheetham, G.M., Knegtel, R.M., Coll, J.T., Renwick, S.B., Swenson, L., Weber P., Austen, D.A. et al. (2002). Crystal structure of aurora-2, an oncogenic serine/threonine kinase. *J Biol Chem*. **277**, 42419-22.

Chen, H.L., Tang, C.J., Chen, C.Y., Tang, T.K. (2005). Overexpression of an Aurora-C kinase-deficient mutant disrupts the Aurora-B/INCENP complex and induces polyploidy. *J Biomed Sci.* **12,** 297-310.

Chen, C.T., Hehnly, H., Doxsey, S.J. (2012). Orchestrating vesicle transport, ESCRTs and kinase surveillance during abscission. *Nat Rev Mol Cell Biol.***13**, 483-8

Chen, Y.J., Chen, C.M., Twu, N.F., Yen, M.S., Lai, C.R., Yuan. C.C. et al., (2009). Overexpression of Aurora B is associated with poor prognosis in epithelial ovarian cancerpatients. *Virchows Arch.* 455, 431-40.

Chu, Y., Yao, P.Y., Wang, W., Wang, D., Wang, Z., Yao, X. et al. (2011). Aurora B kinase activation requires survivin priming phosphorylation by PLK1. *J Mol Cell Biol.* **3**, 260-7.

Dar, A.A., Goff , L.W., Majid, S., Berlin, J., El-Rifai, W. (2010). Aurora kinase inhibitors: rising stars in cancer therapeutics?. *Mol Cancer Ther.* **9**, 268-78.

Davis, D.A., Sarkar, S.H., Hussain, M., Li, Y., Sarkar, F.H. (2006). Increased therapeutic potential of an experimental anti-mitotic inhibitor SB715992 by genistein in PC-3 human prostate cancer cell line. *BMC Cancer*. **6**, 22.

De la Barre, A.E., Angelov, D., Molla, A., Dimitrov, S. (2001). The N-terminus of histone H2B, but not that of histone H3 or its phosphorylation, is essential for chromosome condensation. *EMBO J.* **20**, 6383-93.

Delacour-Larose, M., Molla, A., Skoufias, D.A., Margolis, R.L., Dimitrov, S. (2004). Distinct dynamics of Aurora B and Survivin during mitosis. *Cell Cycle.* **3,** 1418-26.

DeLuca, J.G., Musacchio, A. (2012). Structural organization of the kinetochore-microtubule interface. *Curr Opin Cell Biol.* **24,** 48-56.

DeLuca, J.G., Gall, W.E., Ciferri, C., Cimini, D., Musacchio, A., Salmon, E.D. (2006). Kinetochore microtubule dynamics and attachment stability are regulated by Hec1. *Cell.* **127**, 969-82.

Dieterich, K., Zouari, R., Harbuz, R., Vialard, F., Martinez, D., Ray, P.F. et al. (2009). The Aurora Kinase C c.144delC mutation causes meiosis I arrest in men and is frequent in the North African population. *Hum Mol Genet.* **18**, 1301-9.

Dodson, C.A., Bayliss, R. (2012). Activation of Aurora-A kinase by protein partner binding and phosphorylation are independent and synergistic. *J Biol Chem.* **287**, 1150-7.

Dodson, C.A., Kosmopoulou, M,, Richards ,M.W., Atrash, B., Bavetsias, V., Blagg, J., Bayliss, R. (2010). Crystal structure of an Aurora-A mutant that mimics Aurora-B bound to MLN8054: insights into selectivity and drug design. *Biochem J.* **427**, 19-28.

Dunleavy, E.M., Roche, D., Tagami, H., Lacoste, N., Ray-Gallet, D., Almouzni-Pettinotti, G. et al. (2009). HJURP is a cell-cycle-dependent maintenance and deposition factor of CENP-A at centromeres. *Cell*. **137**, 485-97.

Dutertre, S., Cazales, M., Quaranta, M., Froment, C., Ducommun, B. et al. (2004). Phosphorylation of CDC25B by Aurora-A at the centrosome contributes to the G2-M transition. *J Cell Sci*. **117**, 2523-31.

Dutertre, S., Hamard-Péron, E., Cremet, J.Y., Thomas, Y., Prigent, C. (2005).The absence of p53 aggravates polyploidy and centrosome number abnormality induced by Aurora-Coverexpression. *Cell Cycle*. **4**, 1783-7.

Elkins, J.M., Santaguida, S., Musacchio, A., Knapp, S. (2012). Crystal structure of human aurora B in complex with INCENP and VX-680. *J Med Chem*. **55**, 7841-8.

Enserink, J.M., Kolodner, R.D. (2010). An overview of Cdk1-controlled targets and processes. *Cell Division.* **5**, 11-52.

Escude, C., Nguyen, C.H., Mergny, J.L., Sun, J.S., Bisagni, E., Garestier, T. and Helene, C. (1995). Selective Stabilization of DNA Triple Helixes by Benzopyridoindole Derivatives. *J. Am. Chem. Soc.* **117,** 10212-10219.

Eyers, P.A., Erikson, E., Chen, L.G., Maller, J.L..(2003). A novel mechanism for activation of the protein kinase Aurora A. *Curr Biol.* **13**, 691-7.

Fink, J., Sanders, K., Rippl, A., Finkernagel, S., Beckers, T.L., Schmidt, M. (2007). Cell type-dependent effects of Polo-like kinase 1 inhibition compared with targeted polo box interference in cancer cell lines. *Mol Cancer Ther.* 6, 3189-97.

Fu, J., Bian, M., Liu, J., Jiang, Q., Zhang, C. (2009). A single amino acid change converts Aurora-A into Aurora-B-like kinase in terms of partner specificity and cellular function. *Proc Natl Acad Sci U S A.* **106**, 6939-44.

Gabillard, J.C., Ulisse, S., Baldini, E., Sorrenti, S., Cremet, J.Y., Arlot-Bonnemains, Y. et al. (2011). Aurora-C interacts with and phosphorylates the transforming acidic coiled-coil 1 protein. *Biochem Biophys Res Commun.* 408, 647-53.

Gadea, B.B., Ruderman JV.(2006). Aurora B is required for mitotic chromatin-induced phosphorylation of Op18/Stathmin. *Proc Natl Acad Sci U S A.* **103**, 4493-8.

Galons, H., Oumata, N., Gloulou, O., Meijer, L. (2013). Cyclin-dependent kinase inhibitors closer to market launch?. *Expert Opin Ther Pat.* [Epub ahead of print]

Gontarewicz, A., Balabanov, S., Keller, G., Colombo, R., Brümmendorf, T.H. et al. (2008). Simultaneous targeting of Aurora kinases and Bcr-Abl kinase by the small molecule inhibitor PHA-739358 is effective against imatinib-resistant BCR-ABL mutations including T315I. *Blood.* **111**, 4355-64.

Guan, R., Tapang, P., Leverson, J.D., Albert, D., Giranda, V.L., Luo, Y. (2005). Small interfering RNA-mediated Polo-like kinase 1 depletion preferentially reduces the survival of p53-defective, oncogenic transformed cells and inhibits tumor growth in animals. *Cancer Res.* 65, 2698-704.

Guse, A., Mishima, M., Glotzer, M. (2005). Phosphorylation of ZEN4/ MKLP1 by aurora B regulates completion of cytokinesis. *Curr Biol.* **15**, 778-86.

Guse, A., Carroll, C.W., Moree, B., Fuller, C.J., Straight, A.F. (2011). *In-vitro* centromere and kinetochore assembly on defined chromatin templates. *Nature.* **477**, 354-8.

Giet, R., Prigent, C. (1999). Aurora/Ipl1p-related kinases, a new oncogenic family of mitotic serine-threonine kinases. *J Cell Sci.* **112**, 3591-601.

Giles, F.J., Cortes, J., Jones, D., Bergstrom, D., Kantarjian, H., Freedman, S.J. (2007). MK-0457, a novel kinase inhibitor, is active in patients with chronic myeloid leukemia or acute lymphocytic leukemia with the T315I BCR-ABL mutation. *Blood.* **109**, 500-2.

Girdler, F., Gascoigne, K.E., Eyers, P.A., Hartmuth, S., Crafter, C., Foote, K.M., Keen, N.J., Taylor, S.S. (2006). Validating Aurora B as an anti-cancer drug target. *J Cell Sci.* **119**, 3664-75.

Girdler, F., Sessa, F., Patercoli, S., Villa, F., Musacchio, A,, Taylor, S. (2008). Molecular basis of drug resistance in aurora kinases. *Chem Biol*. **15**, 552-62.

Giubettini, M., Asteriti, I.A., Scrofani, J., De Luca, M., Lindon, C., Lavia, P., Guarguaglini, G. (2011). Control of Aurora-A stability through interaction with TPX2. *J Cell Sci.* **124**, 113-22.

Gizatullin, F., Yao, Y., Kung, V., Harding, M.W., Loda, M., Shapiro, G.I. (2006). The Aurora kinase inhibitor VX-680 induces endoreduplication and apoptosis preferentially in cells with compromised p53-dependent postmitotic checkpoint function. *Cancer Res.* **66**, 7668-77.

Han, Z., Riefler, G.M., Saam, J.R., Mango, S.E., Schumacher, J.M. (2005). The *C. elegans* Tousled-like kinase contributes to chromosome segregation as a substrate and regulator of the Aurora B kinase. *Curr Biol.* **15**, 894-904.

Hans, F., Skoufias, D.A., Dimitrov, S., Margolis, R.L. (2009). Molecular distinctions between Aurora A and B: a single residue change transforms Aurora A into correctly localized and functional Aurora B. *Mol Biol Cell*. **20**, 3491-502.

Hans, F., Dimitrov, S. (2001). Histone H3 phosphorylation and cell division. *Oncogene*. **20**, 3021-7.

Hardie, D.G. (2011). AMP-activated protein kinase: an energy sensor that regulates all aspects of cell function. *Genes Dev.* **25**, 1895-908.

Hari, M., Loganzo, F., Annable, T., Tan, X., Musto, S., Morilla, D.B., Greenberger, L.M. et al. (2006). Paclitaxel-resistant cells have a mutation in the paclitaxel-binding region of beta-tubulin (Asp26Glu) and less stable microtubules. *Mol Cancer Ther*. 5, 270-8.

Harrington, E.A., Bebbington, D., Moore, J., Rasmussen, R.K., Miller, K.M. et al. (2004). VX-680, a potent and selective small-molecule inhibitor of the Aurora kinases, suppresses tumor growth in vivo. *Nat Med.* **10,** 262-7.

Hauf, S., Watanabe, Y. (2004). Kinetochore orientation in mitosis and meiosis. *Cell.* 119, 317-27.

Herzog , F., Primorac, I., Dube, P., Lenart, P., Sander, B., Mechtler, K., Stark, H., Peters, J.M. (2009). Structure of the anaphase-promoting complex/cyclosome interacting with a mitotic checkpoint complex. *Science.* **13**, 1477-81.

Hewitt, L., Tighe, A., Santaguida, S., White, A.M., Taylor, S.S. (2010). Sustained Mps1 activity is required in mitosis to recruit O-Mad2 to the Mad1-C-Mad2 core complex. *J Cell Biol*. **190**, 25-34.

Hirano, T. (2005). Condensins: organizing and segregating the genome. *Curr Biol*. **15**, 265-75.

Hirota, T., Kunitoku, N., Sasayama, T., Marumoto, T., Zhang, D., Saya, H. et al. (2003). Aurora-A and an interacting activator, the LIM protein Ajuba, are required for mitotic commitment in human cells. *Cell.* **114**, 585-98.

Hoang, T.M., Favier, B., Valette, A., Barette, C., Nguyen, C.H., Molla, A. et al. (2009). Benzo[e]pyridoindoles, novel inhibitors of the aurora kinases. *Cell Cycle.* **8**, 765-72.

Honda, K., Mihara, H., Kato,Y., Yamaguchi, A., Tanaka, H., Urano, T. et al. (2000). Degradation of human Aurora2 protein kinase by the anaphase-promoting complex-ubiquitin-proteasome pathway. *Oncogene*. **19**, 2812-9.

Honda, R., Körner, R., Nigg, E.A. (2003). Exploring the functional interactions between Aurora B, INCENP, and survivin in mitosis. *Mol Biol Cell.***14**, 3325-41.

Honma, K., Nakanishi, R., Nakanoko, T., Ando, K., Maehara, Y. et al. (2013). Contribution of Aurora-A and -B expression to DNA aneuploidy in gastric cancers. *Surg Today.* [Epub ahead of print].

Hu, C.K., Coughlin, M., Field, C.M., Mitchison, T.J. (2011). KIF4 regulates midzone length during cytokinesis. *Curr Biol.* **21**, 815-24.

Hu, C.K., Coughlin, M., Mitchison, T.J. (2012). Midbody assembly and its regulation during cytokinesis. *Mol Biol Cell*. **23**, 1024-34.

Hutterer, A., Berdnik, D., Wirtz-Peitz, F., Zigman, M., Schleiffer, A., Knoblich, J.A. (2006). Mitotic activation of the kinase Aurora-A requires its binding partner Bora. *Dev Cell*. **11**, 147-57.

Hutterer, A., Glotzer, M., Mishima, M.. (2009). Clustering of centralspindlin is essential for its accumulation to the central spindle and the midbody. *Curr Biol.* **19**, 2043-9.

Ikezoe, T. (2008). Aurora kinases as an anti-cancer target. *Cancer Lett.* **262**, 1-9.

Ikezoe,T., Nishioka, C., Tasaka, T., Yang ,Y., Komatsu, N., Togitani, K., Koeffler, H.P., Taguchi, H. (2006). The antitumor effects of sunitinib (formerly SU11248) against a variety of human hematologicmalignancies: enhancement of growth inhibition via inhibition of mammalian target of rapamycin signaling. *Mol Cancer Ther.* 5, 2522-30.

Jabbour, E., Cortes, J.E., Ghanem, H., O'Brien, S., Kantarjian, H.M. (2008). Targeted therapy in chronic myeloid leukemia. *Expert Rev Anticancer Ther.* **8**, 99-110.

Jares, P., Donaldson, A., Blow, J.J. (2000). The Cdc7/Dbf4 protein kinase: target of the S phase checkpoint?. *EMBO Rep*. **1**, 319-22.

Jeremy, P. H. C. and Randy. Y. C. P. (2010). DNA Damage and Polyploidization. From the book "Polyploidization and Cancer".

Johnson, N., Shapiro, G.I. (2010). Cyclin-dependent kinases (cdks) and the DNA damage response: rationale for cdk inhibitor-chemotherapy combinations as an anticancer strategy for solid tumors. *Expert Opin Ther Targets.* **14**, 1199-212.

Karess, R. (2005). Rod-Zw10-Zwilch: a key player in the spindle checkpoint. *Trends Cell Biol.* **15**, 386-92.

Katayama, H., Brinkley, W.R., Sen, S. (2003). The Aurora kinases: role in cell transformation and tumorigenesis. *Cancer Metastasis Rev.* **22,** 451-64.

Katayama, H., Sasai, K., Kawai, H., Yuan, Z.M., Sen, S. et al. (2004). Phosphorylation by aurora kinase A induces Mdm2-mediated destabilization and inhibition of p53. *Nat Genet.* **36**, 55-62.

Kawajiri, A., Yasui, Y., Goto, H., Tatsuka, M., Takahashi, M., Nagata, K., Inagaki, M.. (2003). Functional significance of the specific sites phosphorylated in desmin at cleavage furrow: Aurora-B may phosphorylate and regulate type III intermediate filaments during cytokinesis coordinatedly with Rho-kinase. *Mol Biol Cell*. **14,** 1489-500.

Keating, P., Rachidi, N., Tanaka, T.U., Stark, M.J. (2009). Ipl1-dependent phosphorylation of Dam1 is reduced by tension applied on kinetochores. *J Cell Sci.***122**, 4375-82.

Kelly, A.E., Ghenoiu, C., Xue, J.Z., Zierhut, .C, Kimura, H., Funabiki, H. (2010). Survivin reads phosphorylated histone H3 threonine 3 to activate the mitotic kinase Aurora B. *Science*. **330**, 235-9.

Kimmins, S., Crosio, C., Kotaja, N., Hirayama, J., Monaco, L., Höög, C., Sassone-Corsi, P. et al. (2007). Differential functions of the Aurora-B and Aurora-C kinases in mammalian spermatogenesis. *Mol Endocrinol*. **21**, 726-39.

Knowlton, A.L., Lan, W., Stukenberg, P.T. (2006). Aurora B is enriched at merotelic attachment sites, where it regulates MCAK. *Curr Biol.* **16,** 1705-10.

Kufer, T.A., Silljé, H.H., Körner, R., Gruss, O.J., Meraldi, P., Nigg, E.A.(2002). Human TPX2 is required for targeting Aurora-A kinase to the spindle. *J Cell Biol.* **158**, 617-23.

Lacroix, M., Toillon, R.A., Leclercq, G. (2006). p53 and breast cancer, an update. *Endocr Relat Cancer.***13,** 293-325.

Lan, W., Cleveland, D.W. (2010). A chemical tool box defines mitotic and interphase roles for Mps1 kinase. *J Cell Biol*. **190**, 21-4.

Lapenna, S., Giordano, A. (2009). Cell cycle kinases as therapeutic targets for cancer. *Nat Rev Drug Discov*. **8**, 547-66.

Lawo, S., Hasegan, M., Gupta, G.D., Pelletier, L. (2012). Subdiffraction imaging of centrosomes reveals higher-order organizational features of pericentriolar material. *Nat Cell Biol.* **14**, 1148-58.

Le, L.T, Vu, H.L., Naud-Martin, D., Bombled, M., Nguyen, C.H., Molla, A.(2013). Hydrosoluble benzo[e]pyridoindolones as potent inhibitors of aurora kinases. *ChemMedChem.* **8,** 289-96.

Lee, E.C., Frolov, A., Li, R., Ayala, G., Greenberg, N.M. (2006).Targeting Aurora kinases for the treatment of prostate cancer. *Cancer Res.* **66**, 4996-5002.

Lee, S., Schmitt, C.A. (2003).Chemotherapy response and resistance. *Curr Opin Genet Dev.* **13**, 90-6.

Lénárt, P., Petronczki, M., Steegmaier, M., Di-Fiore, B., Peters, J.M. et al. (2007). The small-molecule inhibitor BI 2536 reveals novel insights into mitotic roles of polo-like kinase 1. *Curr Biol.* **17**, 304-15.

Lin, Y.G., Immaneni, A., Merritt, W.M., Mangala, L.S., Sood, A.K. et al. (2008). Targeting aurora kinase with MK-0457 inhibits ovarian cancer growth. *Clin Cancer Res*, **14**, 5437–5446.

Lin, Z.Z., Jeng, Y.M., Hu, F.C., Pan, H.W., Tsao, H.W., Lai, P.L., Lee, P.H., Cheng, A.L., Hsu, H.C. (2010). Significance of Aurora B overexpression in hepatocellular carcinoma. Aurora B Overexpression in HCC. *BMC Cancer.* 10, 461

Lipp, J.J., Hirota, T., Poser, I., Peters, J.M. (2007). Aurora B controls the association of condensin I but not condensin II with mitotic chromosomes. *J Cell Sci.* **120,** 1245-55.

Lister-Sharp, D., McDonagh, M.S., Khan, K.S., Kleijnen, J. (2004). A rapid and systematic review of the effectiveness and cost-effectiveness of the taxanes used in the treatment of advanced breast and ovarian cancer. *Health Technol Assess,* **4**, 1-113.

Liu, X., Gong, H., Huang, K.. (2013). Oncogenic role of kinesin proteins and targeting kinesin therapy. *Cancer Sci.* [Epub ahead of print]

Liu, D., Lampson, M.A. (2009). Regulation of kinetochore-microtubule attachments by Aurora B kinase. *Biochem Soc Trans.* **37**, 976-80.

Liu, L., Ulbrich, J., Müller, J., Wüstefeld, T., Aeberhard, L., Murphy, D.J. (2012). Deregulated MYC expression induces dependence upon AMPK-related kinase 5. *Nature.* **483**, 608-12.

Liu, Q., Kaneko, S., Yang, L., Feldman, R.I., Nicosia, S.V., Chen, J., Cheng, J.Q. (2004). Aurora-A abrogation of p53 DNA binding and transactivation activity by phosphorylation of serine 215. *J Biol Chem.* **279,** 52175-82.

Liu, X., Erikson, R.L.(2003). Polo-like kinase (Plk)1 depletion induces apoptosis in cancer cells. *Proc Natl Acad Sci U S A.* **100**, 5789-94.

Liu, Y., Gray, N.S. (2006). Rational design of inhibitors that bind to inactive kinase conformations. *Nat Chem Biol.* **2**, 358-64.

López-Ríos, F., Ladanyi, M.. (2006). Malignant mesothelioma. *N Engl J Med.* **354,** 305-7.

Lowery, D.M., Lim, D., Yaffe, M.B. (2005), Structure and function of Polo-like kinases. *Oncogene*, **24**, 248–59

Maciejowski, J., George, K.A., Terret, M.E., Zhang, C., Shokat, K.M., Jallepalli, P.V. (2010). Mps1 directs the assembly of Cdc20 inhibitory complexes during interphase and mitosis to control M phase timing and spindle checkpoint signaling. *J Cell Biol.* **190,** 89-100.

Macůrek, L., Lindqvist, A., Lim, D., Lampson, M.A., Medema, R.H. et al. (2008). Polo-like kinase-1 is activated by aurora A to promote checkpoint recovery. *Nature.* **455**, 119-23.

Macurek, L., Lindqvist, A., Medema, R.H. (2009). Aurora-A and hBora join the game of Polo. *Cancer Res.* **69,** 4555-8.

Maerki, S., Olma, M.H., Staubli, T., Steigemann, P., Gerlich, D.W., Quadroni, M., Sumara, I., Peter, M. (2009). The Cul3-KLHL21 E3 ubiquitin ligase targets aurora B to midzone microtubules in anaphase and is required for cytokinesis. *J Cell Biol.* **187**, 791-800.

Mahadevan, D., Stejskal, A., Cooke, L.S., Manziello, A., Morales, C., Persky, D.O., Fisher, R.I., Miller, T.P., Qi, W. (2012). Aurora A inhibitor (MLN8237) plus vincristine plus rituximab is synthetic lethal and a potential curative therapy in aggressive B-cell non-Hodgkin lymphoma. *Clin Cancer Res*. **18**, 2210-9.

Malvezzi, F., Litos, G., Schleiffer, A., Heuck, A., Mechtler, K., Clausen, T., Westermann, S. (2013). A structural basis for kinetochore recruitment of the Ndc80 complex via two distinct centromere receptors. *EMBO J.* **32**, 409-23.

Manley, P.W., Cowan-Jacob, S.W., Buchdunger, E., Fabbro, D., Fendrich, G., Furet, P., Meyer, T., Zimmermann, J. (2002). Imatinib: a selective tyrosine kinase inhibitor. *Eur J Cancer.* **38**, 19-27.

Mao, Y., Desai, A., Cleveland, D.W. (2005). Microtubule capture by CENP-E silences BubR1-dependent mitotic checkpoint signaling. *J Cell Biol.* **170,** 873-80.

Mao, Y., Varma, D., Vallee, R. (2010). Emerging functions of force-producing kinetochore motors. *Cell Cycle.* **9,** 715-9.

Martin, M.P., Zhu, J.Y., Lawrence, H.R., Pireddu, R., Schönbrunn, E. et al. (2012). A novel mechanism by which small molecule inhibitors induce the DFG flip in Aurora A. *ACS Chem Biol.* **7**, 698-706.

May, K.M., Hardwick KG. (2006). The spindle checkpoint. *J Cell Sci.* **119,** 4139-42.

Mayer , T.U., Kapoor, T.M., Haggarty, S.J., King, R.W., Schreiber, S.L., Mitchison, T.J. (1999). Small molecule inhibitor of mitotic spindle bipolarity identified in a phenotype-based screen. *Science*. **286,** 971-4.

Meldi, L., Brickner, J.H. (2011). Compartmentalization of the nucleus. *Trends Cell Biol.* **21**, 701-8.

Meraldi, P., Honda, R., Nigg, E.A. (2002). Aurora-A overexpression reveals tetraploidization as a major route to centrosome amplification in p53-/- cells. *EMBO J.* **21**, 483-92.

Molla, A. (2010). Aurora kinases orchestrate mitosis; who are the players?. *BioMolecular Concepts*. **1**, 147-155.

Molli, P.R., Li, D.Q., Bagheri-Yarmand, R., Pakala, S.B., Kumar, R. et al. (2010). Arpc1b, a centrosomal protein, is both an activator and substrate of Aurora A. *J Cell Biol.* **190,** 101-14.

Motoshima, H., Goldstein, B.J., Igata, M., Araki, E. (2006). AMPK and cell proliferation: AMPK as a therapeutic target for atherosclerosis and cancer. *J Physiol.* ***574,*** 63-71.

Musacchio, A., Salmon, E.D. (2007). The spindle-assembly checkpoint in space and time. *Nat Rev Mol Cell Biol.* **8**, 379-93.

Nachury, M.V., Maresca, T.J., Salmon, W.C., Waterman-Storer, C.M., Heald, R., Weis, K. (2001). Importin beta is a mitotic target of the small GTPase Ran in spindle assembly. *Cell.***104**, 95-106.

Nair, J.S., Tse, A., Keen, N. et al. (2004). A novel Aurora B kinase inhibitor with potent anticancer activity either as a single agent or in combination with chemotherapy. *J Clin Oncol.* **22**.

Nasmyth, K., Haering, C.H. (2009). Cohesin: its roles and mechanisms. *Annu Rev Genet.* **43**, 525-58.

Nigg, E.A., Raff, JW.(2009). Centrioles, centrosomes, and cilia in health and disease. *Cell.* **139**, 663-78.

Nilsson, J., Yekezare, M., Minshull, J., Pines, J. (2008). The APC/C maintains the spindle assembly checkpoint by targeting Cdc20 for destruction. *Nat Cell Biol.* **10**, 1411-20.

Nguyen, C.H. , Marchand, C., Delage, S. , Sun, J.S. , Garestier, T. , Hélène, C. and Bisagni, E. (1998). Synthesis of 13H-Benzo[6,7]- and 13H-Benzo[4,5]indolo[3,2-c]- quinolines: A New Series of Potent Specific Ligands for Triplex DNA. *J. Am. Chem. Soc.* **120**, 2501–2507.

Nguyen, C.H., Bisagni, E., Lavelle, F., Bissery, M.C., Huel, C. (1992). Synthesis and antitumor properties of new 4-methyl-substituted- pyrido[4,3-b]indoles (gamma-carbolines). *Anticancer Drug Des.* **7**, 219-33.

Nguyen, C.H., Lhoste, J.M., Lavelle, F., Bissery, M.C., Bisagni, E. (1990). Synthesis and antitumor activity of 1-[[(dialkylamino)alkyl]amino]-4-methyl-5H-pyrido[4,3-b]benzo[e]- and -benzo[g])indoles- A new class of antineoplastic agents. *J Med Chem.* **33**, 1519-28.

Nguyen, H.G., Chinnappan, D., Urano, T., Ravid, K. (2005). Mechanism of Aurora-B degradation and its dependency on intact KEN and A-boxes: identification of an aneuploidy-promoting property. *Mol Cell Biol.* **25**, 4977-92.

O'Connor, C. (2008). Cell Division: Stages of Mitosis. *Nature Education,* **1**.

Olmos, D., Barker, D., Sharma, R., Brunetto, A.T., Yap, T.A., Blagden, S.P. (2013). Phase I study of GSK461364, a specific and competitive Polo-like kinase 1 inhibitor, in patients with advancedsolid malignancies. *Clin Cancer Res.* **17,** 3420-30.

O'Shaughnessy, J., Gradishar, W.J., Bhar, P., Iglesias, J. (2013). nab-Paclitaxel for first-line treatment of patients with metastatic breast cancer and poor prognostic factors: a retrospective analysis. *Breast Cancer Res Treat*. **138**, 829-37.

Pan, C., Yan, M., Yao, J. et al. (2008). Aurora kinase small molecule inhibitor destroys mitotic spindle, suppresses cell growth, and induces apoptosis in oral squamous cancer cells. *Oral Oncol*. **44**, 639 – 645.

Pan, D. (2010). The hippo signaling pathway in development and cancer. *Dev Cell*. **19,** 491-505.

Petersen, J., Paris, J., Willer, M., Philippe, M., Hagan, I.M. (2001). The S. pombe aurora-related kinase Ark1 associates with mitotic structures in a stage dependent manner and is required for chromosome segregation. *J Cell Sci.* **114,** 4371-84.

Petsalaki , E., Akoumianaki, T., Black, E.J., Gillespie, D.A., Zachos, G. (2011). Phosphorylation at serine 331 is required for Aurora B activation. *J Cell Biol.* **195,** 449-66.

Petretti, C., Savoian, M., Montembault, E., Glover, D.M., Prigent, C., Giet, R. (2006). The PITSLRE/CDK11p58 protein kinase promotes centrosome maturation and bipolar spindle formation. *EMBO Rep*. **7**, 418-24.

Petronczki, M., Lénárt, P., Peters, J-M. (2008). Polo on the rise-from mitotic entry to cytokinesis with Plk1. *Dev Cell*. **14**, 646–59.

Pihan, G.A., Wallace, J., Zhou, Y., Doxsey, S.J. (2003). Centrosome abnormalities and chromosome instability occur together in pre-invasive carcinomas. *Cancer Res.* **63,** 1398-404.

Prigent, C., Dimitrov, S. (2003). Phosphorylation of serine 10 in histone H3, what for?. *J Cell Sci.* **116**, 3677-85.

Przewloka, M.R., Venkei, Z., Bolanos-Garcia, V.M., Debski, J., Dadlez, M, Glover, D.M. (2011). CENP-C is a structural platform for kinetochore assembly. *Curr Biol.* **21,** 399-405.

Pugacheva, E.N., Jablonski, S.A., Hartman, T.R., Henske, E.P., Golemis E.A. (2007). HEF1-dependent Aurora A activation induces disassembly of the primary cilium. *Cell.* **129**, 1351-63.

Qi, W., Liu, X., Cooke, L.S., Persky, D.O., Miller, T.P., Squires, M., Mahadevan, D. (2012). AT9283, a novel aurora kinase inhibitor, suppresses tumor growth in aggressive B-cell lymphomas. *Int J Cancer*. **130,** 2997-3005.

Reboutier, D., Troadec, M.B., Cremet, J.Y., Fukasawa, K., Prigent, C. (2012). Nucleophosmin/B23 activates Aurora A at the centrosome through phosphorylation of serine 89. *J Cell Biol.* **197,** 19-26.

Remeseiro, S., Losada, A. (2013). Cohesin, a chromatin engagement ring. *Curr Opin Cell Biol.* **25***,* 63-71.

Rosasco-Nitcher, S.E., Lan, W., Khorasanizadeh, S., Stukenberg, P.T. (2008). Centromeric Aurora-B activation requires TD-60, microtubules, and substrate priming phosphorylation. *Science.* **319**, 469-72.

Sabino, D., Brown, N.H., Basto, R. (2011). Drosophila Ajuba is not an Aurora-A activator but is required to maintain Aurora-A at the centrosome. *J Cell Sci.* **124,** 1156-66.

Sakurikar, N., Eichhorn, J.M., Chambers, T.C. (2012). Cyclin-dependent kinase-1 (Cdk1)/cyclin B1 dictates cell fate after mitotic arrest via phosphoregulation of antiapoptotic Bcl-2 proteins. *J Biol Chem*. **287,** 39193-204.

Sampath, S.C., Ohi, R., Leismann, O., Salic, A., Pozniakovski, A., Funabiki, H. (2004). The chromosomal passenger complex is required for chromatin-induced microtubule stabilization andspindle assembly. *Cell*. **118,** 187-202.

Sasai, K., Katayama, H., Stenoien, D.L., Fujii, S., Honda, R., Sen, S. et al. (2004). Aurora-C kinase is a novel chromosomal passenger protein that can complement Aurora-B kinase function in mitotic cells. *Cell Motil Cytoskeleton.* **59**, 249-63.

Screpanti, E., De Antoni, A., Alushin, G.M., Petrovic, A., Melis, T., Nogales, E., Musacchio, A. (2011). Direct binding of Cenp-C to the Mis12 complex joins the inner and outer kinetochore. *Curr Biol*. **21**, 391-8.

Schmitt, A., Gutierrez, G.J., Lénárt, P., Ellenberg, J., Nebreda, A.R. (2002). Histone H3 phosphorylation during Xenopus oocyte maturation: regulation by the MAP kinase/p90Rsk pathway and uncoupling from DNA condensation. *FEBS Lett.*, **518**, 23-8.

Schumacher, J.M., Ashcroft, N., Donovan, P.J., Golden, A. (1998). A highly conserved centrosomal kinase, AIR-1, is required for accurate cell cycle progression and segregation of developmental factors in Caenorhabditis elegans embryos. *Development*. **125**, 4391-402.

Schumacher, J.M., Golden, A., Donovan, P.J. (1998). AIR-2: An Aurora/Ipl1-related protein kinase associated with chromosomes and midbody microtubules is required for polar body extrusion and cytokinesis in Caenorhabditis elegans embryos. *J Cell Biol.* **143**, 1635-4.

Seki, A., Coppinger, J.A., Du, H., Jang, C.Y., Yates, J.R., Fang, G. (2008). Plk1- and β-TrCP-dependent degradation of Bora controls mitotic progression. *J Cell Biol*. **181,** 65–78.

Seki, A., Coppinger, J.A., Jang, C.Y., Yates, J.R., Fang, G. (2008). Bora and the kinase Aurora a cooperatively activate the kinase Plk1 and control mitotic entry. *Science.* **320,** 1655-8.

Sessa, F., Mapelli, M., Ciferri, C., Tarricone, C., Areces, L.B., Schneider, T.R., Stukenberg, P.T.,, Musacchio, A. (2005). Mechanism of Aurora B activation by INCENP and inhibition by hesperadin. *Mol Cell.* **18**, 379-91.

Sharma, A., Madhunapantula, S.V., Gowda, R., Berg, A., Neves, R.I., Robertson, G.P.. (2013). Identification of aurora kinase B and Wee1-like protein kinase as downstream targets of (V600E)B-RAF in melanoma. *Am J Pathol.* **182**, 1151-62.

Signorovitch, J.E., Wu, E.Q., Betts, K.A., Parikh, K., DeAngelo, D.J. et al. (2011). Comparative efficacy of nilotinib and dasatinib in newly diagnosed chronic myeloid leukemia: a matching-adjusted indirect comparison of randomized trials. *Curr Med Res Opin.* **27,** 1263-71.

Socinski, M.A., Govindan, R., Spigel, D. (2012). Clinical roundtable monograph: Recent advances in taxanes for the first-line treatment of advanced non-small cell lung cancer. *Clin Adv Hematol Oncol.* **10,** 1-16.

Steegmaier, M., Hoffmann, M., Baum, A., Lénárt, P., Petronczki, M., Rettig. W.J. et al. (2007). BI 2536, a potent and selective inhibitor of polo-like kinase 1, inhibits tumor growth in vivo. *Curr Biol.* **17,** 316-22.

Steigemann, P., Wurzenberger, C., Schmitz, M.H., Held, M., Guizetti, J., Maar, S., Gerlich, D.W. (2009). Aurora B-mediated abscission checkpoint protects against tetraploidization. *Cell.* **136**, 473-84.

Stein, MA.**, Rubin, E.H., Scott, P.D., Fernandez, R., Wilding, G. et al. (2006). Phase I clinical and pharmacokinetic (PK) trial of the kinesin spindle protein (KSP) inhibitor MK-0731 in cancer patients.* Journal of Clinical Oncology. ***24.

Strebhardt, K., Ullrich, A. (2006). Targeting polo-like kinase 1 for cancer therapy. *Nat Rev Cancer*. **6**, 321-30.

Sumara, I., Giménez-Abián, J.F., Gerlich, D., Hirota, T., Peters, J.M. (2004). Roles of polo-like kinase 1 in the assembly of functional mitotic spindles. *Curr Biol.* **14**, 1712-22.

Sumara, I., Quadroni, M., Frei, C., Olma, M.H., Sumara, G., Ricci, R., Peter, M. (2007). A Cul3-based E3 ligase removes Aurora B from mitotic chromosomes, regulating mitotic progression and completion of cytokinesis in human cells. *Dev Cell.* **12,** 887-900.

Suzuki, A., Lu, J., Kusakai, G., Kishimoto, A., Ogura, T., Esumi, H. (2004). ARK5 is a tumor invasion-associated factor downstream of Akt signaling. *Mol Cell Biol.* **24**, 3526-35.

Takai, N., Hamanaka, R., Yoshimatsu, J., Miyakawa, I. (2005). Polo-like kinases (Plks) and cancer. *Oncogene.* **24,** 287-91.

Takemoto, A., Murayama, A., Katano, M., Urano, T., Kimura, K. et al. (2007). Analysis of the role of Aurora B on the chromosomal targeting of condensin I. *Nucleic Acids Res.* **35**, 2403-12.

Takeuchi, K., Fukagawa, T. (2012). Molecular architecture of vertebrate kinetochores. *Exp Cell Res.* **318,** 1367-74.

Tanaka, R., Squires, M.S., Kimura, S. et al. (2008). Activity of the multi-targeted kinase inhibitor, AT9283 on Imatinib-resistant CML models. *Blood*. **112.**

Tang, C.J., Lin, C.Y., Tang, T.K. (2006). Dynamic localization and functional implications of Aurora-C kinase during male mouse meiosis. *Dev Biol.* **290**, 398-410.

Tao, Y., Zhang, P., Girdler, F. et al. (2008). Enhancement of radiation response in p53-deficient cancer cells by the Aurora-B kinase inhibitor AZD1152. *Oncogene.* **27**, 3244 –3255.

Tao, W., South ,V.J., Zhang, Y., Davide, J.P., Farrell, L., Kohl, N.E., Sepp-Lorenzino, L., Lobell, R.B. (2005). Induction of apoptosis by an inhibitor of the mitotic kinesin KSP requires both activation of the spindle assembly checkpoint and mitotic slippage. *Cancer Cell.* **8**, 49-59.

Tao, W., South, V.J., Diehl, R.E., Davide, J.P., Sepp-Lorenzino, L., Fraley, M.E., Arrington, K.L., Lobell, R.B. (2007). An inhibitor of the kinesin spindle protein activates the intrinsic apoptotic pathway independently of p53 and de novo protein synthesis. *Mol Cell Biol.***27**, 689-98.

Tsai, Y., Wiese, C., Cao, K., Martin, O., Zheng, Y. et al. (2003). A Ran signalling pathway mediated by the mitotic kinase Aurora A in spindle assembly. *Nat Cell Biol.* **5**, 242-8.

Tsou, J.H., Chang, K.C., Chang-Liao, P.Y., Yang, S.T., Hung, L.Y. et al. (2011). Aberrantly expressed AURKC enhances the transformation and tumourigenicity of epithelial cells. *J Pathol.* **225**, 243-54.

Thaiparambil, J.T., Eggers, C.M., Marcus, A.I. (2012). AMPK regulates mitotic spindle orientation through phosphorylation of myosin regulatory light chain. *Mol Cell Biol.* **32**, 3203-17.

Trakala, M., Fernández-Miranda, G., Pérez de Castro, I., Heeschen, C., Malumbres, M. (2013). Aurora B prevents delayed DNA replication and premature mitotic exit by repressing p21(Cip1). *Cell Cycle.* **12,** 1030-41.

Ueda, Y., Enomoto, T., Matsuzaki, S., Kobayashi, E., Kimura, T., Yoshino, K., Fujita, M., Tsutsui, T., Kimura, T. (2013). Taxane-sensitivity of ovarian carcinomas previously treated with paclitaxel and carboplatin. *Cancer Chemother Pharmacol.* [Epub ahead of print]

Vader, G., Lens, S.M. (2008). The Aurora kinase family in cell division and cancer. *Biochim Biophys Acta.* **1786**, 60-72.

Van der Waal, M.S., Hengeveld, R.C., van der Horst, A., Lens, S.M. (2012). Cell division control by the Chromosomal Passenger Complex. *Exp Cell Res.* **318**, 1407-20.

Van Hooser, A., Goodrich, D.W., Allis,C.D., Brinkley, B.R., Mancini, M.A. (1998). Histone H3 phosphorylation is required for the initiation, but not maintenance, of mammalian chromosome condensation. *J Cell Sci*. **111**. 3497-506.

Van Vugt, M.A., Brás, A., Medema, R.H. (2004). Polo-like kinase-1 controls recovery from a G2 DNA damage-induced arrest in mammalian cells. *Mol Cell.* **15**, 799-811.

Van Vugt, M.A., Medema, R.H. (2005). Getting in and out of mitosis with Polo-like kinase-1. *Oncogene.* **24**, 2844-59.

VanderPorten, E.C., Taverna, P., Hogan, J.N., Ballinger, M.D., Flanagan, W.M., Fucini, R.V. (2009). The Aurora kinase inhibitor SNS-314 shows broad therapeutic potential with chemotherapeutics and synergy with microtubule-targeted agents in a colon carcinoma model. *Mol Cancer Ther.* **8,** 930-9.

Veerakumarasivam, A., Goldstein, L.D., Saeb-Parsy, K., Scott, H.E., Warren, A., Kelly, J.D. et al. (2008). AURKA overexpression accompanies dysregulation of DNA-damage response genes in invasive urothelial cell carcinoma. *Cell Cycle.* **7**, 3525-33.

Vu, H.L. (2011). Les Benzo[e]pyridoindoles, une novelle famille d'inhibiteurs de kinase à activité anti-proliférative. *Ph.D thesis, UJF*.

Walter, A.O., Seghezzi, W., Korver, W., Sheung, J., Lees, E. (2000). The mitotic serine/threonine kinase Aurora2/AIK is regulated by phosphorylation and degradation. *Oncogene.* **19**, 4906-16.

Wang, F., Ulyanova, N.P., van der Waal, M.S., Patnaik, D., Lens, S.M., Higgins, J.M. (2011). A positive feedback loop involving Haspin and Aurora B promotes CPC accumulation at centromeres in mitosis. *Curr Biol.* **21,** 1061-9.

Warner, S.L., Munoz, R.M., Stafford, P., Koller, E., Hurley, L.H., Von Hoff, D.D., Han, H. (2006).Comparing Aurora Aand Aurora B as molecular targets for growth inhibition of pancreatic cancer cells. *Mol Cancer Ther.* **5,** 2450-8.

Weaver, B.A., Bonday, Z.Q., Putkey, F.R., Kops, G.J., Silk, A.D., Cleveland, D.W. (2003). Centromere-associated protein-E is essential for the mammalian mitotic checkpoint to prevent aneuploidy due to single chromosome loss. *J Cell Biol.* **162**, 551-63.

Wei, Y., Yu, L., Bowen, J., Gorovsky, M.A., Allis, C.D. (1999). Phosphorylation of histone H3 is required for proper chromosome condensation and segregation. *Cell*. **97**, 99-109.

Westermann, S., Schleiffer, A. (2013). Family matters: structural and functional conservation of centromere-associated proteins from yeast to humans. *Trends Cell Biol.* [Epub ahead of print]

Wilson, L., Jordan, MA. (2004). New microtubule/tubulin-targeted anticancer drugs and novel chemotherapeutic strategies. *J Chemother.* **16**, 83-5.

Woessner, R., Tunquist, B., Lemieux, C., Chlipala, E., Walker, D. (2009). ARRY-520, a novel KSP inhibitor with potent activity in hematological and taxane-resistant tumor models. *Anticancer Res.* **29**, 4373-80.

Wordeman, L. (2010). How kinesin motor proteins drive mitotic spindle function: Lessons from molecular assays. *Semin Cell Dev Biol.* **21**, 260-8.

Xu, Z., Ogawa, H., Vagnarelli, P., Bergmann, J.H., Samejima, K. (2009). INCENP-aurora B interactions modulate kinase activity and chromosome passenger complex localization. *J Cell Biol.* **187,** 637-53.

Yabe, T., Ge, X., Lindeman, R., Nair, S., Runke, G., Mullins, M.C., Pelegri, F. (2009). The maternal-effect gene cellular island encodes aurora B kinase and is essential for furrow formation in the early zebrafish embryo. *PLoS Genet*. **5**, e1000518.

Yabuta, N., Okada, N., Ito, A., Hosomi, T., Nojima, H. et al. (2007). Lats2 is an essential mitotic regulator required for the coordination of cell division. *J Biol Chem.* **282**, 19259-71.

Yang, J., Ikezoe, T., Nishioka, C. et al. (2007). AZD1152, a novel and selective aurora B kinase inhibitor, induces growth arrest, apoptosis, and sensitization for tubulin depolymerizing agent or topoisomerase II inhibitor in human acute leukemia cells in vitro and in vivo. *Blood.* **110**, 2034 –2040.

Yang, H., Ou, C.C., Feldman, R.I., Nicosia, S.V., Kruk, P.A., Cheng, J.Q. (2004). Aurora-A kinase regulates telomerase activity through c-Myc in human ovarian and breast epithelial cells. *Cancer Res.* **64,** 463-7.

Yasui, Y., Urano, T., Kawajiri, A., Nagata, K., Tatsuka, M., Saya, H., Furukawa, K., Takahashi ,T., Izawa, I., Inagaki, M. (2004). Autophosphorylation of a newly identified site of Aurora-B is indispensable for cytokinesis. *J Biol Chem.* **279,** 12997-3003.

Young, M.A., Shah, N.P., Chao, L.H., Seeliger. M., Kuriyan, J. et al. (2006). Structure of the kinase domain of an imatinib-resistant Abl mutant in complex with the Aurora kinase inhibitor VX-680. *Cancer Res.* **66**, 1007-14.

Yuan, K., Li, N., Huo, Y., Yan, F., Yang, Y., Ward, T., Jin, C., Yao, X. (2009). Recruitment of separase to mitotic chromosomes is regulated by Aurora B. *Cell Cycle.* **8**, 1433-43.

Zeng, W.F., Navaratne, K., Prayson, R.A., Weil, R.J. (2007). Aurora B expression correlates with aggressive behaviour in glioblastoma multiforme. *J Clin Pathol.* **60**, 218-21.

Zhao, Z.S., Lim, J.P., Ng, Y.W., Lim, L., Manser, E. (2005). The GIT-associated kinase PAK targets to the centrosome and regulates Aurora-A. *Mol Cell.* **20**, 237-49.

Zhou, B.B., Bartek, J. (2004). Targeting the checkpoint kinases : chemosensitization versus chemoprotection. *Nat Rev Cancer.* **4**, 216-25.

Zhou, J., Giannakakou, P. (2005). Targeting microtubules for cancer chemotherapy. *Curr Med Chem Anticancer Agents.* **5,** 65-71.

Zou, J., Luo, S.D., Wei, Y.Q., Yang, S.Y. (2011). Integrated computational model of cell cycle and checkpoint reveals different essential roles of Aurora-A and Plk1in mitotic entry. *Mol Biosyst.* **7,** 169-79.

ABSTRACT

Benzo[e]pyridoindoles are novel potent inhibitors of aurora kinases. We performed a SAR study to improve their activity and water solubility. Amino-benzo[e]pyridoindolones were found to be potent hydrosoluble anti-proliferative molecules. They induced a massive arrest in mitosis, prevented histone H3 phosphorylation as well as disorganizing the mitotic spindles. Upon a delay, cells underwent binucleated and finally died. Taking into account their interesting preclinal characteristics, their efficiency towards xenografts in nude mice and their apparent safety in animals, these molecules are promising new anti-cancer drugs. They probably target a metabolic signaling pathway, besides aurora B inhibition.

In addition to their possible applications, these inhibitors are tools for cell biology studies. C4, a low ATP affinity inhibitor of aurora B kinase, revealed that the basal activity of the kinase is required for histone H3 phosphorylation in prophase and for chromosome compaction in anaphase. These waves of activation/deactivation of the kinase, during mitosis, corresponded to different conformations of the passenger chromosomal complex.

Key words: *Cancer, mitotic kinases, kinase inhibitor, histone H3 phosphorylation, chromosome compaction.*

RÉSUMÉ

Les benzo[e]pyridoindoles sont de puissants inhibiteurs des kinases aurora. Nous avons réalisé une étude structure/activité pour améliorer leur activité et leur solubilité. Les amino-benzopyridoindolones se révèlent être des puissantes molécules antiprolifératives. Elles induisent un fort arrêt mitotique qui s'accompagne de l'absence de phosphorylation de l'histone H3 ainsi que de la désorganisation du fuseau mitotique. Après un délai, les cellules deviennent binuclées puis, elles meurent. Compte tenu de leurs caractéristiques précliniques, de leur efficacité sur des xénogreffes implantées chez la souris nude et de leur absence apparente de toxicité chez l'animal, ces molécules sont prometteuses pour les traitements anticancéreux. Elles ciblent probablement une voie métabolique tout en inhibant la kinase Aurora B.

Au de là de leurs possibles applications, ces inhibiteurs sont des outils pour la biologie cellulaire. La molécule C4, un inhibiteur d'Aurora de faible affinité pour l'ATP, révèle l'existence d'une activité basale de la kinase requise pour la phosphorylation de l'histone H3 en prophase et pour la compaction des chromosomes en anaphase. Ces vagues d'activation/désactivation de la kinase Aurora B correspondent à différentes conformations du complexe passager.

Mots clés : *Cancer, kinases mitotiques, inhibiteur de kinase, phosphorylation de l'histone H3, compaction des chromosomes*